Provenance analysis of the Late Cretaceous to Paleocene Rakopi, North Cape, and Farewell formations, northwest Nelson, New Zealand

---

A thesis submitted in partial fulfilment of the requirements for the degree of Master of Science in Geology

in the University of Canterbury

by

Sarah Lynette Smithies

2018

Frontispiece: sunset over conglomerate sea stacks at Whararikі Beach

ABSTRACT

The Taranaki Basin of New Zealand first developed in the middle of the Cretaceous as Zealandia rifted from Gondwana. Rift basins were active depocentres throughout the Late Cretaceous to Paleocene when rifting slowed. The only outcrops are located in northwest Nelson in the Pakawau sub-basin, a northeast trending graben bound by the Wakamarama Fault to the southeast and the Kahurangi Fault to the northwest. This study focuses on the provenance of the Late Cretaceous Rakopi and North Cape formations of the Pakawau Group and the Paleocene Farewell Formation deposited within the Pakawau Sub-basin. There are a range of potential basement sources, including the metasedimentary units of the Buller and Takaka terranes, granitoids of the Separation Point Suite and Karamea Suite, volcanics of the Takaka Terrane, and a variety of schists.

The depositional environments of the Rakopi, North Cape, and Farewell formations provides the context for the provenance analysis undertaken in this thesis. Previous studies were reviewed, and additional data added from outcrop description, paleoflow measurements, and measured stratigraphic columns. The oldest unit is the Late Cretaceous Rakopi Formation which contains sandstones, carbonaceous mudstones, siltstones, minor conglomerates, and coal, interpreted as a meandering river and floodplain environment. Locally at the base of the Rakopi Formation is the Otimataura Conglomerate; conglomerates, breccias, and sandstones interpreted as alluvial fans fed from the Wakamarama fault scarps. The Late Cretaceous North Cape Formation conformably overlies the Rakopi Formation and contains sandstones, siltstones, carbonaceous mudstones, thin coal seams, and rare conglomerates. It is interpreted as a marginal marine deposit with sediment contributions from fan deltas prograding from the Wakamarama Fault into a shallow marine embayment. New work on the Paleocene Farewell Formation has led to three lithofacies associations being proposed. Association FM has trough cross-bedded sandstone beds in channels interbedded with thick carbonaceous mudstone units, interpreted as sandy meandering river deposits. Association FS has complex stacked trough cross-bedded sandstone channels sometimes capped by thin siltstone and carbonaceous mudstone beds, interpreted as sandy braided river deposits. Association FG has thick conglomerate beds, sometimes with tabular cross-bedding, interbedded with sandstone and rare siltstone, interpreted as gravelly braided river deposits.

The north to northeast paleoflow direction shows drainage down the axis of the Pakawau sub-basin, and flow to the west away from the fault in outcrops adjacent to it.

For all formations, conglomerate composition was analysed by clast counts, followed by comparison of clast petrology and whole-rock geochemistry to potential basement sources. The Otimataura Conglomerate is dominantly composed of local basement. The North Cape and Farewell formations contain abundant metasedimentary clasts and minor vein quartz, likely from the Takaka Terrane Ellis Group; minor granitoid clasts from a mixture of Separation Point Suite intrusives and a previously unknown A-type granite; minor volcanic clasts from the Takaka Terrane; minor intrabasinal sedimentary clasts; and rare schist and chert. The granitoid and volcanic clasts become less abundant and more weathered towards the top of the Farewell Formation.

The composition of the sandstones was investigated by petrographic point counts. The Rakopi Formation Otimataura Conglomerate has litharenites and sublitharenites, with lithics dominated by schist in the southern field area (Paturau River), and sedimentary lithics further north (Pakawau Bush Road), reflecting the local basement composition. The Rakopi Formation (excluding the Otimataura Conglomerate) and the North Cape Formation sandstones are feldsarenites and lithic feldsarenites. The lithics are dominantly metasedimentary and sedimentary, with some volcanics, plutonic fragments, and schist. The Farewell Formation has mostly lithic feldsarenites and becomes more quartzose upsection. It has more metasedimentary and sedimentary lithics, which become more abundant up the stratigraphy.

The whole-rock geochemistry of fifty-four sedimentary samples was analysed by ICP-MS, ICP-OES, and XRF. The geochemistry shows elevated S and P_2O_5 in the North Cape Formation, indicating a marine-influenced depositional environment. A marine influence is also suggested for the Rakopi Formation by elevated P_2O_5 content and the presence of rare glauconite. The Rakopi Formation has elevated chemical index of alteration (CIA) values, and high Rb/Sr suggesting the presence of illite/smectite clays, likely diagenetic. The North Cape Formation has very low clays. The Farewell Formation has increasing CIA values and Ga/Rb up-section, suggesting increasing amounts of kaolinite clays likely due to weathering. A more granitic provenance for the North Cape Formation and upper Rakopi Formation is suggested

by elevated Na_2O and K_2O showing the presence of plagioclase, lower Zr indicating less zircon, and higher light rare earth element concentration.

When rifting began in the Late Cretaceous, deposition was highly localised resulting in local provenance of the Otimataura Conglomerate. The remainder of the Rakopi Formation and the North Cape Formation have a mixed provenance of Takaka Terrane metasedimentary and volcanic units, Separation Point Suite, and A-type granites, showing drainage away from the Wakamarama Fault. The Farewell Formation provenance is also dominated by Takaka Terrane metasedimentary units, showing drainage from the Wakamarama Fault, although high degrees of weathering show that fault movement was slowing creating greater residence times for sediments in the system. The composition of the Rakopi, North Cape, and Farewell formations has implications for their hydrocarbon reservoir potential offshore, for example high clay contents in the Rakopi and North Cape formations are expected to decrease their permeability and reservoir potential.

TABLE OF CONTENTS

TABLE OF FIGURES

TABLE OF TABLES

ACKNOWLEDGEMENTS

Firstly, I'd like to thank my supervisors, Kari Bassett, Greg Browne, and Alex Nichols. I couldn't have done this thesis without Kari's sedimentology expertise, many hours spent editing, and time spent in meetings asking hard questions. Greg's local knowledge, extensive knowledge of the literature, and help in the field (even in the mud and rain) was invaluable. Alex's geochemical insight and eye for detail significantly improved the quality of my work.

Thanks to all the technical staff at UC for their support, especially to Rob Spiers and Chris Grimshaw for finding time to make thin sections despite moving the geology department twice. All of the geology staff went above and beyond in a very difficult year. Thank you also to Craig at Spectrachem for running XRF analyses on such short notice.

Funding for this thesis came from an Orion Master's Energy Scholarship. Field work was funded by the Mason Trust Fund and by a GNS field work grant. The sedimentary geochemistry portion of my research was made possible by Stuart Munday and Chemostrat Ltd., who provided access to their excellent facilities for my samples.

The use of the Victoria University of Wellington Onekaka field station made field work significantly more comfortable, thank you to Kosta Tashkoff and Irene Turner for making this available. Thanks also to the landowners in the Whanganui Inlet who kindly gave me access across their land, many key outcrops would be missing from this study without them. The Department of Conservation gave access and sampling permission for the many locations on Crown land.

Thanks to Rebecca Joyce for being a fantastic field partner, especially for bashing up the Paturau with me. Thanks also to Sophie Hill and Marlene Villeneuve for adding their perspectives in the field. A huge thank you to my fellow students and the room 323 crew for the moral support and well-deserved treat breaks. Finally, thanks to my family for their unwavering support. I couldn't have finished this without you.

1. INTRODUCTION

The sub-continent of Zealandia began to rift from Gondwana in the middle of the Cretaceous at ~105 Ma (King and Thrasher 1996; Laird and Bradshaw 2004). As a result, active extensional structures were widespread throughout Zealandia in the Late Cretaceous. Numerous rift basins developed and were major sediment depocentres throughout the Late Cretaceous and into the Paleocene (Bache et al. 2014; Strogen et al. 2017). The Tasman Sea opened in the Late Cretaceous (~85 Ma), and continued to spread until the Paleocene, when the spreading centre slowed and eventually stopped in the earliest Eocene (Bache et al. 2014; Strogen et al. 2017). Extension in the sedimentary basins also slowed and stopped, transitioning into passive margin sedimentation.

This thesis focuses on sedimentary rocks deposited during this time of tectonic change as rift basins opened and developed in the Late Cretaceous through the transition into a passive margin setting in the Paleocene. The sedimentary succession studied was deposited within a graben that developed during Late Cretaceous rifting (the Pakawau sub-basin of the Taranaki Basin). This project focuses on the provenance of these sedimentary rocks, and how the provenance changed through time in response to the changing tectonic regime.

1.1 Taranaki Basin

This study focuses on the Taranaki Basin (Fig. 1.1), which first formed in the Late Cretaceous due to extension of the Zealandia continental crust (King and Thrasher 1996; Strogen et al. 2017). Dominantly terrestrial successions were deposited in extensional sub-basins. The majority of the Taranaki Basin is now offshore, and the only outcrop of the Late Cretaceous and Paleocene lithologies is found in northwest Nelson in the northern South Island, the field area for this research.

The Late Cretaceous and Paleocene succession is of particular interest for petroleum exploration. The Taranaki Basin is currently the only petroleum-producing basin in New Zealand (PBE 2017). The Late Cretaceous units are the main hydrocarbon source rocks in the

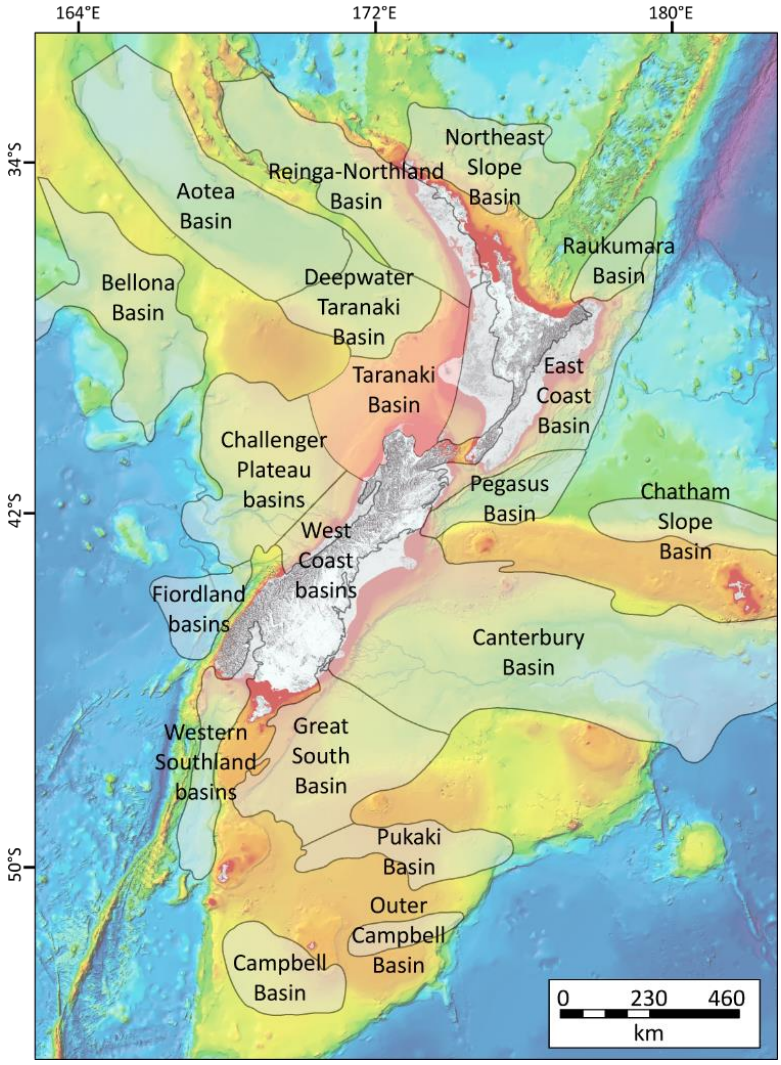

Fig. 1.1: Location of key sedimentary basins in Zealandia, including the Taranaki Basin (red). Base map shows bathymetry. Modified from PBE (2017).

Taranaki petroleum system, as well as being potential reservoirs (Killops et al. 1994; Higgs et al. 2010; Joyce 2018). The Paleocene units are actively producing units in several gas condensate and oil fields (PBE 2017).

There has been extensive exploration of the offshore Taranaki Basin (Fig. 1.2), but relatively little work on the corresponding onshore outcrops in northwest Nelson, especially the Paleocene stratigraphy. This study will use provenance analysis to refine the paleogeographic models for the Late Cretaceous and Paleocene southern Taranaki Basin, by reconstructing sediment drainage patterns from basement source to site of deposition. The paleogeography is useful for understanding the offshore petroleum system, as it models the location of potential source, reservoir, and seal lithologies. Sandstone composition has also been shown to be a primary control of sandstone porosity and permeability, and therefore reservoir quality, in the Taranaki Basin (Higgs et al. 2010). Understanding how the basement type

influences the composition of sedimentary rocks infilling the sedimentary basin will therefore aid prediction of potential reservoir units off shore.

1.2 Summary of stratigraphy

The oldest unit in the southern Taranaki Basin is the Late Cretaceous Rakopi Formation of the Pakawau Group, which rests unconformably on basement in the northwest Nelson area (Rattenbury et al. 1998). It is a succession of sandstones interbedded with carbonaceous mudstone, siltstone, conglomerate, and coal beds, interpreted as meandering stream, overbank, and swamp deposits (Thrasher 1992; Rattenbury et al. 1998; Browne et al. 2008). Locally at the base of the Rakopi Formation is the Otimataura Conglomerate. This member

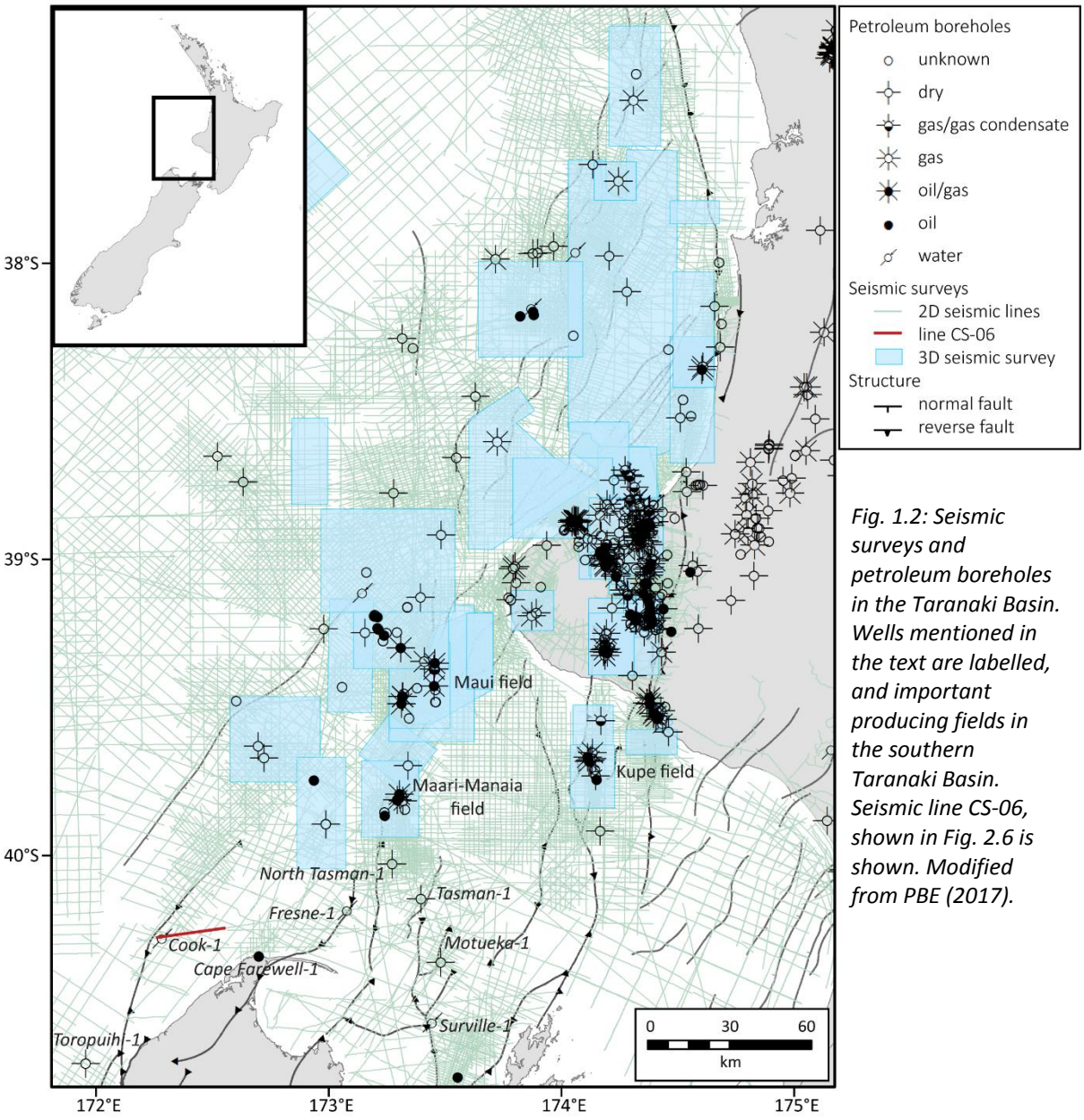

Fig. 1.2: Seismic surveys and petroleum boreholes in the Taranaki Basin. Wells mentioned in the text are labelled, and important producing fields in the southern Taranaki Basin. Seismic line CS-06, shown in Fig. 2.6 is shown. Modified from PBE (2017).

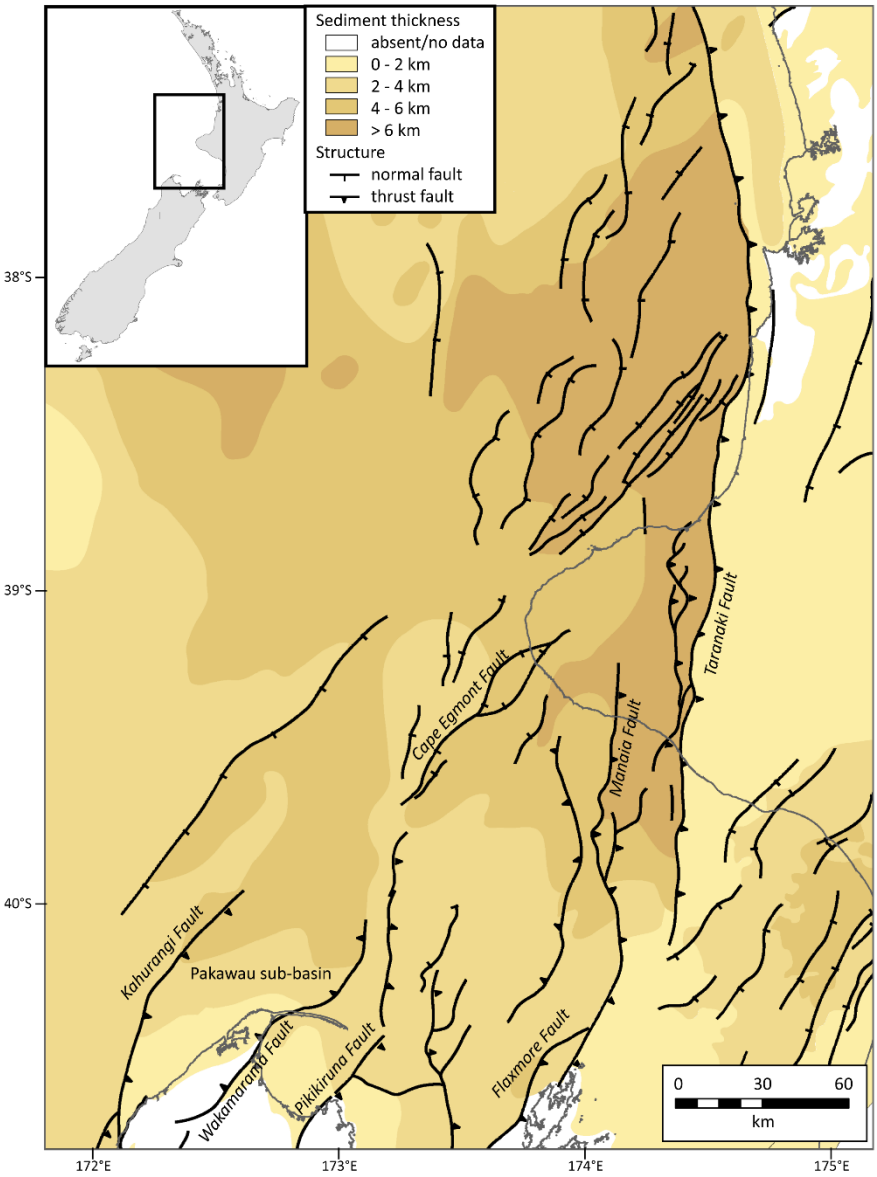

Fig. 1.3: Modern structure of the Taranaki Basin, and thickness of Late Cretaceous to recent sedimentary rocks. Many of the thrust faults in the Southern Taranaki Basin are inverted Late Cretaceous to Paleocene normal faults. Data from King and Thrasher (1996) via. New Zealand Petroleum and Minerals.

contains sandstones, conglomerates, and breccias interpreted as alluvial fan deposits adjacent to active fault scarps (Thrasher 1992).

The Late Cretaceous North Cape Formation of the Pakawau Group is a succession of sandstones interbedded with siltstones, minor conglomerates, and rare coal seams (Thrasher 1992; Rattenbury et al. 1998; Higgs et al. 2010). It is interpreted as paralic and marginal marine deposits, with coastal plain and fluvial environments, estuary deposits, and tidal channels (Bal and Lewis 1994; Higgs et al. 2010; Joyce 2018).

The contact between the North Cape Formation and overlying Paleocene Farewell Formation of the Kapuni Group is well exposed in northwest Nelson. It is unconformable due to a marine regression as rifting slowed (Bal 1994). The Farewell Formation contains sandstones, siltstones, pebbly sandstones, conglomerates, and minor coals (King and Thrasher 1996;

Rattenbury et al. 1998). The formation is interpreted as a floodplain environment with braided to meandering rivers. The Farewell Formation is separated from overlying units by a significant regional unconformity spanning the late Waipawan into at least the Bortonian (Early to Middle Eocene).

1.3 Field area

The field area for this study is the region in northwest Nelson where the Late Cretaceous Rakopi and North Cape formations and Paleocene Farewell Formation crop out (Fig. 1.4). Also well exposed in northwest Nelson is the contact of the Farewell Formation with the overlying Oligocene to Pliocene sedimentary rocks.

These northwest Nelson sedimentary rocks are contained within the Pakawau sub-basin, bounded by the Wakamarama Fault to the southeast and the Kahurangi Fault offshore to the northwest (Fig. 1.3). Both these faults had normal offset during the Late Cretaceous and Paleocene, and the graben between the faults was an active depocentre. Both faults were inverted during the Miocene, and are now active reverse faults (Reilly et al. 2015). Compression along the Wakamarama Fault caused the uplift of the Wakamarama and Burnett

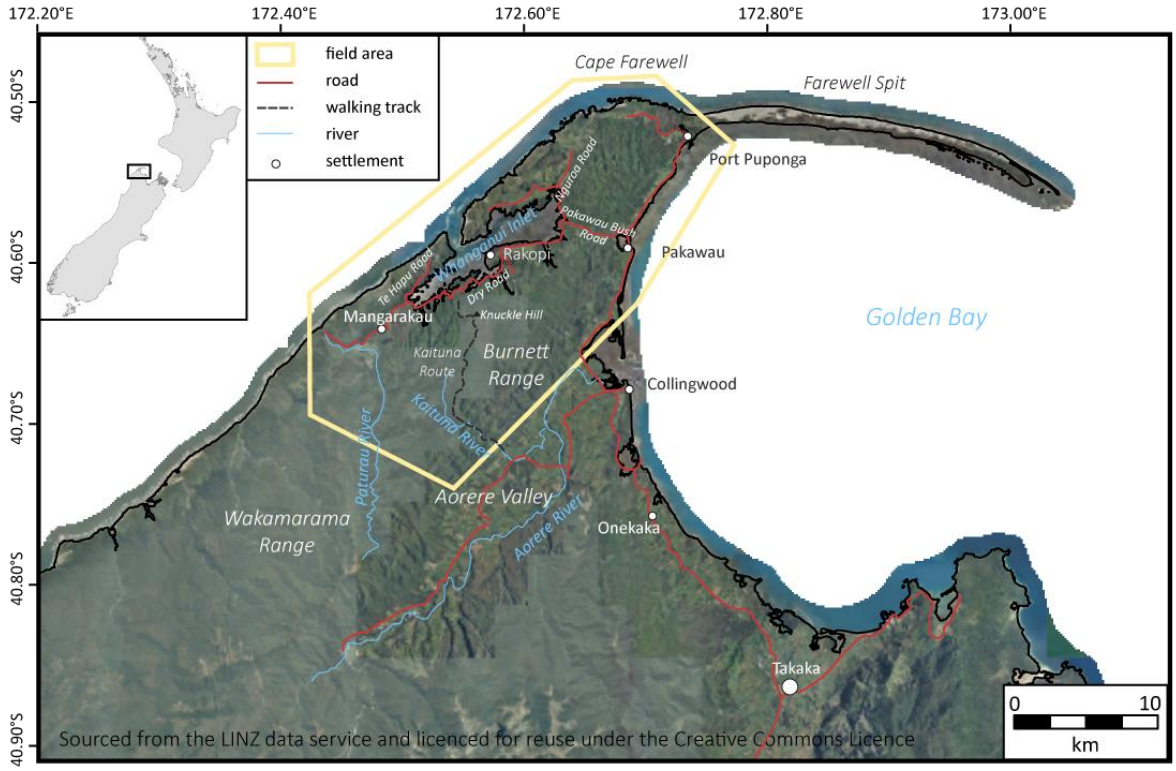

Fig. 1.4: Map of northwest Nelson region with key place names and field area of this project outlined.

Ranges in northwest Nelson (Fig. 1.4) and exposure of the Late Cretaceous to Paleocene succession.

Outcrops of the Rakopi Formation are mostly located in the Burnett Ranges, typically on roadside cuttings and river banks. The North Cape Formation mostly outcrops around the shores of the Whanganui Inlet. The Farewell Formation is well exposed on the coast around Cape Farewell (Fig. 1.4).

1.4 Aims and scope

The aim of this research is to determine the composition and provenance of the Rakopi, North Cape and Farewell formations where they outcrop in the northwest Nelson area, and how this changed through time. Chapter 2 will review the current understanding of Late Cretaceous and Paleocene tectonics, the northwest Nelson stratigraphy and sedimentological interpretations, and previous provenance studies. It will also summarise the basement lithologies in northwest Nelson, as the basement is the potential source material for the younger sedimentary rocks.

To provide the context of the provenance study, the depositional setting of the Rakopi, North Cape, and Farewell formations were investigated from field studies (Chapter 3). This is particularly relevant for the Farewell Formation, which has little literature on its sedimentology.

The composition of the sedimentary rocks was examined using multiple techniques. The overall composition of the conglomerates was described by clast counts in the field, and the different clast types compared to possible basement sources by their petrology and whole-rock geochemistry (Chapter 4). The composition and provenance of the Pakawau Group and Farewell Formation sandstones were examined by petrographic techniques (Chapter 5). The whole-rock geochemistry of sandstone and mudstone samples was analysed and compared to basement geochemistry (Chapter 6). The whole-rock sedimentary geochemistry was then compared to the petrographic results to validate the geochemical technique.

The provenance was used to refine the paleogeographic models already available for the southern Taranaki Basin (Chapter 7). The impact of the paleogeography and sandstone composition on petroleum reservoir potential will also be discussed (Chapter 7).

In summary, the aims of this research are:

- Review existing knowledge of Taranaki Basin tectonics; northwest Nelson paleogeography, sedimentology, and provenance; and potential basement source lithologies (Chapter 2).
- Describe the sedimentology of the Rakopi, North Cape, and Farewell formations in northwest Nelson and implications for depositional environment and paleogeography (Chapter 3).
- Describe the composition of Late Cretaceous and Paleocene mudstones, sandstones, and conglomerates in northwest Nelson from conglomerate composition (Chapter 4), sandstone petrology (Chapter 5), and sandstone and mudstone whole-rock geochemistry. (Chapter 6)
- Investigate temporal variation of the composition and provenance of the Rakopi, North Cape, and Farewell formations (Chapter 4, 5, 6).
- Use temporal changes in sedimentary rock provenance to examine the changing tectonic setting in the Pakawau sub-basin across the Late Cretaceous and Paleocene (Chapter 7)
- Refine paleogeographic models of the southern Taranaki Basin for the Late Cretaceous and Paleocene based on sediment transport pathways (Chapter 7)
- Relate sandstone composition to reservoir quality (Chapter 7)

2. GEOLOGICAL BACKGROUND

2.1 Introduction

This chapter reviews the previous provenance and sedimentological studies of the Rakopi, North Cape, and Farewell formations. The first portion of the chapter describes the tectonic setting of the Taranaki Basin, and then describes the sedimentary succession in the southern Taranaki Basin as presented in the literature. The depositional setting through the Late Cretaceous and Paleocene and the impact of tectonics is reviewed.

The second portion of this chapter describes the basement lithologies in the northwest Nelson region, as the basement is the main source material for the younger sedimentary units. Previous provenance studies on the Rakopi, North Cape, and Farewell formations are then reviewed.

2.2 Late Cretaceous and Cenozoic tectonic setting

The middle of the Cretaceous (~105 Ma) marks an abrupt tectonic change from a subduction system at the margin of Gondwana, to an extensional regime related to the breakup of Gondwana and the opening of the Tasman Sea (King and Thrasher 1996; Laird and Bradshaw 2004; Strogen et al. 2017). In the Taranaki Basin there were two phases of extension separated by a short phase of uplift and erosion (King and Thrasher 1996; Strogen et al. 2017).

The first phase of rifting (the "Zealandia Rift" phase of Strogen et al. 2017) occurred in the late Early and early Late Cretaceous between 105 and 83 Ma, immediately prior to the opening of the Tasman Sea rift (Strogen et al. 2017). Normal faults and associated half-grabens and grabens opened in the northern and western Taranaki Basin. The faults were dominantly oriented NW to NNW, approximately parallel to the Tasman Sea spreading. The fault-controlled basins were filled by the Taniwha Formation, an early synrift terrestrial deposit, followed by late synrift marginal marine and marine deposits (Strogen et al. 2017). The Taniwha Formation and equivalents are absent in the northwest Nelson area.

Two tectonic models for this first phase of rifting have been proposed (Strogen et al. 2017). Laird (1981) proposed that a rift arm propagated from a triple junction southwest of the South

Island, through the West Coast and into the Taranaki Basin (Fig. 2.1A). This rift arm failed, while the other two arms became the Tasman Sea Rift. The second model, proposed by Thrasher (1990) and King and Thrasher (1996), is that the extension was oblique, as a result of a sinistral transform system propagating from the Tasman Sea rift (Fig. 2.1B). Lamb (2016) have also suggested that there was significant (~250 km) sinistral offset in the Late Cretaceous along what is now the Alpine Fault zone, on the basis of the geometry of the basement terranes, and paleomagnetic data indicating their orientation prior to Cenozoic displacement. This strike-slip offset could have been the same strike-slip motion suggested by Thrasher (1990) and King and Thrasher (1996). However, Reilly (2015) found no evidence for oblique motion in seismic profiles of the southern Taranaki Basin such as pop-up structures, pull-apart basins at fault relays, and out-of-plane displacements on vertical profiles. This calls into doubt the reconstruction of large-scale strike-slip faulting.

The Zealandia Rift was followed by a short period of uplift and erosion from 83 to 80 Ma, concurrent with the onset of Tasman seafloor spreading (Strogen et al. 2017). The start of rifting is marked by a widespread regional unconformity separating the older basement rocks from the younger "cover" sequence (Laird 1981; Laird and Bradshaw 2004). This may have resulted from uplift and erosion due to mantle upwelling and thermal expansion immediately preceding rifting (Laird 1981; Laird and Bradshaw 2004). The uplift created an angular unconformity, truncating or removing the Taniwha Formation. A large wedge of sediment up to 2.5km thick (the Taranaki Delta) prograded westward into the central Taranaki Basin (Strogen et al. 2017). The volume of sediment suggests reworking of Zealandia Rift phase sediments, as well as erosion of basement.

A second phase of extension (the "West Coast-Taranaki Rift") occurred from 80 to 55 Ma (Late Cretaceous to end Paleocene) (Strogen et al. 2017). During this extension, normal faults developed generally striking north to northeast. The resulting grabens and half-grabens were filled by terrestrial and shallow marine deposits (Fig. 2.2). In the northwest Nelson region, the Pakawau Sub-basin developed. This is a northeast-trending graben bounded to the southeast by the Wakamarama Fault and to the northwest by the Kahurangi Fault. Normal movement on the Wakamarama Fault began at ~80 Ma (Late Cretaceous) and ceased by ~65 Ma (earliest Paleocene) (Reilly et al. 2015).

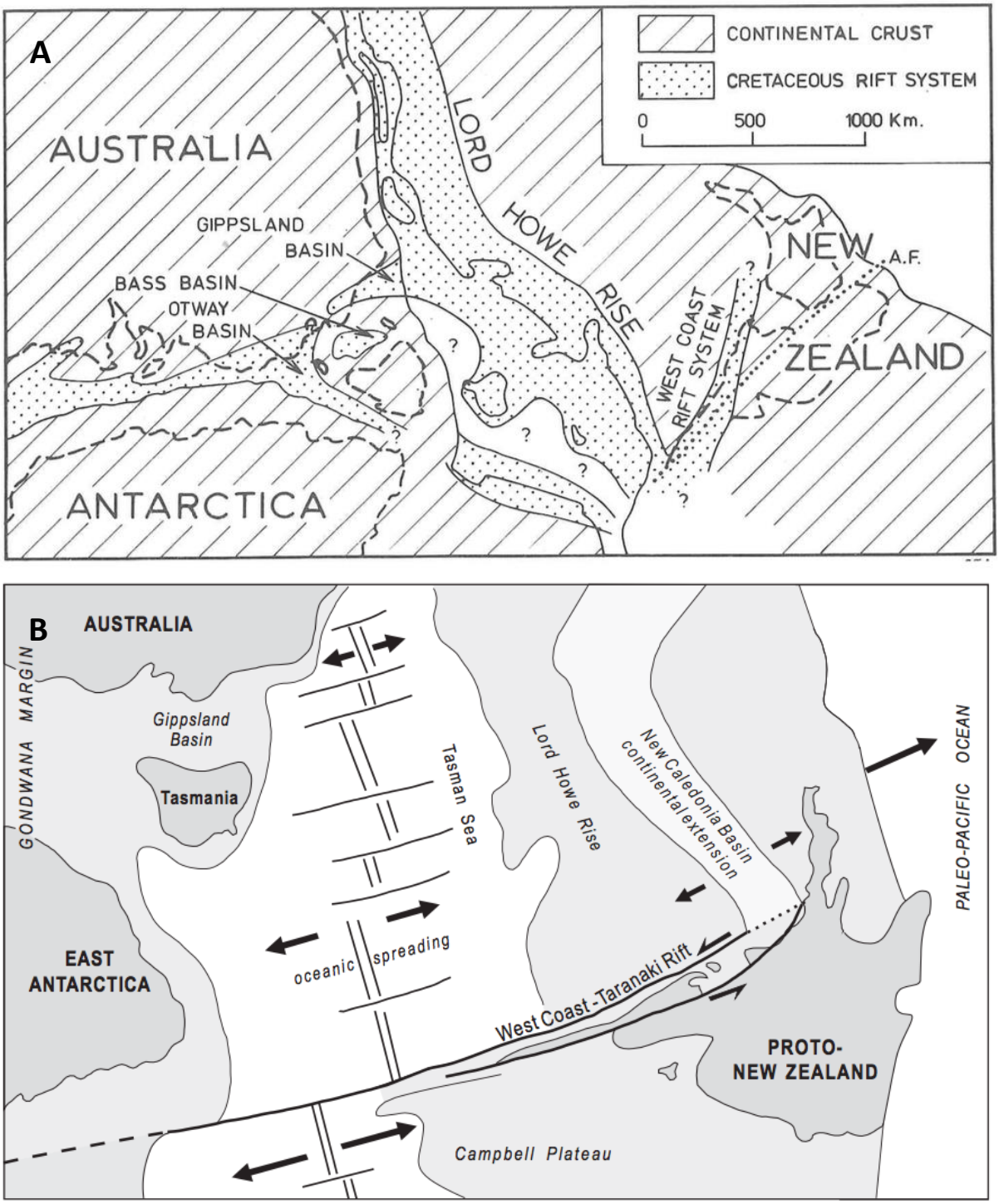

Fig. 2.1 A: Failed rift arm model of the first phase of Taranaki rifting, proposed by Laird (1981). Figure from Laird (1981, p. 317). B: strike-slip extension model of the first phase of Taranaki rifting, proposed by Thrasher (1990) and King and Thrasher (1996). Figure from King and Thrasher (1996, p. 95).

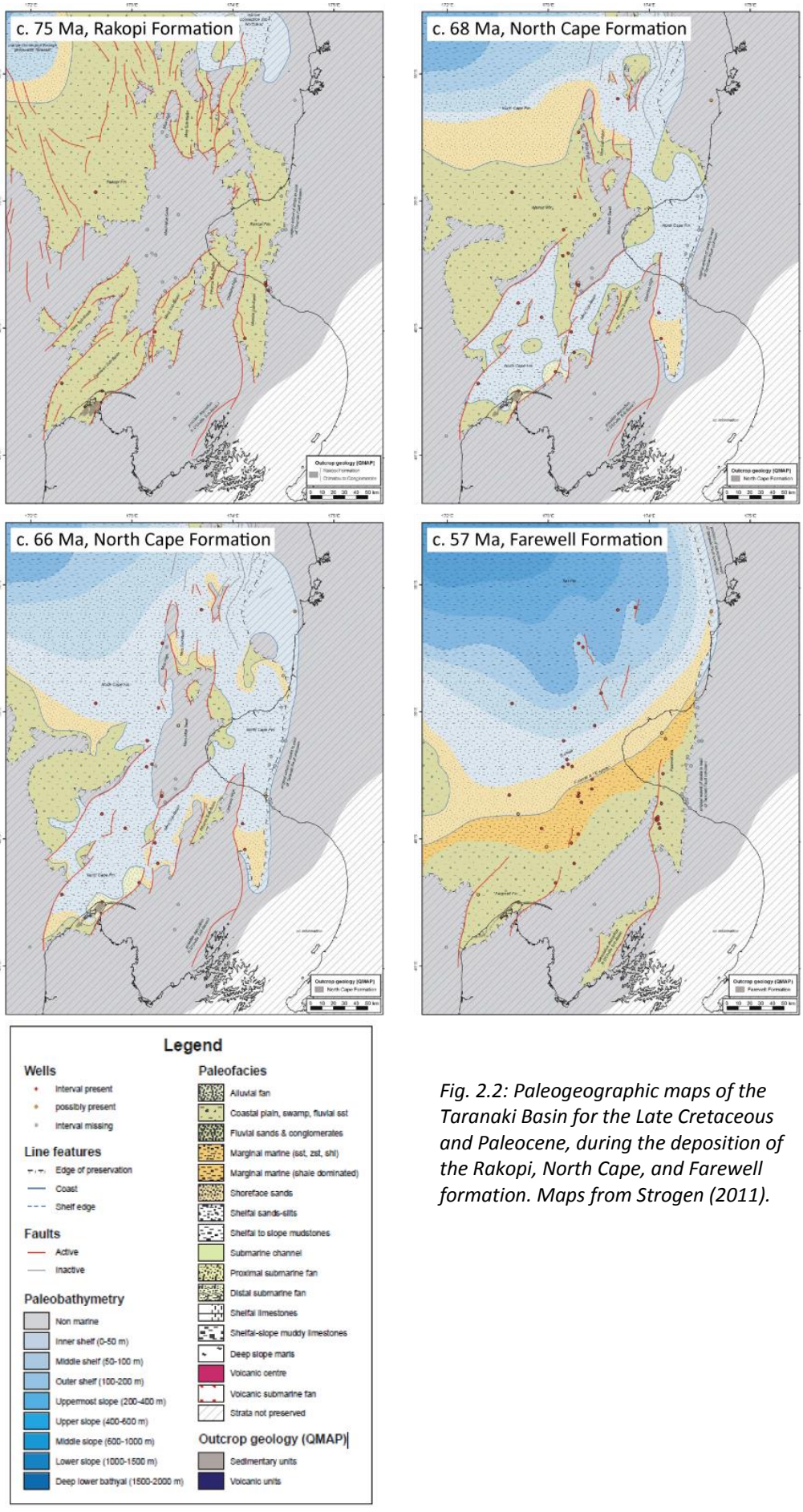

Fig. 2.2: Paleogeographic maps of the Taranaki Basin for the Late Cretaceous and Paleocene, during the deposition of the Rakopi, North Cape, and Farewell formation. Maps from Strogen (2011).

From the end of the Paleocene, the Taranaki Basin transitioned into a relatively tectonically quiescent period of passive margin subsidence and sedimentation (King and Thrasher 1996; Reilly et al. 2015). In the northwest Nelson area, there is a regional unconformity spanning the Early to Middle Eocene. This is followed by a Late Eocene and Oligocene marine succession.

Following the development of the Pacific-Australian plate boundary in the Miocene, the eastern and southern Taranaki Basin structure was overprinted by compressional tectonics (King and Thrasher 1996; Reilly et al. 2015). Many Late Cretaceous normal faults were inverted, including the Wakamarama and Kahurangi Faults. Along the Wakamarama Fault, the Late Cretaceous and Paleogene fill in the Pakawau Sub-basin has been uplifted and gently folded into the Wakamarama Anticline, a northeast-plunging anticline (Figs. 2.3, 2.4).

2.3 Late Cretaceous and Cenozoic stratigraphy

The Pakawau Group, which includes the Rakopi and North Cape formations, is the oldest group in the northwest Nelson cover sequence (Thrasher 1992). The Pakawau Group was deposited in the Late Cretaceous during the second phase of extension in the Taranaki Basin. These two formations are distinguishable from seismic facies mapping, in offshore wells, and in outcrops in northwest Nelson (King and Thrasher 1996).

The Pakawau Group is overlain by the Kapuni Group, which in the northwest Nelson area is only represented by the Farewell Formation, the oldest of the constituent formations of the Kapuni Group. The Farewell Formation is Teurian to Waipawan (Paleocene-earliest Eocene) in age.

2.3.1 Previous work

The Late Cretaceous and Cenozoic stratigraphy of the southern Taranaki Basin has been described and redefined by many authors (Fig. 2.5, Table 2.1) (Suggate 1956; Titheridge 1977; Thrasher 1992; Higgs et al. 2010). The stratigraphy described here is based on Thrasher (1992) and Higgs et al. (2010).

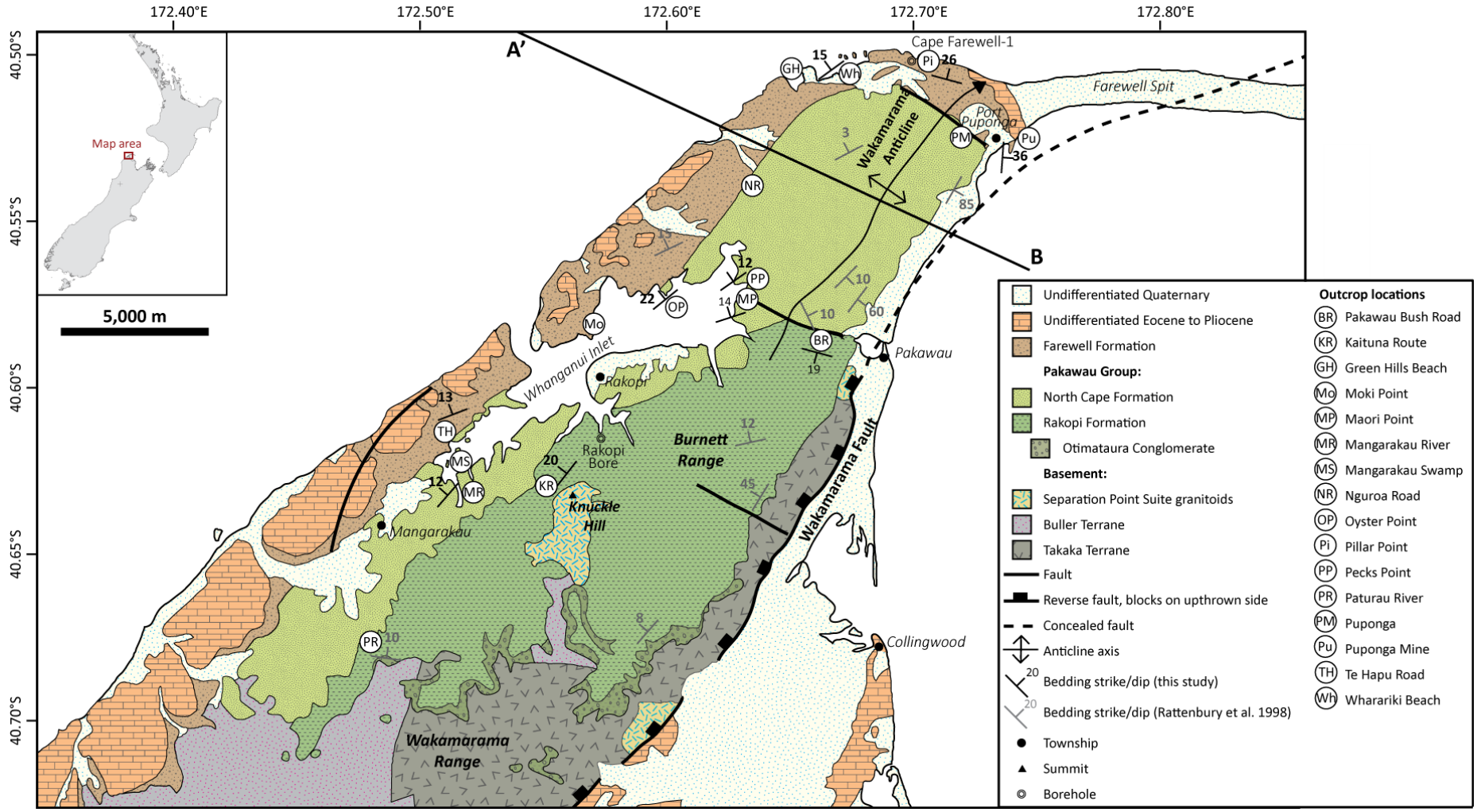

Fig. 2.3: Geological map showing Late Cretaceous and Paleocene outcrop in the northwest Nelson region. Modified from Rattenbury et al. (1998).

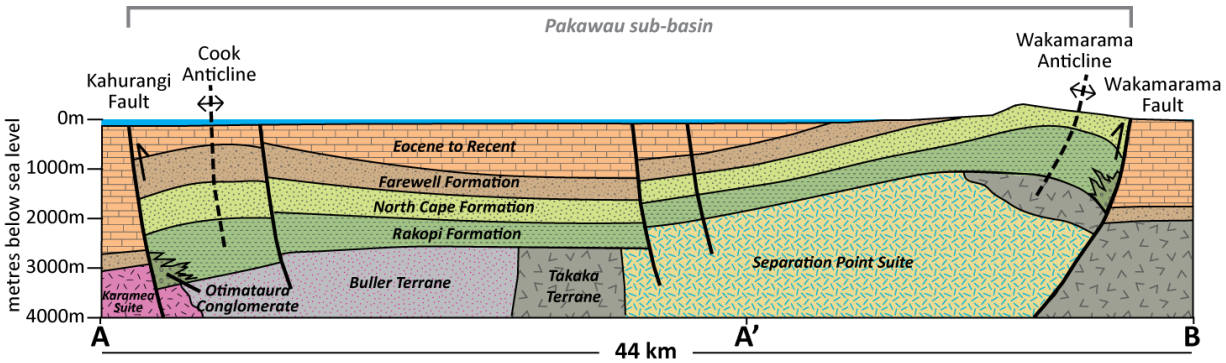

Fig. 2.4 cross section through the Pakawau sub-basin showing key structures. Cross-section line A' to B is shown on Fig. 2.3, and A to B is shown on Fig. 2.8. Vertical scale 2x exaggerated. Modified from King and Thrasher (1996), surface data from Rattenbury (1998), basement data from Tulloch and Mortimer (2017).

Early studies in the late nineteenth century focused on the coal resource in the northwest Nelson area (Ongley and Macpherson 1923; Suggate 1956; Bussell 1985). Coal was mined on a small scale in the Whanganui Inlet (previously called "Westhaven Inlet" or "West Haven Inlet") and Cape Farewell region as early as 1840, and continued until the Puponga Mine closed in 1974 (Ongley and Macpherson 1923; Bussell 1985; Thrasher 1992). There were several boreholes drilled at Puponga and in the Whanganui Inlet for the purpose of assessing coal resources (Ongley and Macpherson 1923; Suggate 1956; Bussell 1985). Particularly important is the Rakopi Bore (also called "Bassett's" Bore) drilled near Rakopi in 1915 (Fig. 2.3), which is the type-section for the Rakopi Formation (Thrasher 1992).

During this phase of coal exploration, the first geological map of the region was published in 1923 (Ongley and Macpherson 1923). It was followed by a more detailed description of the stratigraphy and coal resource of the Puponga region by Suggate (1956) and Bussell (1985), and a further 1:63,360 scale geological map by Bishop (1971).

The modern era of oil exploration in the wider Taranaki Basin began in the 1950s (King and Thrasher 1996). In the 1970s and 1980s, several wells were drilled in the Southern Taranaki Basin, including Cook-1 (1970), Fresne-1 (1976), and Cape Farewell-1 (1985 to 1986) (Fig. 1.2) (van Oyen and Branger 1970; NZ Aquitaine Petroleum Ltd 1976; Carter and Kintanar 1987). With the availability of well and seismic reflection data, there was renewed interest in the outcrop sedimentology and its relationship to the offshore units (Thrasher 1992). The older interpretations of Titheridge (1977) that had been used through the 1980s were revisited, and Titheridge's (1977) fluvial model of North Cape deposition was replaced by Wizevich

et al.'s (1992) marginal marine to estuarine interpretation. Detailed lithofacies analysis of the North Cape and Farewell formations were also presented (Bal 1992; Bal and Lewis 1994; Stark 1996). The stratigraphy of the Nelson region was summarised by Rattenbury et al. (1998) in the Institute of Geological and Nuclear Science 1:250,000 geological map series.

There was renewed interest in the northwest Nelson outcrops from the late 2000's, particularly the petrology and composition of the sedimentary rocks and coals, and how the composition and sedimentology relates to the petroleum system in the wider Taranaki Basin (Browne et al. 2008; Higgs et al. 2010; Joyce 2018). In the modern era of petroleum exploration, the Rakopi Formation had been little studied due to the remote and poor-quality nature of its outcrops. The first detailed lithofacies analysis of the Rakopi Formation was presented by Browne et al. (2008).

2.3.2 Rakopi Formation sedimentology and depositional environment

The Late Cretaceous Rakopi Formation is the oldest cover unit in the northwest Nelson region, where it rests unconformably on basement (Fig. 2.3) (Rattenbury et al. 1998). Exhumation of basement intrusives was relatively rapid, as the Rakopi Formation locally onlaps the Separation Point Suite granitoids dated at 105 Ma at Knuckle Hill (Tulloch 2017 personal communication). Exhumation of this young basement may be related to the phase of uplift between 83 and 80 Ma as described by Strogen et al. (2017).

The Rakopi Formation is a succession of sandstones interbedded with carbonaceous mudstone, siltstone, conglomerate, and thin coal beds (Thrasher 1992; Rattenbury et al. 1998). The unit thickens towards contemporaneously active faults such as the Wakamarama Fault, reaching a maximum thickness of over 1500m (Fig. 2.4) (Thrasher 1992; Browne et al. 2008).

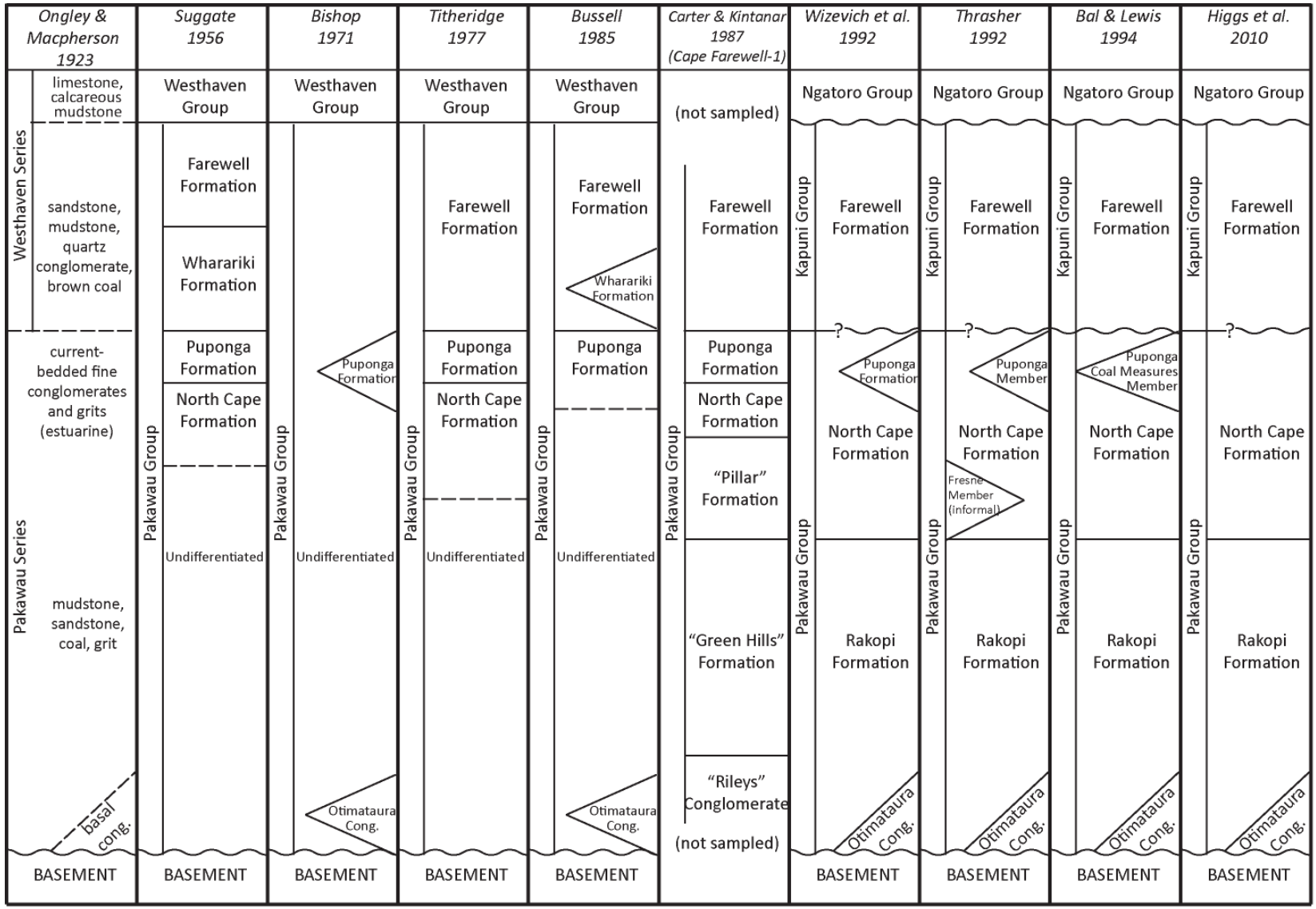

Fig. 2.5: Stratigraphic schemes from key publications that revised the naming schemes for Late Cretaceous and Paleocene sedimentary rocks in northwest Nelson. This study uses the naming scheme of Higgs et al. (2010).

Table 2.1: Summary of significant literature dealing with the sedimentology and stratigraphy of Late Cretaceous and Paleocene sedimentary rocks in the northwest Nelson area. For clarity, the naming scheme of Higgs et al. (2010) (Fig. 2.5) has been used; square brackets indicate where older names have been substituted.

Reference	Publication type	Units	Objectives	Methods	Key findings
Ongley and Macpherson (1923)	Bulletin	[Otimataura Conglomerate], [Rakopi Fm], [North Cape Fm], [Farewell Fm], [Ngatoro Group]	Description of the geology and resources (coal, mineral) of the northwest Nelson region	Outcrop description Boreholes for coal exploration	Conglomerate (Otimataura Conglomerate) at the base of the Pakawau Group, with clasts of greywacke, schist, granite, and quartz. Describes interbedded sandstone, mudstone, coal (Rakopi Fm), onlapping onto Knuckle Hill. North Cape Fm on the eastern shores of the Whanganui Inlet is estuarine. North Cape Fm passes conformably into "quartz conglomerate" (Farewell Fm), which is conformable with overlying Ngatoro Group.
Suggate (1956)	Peer reviewed article	North Cape Fm, [Farewell Fm], [Ngatoro Group]	Description of sedimentology and extent of the stratigraphy in the Puponga/Cape Farewell Assess the coal resource	Outcrop description Drillholes for coal exploration	North Cape Fm: 240m + Upper North Cape Fm: 46-58m of fine sandstone, mudstone, coal. Conglomerates become thicker to the west. Farewell Fm: 490m total thickness of conglomerate, pebbly sand, quartzose sandstone, and mudstone. Conglomerates have increasingly leached granite and greywacke clasts towards the top.
Titheridge (1977)	MSc thesis	North Cape Fm, Farewell Fm, [Ngatoro Group]	Description and interpretation of the Late Cretaceous to Oligocene strata based on stratigraphy, thickness and age of units, sedimentary structures, textures, and composition	Measured sections in the Whanganui Inlet, at Cape Farewell, and Kahurangi Point. Paleocurrent measurements Thin section analysis, palynological and foraminiferal analysis of sedimentary samples	North Cape Fm: braided stream and overbank deposits; transitions upwards to floodplain deposits as a result of tectonic quiescence. Farewell Fm: braided stream deposits due to increasing tectonic activity.
Bussell (1985)	Unpublished coal report	[North Cape Fm], [Farewell Fm], [Ngatoro Gp]	Detailed assessment of the coal resource in the Whanganui Inlet region	Geological mapping and outcrop description Measured sections in the Whanganui Inlet	Minor (normal) faulting and folding in the Whanganui Inlet region Correlates coal measures at Puponga with coal in the Inlet (Puponga Member) Interprets Pakawau Group deposits as braided rivers, transitioning upwards to lower energy meandering river deposits.
Wizevich et al. (1992)	Peer reviewed article	North Cape Fm	Interpretation of the depositional environment of the North Cape Fm	Measured sections in the Whanganui Inlet Dinoflagellate and palynological assemblages in three samples	North Cape Fm: marine/tidal influence suggested by sedimentological evidence (ripple cross-laminations, herringbone cross-beds, opposing paleocurrent, mud draped cross-bedding, bioturbation) and paleontological evidence (marine dinoflagellates and marine algae)

Reference	Publication type	Units	Objectives	Methods	Key findings
Wizevich (1994)	Conference proceeding	Otimataura Conglomerate, Rakopi Fm, North Cape Fm, Farewell Fm	Description of Late Cretaceous and Paleocene succession in the Pakawau sub-basin Interpretation of depositional setting and controls on sedimentation, related to the opening of the Tasman Sea	Description of outcrops in the Wakamarama and Burnett Ranges and Whanganui Inlet Review of published data, including Rakopi Bore	Otimataura Conglomerate: Basal marron-coloured unit of sandstone, breccia and conglomerate, with paleocurrent trending north, away from the away from the Wakamarama Fault. Interpreted as alluvial fan and debris flow deposits. Rakopi Fm: generally fine-grained and organic/coal rich. Infer meandering stream deposits on a low-gradient coastal plain. North Cape Fm: three facies associations: conglomeritic proximal association in the NE of the Inlet; medial, sandstone dominated association; distal mudstone and fine sandstone in the SW of the inlet. Interpreted as tide influenced braid delta system. Paleocurrents to the NW, away from the Wakamarama Fault. Sedimentation in the Pakawau Sub-basin was dominantly controlled by the Wakamarama Fault. Eustatic sea level rise at 66.5Ma may have caused the marine transgression that lead to North Cape Fm deposition
Thrasher (1992)	PhD thesis	Rakopi Fm, North Cape Fm, Farewell Fm, Ngatoro Group	Describe the Late Cretaceous structure and tectonic history of the Taranaki Basin Describe the relationship between tectonics and Late Cretaceous sedimentation Evaluation of the stratigraphy of the Pakawau Group Offshore stratigraphy and seismic facies mapping of the Late Cretaceous sedimentary rocks Late Cretaceous paleogeography of the Taranaki Basin	Interpretation of seismic reflection data and seismic facies mapping Outcrop description in the northwest Nelson area Petroleum exploration well data (lithologic, palaeontological, wireline log, and geochemical data)	Late Cretaceous tectonics were dominated by high angle normal faulting. No significant strike-slip faulting occurred in the Late Cretaceous. Subdivision of the Pakawau Group into the Rakopi Fm and the North Cape Fm: Rakopi is entirely terrestrial, North Cape is marine to paralic. The formations are distinguishable in well data and in seismic reflection surveys. Definition of the Otimataura Conglomerate Member and the Fresne Conglomerate Member. Rakopi Fm is a good potential source rock, Rakopi, North Cape, and Farewell Fms are all potential reservoirs.
Bal (1992)/Bal and Lewis (1994)	BSc Hons dissertation/ peer reviewed article	North Cape Fm, Farewell Fm	Description of the upper North Cape Fm (Puponga Mbr), its extent and lateral and vertical variation, and interpretation of depositional setting.	Five measured sections in the Whanganui Inlet, North Cape Fm and overlying Farewell Fm. Description of lithofacies and lithofacies associations Paleocurrent measurements Samples for dinoflagellates, palynomorph dating, clay assemblage from XRD	North Cape Fm: three lithofacies associations: A1 - High energy subtidal channels and intertidal sand shoals A2 - Intertidal and supratidal mudflats, salt marsh and mires A3 - Distributary/crevasse channel splays, levees, mouth bars into freshwater bays; mires Farewell Formation: lithofacies association B - braided or coarse-grained meandering river or floodplain deposits. North Cape Fm has paleocurrent trending SW/NE; Farewell Fm paleocurrent trends NW.
Stark (1996)	MSc thesis	North Cape Fm, Farewell Fm	Description of the Farewell Fm, its extent and lateral and vertical variation, and interpretation of depositional setting.	Fifteen measured sections in the Whanganui Inlet and around Cape Farewell, of Farewell Fm Description of lithofacies and	Adds additional lithofacies associations to Bal (1994)'s A1-A3, covering Farewell Fm: A4 - lacustrine A5, A6, A7 - fluvial, low energy meandering (A5) to high energy braided (A7)

Reference	Publication type	Units	Objectives	Methods	Key findings
				lithofacies associations Paleocurrent measurements Samples for thin section analysis, clay assemblage from XRD Conglomerate clast counts	B1, B2, B3 - fluvial, coarse grained braided river Paleocurrent: B2 - N-NE; A5, A6, B1 - W-NW Argues that the Farewell Fm does not outcrop in the northern Whanganui Inlet (cf. Bal 1992), i.e. lithofacies associations A4 - A7 are North Cape Fm.
Browne et al. (2008)	Peer reviewed article	Rakopi Fm	Description of the Rakopi Fm, its sedimentology, stratigraphy, petrography, and depositional environment Preliminary interpretation of basin-scale architecture of the Pakawau Group Assess Rakopi Fm source rock and reservoir potential	Description of two sections: Paturau River, and a forestry block west of Pakawau Lithofacies description Samples from sections for petrographic description; dinoflagellate assemblage	Rakopi Fm interpreted as fluvial channel sandstones and overbank deposits. Minor marine influence suggested by presence of glauconite, dinoflagellate cysts, and elevated sulfur content in coal. This suggests overall depositional environment was a low-gradient coastal plain with periodic marine transgression.
Higgs et al. (2010)	Peer reviewed article	Rakopi Fm, North Cape Fm	Assess reservoir potential of Pakawau Group	Three measured sections in the Whanganui Inlet Description of lithofacies and lithofacies associations 42 samples from Whanganui Inlet outcrop, offshore petroleum wells, and Browne et al. (2008)	Best reservoir facies is A1 (shoreface and intertidal estuarine paralic deposits) High spatial variability in reservoir quality Suggests discontinuation of the Puponga Mbr, as coals are present throughout the North Cape Fm on a regional scale.
Joyce (2018)	MSc thesis	North Cape Fm	High detail lithofacies analysis and paleogeographic models of North Cape Fm in northwest Nelson Use northwest Nelson outcrops to investigate reservoir potential of North Cape Fm	High detail sections and outcrop descriptions in the Whanganui Inlet Petrophysical measurements of samples (thin section porosity, porosity and permeability measurements)	North Cape Fm in the southern Whanganui Inlet was sheltered estuarine tidal embayment with salt marshes, distributary channels. Bay-head fan delta in the northern Whanganui Inlet. North Cape Fm has good quality hydrocarbon reservoirs especially conglomeritic and cross-bedded/wavy bedded sandstones.

The Otimataura Conglomerate is found locally at the base of the Rakopi Formation, both in northwest Nelson outcrops (Fig. 2.3) and in wells (for example, Cape Farewell-1). The Otimataura Conglomerate is up to 300m thick on the east side of the Burnett Ranges in the Otimataura Creek and Coal Creek area, but thins to around 60m in Marble Creek, and 36m in the Paturau River (Wizevich 1994; Browne et al. 2008). Where the Otimataura Conglomerate is thickest in the Otimataura Creek and Coal Creek area, it consists of cobble-sized clasts of basement lithologies, generally rounded but with some angular clasts (Wizevich 1994). In this area, there is a basal unit up to 30m thick of maroon-coloured breccias, sandstones and conglomerates. In the Paturau River area, the Otimataura Conglomerate is pebbly, and has interbedded sandstones, mudstones and coals at the base (Wizevich 1994; Browne et al. 2008).

In seismic sections, the Rakopi Formation is characterised by hummocky, high-amplitude, discontinuous reflectors (Fig. 2.6) (Thrasher 1992; King and Thrasher 1996; Browne et al. 2008). In gamma and spontaneous potential wireline well logs the Rakopi Formation shows heterolithic, interbedded, fining upwards cycles (Fig. 2.6) (King and Thrasher 1996; Browne et al. 2008). The Rakopi Formation is continuous through much of the Taranaki Basin.

Movement on the Wakamarama and associated Kahurangi faults strongly controlled the deposition of the Rakopi Formation. The Otimataura Conglomerate, at the base of the Rakopi Formation, is interpreted as alluvial fan deposits proximal to the active fault scarps of the Wakamarama and Kahurangi faults (Thrasher 1992; Wizevich 1994). The Rakopi Formation is interpreted as meandering stream, overbank, and swamp deposits formed on a coastal plain (King and Thrasher 1996). It thickens towards the Wakamarama Fault, indicating that the fault was locally controlling subsidence.

In older literature, the Rakopi Formation is considered entirely terrestrial (Titheridge 1977; Thrasher 1992; King and Thrasher 1996). However, recent work by Browne et al. (2008) has shown that at least some marine influence is likely, as evidenced by the presence of dinoflagellates, glauconite, and elevated sulfur content in Rakopi coals. This could be explained by periodic marine transgressions over a low-gradient coastal plain from minor sea-level fluctuations.

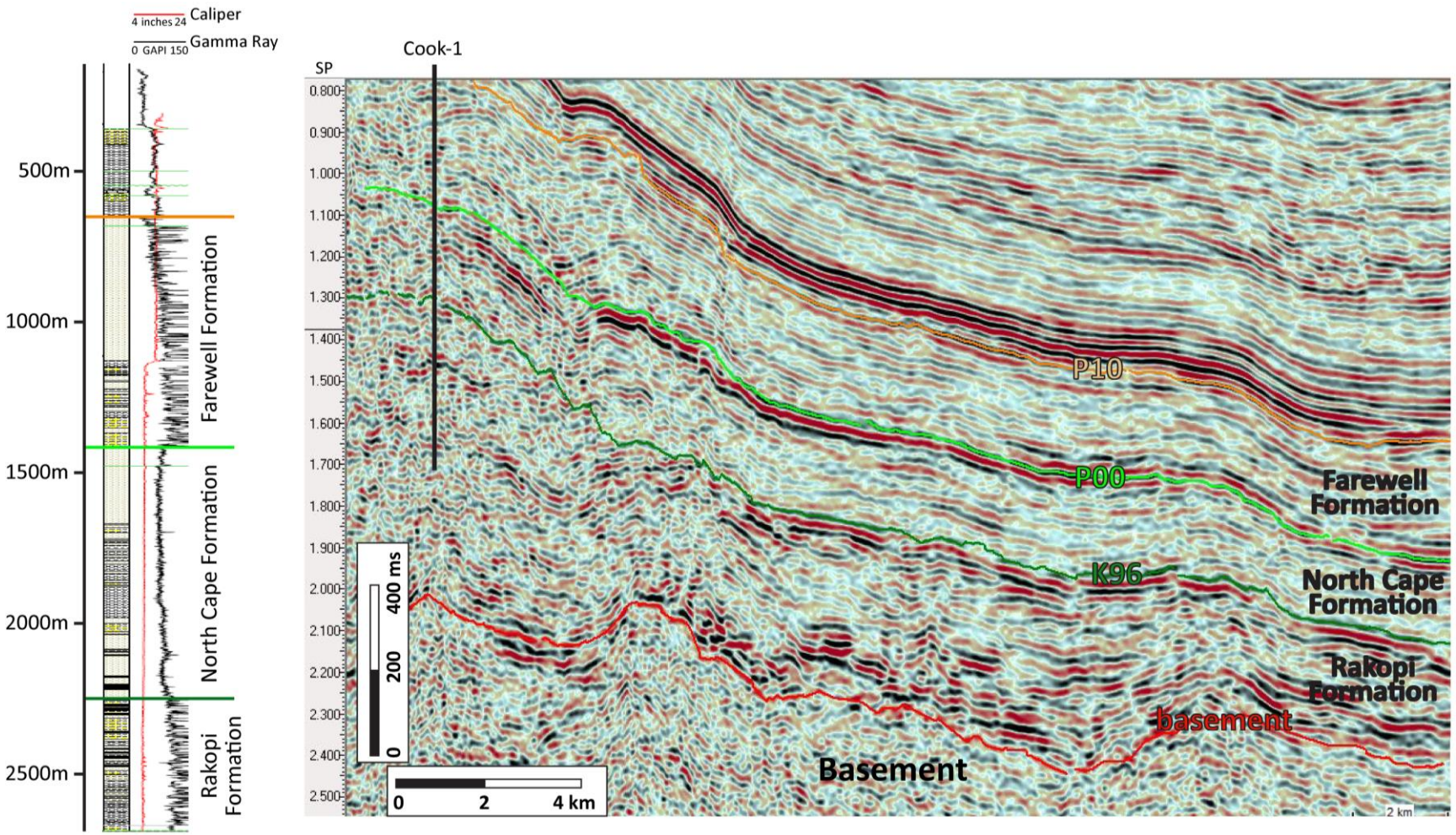

Fig. 2.6. Example of seismic reflection character and well gamma log of the Rakopi, North Cape, and Farewell formations. Well log from Cook-1 (Roncaglia et al. 2013), seismic line is CS-06, shown on Fig. 1.2. Seismic interpretation from Bull et al. (2016).

2.3.3 North Cape Formation sedimentology and depositional environment

The contact between the Rakopi and North Cape formations marks a transition from the terrestrial-dominated Rakopi Formation to the shallow-marine dominated North Cape Formation (King and Thrasher 1996; Rattenbury et al. 1998). The contact is predominantly conformable, aside from in some offshore seismic sections where the Rakopi Formation is truncated by the North Cape in a minor unconformity (Thrasher 1992; King and Thrasher 1996).

The North Cape Formation is a succession of sandstones interbedded with siltstones, minor conglomerates, and rare coal seams (Thrasher 1992; Rattenbury et al. 1998). Thrasher (1992) differentiates the coal-bearing Puponga Member near the top of the North Cape Formation from the rest of the North Cape Formation. However, Higgs et al. (2010) describe coal measures occurring throughout the North Cape Formation and suggest discontinuation of the Puponga Member nomenclature (Fig. 2.5).

The seismic character of the North Cape Formation is distinct from that of the Rakopi Formation. It typically has more uniform, parallel-layered, and lower amplitude reflections (Fig. 2.6) (Thrasher 1992; King and Thrasher 1996; Browne et al. 2008). Locally, coaly facies of the North Cape Formation exhibit higher amplitude, more discontinuous reflectors. In well logs the North Cape Formation is more uniform, in contrast to the Rakopi Formation (Fig. 2.6) (Browne et al. 2008).

Earlier workers such as Ongley and Macpherson (1923) interpreted the North Cape Formation as “estuarine”, however Titheridge (1977) argued that the North Cape Formation was a non-marine braided river and overbank succession. Based on sedimentary structures such as ripple cross-laminations and herringbone cross-beds, and the presence of marine dinoflagellates, the North-Cape Formation has since been re-interpreted as marine and marginal marine (Thrasher 1992; Wizevich et al. 1992).

In the Whanganui Inlet, the North Cape Formation is dominantly fluvio-estuarine, with deltas fed from the Wakamarama Fault and from the southwest. There are three main depositional environments represented: delta plain distributary channels; a tidally dominated delta front; and the sub-tidal delta front (Higgs et al. 2010; Joyce 2018). In the Fresne-1 well, immediately adjacent to the Wakamarama Fault scarp, a 900m thick conglomeratic sequence (the Fresne

Conglomerate Member) is present at the base of the North Cape Formation (Thrasher 1992; King and Thrasher 1996). Thrasher (1992) suggests that Fresne-1 was drilled at or near the apex of a fan delta. A second fan delta had an apex near Puponga, resulting in conglomeratic facies in the northern part of the Whanganui Inlet outcrop.

2.3.4 Farewell Formation sedimentology and depositional environment

The Teurian to Waipawan (Paleocene) Farewell Formation is a succession of interbedded quartzofeldspathic sandstones, siltstones, pebbly sandstones, conglomerates, and coals (King and Thrasher 1996; Stark 1996; Rattenbury et al. 1998). The Farewell Formation is interpreted as a floodplain environment with braided to meandering rivers (King and Thrasher 1996; Stark 1996; Rattenbury et al. 1998). In seismic reflection profiles the Farewell Formation has a bland signature, with continuous to semi-continuous reflectors separated by high amplitude reflectors (Fig. 2.6) (Bull et al. 2016).

By the start of Farewell Formation deposition (~65 Ma), movement on the Wakamarama Fault is inferred to have slowed significantly based on displacement backstripping of seismic profiles (Reilly et al. 2015). The paleocurrent of the Farewell Formation is dominantly north to northeast, parallel to the Wakamarama Fault (Bal and Lewis 1994; Stark 1996), indicating that the river system was still constrained by the graben. There is no evidence for significant fans draining the Wakamarama Fault, suggesting little or no uplift along the fault (Stark 1996).

The North Cape Formation - Farewell Formation contact is poorly constrained. It is generally taken as the K-T boundary, to correlate with the top Cretaceous seismic reflection horizon observed in offshore seismic profiles (Thrasher 1992). However, at Moki Point and the Whanganui Inlet entrance, the palynomorph assemblage indicates that both the North Cape and the Farewell Formation are Early Paleocene (Bal 1994), suggesting that the contact may not coincide exactly with the K-T boundary.

The location of the contact in outcrop is also contested. Bal and Lewis (1994) and Bal (1994) defined the contact in the northern Whanganui Inlet based on a change in lithofacies, from interbedded sandstones, mudstones, and coal seams, to thick sandstones with minor gravel, coal, and mudstone. In contrast, Stark (1996) argues that the Farewell Formation does not outcrop around the northern and northwest Whanganui Inlet, on the basis that the Farewell

Formation imaged in seismic surveys offshore of the region is much thinner than the onshore equivalent.

The contact between the North Cape and Farewell formations is unconformable and erosional (Bal 1994). The contact records a marine regression across much of the southern Taranaki Basin, as the depositional environment changed from coastal plain, estuarine, and marginal marine in the North Cape Formation to fluvial in the Farewell Formation. The reason for this regression is not well understood (Thrasher 1992). It may have occurred as a result of dramatic increase in sediment supply, or due to slowing subsidence rates decreasing accommodation space. Bal (1994) suggests that the erosion and subsequent marine regression may have been related to the changing tectonic regime at the cessation of Tasman Sea spreading.

2.3.5 Eocene to Miocene sedimentary succession and depositional environment

In the northwest Nelson region, the Farewell Formation is separated from overlying units by a significant regional unconformity spanning the late Waipawan into at least the Bortonian (Early to Middle Eocene) (King and Thrasher 1996; Rattenbury et al. 1998). The contact is well exposed at Puponga Point (Fig. 2.3). The Farewell Formation is overlain by a glauconitic sandstone, the Matapo Sandstone Member of the Otaraoa Formation. The Matapo Member is overlain by calcareous siltstones and sandstones of the Abel Head Formation, which is overlain by the early Waitakian (Oligocene) Takaka Limestone, a lateral correlative of the Tikorangi Formation in the central part of the Taranaki Basin.

The depositional hiatus during the Eocene is likely to represent tectonic quiescence and peneplanation after the cessation of rifting (King and Thrasher 1996). The top of the Farewell Formation exposed at Puponga Point is deeply weathered, probably a result of sub-aerial exposure and leaching. The unconformity may also be related to uplift associated with the opening of the Emerald Sea Basin at ~45 Ma (King and Thrasher 1996). The Ngatoro Group are the passive margin shelf and slope deposits related to a phase of subsidence and marine transgression.

The Wai-iti Group in northwest Nelson is Waitakian to Altonian in age, and is dominated by siliciclastic sedimentary units (Bishop 1971; King and Thrasher 1996). The group includes the

Kaipuke Siltstone and the Tarakohe Mudstone. Sedimentary rocks younger than Altonian, aside from surficial Quaternary deposits, are absent.

Compression along the Pacific-Australian plate boundary began in the Early Miocene (King and Thrasher 1996). This resulted in an influx of siliciclastic sediments and the deposition of the Wai-iti Group. Continued uplift meant that deposition ceased in the northwest Nelson region.

2.4 Basement geology

An understanding of the basement lithologies is crucial for reconstructing sedimentary provenance, as the basement lithologies are the source material for the younger sedimentary rocks. The basement of the southern Taranaki Basin and northwest Nelson region is highly varied but is relatively well-known, especially from outcrops (Figs. 2.7, 2.8).

The basement of New Zealand is generally defined as the lithologies older than mid-Cretaceous (Mortimer 2004; Mortimer et al. 2014), which is grouped into the Austral Superprovince by Mortimer et al. (2014). The Austral Superprovince is further divided into three main sedimentary, plutonic, and metamorphic basement provinces (Western and Eastern Province and the Median Batholith), which comprise seven, fault-bounded terranes. The igneous intrusions older than mid-Cretaceous that intrude the Western Province, including most of the Median Batholith, are grouped by Mortimer et al. (2014) into the Tuhua Intrusives.

For much of the Paleozoic and Mesozoic, until the middle of the Cretaceous, Zealandia was part of the subduction zone on the margin of Gondwana (Mortimer 2004). The Austral Superprovince are the volcano-sedimentary rocks accreted to the Gondwana margin over this time with associated metamorphics. The Tuhua Intrusives which intrude the Austral Superprovince are typically associated with the subduction margin. Complex faulting, folding, and regional metamorphism in the basement reflects the compressional tectonic regime.

2.4.1 Western Province - Buller Terrane

The Buller Terrane occurs in the western portion of northwest Nelson, west of the Anatoki Fault, and comprises sedimentary and metamorphic rocks of Late Cambrian to Silurian age

(Figs. 2.7, 2.8) (Rattenbury et al. 1998). Most of the succession is made up of over 5000 m of the Greenland Group, which are quartz-muscovite sandstone, siltstone, and mudstone turbidite units (Laird 1972; Cooper 1989; Roser et al. 1996; Rattenbury et al. 1998). In the Wakamarama Range in northwest Nelson, the Greenland Group is conformably overlain by the Golden Bay Group. The Golden Bay Group includes the Aorangi Mine Formation, a quartzite, quartz sandstone, and black siliceous shale with minor chert; the Leslie and Slaty Creek formations, a turbidite quartz sandstone, siltstone, and black shale; and the Douglas and Peel formations, fine-grained sandstones and quartzite (Fig. 2.7) (Harrison 1993; Rattenbury et al. 1998).

In some regions the Golden Bay Group has been metamorphosed to the Bay schist (Stallard 1994; Rattenbury et al. 1998). In the Mount Olympus and Aorere Valleys areas the Bay Schist is a dark quartz, muscovite, chlorite and quartz-biotite pelitic schist (Fig. 2.8). South of Knuckle Hill the Bay Schist is a quartz-muscovite-chlorite and quartz-biotite schist.

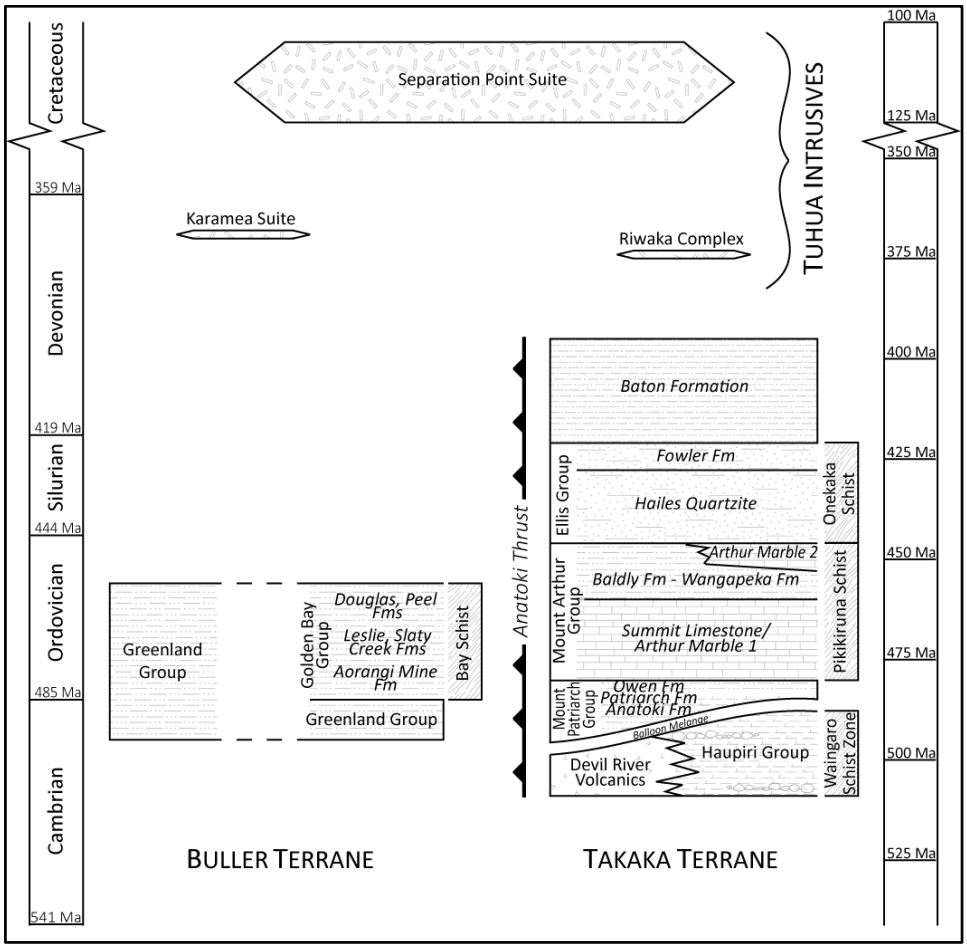

Fig. 2.7: Summary of Western Province stratigraphy and ages for the northwest Nelson region. Summarised from Rattenbury et al. (1998), Mortimer *et al. (2014); ages from Rattenbury et al. (1998), Turnbull et al. (2013), Turnbull et al. (2017).*

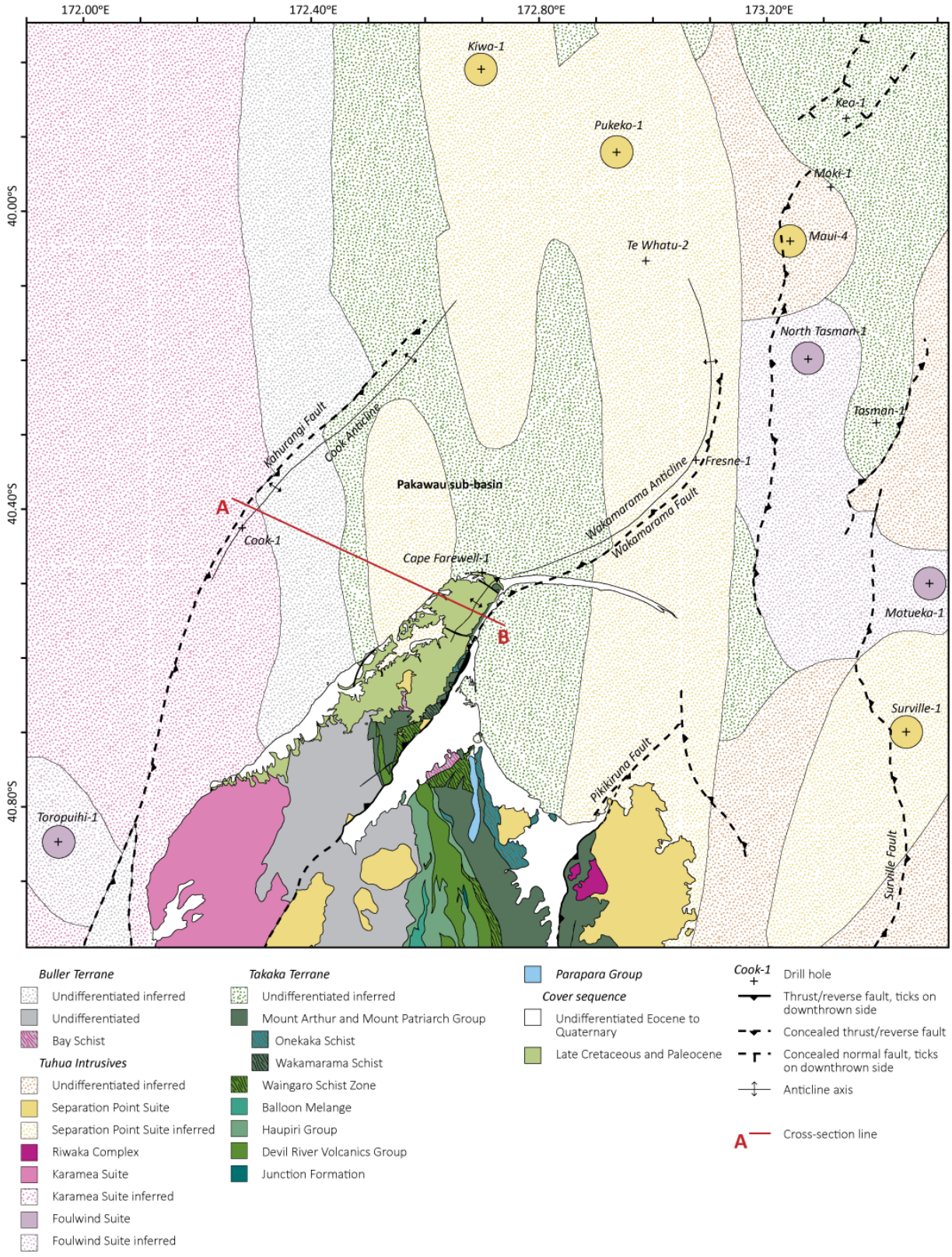

Fig. 2.8: Geological map of the southern Taranaki Basin, showing key basement lithologies and structures. Cross-section line for Fig. 2.4 is shown. Coordinates are in WGS84. Onshore geology modified from Rattenbury et al. (1998), offshore geology modified from Tulloch and Mortimer (2017), structure from King and Thrasher (1996).

2.4.2 Western Province - Takaka Terrane

The Takaka Terrane is separated from the Buller Terrane by the Anatoki Thrust Fault (Mortimer 2004). The Takaka Terrane is significantly more geologically complex than the Buller Terrane, containing Cambrian to Early Devonian siliciclastic, carbonate, and volcanic rocks (Fig. 2.7). The Takaka Terrane has undergone significant folding and faulting. The stratigraphy of the Takaka Terrane is present in discrete thrust fault slices, juxtaposing parts of the succession (Rattenbury et al. 1998).

The Junction Formation is the oldest unit in the Takaka Terrane (Rattenbury et al. 1998). It is composed of turbiditic sandstone, siltstones, and debris flow conglomerates. On the basis of trilobite fossils the Junction Formation is estimated to be of Middle Cambrian age (Rattenbury et al. 1998).

The Middle to Late Cambrian Haupiri Group sedimentary rocks and the Devil River Volcanics are interpreted as a volcanic arc sequence (Cooper 1989; Rattenbury et al. 1998; Münker and Cooper 1999). The Haupiri Group sedimentary units comprise non-volcanic to volcanic and tuffaceous sandstones and siltstones, cherts, carbonates, and conglomerates. Conglomerate clasts include chert, volcanic and non-volcanic sandstones, carbonates, clasts of the Junction Formation, and volcanic and plutonic clasts likely derived from the Devil River Volcanics. The Haupiri Group is interpreted as back-arc or intra-arc basin fill (Münker and Cooper 1999).

Interfingered with the Haupiri Group are the Middle Cambrian to earliest Ordovician Devil River Volcanics Group (Cooper and Tulloch 1992; Rattenbury et al. 1998; Münker and Cooper 1999). The Devil River Volcanics comprise three volcanogenic formations: the Benson Volcanics (dominantly basaltic to basaltic-andesitic with some andesite, dacite, and rhyolite), the Mataki Volcanics (tholeiitic basalt), and the Cobb Igneous Complex (gabbro, serpentinised peridotite and websterite) (Rattenbury et al. 1998; Münker and Cooper 1999). Each of these formations is further subdivided into volcanic suites.

The Balloon Melange is a zone of deformation, with blocks of Junction Formation, Devil River Volcanics, and Haupiri Group (Rattenbury et al. 1998; Münker and Cooper 1999). Clast ages suggest that the melange formed in the Late Cambrian. Melange formation was followed by a significant tectonic episode, which resulted in folding, thrust development and formation of the greenschist facies Waingaro Schist zone (Cooper and Tulloch 1992).

In the Late Cambrian to Devonian a sedimentary passive margin succession was deposited (Rattenbury et al. 1998). The oldest group in this succession is the Late Cambrian to Early Ordovician Mount Patriarch Group (Wright et al. 1994). This group contains the quartz-mica sandstones, volcaniclastic sandstones, and granule conglomerates of the Anatoki Formation, which grades up into the calcareous siltstone, carbonaceous limestone, and carbonaceous shale of the Patriarch Formation and the limestone, calcareous sandstone, and more quartzose sandstone and siltstone of the Owen Formation.

The Mount Patriarch Group is overlain by the Mount Arthur Group, which is Late Cambrian to Early Devonian in age (Roser et al. 1996; Rattenbury et al. 1998). This group marks the start of significant carbonate sedimentation. The basal unit contains the limestones, calcareous mudstone and sandstone, and minor dolomite bands of the Summit Limestone of the Arthur Marble 1. This is overlain by either the siliceous siltstone, quartz sandstone, calcareous siltstone, and local carbonaceous shale and limestone of the Baldly Formation and laterally equivalent Wangapeka Formation; or by the black limestone and calcareous mudstone of the Arthur Marble 2.

The Mount Arthur Group is overlain by the Middle to Late Silurian Ellis Group, which contains quartz sandstone, quartzite and siliceous siltstone (Grindley 1980; Roser et al. 1996; Rattenbury et al. 1998). This may grade conformably into the Baton Formation, the youngest unit of the Takaka Terrane. The Early Devonian Baton Formation is only present in the southeast of the Nelson region. It contains mudstone, fine-grained sandstone, and minor limestone and conglomerate.

The Ellis Group is locally metamorphosed to the Onekaka Schist (Bishop 1971; Rattenbury et al. 1998). This unit includes thick-bedded quartzite, metavolcanics, and siliceous quartz±albite/oligoclase-biotite-muscovite schist.

2.4.3 Western Province – Tuhua Intrusives

The Tuhua Intrusives are all Cambrian to Early Cretaceous plutonic and hypabyssal rocks that intrude the Western Province Takaka and Buller terranes (Mortimer et al. 2014). In northwest Nelson, they include the Karamea Suite, Riwaka Complex, and Separation Point Suite (Fig. 2.7).

The Buller Terrane was intruded during the Late Devonian by the Karamea Suite, a series of S-type, alkali granites (Mortimer et al. 1997). The Karamea Suite was emplaced between 370 and 368 Ma (Turnbull et al. 2013).

The Takaka Terrane was intruded at c. 364 Ma (Late Devonian) by the Riwaka Complex (Turnbull et al. 2017). This is an ultramafic to intermediate suite of plutonic rocks, including peridotite, pyroxenite, gabbro, diorite, and monzodiorite with associated Ni-Cu-platinum group element sulphide mineralisation (Turnbull et al. 2017).

The Median Batholith intrudes the Takaka Terrane. It is composed of a range of Devonian to Early Cretaceous, I-type, subalkaline, gabbros to granites (Mortimer 2004). The Early Cretaceous Separation Point Suite is particularly important in northwest Nelson. It is not confined to the fault-bounded zone between the Eastern and Western Provinces, but also occurs in isolated intrusions in the Takaka Terrane, such as at Knuckle Hill (Fig. 2.3) (Tulloch and Rabone 1993; Rattenbury et al. 1998). The age of Separation Point Suite intrusives typically ranges between 125 and 105 Ma (Mortimer et al. 1999). At Knuckle Hill, the Separation Point Suite has been dated at 105 ± 1 Ma using uranium-lead zircon dating (Tulloch 2017 personal communication).

2.5 Previous provenance studies

The provenance of the northwest Nelson Pakawau Group and Farewell Formation is not well understood due to a lack of detailed provenance studies of the outcrops (Table 2.2). The available literature points to a mixture of sources from the above sedimentary, metamorphic, plutonic, and volcanic basement lithologies (Stark 1996; Higgs et al. 2010). Many studies used small sample sets, sometimes less than ten (Wizevich 1992; Browne et al. 2008) and up to thirty at the most (Titheridge 1977; Stark 1996). Higgs et al. (2010) had more samples (52 in addition to six from the Browne et al. (2008) study), many of which were from offshore wells. There are discrepancies between these publications, possibly due to the small sample sets.

2.5.1 Pakawau Group provenance

Pakawau Group sandstones are generally feldsarenites, lithic feldsarenites, and feldspathic litharenites, following the nomenclature of Folk et al. (1970) (Fig. 2.9) (Wizevich 1992; Stark

1996; Browne et al. 2008; Higgs et al. 2010). However, according to Titheridge (1977) Pakawau Group and Kapuni Group samples are much more quartz-rich, classified as feldsarenites and subfeldsarenites (Fig. 2.9). This discrepancy may be because Titheridge (1977) used a visual estimate of composition rather than point counting.

Lithic fragments in the Pakawau Group include metamorphic, sedimentary, plutonic, and volcanic lithics (Titheridge 1977; Wizevich 1992; Stark 1996; Higgs et al. 2010). Conglomerate clasts also range in composition, including metasedimentary clasts, schists, vein quartz, quartzite, granite, volcanics, gneiss, and syn-sedimentary mudstone and siltstone (Titheridge 1977; Wizevich 1994). The variation in lithic composition reflects the wide variety of different source rocks in the basement, as well as reworking of basin sediments.

In the Rakopi Formation, Browne et al. (2008) found that the samples from the Paturau River in the southern part of the region are litharenites, whereas samples taken from further north in a forestry block near Pakawau are predominantly lithic feldsarenites (Fig. 2.9). These spatial trends could reflect changing source areas. Browne et al. (2008) suggest that the litharenites are from a metamorphic source such as the Takaka Terrane, and the lithic feldsarenites from a granitic source such as the Karamea Suite or the Separation Point Granite. From detrital zircon analysis, Adams et al. (2017) found that the Rakopi Formation in the Paturau River has dominantly Early Cretaceous Separation Point Suite/Median Batholith zircons, with minor Carboniferous Karamea Suite zircons, and recycled zircons from Buller and/or Takaka Terrane sedimentary rocks. There are also two very young 81 ± 2 and 84 ± 2 Ma zircons, possibly from rift-related magmatism.

In the North Cape Formation some spatial trends are apparent. Stark (1996) found that the total sandstone lithic content increased from the Paturau River, northeast to the Whanganui Inlet entrance and to the Moki Point South section, and then decreased further northeast towards Moki Point. Stark (1996) also found that lithic compositions varied, with North Cape Formation sandstones at the Paturau River containing fine-grained, highly altered volcanics, compared to sedimentary lithics in the rest of the unit.

There is conflicting evidence for temporal changes through the Pakawau Group. Wizevich (1992) found that from the base of the Pakawau Group to the top, the feldspar content of the sandstones increases while lithics decreases. He attributes this to erosion of a

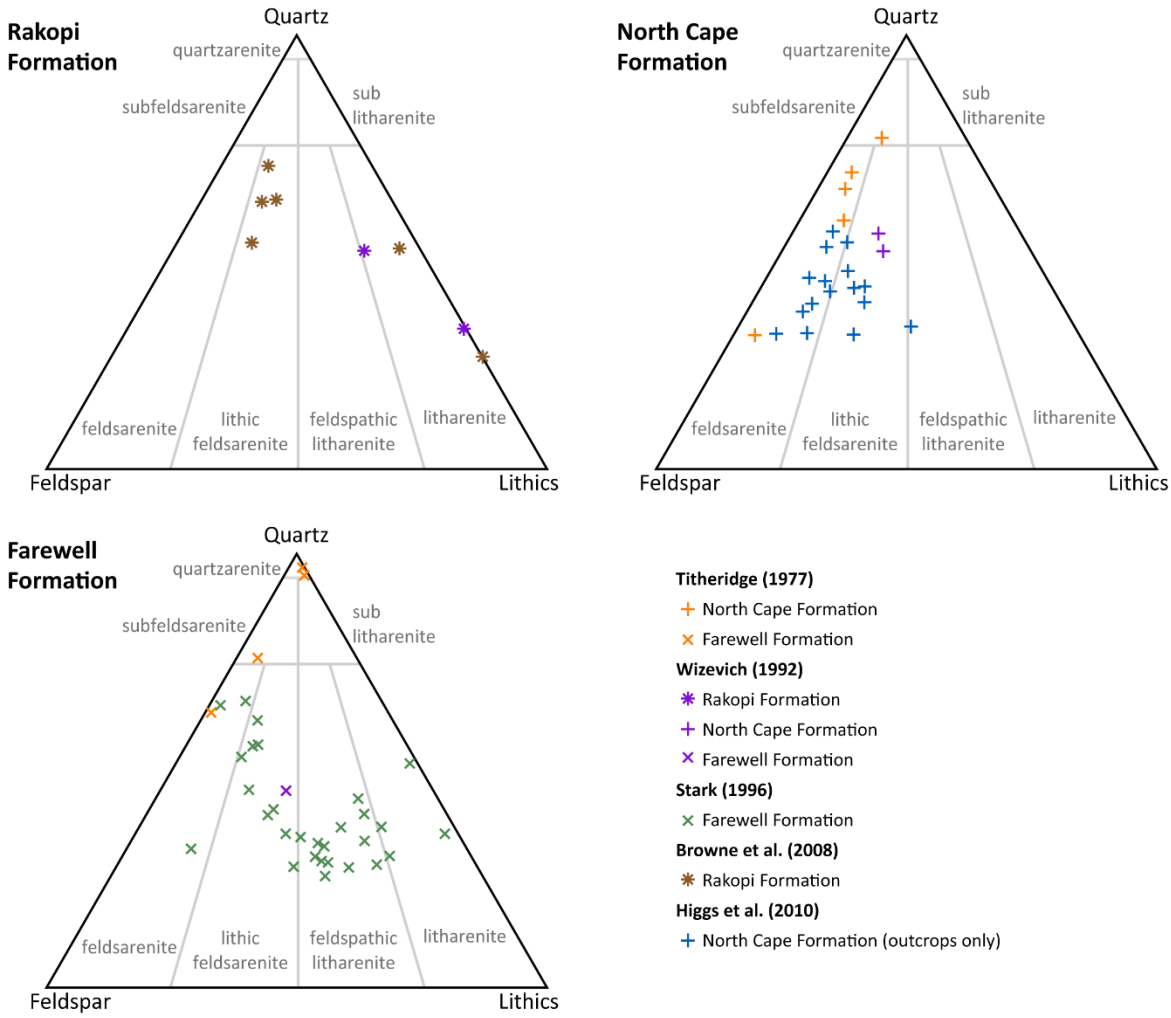

Fig. 2.9: Rakopi, North Cape, and Farewell Formation sandstone composition in northwest Nelson, from previous provenance studies. Ternary diagram after Folk et al. (1970).

metasedimentary source and unroofing of granites. However, other authors found no strong temporal trends (Browne et al. 2008).

Offshore wells close to northwest Nelson have a similar composition and provenance to onshore outcrops (Smale 1996). Further offshore the Pakawau Group is dominated by granitic sources, likely from the widespread Separation Point Suite (Smale 1996; Adams et al. 2017). The Pakawau Group is influenced by a low-grade metamorphic source in Surville-1 and Cook-1, as well as further north in Maui-1 and North Tasman-1. Acidic and basic volcanic detritus is also found in Fresne-1, Surville-1 and Cape Farewell-1, possibly sourced from the Devil River Volcanics in the Takaka Terrane. The influence of the Devil River Volcanics from northwest Nelson may extend as far north as Ariki-1 and Tangaroa-1 in the North Taranaki Bight.

No detailed study of the provenance or composition of the Otimataura Conglomerate has been published. Wizevich (1992; 1994) reported that the sandstones interbedded with the

conglomerate are metamorphic litharenites (Fig. 2.9), and the clasts themselves are dominated by green micaceous schist and phyllite with some green volcanic sandstone, vein quartz, and granite. These observations were made at outcrops in the Coal Creek area on the east side of the Wakamarama Ranges, so the likely source material are adjacent basement schists. Wizevich (1994) notes an upwards decrease in schist and phyllite conglomerate clasts, and an increase in rounded quartz clasts. A possible equivalent to the Otimataura Conglomerate in Cape Farewell-1 ("Riley's Conglomerate") is composed of pebbles and granules of sandstone, quartzite, vein quartz, glauconitic sandstone, coal, siltstone, and minor metamorphics (Carter and Kintanar 1987).

2.5.2 Farewell Formation provenance

The Farewell Formation is typically described as more quartzose than the Pakawau Group due to the lighter colour of the outcrops (Ongley and Macpherson 1923; Suggate 1956). Stark (1996) found that Farewell Formation sandstones are dominantly lithic feldsarenites and feldspathic litharenites (Fig. 2.9). Titheridge (1977) found that Farewell Formation sandstones are dominantly feldsarenites and subfeldsarenites, with quartzarenites at the top of the unit (Fig. 2.9).

Conglomerates in the Farewell Formation have similar clast types to the North Cape Formation; they are dominated by metasedimentary clasts and vein quartz, with minor schists, chert, quartzite, granite, volcanics, and gneiss (Titheridge 1977; Stark 1996). Several authors have reported a temporal change in the Farewell Formation conglomerate composition. Titheridge (1977) found that there is a higher proportion of granitic and volcanic clasts in the lower North Cape Formation; fewer, more weathered granitic and volcanic clasts in the lower Farewell Formation; and no granitic or volcanic clasts in the upper Farewell Formation. Titheridge (1977) interpreted the increasing quartz content of the Farewell Formation as being a result of increased weathering and reworking of material. Similarly, Suggate (1956) found that in the Puponga area greywacke and granite clasts in the Farewell Formation are increasingly leached towards the top of the stratigraphy.

Table 2.2: Summary of significant literature dealing with the provenance of Late Cretaceous and Paleocene sedimentary rocks in the northwest Nelson area. For clarity, the naming scheme of Higgs et al. (2010) (see Fig. 2.5) has been used; square brackets indicate where older names have been substituted

Reference	Publication type	Units	Objectives	Methods	Key findings
Titheridge (1977)	MSc thesis	North Cape Fm, Farewell Fm	Description and interpretation of the Late Cretaceous to Oligocene strata based on stratigraphy, thickness and age of units, sedimentary structures, textures, and composition	Ten sandstone samples: thin sections stained for alkali feldspars and plagioclase, most sample compositions visually estimated, and calibrated with one sample with 300-400 point counts. "X-ray identification" of clay mineralogies Conglomerate composition counted volumetrically	Pakawau Group: sandstones are dominantly feldsarenites and subfeldsarenites Farewell Formation: sandstones dominantly feldsarenites and subfeldsarenites with some quartzarenites towards the top. Lithics dominantly micaceous and cherty mudstone and semischist, minor quartzarenite and chert, rare volcanics. Conglomerates in the Farewell and North Cape Fms dominated by quartz sandstone and vein quartz, with minor volcanics, granite, gneiss, schist, and subschist. Upward increase in clast weathering and decrease in proportion of volcanic and granite clasts.
Wizevich (1992)	Conference abstract	Otimataura Conglomerate, Rakopi Fm, North Cape Fm, Farewell Fm.	Description of Pakawau Group and Farewell Fm petrography, interpretation of provenance	Thin section and XRD analysis of five samples	Otimataura Conglomerate: sandstones are metamorphic litharenites Rakopi Fm: sandstones are litharenites, higher spatial and temporal variability North Cape and Farewell Fms: sandstones are lithic feldsarenites. Suggest unroofing of metasedimentary rocks and exposure of older granites.
Wizevich (1994)	Conference proceeding	Otimataura Conglomerate	Description of Late Cretaceous and Paleocene sedimentary rocks in the Pakawau sub-basin Interpretation of depositional setting and controls on sedimentation, related to the opening of the Tasman Sea	Description of outcrops in the Wakamarama and Burnett Ranges and Whanganui Inlet Review of published data, including Rakopi Bore	In the Coal Creek area, Otimataura Conglomerate clasts are dominantly green micaceous schist/phyllite with some green volcanic sandstone, vein quartz, and granite (“white with a few percent biotite”). Gradational composition changes with upward increase in rounded qz and decreasing schist/phyllite. Schist in underlying basement is suggested source.
Smale (1996)	Unpublished petroleum report	Pakawau Group, Kapuni Group	Summary of key conclusions of petroleum reports related to provenance and diagenesis in the Taranaki Basin	Review of petroleum reports, mostly studies of well cuttings and cores	Pakawau Group: in the Taranaki Bight are dominated by granites, likely Separation Point Suite. Near the South Island (Cook-1, Surville-1, Maui-1, North Tasman-1) influence from metamorphics, likely northwest Nelson metamorphic basement. Altered volcanics in Cape-Farewell-1, Fresne-1, Surville-1, and as far away as Ariki-1 and Tangaroa-1. Likely source is Takaka Terrane. Greywacke pebbles in North Tasman-1 either from Maitai Group or northwest Nelson. Kapuni Group: dominated by alkali granite, suggested Karamea Granite or mixed Karamea/Separation Point source. Volcanic (Kupe South field, Okoki-1, Awakino-1, Te Ranga-1) and metamorphic (Kupe South field, Maui-6, Okoki-1) detritus from suggested northwest Nelson source

Reference	Publication type	Units	Objectives	Methods	Key findings
Stark (1996)	Unpublished MSc thesis	North Cape Fm, Farewell Fm	Description of the Farewell Fm, its extent and lateral and vertical variation, and interpretation of depositional setting.	Twenty-eight sandstone samples from the North Cape (16) and Farewell (12) Fms. Clast counts of Farewell Formation conglomerates	Sandstones dominantly lithic feldsarenites and feldspathic litharenites. Increase in lithic fragments from the Paturau River north to Moki Point, then decrease towards Oyster Point. Conglomerates dominated by metasedimentary rocks, vein quartz, quartzite, granite, gneiss with minor chert, schist. No strong spatial or temporal trends. Lithics are dominantly sedimentary (quartzose siltstone, altered mudstone, chert), except for in the Farewell Fm at the Paturau River where they are highly altered, fine-grained volcanics. Minor metamorphic (undulose quartz, muscovite, biotite, minor albite)
Browne et al. (2008)	Peer reviewed article	Rakopi Fm	Description of the Rakopi Fm, its sedimentology, stratigraphy, petrography, and depositional environment Preliminary interpretation of basin-scale architecture of the Pakawau Group Assess Rakopi Fm source rock and reservoir potential	Five samples from two sections: Paturau River (two), and a forestry block west of Pakawau (three) Thin sections: blue-dyed resin, stained for K-feldspar with sodium cobaltinitrate, 300 point counts	Paturau River section: sandstones are litharenites with schist lithics, source is likely Takaka Terrane. Forestry block section: sandstones are quartz-rich lithic feldsarenites, source is likely Buller Terrane and Karamea Suite granites OR Separation Point Suite granites.
Higgs et al. (2010)	Peer reviewed article	Rakopi Fm, North Cape Fm	Assess reservoir potential of the Pakawau Group	42 samples from Whanganui Inlet outcrop, offshore petroleum wells, and Browne et al. (2008) Thin sections: blue-dyed resin, stained for K-feldspar with sodium cobaltinitrate, and carbonates with alizarin red and potassium ferricyanide, 300 point counts	Pakawau Group sandstones are dominantly feldsarenites or lithic feldsarenites with rare feldspathic litharenites and litharenites. No temporal trends or strong difference between the Rakopi and North Cape Fms, but some spatial variation Likely source rocks include Separation Point Suite and Karamea Suite granitoids, Median Batholith granodiorites or gabbros, Takaka Terrane metamorphics, Brook Street Terrane Diagenetic features suggest burial of >3km.

Lithic fragments in the Farewell Formation are dominated by sedimentary fragments, particularly quartz rich siltstones and fine sandstones, and minor chert (Titheridge 1977; Stark 1996). There are also minor metamorphic and volcanic lithics.

In offshore wells, the Kapuni Group provenance is dominated by an alkali granite source, predominantly Karamea Suite-type granites, with Separation Point influence in some areas (Smale 1996). Northwest Nelson sources are still important; a low-grade metamorphic influence is present as far north as New Plymouth (Okoki-1, Maui-6). Acidic to intermediate volcanic detritus is found in wells in the northern Taranaki Basin (Okoki-1, Te Ranga-1 and Awakino-1).

2.6 Conclusion

The Taranaki Basin developed in the Late Cretaceous as Zealandia rifted from Gondwana. Extension in the Taranaki Basin occurred in two phases: the Zealandia Rift (105 – 83 Ma) followed by a short phase of uplift and erosion (83 – 80 Ma), and then the West Coast-Taranaki Rift (80 – 55 Ma). During the second phase of rifting the Pakawau sub-basin developed in northwest Nelson. The Pakawau sub-basin is a northeast striking graben bound by the Wakamarama Fault to the southeast and the Kahurangi Fault to the northwest. These faults were inverted in the Miocene, and the graben fill was uplifted and folded into the Wakamarama and Cook anticlines.

Through the Late Cretaceous and Paleocene the Pakawau sub-basin was a major depocentre. The oldest unit is the Late Cretaceous Rakopi Formation, which rests unconformably on basement. The Rakopi Formation contains interbedded sandstone, carbonaceous mudstone, siltstone, coal, and minor conglomerate interpreted as meandering stream, overbank, and swamp deposits formed on a coastal plain. Locally at the base of the Rakopi Formation is the Otimataura Conglomerate member: conglomerates, breccias, and sandstones interpreted as alluvial fans fed from the Wakamarama and Kahurangi faults.

The Late Cretaceous North Cape Formation conformably overlies the Rakopi Formation. The North Cape Formation comprises sandstones interbedded with siltstones, minor conglomerates, and rare coal seams. In northwest Nelson, it is interpreted as fluvio-estuarine.

Fan-deltas were fed from the Wakamarama Fault into a tidally-dominated shallow marine embayment.

The North Cape Formation is unconformably overlain by the Paleocene Farewell Formation. The Farewell Formation is a succession of interbedded sandstones, conglomerates, siltstones, and rare coal. It is interpreted as entirely fluvial, with both meandering and braided fluvial styles.

The Pakawau Group Rakopi and North Cape formations and the Farewell Formation in northwest Nelson have a mixed provenance of Western Provence basement lithologies, although this not been studied in detail. Possible basement sources include the quartzose sedimentary rocks of the Buller Terrane Greenland Group and Golden Bay Group; the metamorphosed volcanics of the Takaka Terrane Devil River Volcanics; carbonate and siliciclastic sedimentary units of the younger Takaka Terrane; and the Tuhua Intrusives Riwaka Complex, Karamea Suite, and Separation Point Suite granitoids.

3. SEDIMENTOLOGY

3.1 Introduction

This chapter provides a description of the sedimentology and depositional interpretation for the Rakopi, North Cape, and Farewell formations. The sedimentology is used to reconstruct paleogeography, which in a provenance context is useful for understanding the sediment transport pathways. The environment in which sediments are transported and deposited can also change their overall composition through processes such as chemical weathering, abrasion and mechanical breakdown, sorting, and mixing (Garzanti 1986; Macaire 1986; Savage et al. 1988; Johnsson 1993).

This chapter will describe the range of lithofacies present in the sampled formations. These will be grouped into lithofacies associations, which are groups of lithofacies that commonly occur together leading to an interpretation of depositional environment. The lithofacies associations will be used in this project as the environmental context for the composition data for samples.

3.2 Fieldwork methods

3.2.1 Outcrop location and quality

Outcrops of the Rakopi Formation are rare and of poor quality due to its fine-grained nature. There are good outcrops along the Paturau River and on Pakawau Bush Road (Fig. 2.3) as described by Browne et al. (2008). The Kaituna Route walking track has patchy, highly weathered outcrop. Outcrops of the Otimataura Conglomerate, a basal coarse-grained unit of the Rakopi Formation (Bishop 1971; Wizevich 1994; Browne et al. 2008) are invariably difficult to access. It outcrops in steep cliffs on the east side of the Burnett Range adjacent to (west of) the Wakamarama Fault in Coal Creek, Otimataura Creek, and Marble Creek. There is also outcrop at the stratigraphic base of the Paturau River section (Figs. 2.3, 3.1E), at the confluence of Thompson Creek with Paturau River, although this outcrop is surrounded by deep water of the Paturau River (Fig. 3.1E).

Well exposed outcrops of the North Cape Formation are found in coastal shore platforms and cliffs typically less than 5m high around the Whanganui Inlet. There are also road cuttings along Dry Road, although the generally weathered nature and discontinuity of these outcrops makes it difficult to distinguish the Rakopi Formation from the North Cape Formation.

The Farewell Formation is exposed in high (>10m) coastal cliffs around the north-western side of the Whanganui Inlet, and a contact with the underlying North Cape Formation at Oyster Point and Moki Point (Fig. 2.3). The Farewell Formation also has good exposure in steep coastal cliffs around Cape Farewell, for example at Whahariki Beach and Green Hills Beach (Fig. 2.3). The top contact with the Matapo Sandstone Member (Otaraoa Formation) is exposed around Puponga Point (also called Abel Head). The type section for the Farewell Formation is along the Pillar Point walking track, where outcrops typically less than two metres high are exposed in small road cuttings.

3.2.2 Outcrop description and measured sections

Sections were measured by tape measure and compass traverses to a decimetre scale, aided by handheld GPS coordinates (GPS unit: Garmin GPSMAP 64). A rangefinder (rangefinder unit: Nikon “Forestry Pro”) was used to measure heights of cliffs and distances traversed across obscured parts of the section, which was used to calculate the stratigraphic thickness obscured.

In locations where good quality sections had already been measured and published (for example Browne et al. 2008 their Fig. 6 and Higgs et al. 2010 their Fig.4), laminated copies of these sections were taken into the field and annotated with additional data, including sample locations, GPS coordinates, paleoflow measurements, and bedding orientation.

Paleoflow measurements were taken from trough cross beds and tabular cross beds with three-dimensional exposure and amplitudes greater than 0.1m. Parting lineations and groove mark orientations were also measured. The paleoflow measurements were rotated to horizontal using a stereonet.

3.3 Lithofacies of the Rakopi Formation

Browne et al. (2008) described the lithofacies of the Rakopi Formation in detail, based on a section in the Paturau River, and in freshly exposed (at the time) outcrop in a forestry block south of Pakawau Bush Road (Fig. 2.3). These are the only known continuous sections of Rakopi Formation. The formation was drilled in 1915 at the Rakopi Bore (also called Bassett's Bore), although no samples remain, and only a generalised lithological log was produced. In the outcrops studied for this project, the following facies occur:

- Hard, bright coal (Browne et al. 2008) 0.1-1m thick. Rootlets from the base of coal beds may extend up to 0.3m into underlying beds (Fig. 3.1A).
- Coaly mudstone (Fig. 3.3). Mudstone is grey to dark brown and includes coaly material and plant fossils. This is often interbedded with coal beds.
- Siltstone, usually laminated and carbonaceous (Fig. 3.1A). Sometimes has leaf fossils. Siltstone is often interbedded with coal.
- Interbedded sandstone and siltstone. Fine to very fine sandstone beds 1-10cm thick are interbedded with siltstone beds 0.5-1cm thick. The bedding may be planar or wavy. The sandstone may have ripples (Fig. 3.1B).
- Fine to coarse sandstone, commonly trough cross-bedded, with bedsets 0.1-0.3m thick (Fig. 3.1C). Planar bedding is also common. Sandstone may contain coaly fragments and leaf fossils. Beds often have normal grading.
- Conglomerates are rare, and in this study only recorded at the base of the Paturau River section. These Paturau River conglomerates are grouped into the Otimataura Conglomerate. Here, the units are up to 4m thick. The lowest conglomerate (Fig. 3.1E) is matrix supported, with sub-angular very coarse pebble to cobble clasts. The upper conglomerate units are clast supported and the clasts are subrounded coarse to very coarse pebbles (Fig. 3.1F). The Otimataura Conglomerate is absent at the Pakawau Bush Road, at the contact between basement and Rakopi Formation west of Knuckle Hill, and in the Rakopi Bore. The Rakopi Bore does contain minor conglomerates (Fig. 3.2) which are described by the drillers as containing "quartz pebbles". These conglomerates grade into sandstones. The Otimataura Conglomerate is present at the base of Cape Farewell-1, where there is at least 120m of clast supported conglomerate (Carter and Kintanar 1987).

Fig. 3.1: Outcrops of Rakopi Formation, measuring stick is 1m long with 10cm gradations. A: rootlets from coal bed above into siltstone. B: interbedded sandstone and siltstone. Sandstone has ripples. C: sandstone unit which has planar bedding and trough cross-bedding. D: outcrop of Rakopi Formation in the Paturau River (~5m tall), showing two fining upwards sandstone – siltstone – coal cycles. E: Otimataura Conglomerate at the base of the Paturau River section, outcrop ~5m high. F: conglomerate at 61m in the Paturau River.

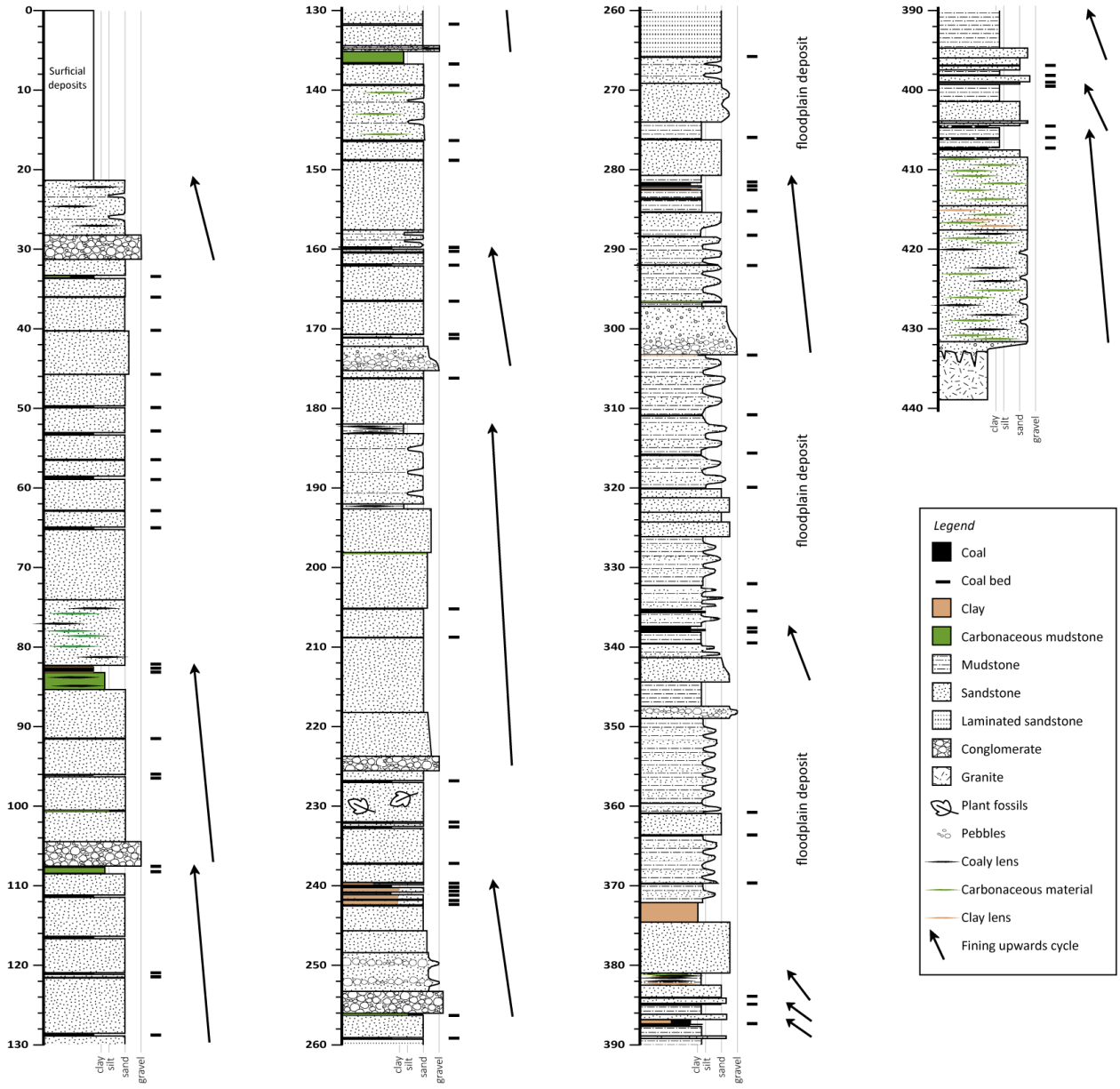

Fig. 3.2: Stratigraphic column of the Rakopi Bore. Scale is in metres. Approximate location of the bore is 40.61°S, 172.57°E (Ongley & Macpherson 1923). Data is from Wellman (1950), included in Appendix A.

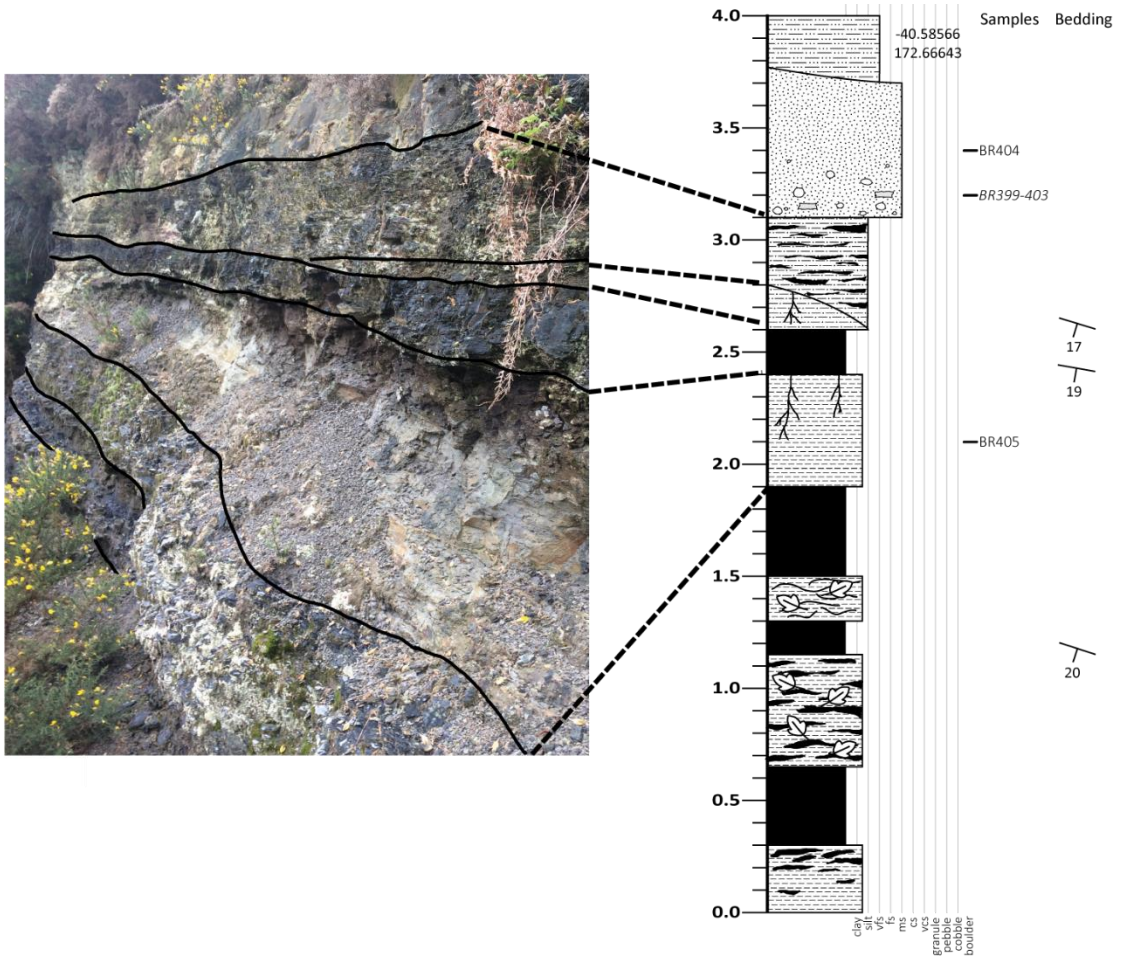

Fig. 3.3: Detailed stratigraphic column and photograph of the Rakopi Formation at the Pakawau forestry block (40.58566°S, 172.66643°E). Interbedded coal, siltstone, and carbonaceous mudstone are eroded by sandstone channel with pebble and siltstone rip up lag at base. Vertical scale is in metres.

These facies are commonly organised into fining upwards cycles, with basal sandstone and possibly conglomerate fining upwards to siltstone, carbonaceous mudstone, and coal (Figs. 3.1D, 3.2).

Browne et al. (2008) interpreted the Rakopi Formation as terrestrial fluvial channels, overbank deposits and levee deposits formed on a low-gradient coastal plain, with some marine influence. This is supported by the outcrops and bores in this study. A terrigenous setting is shown by the presence of coal and rootlets. The fining upwards cycles are characteristic of a meandering river system. The cycles form in avulsing channels where the sandstone and conglomerates are the main fluvial channel fill, and the finer siltstone are the overbank deposits formed as the main channel migrates across the flood plain (Miall 2010). Coal deposits form as mires develop in abandoned channels. In parts of the stratigraphy in the Rakopi Bore, the fining upwards cycles are less well-developed and instead comprise

interbedded siltstone, sandstone, and coal (Fig. 3.2 at 334m-303m; 345-372m). These are likely to be the floodplain deposits, where soils and mires develop, and sediment is only deposited during flood events.

The Otimataura Conglomerate was interpreted as alluvial fan deposits fed from the Wakamarama Fault scarp by Wizevich (1994). This is supported by the presence of more angular, poorly sorted, matrix-supported conglomerates at the base of the Paturau River section (Fig. 3.1E), which are likely to be a debris flow deposit. The clast-supported, more rounded conglomerates upsection and further northwest (Fig. 3.1F) are more likely deposited by streamflow. Debris flows and high energy stream flows able to transport gravels are features of alluvial fans (Blair and McPherson 1994, 2009; Miall 2010). On the Paturau River section, the conglomerates alternate with the coaly fluvial deposits, suggesting this region is the edge of the fan where it interfingered with the main floodplain deposits.

3.4 Lithofacies of the North Cape Formation

Bal (1992), Bal and Lewis (1994), and Higgs et al. (2010) presented detailed descriptions of North Cape Formation lithofacies grouped into three lithofacies associations (A1-A3). The lithofacies associations were described in more detail by Joyce (2018) and renamed according to adjusted environmental interpretations. It is outside the scope of this project to present a detailed review of lithofacies and lithofacies associations, so a summary of lithofacies from outcrops sampled in this study is presented here, following the published nomenclature of Higgs et al. (2010).

3.4.1 Lithofacies Association A1: thick-bedded, cross-bedded sandstone and minor conglomerate

Lithofacies Association A1 (tidally influenced delta front association DF of Joyce 2018) crops out at Maori Point, Pecks Point, and the base of the Oyster Point section (Figs. 2.3,s 3.4-3.7). This facies association contains the following facies, in decreasing order of abundance:

- Trough cross-bedded fine to coarse sandstone (Fig. 3.8A-C). Trough cross-beds are commonly bidirectional, with bedsets typically 0.15-0.5m thick. The bedsets reach up to 1.5m thickness at the top of the Pecks Point section. Mud drapes 0.1-1cm thick are

abundant on the foresets of the trough cross-beds and are characteristic of this lithofacies association. The base of the trough cross-bed sets often has pebbles and siltstone rip-up clasts. At the top of the Pecks Point section this facies has burrows including *Ophiomorpha*. Some beds have logs or branches replaced by iron oxide precipitates. The base of the trough cross-bedded sandstone units may be erosive and have a concentration of subrounded to rounded pebbles.

- Planar cross-bedded sandstone beds 0.5-1m thick (Fig. 3.8D). Pebbles are concentrated at the base of these units and may occur in horizons along the foresets.
- Pebble conglomerates 0.1-1m thick (Fig. 3.8H). These are often at the base of trough cross-bedded sandstone. The base is often erosive, forming channels eroding into the underlying units. The conglomerates therefore often vary laterally in thickness. The conglomerates are typically clast supported, with moderately to well-sorted, sub-rounded to rounded, medium to coarse pebble clasts.
- Interbedded siltstone and very fine sandstone. This occurs as beds up to 0.5m thick that may be laterally continuous for up to 20m of outcrop or may be lenses often in the trough cross-bedded sandstone. Beds and laminae of siltstone and sandstone are 0.1 to 2cm thick and are wavy or lenticular. The sandstone often has asymmetrical ripples (Fig. 3.8E-F). The siltstone is often organic rich.
- Planar bedded sandstone. The trough cross-bedded sandstone may pass upwards into planar bedding, which has parting lineations where the bedding surface is exposed.
- Organic-rich very fine to fine sandstone (Fig. 3.8G). These sandstone units have abundant carbonaceous stringers and some have wavy bedding.
- Tabular cross-bedded conglomerate with beds up to 3m thick. This only occurs at the top of the Pecks Point South section. The conglomerate is clast supported, with moderately to well sorted, subrounded to rounded, very coarse pebbles. Cross beds are marked by sandstone lenses. The base of the unit is erosive.

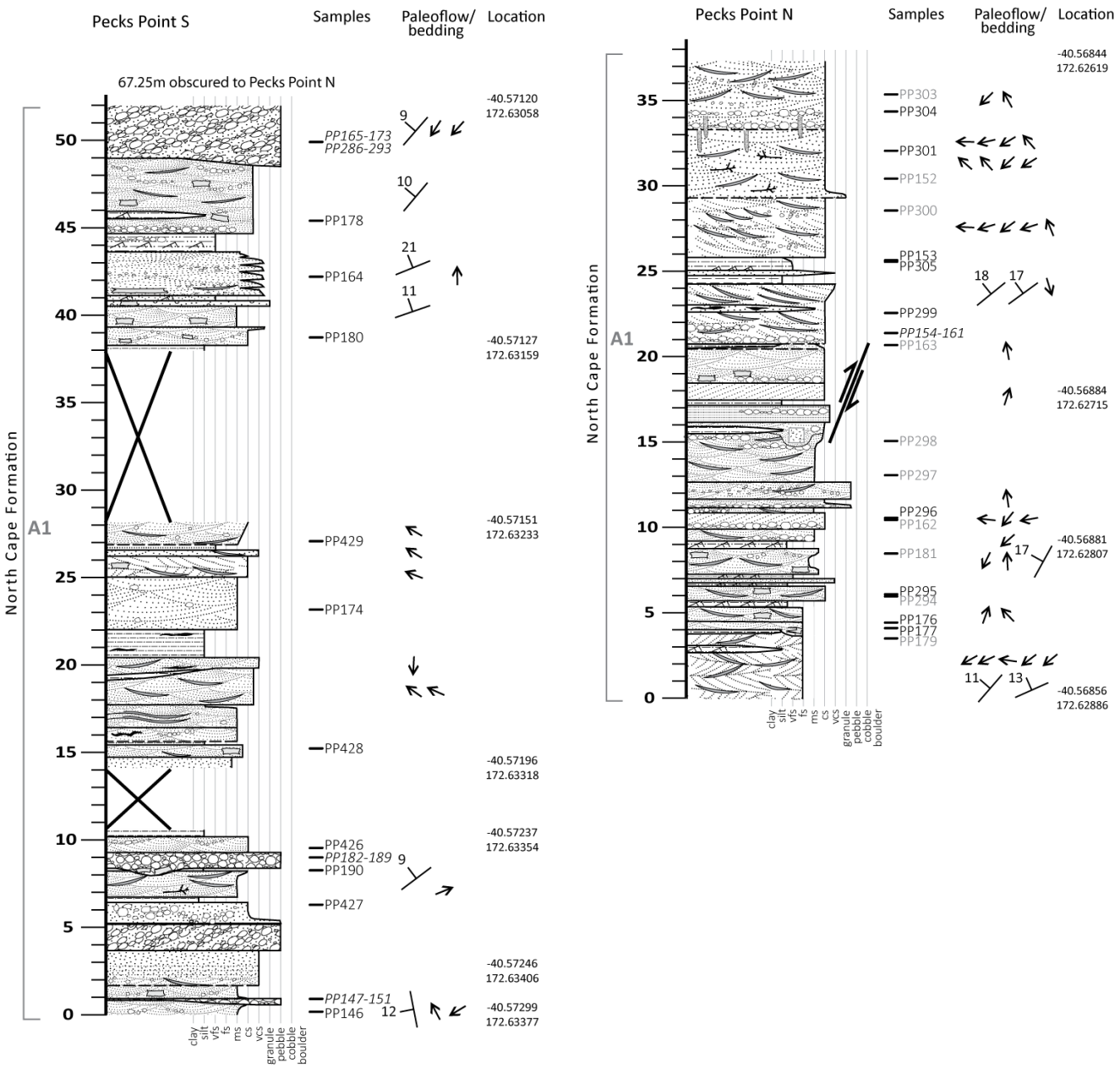

Fig. 3.4: Stratigraphic column of the North Cape Formation at Pecks Point. Sections are lithofacies association A1. See Fig. 3.5 for legend.

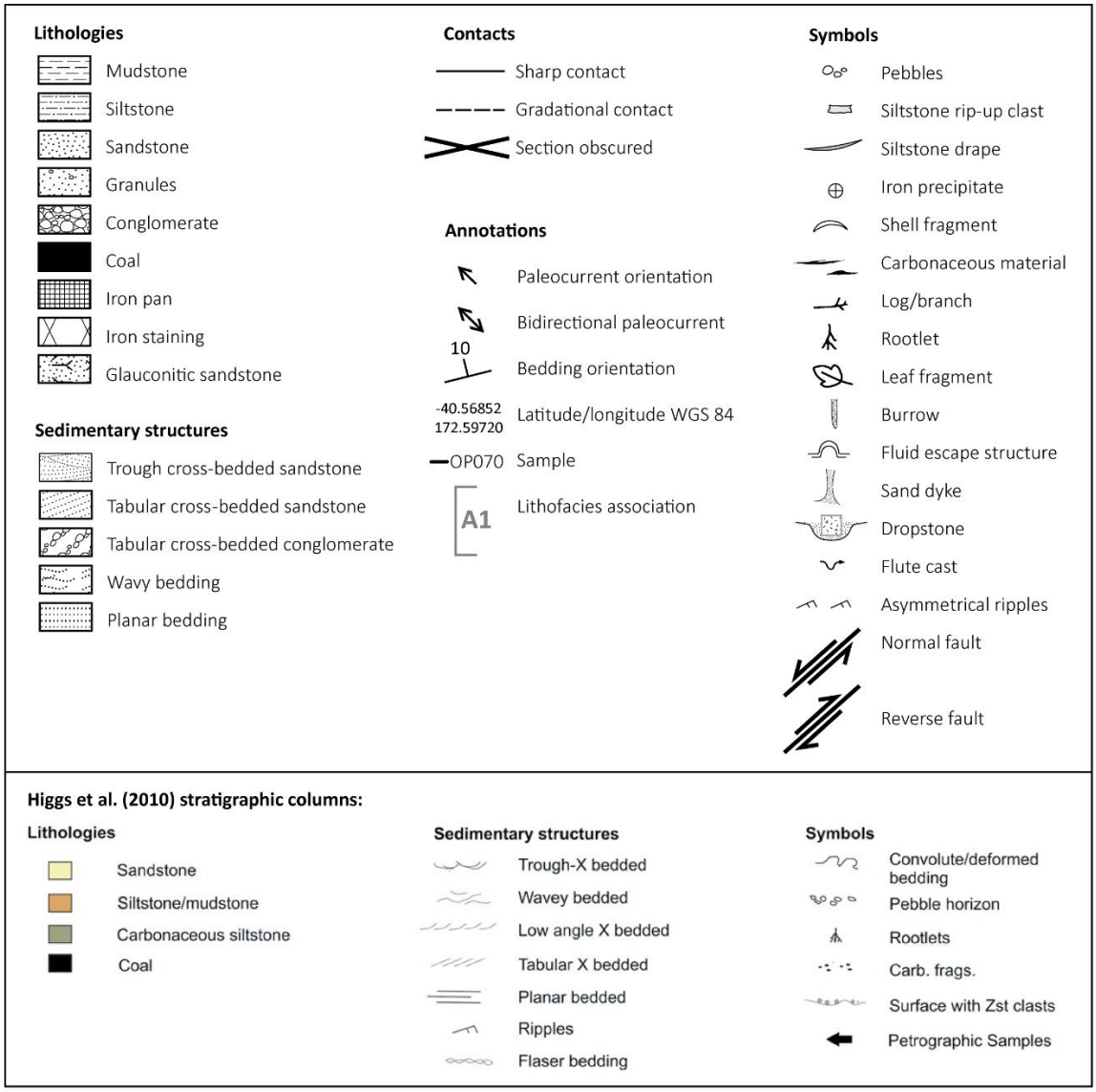

Fig. 3.5: Legend for stratigraphic columns, including columns from Higgs et al. (2010).

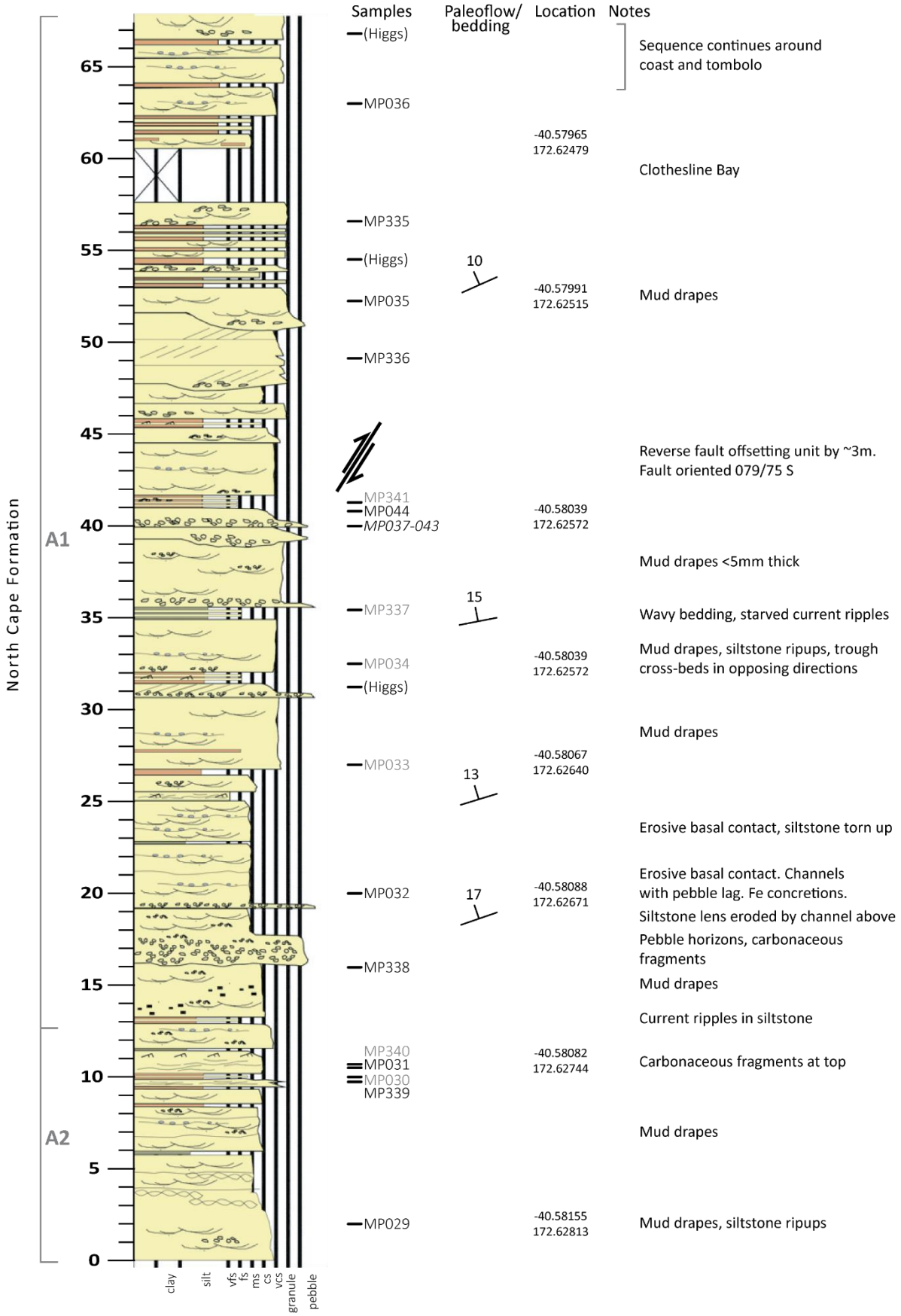

Fig. 3.6: Stratigraphic column of the North Cape Formation at Maori Point. Stratigraphic column is from Higgs et al. (2010), all additional notes and data from this study. See Fig. 3.5 for legend.

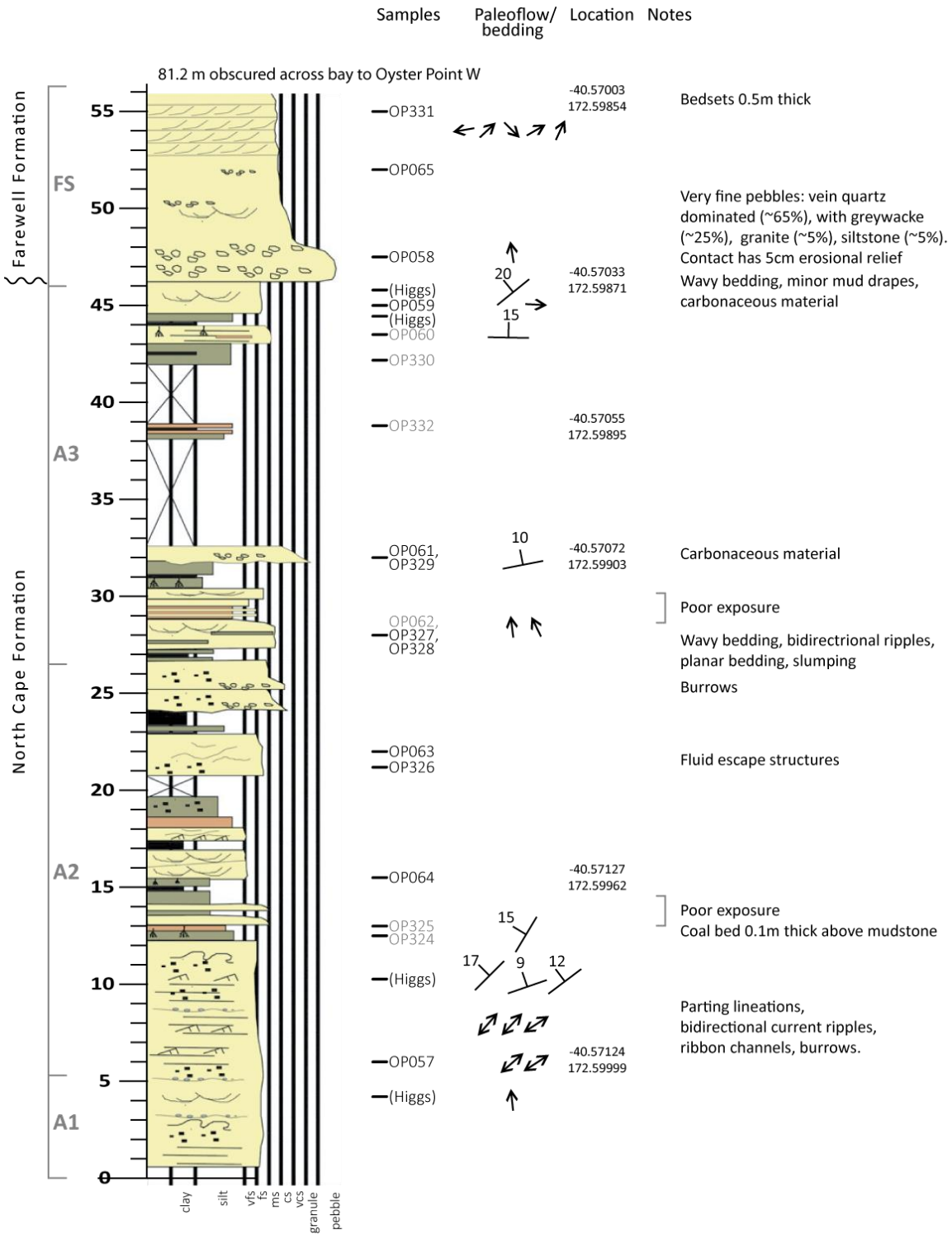

Fig. 3.7: Stratigraphic column of the North Cape Formation at Oyster Point. Stratigraphic column is from Higgs et al. (2010), all additional notes and data from this study. See Fig. 3.5 for legend.

Bal and Lewis (1994) interpreted this lithofacies association as tidally dominated channels and sand shoals. Higgs et al. (2010) suggested that the tidal channels were the front of a fan-delta, fed by material from the Wakamarama Fault scarp. Joyce's (2018) overlapping DF

association was interpreted as a tidally influenced delta-front environment with mixed tidal and fluvial processes.

From the outcrops in this study, a submarine setting is supported by the lack of terrigenous indicators such as coal beds, rootlets, and desiccation cracks. A tidal influence is strongly indicated by structures such as bidirectional cross-bedding and mud drapes. The abundance of sandstone units, channels with pebble lag deposits, and cross-bedding sets up to 1.5m thickness suggests a high-energy environment. The thickness of the cross-bed sets indicates large-scale channels multiple metres deep.

The fan-delta environment suggested by Higgs et al. (2010) is less clear from the sedimentological evidence in association A1. However, the proximity of the outcrops to the Wakamarama Fault Scarp and the transition from association A1 to shallower water and terrigenous deposits does suggest that this association was part of a delta prograding from the fault scarp.

Joyce (2018) suggested that the conglomeritic facies at Pecks Point South in the northeast of the field area (Fig. 3.4) are part of a delta plain with meandering to braided rivers transitioning upwards to the sub-tidal delta front. She interpreted this system as a bayhead delta. The overall north to northwest paleoflow direction for the North Cape Formation (Fig. 3.21, Section 3.7) suggests that the southeast of the field area was the head of the estuary, not the northwest so this is unlikely to be a “bayhead” delta. However, a delta prograding from the Wakamarama Fault in the north at Pecks Point is a good explanation for the presence of coarser sandstones and conglomerates and is supported by the west-northwest paleoflow at Pecks Point.

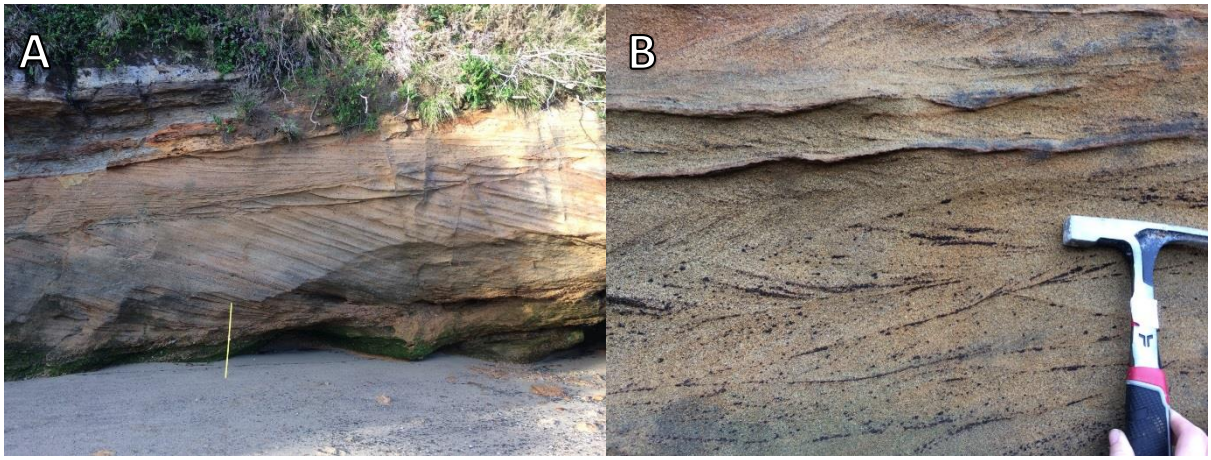

Fig. 3.8 cont.

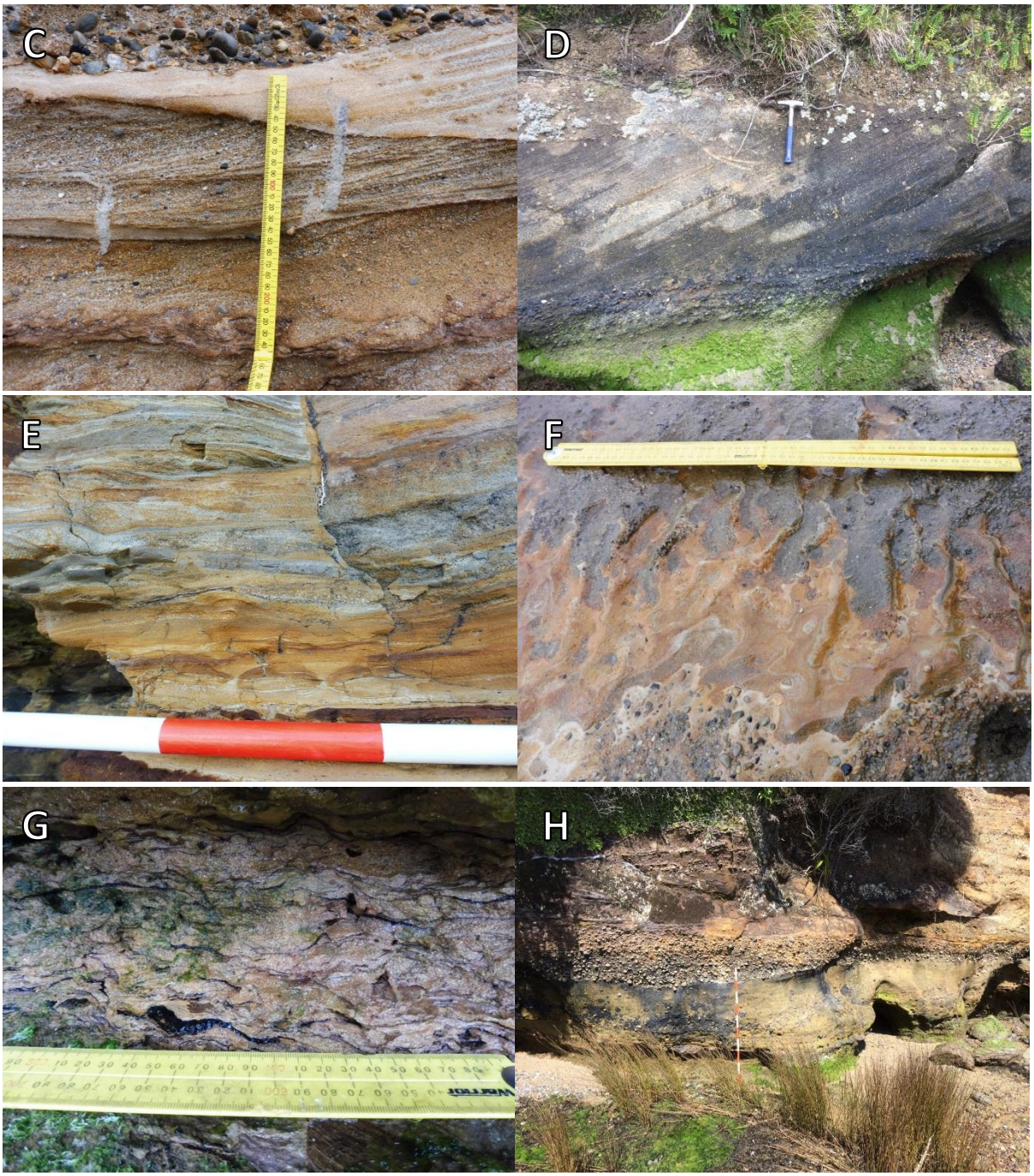

Fig. 3.8: Outcrop photographs of North Cape Formation lithofacies association A1. A: trough-cross bedded sandstone at Pecks Point with mud drapes. B: herringbone cross-beds in sandstone at Pecks Point. C: Ophiomorpha burrows at Pecks Point. D: tabular cross-bedded sandstone with pebble conglomerate at base. E: interbedded sandstone and siltstone with ripples in sandstone. F: the same unit as E but showing linear wave ripples exposed on the bedding surface. G: highly carbonaceous sandstone with coal strings. H: pebble conglomerate in channel form, grades into trough cross-bedded sandstone.

3.4.2 Lithofacies Association A2: interbedded siltstone and sandstone, mudstone, claystone, and coal

Lithofacies association A2 (sub-tidal association ST of Joyce 2018) is present at Oyster Point, Moki Point, and Mangarakau Swamp (Figs. 2.3, 3.7, 3.9). Association A1 often passes upwards into association A2. A2 is composed of the following facies progression:

i) Interbedded siltstone and very fine to medium sandstone. Interbeds are on a millimetre to centimetre scale. Interbeds are dominantly very fine to fine sandstones, but also have siltstone and mudstone (Fig. 3.10A). Sedimentary structures include asymmetric and symmetric ripples 0.5-5cm tall, herringbone ripples, small channels, small burrows up to 15cm deep and 1cm wide, and convolute bedding. Mudstone units may be pushed into small flame structures at the top of the bed. The interbeds are alternating sequences of upper plane bed laminations, ripples, lower plane bed laminations, smaller climbing ripple, and a sharp contact with a final mud drape (Fig. 3.10B). At Wairoa River, herringbone ripples and mud drapes alternating with sand-starved ripples and thicker mud-drapes show spring and neap tidal cycles (Fig. 3.10C). The structures interpreted by Browne (2009) as titanosaurid dinosaur footprints occur within this facies.
ii) Massive, flaky, organic-rich mudstone often gradationally overlies the interbedded sandstone and siltstone. The mudstone has rootlets extending down into it (by up to 0.5m) from the overlying coal (Fig. 3.10D).
iii) Thin coal seam 0.1-0.3m thick, laterally continuous (Fig. 3.10D).

Association A2 was interpreted by Bal and Lewis (1994) and Higgs et al. (2010) as intertidal and supratidal mudflats, salt marshes, and paralic mires. The equivalent association ST of Joyce (2018) was interpreted as sub-tidal sand flats to supra-tidal salt marshes. These interpretations are supported by the observations of this study. The interbedded siltstone and sandstone is tidally influenced, as evidenced by the presence of structures such as paired mud-drapes, herringbone cross-bedding and spring-neap tidal bundles. The presence of dinosaur footprints suggests the environment was intertidal to shallow sub-tidal, allowing the dinosaurs to walk onto the mudflats at low tide or in shallow water. Progradation of the shoreline is shown by the facies progression from interbedded sandstone and siltstone to

mudstone and coal. The top of the heterolithic sandstone is usually reworked and may have rootlets penetrating into it. The coal represents coastal mires.

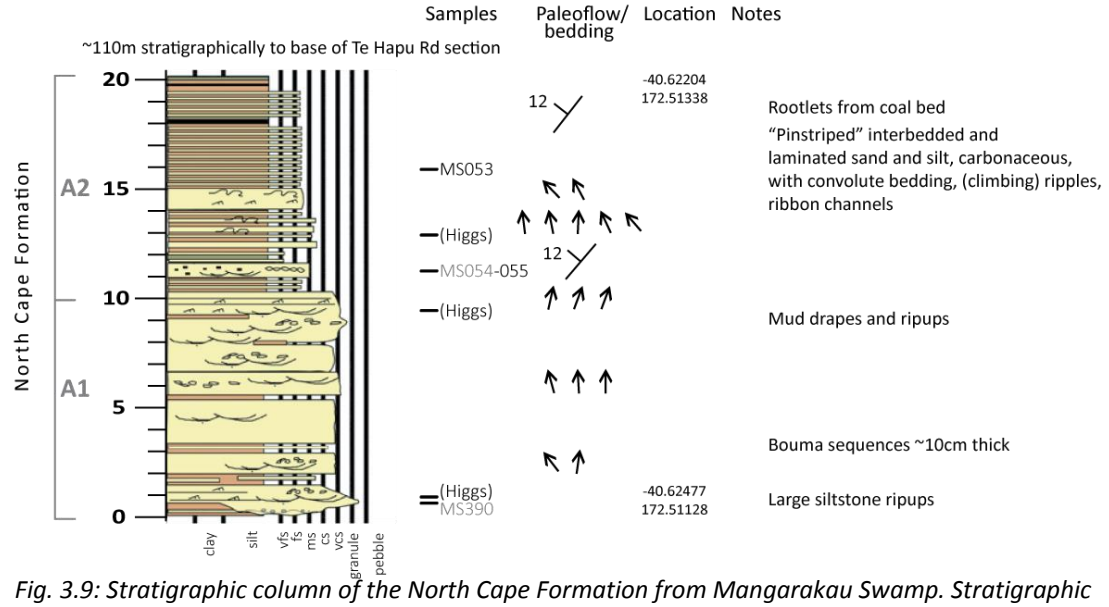

Fig. 3.9: Stratigraphic column of the North Cape Formation from Mangarakau Swamp. Stratigraphic column is from Higgs et al. (2010), all additional notes and data from this study. See Fig. 3.5 for legend.

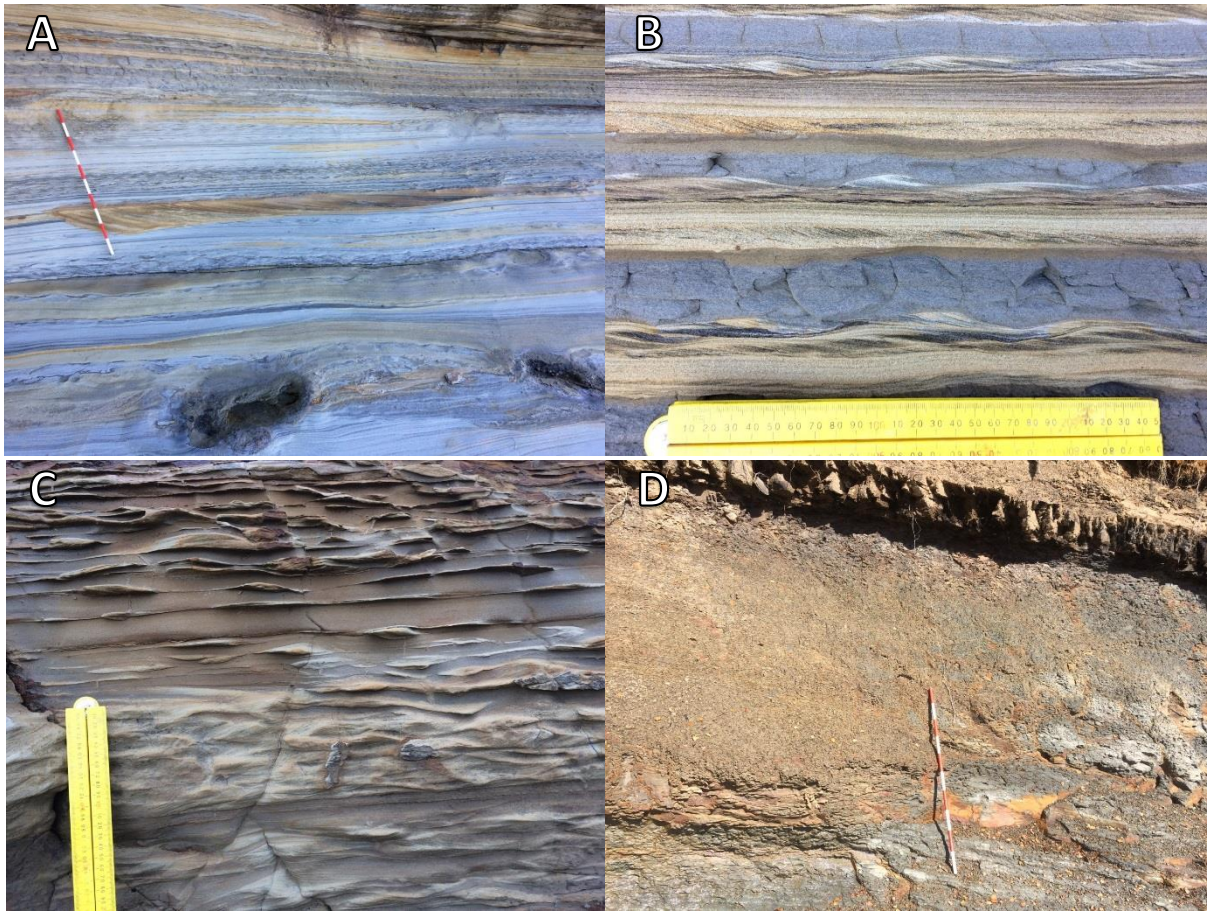

Fig. 3.10: North Cape Formation lithofacies association A2 at Mangarakau Swamp. Measuring stick is 1m with 10cm gradations. Ruler is 25cm. A: heterolithic sandstone and siltstone facies with plane-bed laminations, carbonaceous laminations, and ripples. B: interbedded siltstone/sandstone with upper and lower plane bed laminations and ripples in sand. C: interbedded sand and silt showing spring-neap cycles from Wairoa River. D: coal bed with massive mudstone underneath.

3.4.3 Lithofacies Association A3: thin-bedded sandstone, with mudstone, coal and rare conglomerate

Lithofacies Association A3 (delta plain association DP of Joyce 2018) is found at Maori Point, Moki Point, Mangarakau River, Puponga Mine, and Oyster Point (Figs. 2.3, 3.6, 3.7). It contains the following facies:

- Sandstone beds between 0.25-2m thick. Trough cross-bedding may be present and is unidirectional with bedsets up to 0.5m thick. Mud drapes are usually absent. Pebbles may be concentrated along base of trough cross-bed sets. Fine sandstones commonly have wavy laminations. Sandstone dykes may be present. Carbonaceous material in small coaly stringers is common.
- Rare pebble conglomerates up to 1m thick. Typically clast supported, clasts are moderately sorted, sub-rounded to rounded, medium pebbles. This unit often grades upwards into sandstone. At Moki Point, it occurs in a channel which erodes the units below. Here, the conglomerate passes laterally into sandstone away from the channel axis.
- Siltstone, commonly laminated. May have soft sediment deformation such as flame structures.
- Mudstone, usually massive and organic rich. May show soft-sediment deformation such as flame structures (Fig. 3.11A).
- Thick coal seams between 0.1-0.5m thick (Fig. 3.11A). Rootlets from the base of coals may extend down into sandstone, siltstone or mudstone units by up to 0.75m.

Association A3 was interpreted by Bal and Lewis (1994) as crevasse splays and interdistributary bars. Higgs et al. (2010) and Joyce (2018) added that this was part of the non-marine to intertidal upper delta plain. A terrigenous setting is strongly supported by the presence of coal and rootlets. Coal seam thicknesses of up to 0.5m are a result of peat accumulations approximately 5m thick, indicating that the mires were relatively stable features of the sedimentary system. The sandstone and rare conglomerates often have erosive bases with a channel morphology. These are interpreted as fluvial channels, and the surrounding siltstones and carbonaceous mudstones as floodplain or overbank fines. This supports an overall setting for lithofacies association A3 as a coastal plain or delta plain with meandering rivers.

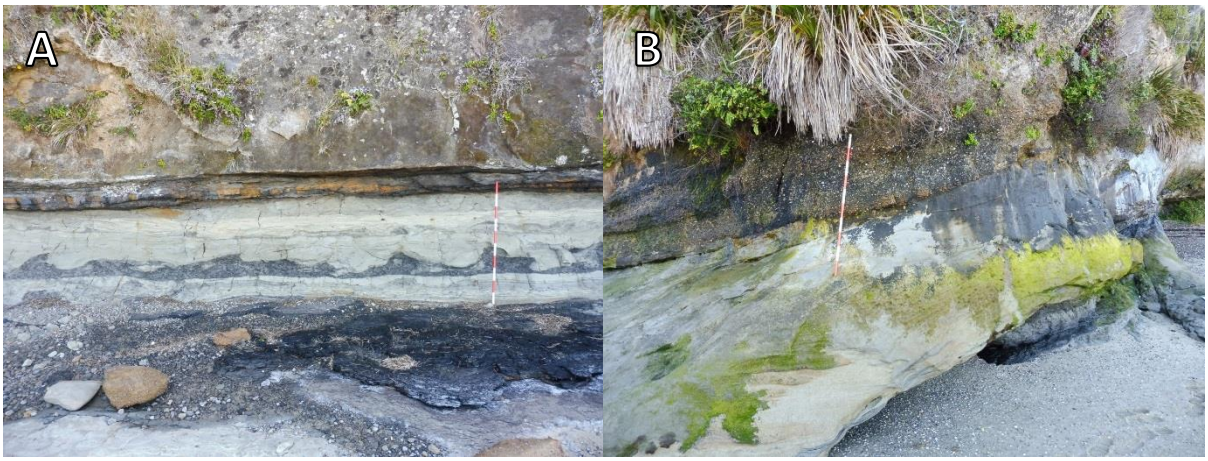

Fig. 3.11: North Cape Formation lithofacies association A3. Measuring stick is 1m with 10cm gradations. A: Moki Point. Coal bed at base of outcrop, siltstone with wavy lamination, carbonaceous mudstone showing flame structures, coal bed under sandstone at top. B: Contact between the North Cape and Farewell formations at Oyster Point. Coal is visible at base of outcrop, overlain by siltstone, and sandstone (Association A3). The Farewell Formation is the pebble conglomerate eroding the sandstone.

3.4.4 Upper contact of the North Cape Formation

The contact between the North Cape Formation and the overlying Farewell Formation is exposed at Oyster Point and Moki Point (Figs. 3.7, 3.11B). The top of the North Cape Formation in both locations is lithofacies association A3. The contact is sharp and erosional, with channels in the Farewell Formation cutting into the North Cape Formation. The contact at Oyster Point has approximately 5cm of erosional relief. There is no other evidence (e.g. paleosols or phosphate accumulation) of a significant time-break.

3.5 Lithofacies of the Farewell Formation

There is a brief description of the lithology of the Farewell Formation in Suggate (1956), and Titheridge (1977). The only detailed lithofacies analysis for the Farewell Formation in the study area is by Stark (1996). He interpreted almost all outcrops along the western shore of the Whanganui Inlet as North Cape Formation, not Farewell Formation (Fig. 2.3). This is based on the thickness of the Farewell Formation shown in Thrasher's (1992) isopach maps constructed from seismic surveys. However, there is almost certainly lateral variation in sediment thickness and structural complexity so close to the basin-bounding Wakamarama Fault, meaning that sediment thickness offshore further from the fault is not useful for onshore interpretation closer to the fault. The lithofacies associations proposed by Stark (1996) were separated into North Cape and Farewell Formation associations despite having

very similar characteristics, so these will not be used in this study. Instead, a simplified scheme of three associations is presented below.

3.5.1 Sandy meandering river association (Association FM)

The meandering river association of the Farewell Formation occurs in outcrops along Te Hapu and Westhaven roads at the southern end of the Whanganui Inlet (Fig. 2.3). The typical facies progression displays fining upwards cycle motifs of which the following description describes most variants:

i) Basal fine to coarse sandstone unit 1 -10m thick. Base of the sandstone unit is often channel shaped and erosional, sometimes with groove marks (Fig. 3.12A). Low-angle unidirectional trough cross-bedding is common, with bedsets typically 0.25-0.5m thick (Fig. 3.12B). Minor pebbles may be present at the base of the bedsets. Coaly stringers are sometimes present. Siltstone lenses are present near the top of the sandstone units.

ii) 0.3-7m thick massive siltstones with abundant leaf fossils and minor coaly stringers overlie the sandstone units.

iii) highly carbonaceous mudstones, 0.1-1m thick, sometimes with coal lenses up to 10cm thick overlie the massive siltstones. This unit may be partially or completely removed by overlying erosive channels of the next fining upward cycle (Fig. 3.12B).

A meandering fluvial setting is indicated by the fining-upwards cycles, channelised sandstones, thick mudstones with abundant plant fossils, and minor coal (Miall 2010). The sandstone units are the main channel deposits, and the mudstones and coal represent the overbank deposits. The isolated channels surrounded by overbank mudstones seen in the Te Hapu Road section (Figs. 3.12A, 3.13) are typical of a meandering river deposit (Miall 2010).

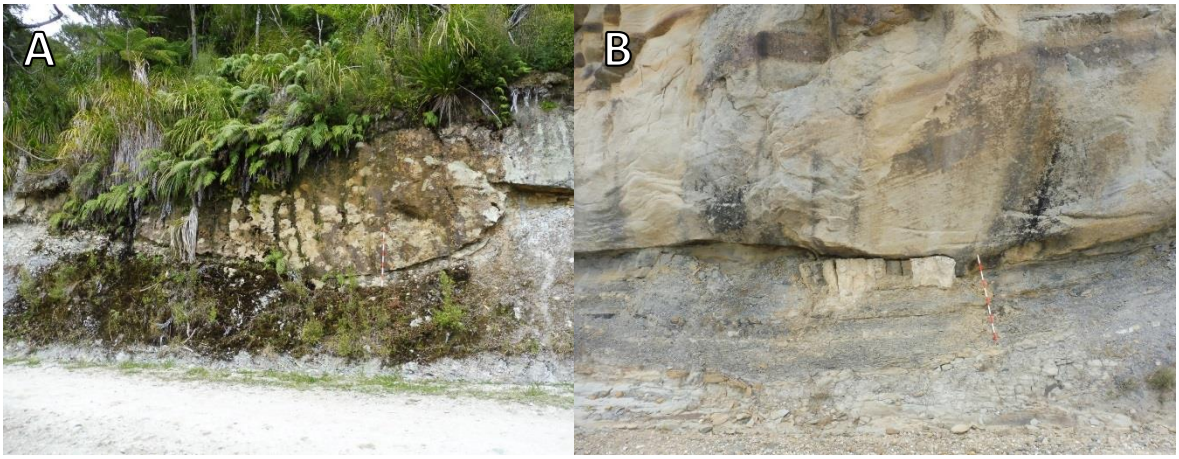

Fig. 3.12: Farewell Formation sandy meandering river association. Measuring stick is 1m with 10cm gradations. A: channel with sandstone fill cutting into massive mudstone with leaf fossils. B: channel with trough cross-bedded sandstone eroding massive mudstone with leaf fossils and coal lens.

3.5.2 Sandy braided river association (Association FS)

The sandy braided river association is present at Oyster Point, Moki Point, and Whahariki Beach (Figs. 2.3, 3.14, 3.15). It is most common in outcrops around the Whanganui Inlet. The dominant feature in this association is thick sandstone units with large-scale trough cross-bedding and complex stacked channels (e.g. Fig. 3.15 26-40m, Fig. 3.17). The typical facies progression from stratigraphic base to top is:

i) Medium to very coarse sandstone units 3-12+m thick. Unidirectional trough cross-bedding is abundant (Fig. 3.16A), with bedsets 0.3-1m thick. Cross-bed sets may be capped with fine sandstone or siltstone lenses. Commonly have siltstone rip-up clasts, large (up to 1m long) carbonaceous stringers, and pebbles at the base of the sandstone (Fig. 3.16B).

ii) Sandstone unit may fine up to carbonaceous fine sandstone unit 0.5-1.5m thick with wavy bedding, asymmetrical ripples, and sandstone dykes.

iii) The sandstone is capped by siltstone 0.3-1m thick with carbonaceous material, and occasionally thin (10cm or less) coal seams.

The complex stacked channels capped by thin finer beds is characteristic of braided river deposits (Bridge and Lunt 2006) (Fig. 3.17). The trough-cross bedded sandstones are the bars and channel fill, and the siltstone and coals are the final channel fill.

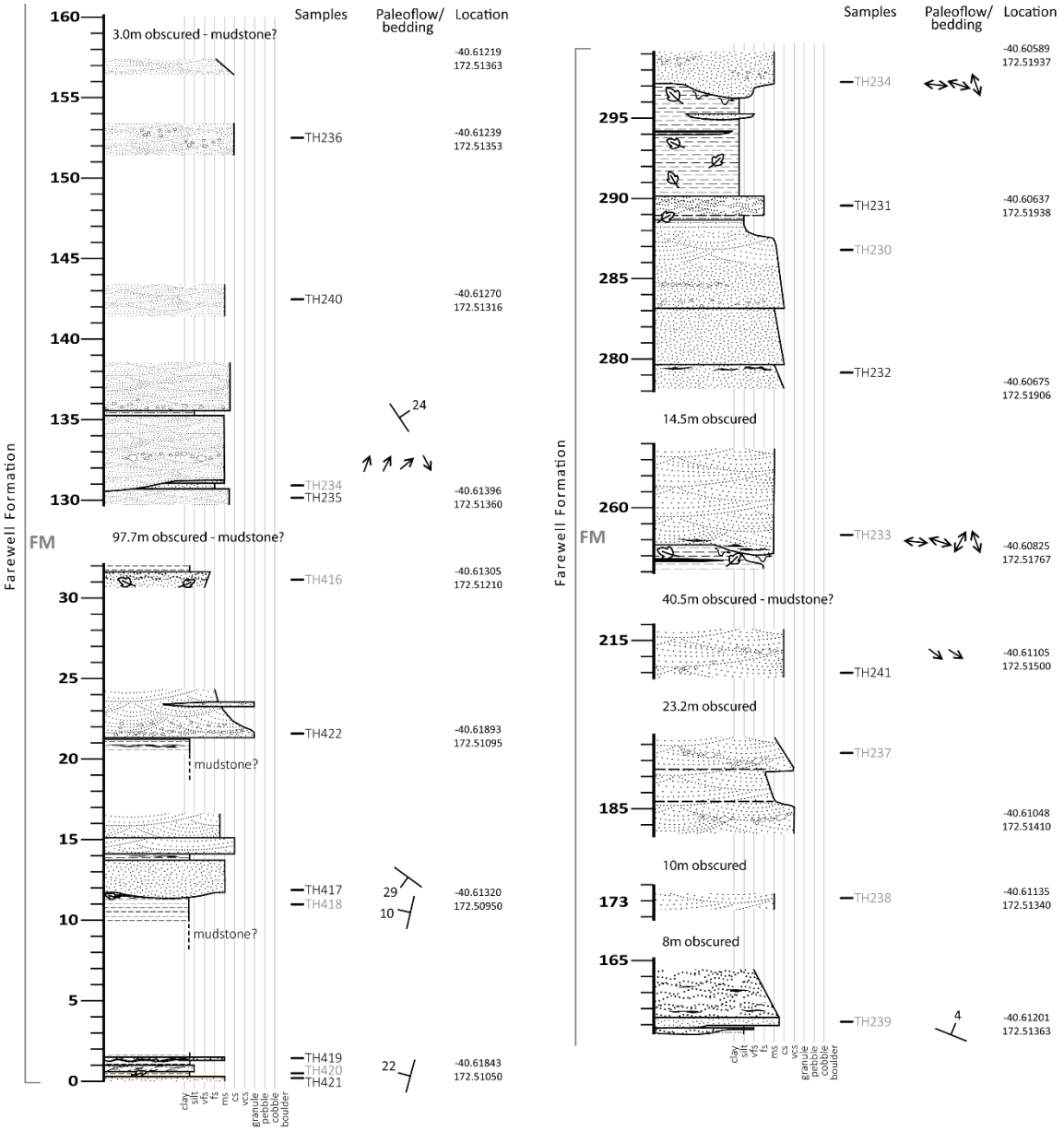

Fig. 3.13: Stratigraphic column of the Farewell Formation from outcrops along Te Hapu and Westhaven roads. Section is meandering river association. The obscured parts of the section are likely to be mudstone, as this is softer and usually eroded out. See Fig. 3.5 for legend.

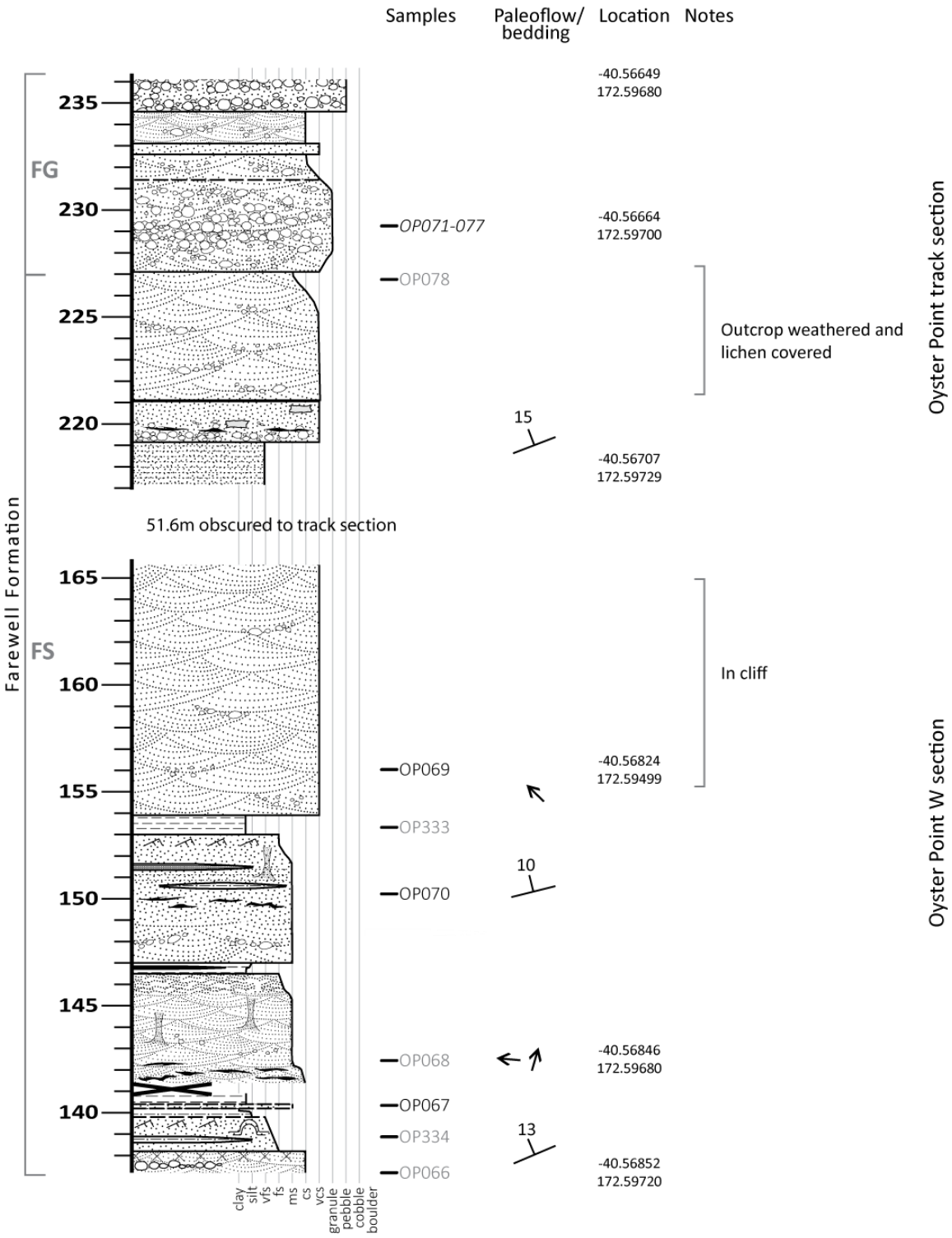

Fig. 3.14: Stratigraphic column of the Farewell Formation at Oyster Point. Lower half of section is sandy braided river association, and transitions to gravelly braided river at 227m. See Fig. 3.5 for legend.

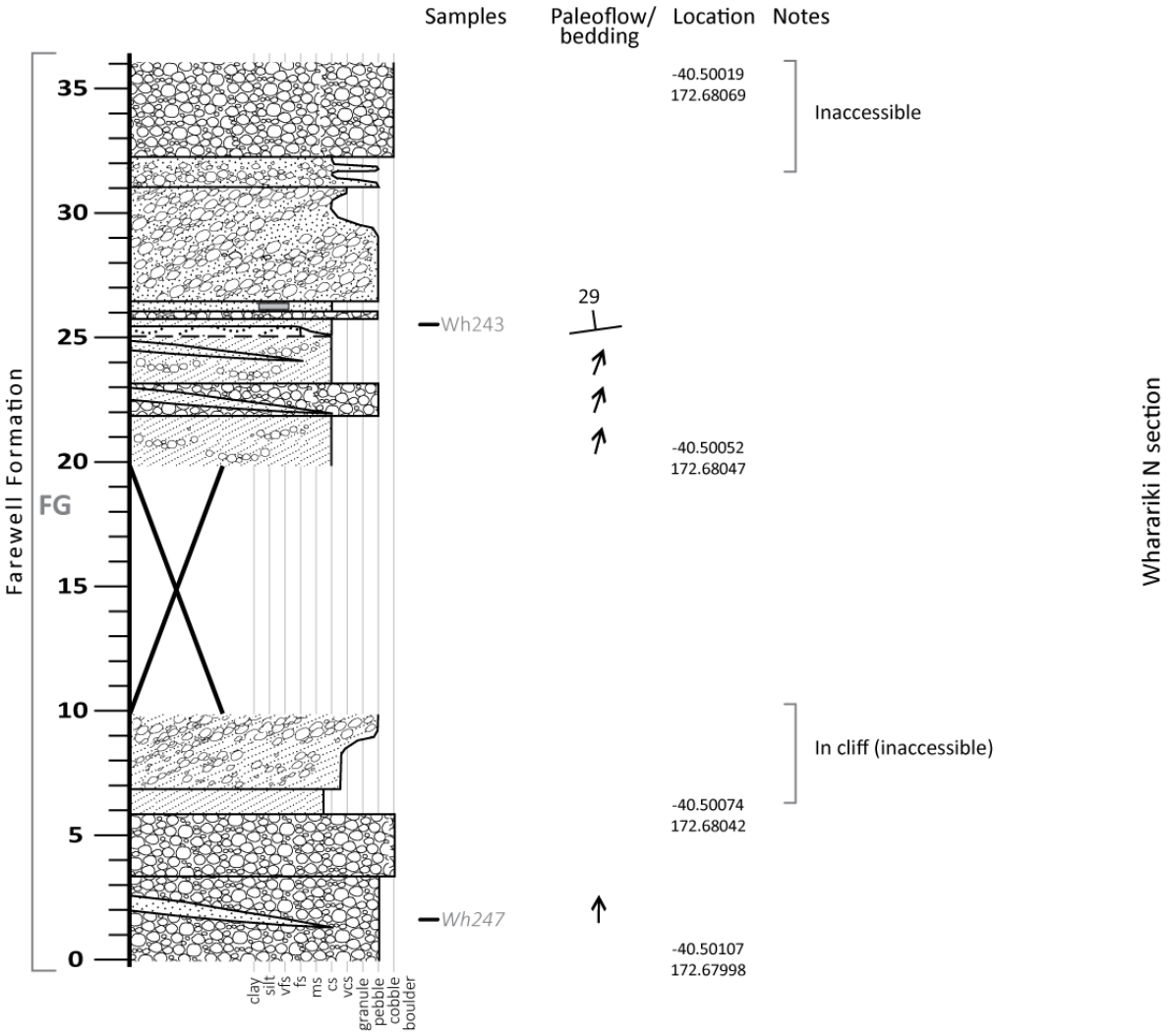
Samples
Paleoflow/ bedding
Location
Notes
-40.50019
172.68069
Inaccessible
29
Wh243
-40.50052
172.68047
Farewell Formation
FG
35
30
25
20
15
10
5
0
In cliff (inaccessible)
-40.50074
172.68042
Wh247
-40.50107
172.67998
clay
silt
vfs
fs
ms
cs
vcs
granule
pebble
cobble
boulder
Whariariki N section

Fig. 3.15 cont.

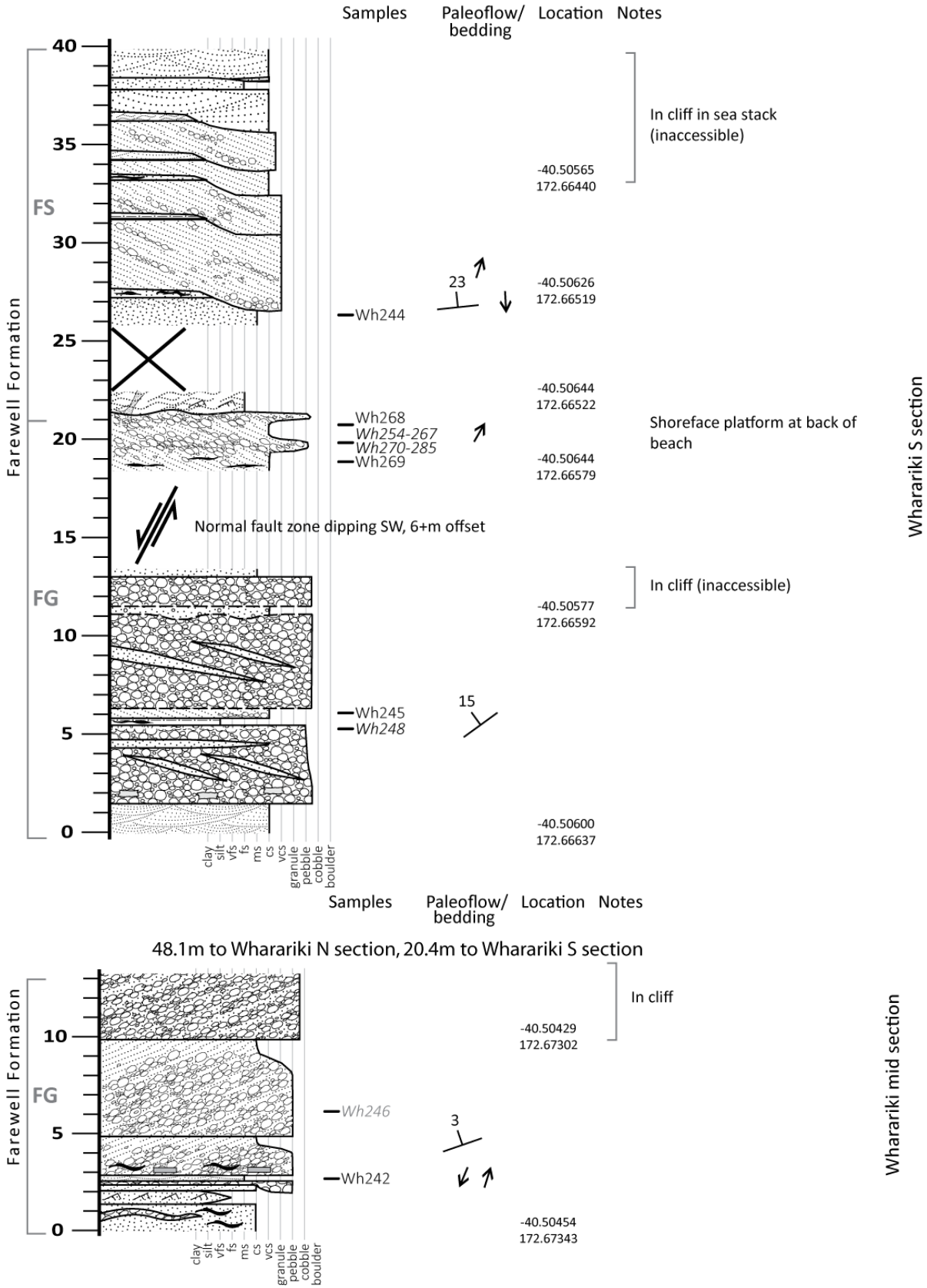

Fig. 3.15: Stratigraphic column of the Farewell Formation at Whararíki Beach. Top half of south section is sand-dominated lithofacies association, remainder is gravel-dominated at 227m. See Fig. 3.5 for legend.

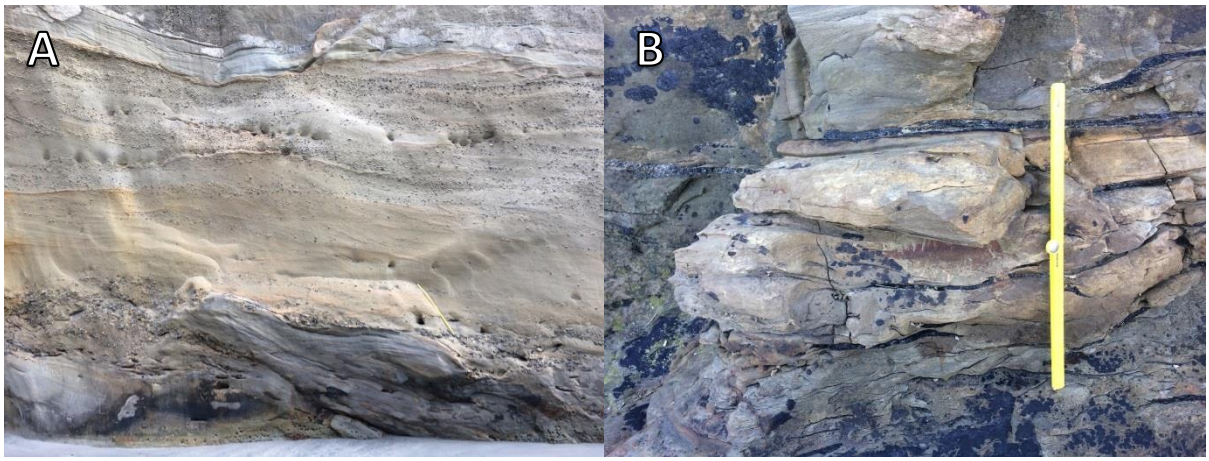

Fig. 3.16: Farewell Formation sand-dominated lithofacies association. A: sandstone with low angle trough-cross beds, pebble horizons, and siltstone lens. Measuring stick is 1m. B: sandstone with coaly stringers. Photo is from base of sandstone unit Measuring stick is 0.5m.

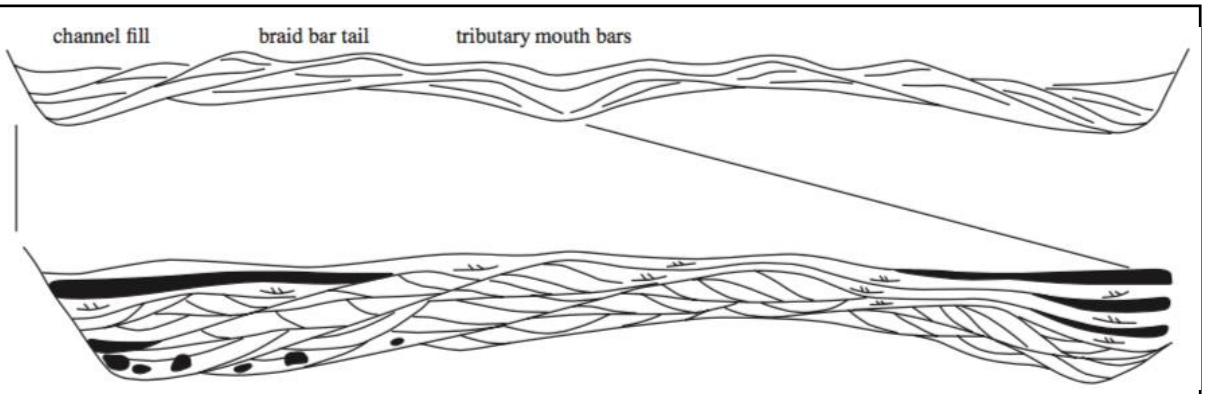

Fig. 3.17: Comparison of Farewell Formation sand-dominated lithofacies association at Whararikí Beach (cliff ~15m high) with model of sand-bed braided river deposit from Bridge and Lunt (2006).

3.5.3 Gravelly braided river association (Association FG)

The gravelly braided river association is present at the top of the Oyster Point section, Pillar Point, Whahariki Beach, Green Hills Beach, and Puponga Point (Figs. 2.3, 3.15, 3.18, 3.19). It is more common in the northern part of the field area. A typical facies progression from stratigraphic base to top is:

i) Clast supported conglomerate 0.5-8m thick. Clast size is typically coarse pebble to cobble, with rare boulders. Clasts are moderately to well-sorted, and sub-rounded rod dominated. The beds may have bedding indicated by crude imbrication, or by lenses of sandstone. This may show large-scale tabular cross-beds, with bedsets 1-4m thick (Fig. 3.20A).

ii) Cross-bedded pebbly sandstone 0.25-3m thick. The pebbly sandstone commonly has low-angle, unidirectional trough cross-beds with bedsets 0.2-0.5m thick. The foresets of the trough cross-beds are often marked by pebbles. The sandstone may be tabular cross-bedded with bedsets ~1m thick (Fig. 3.20B). Coaly stringers are abundant, typically between 0.1 and 0.4 m in length.

iii) Very fine to medium sandstone 0.25-1.5m thick. May have asymmetrical ripples up to 15cm thick, or wavy bedding marked by organic laminations. Coaly stringers are common.

iv) Siltstone 0.25-1m thick (rarely present). The siltstone may have lamination or fine bedding and asymmetrical ripples 0.5-2cm high (Fig. 3.20C). The siltstone may fine upwards to massive, organic rich mudstone.

This association is terrigenous, as demonstrated by the abundance of coaly stringers (leaf mats or coalified branches) and absence of marine indicators such as marine fossils. A braided river system is suggested by the complex stacked channels, clast-supported sub-rounded conglomerates, and absence/rarity of overbank and floodplain deposits (Bridge and Lunt 2006). A fining upwards progression from conglomerate to pebbly sandstone capped by fine sandstone or silt is sometimes seen (e.g. Figs. 3.19 85-332m). This association is likely to represent a series of channel-fills in an avulsing channel fluvial system (Godin 1991; Lunt et al. 2013).

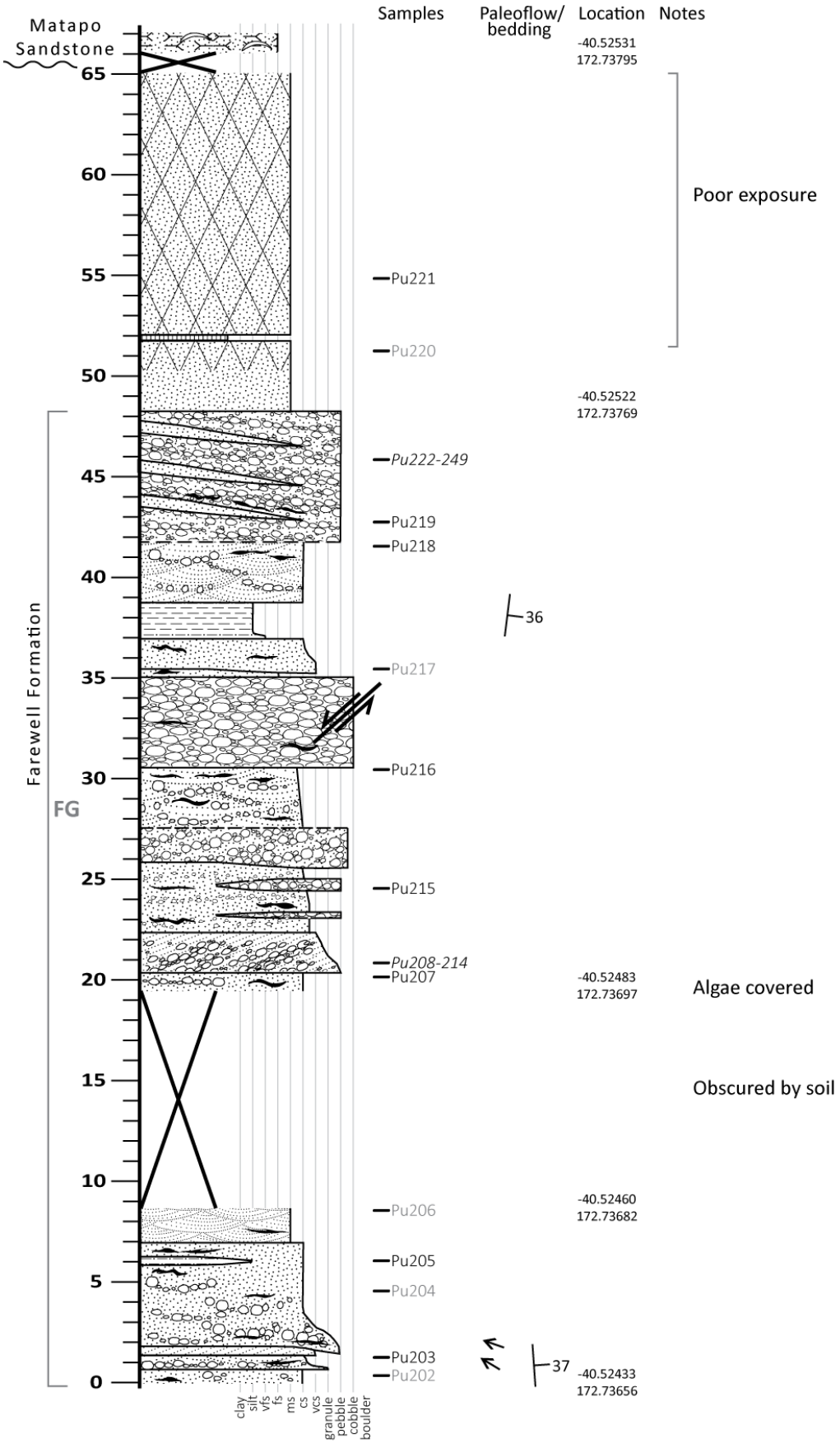

Fig. 3.18: Stratigraphic column of the Farewell Formation and contact with the Matapo Member at Puponga Point. Section is gravelly braided river association. See Fig. 3.5 for legend.

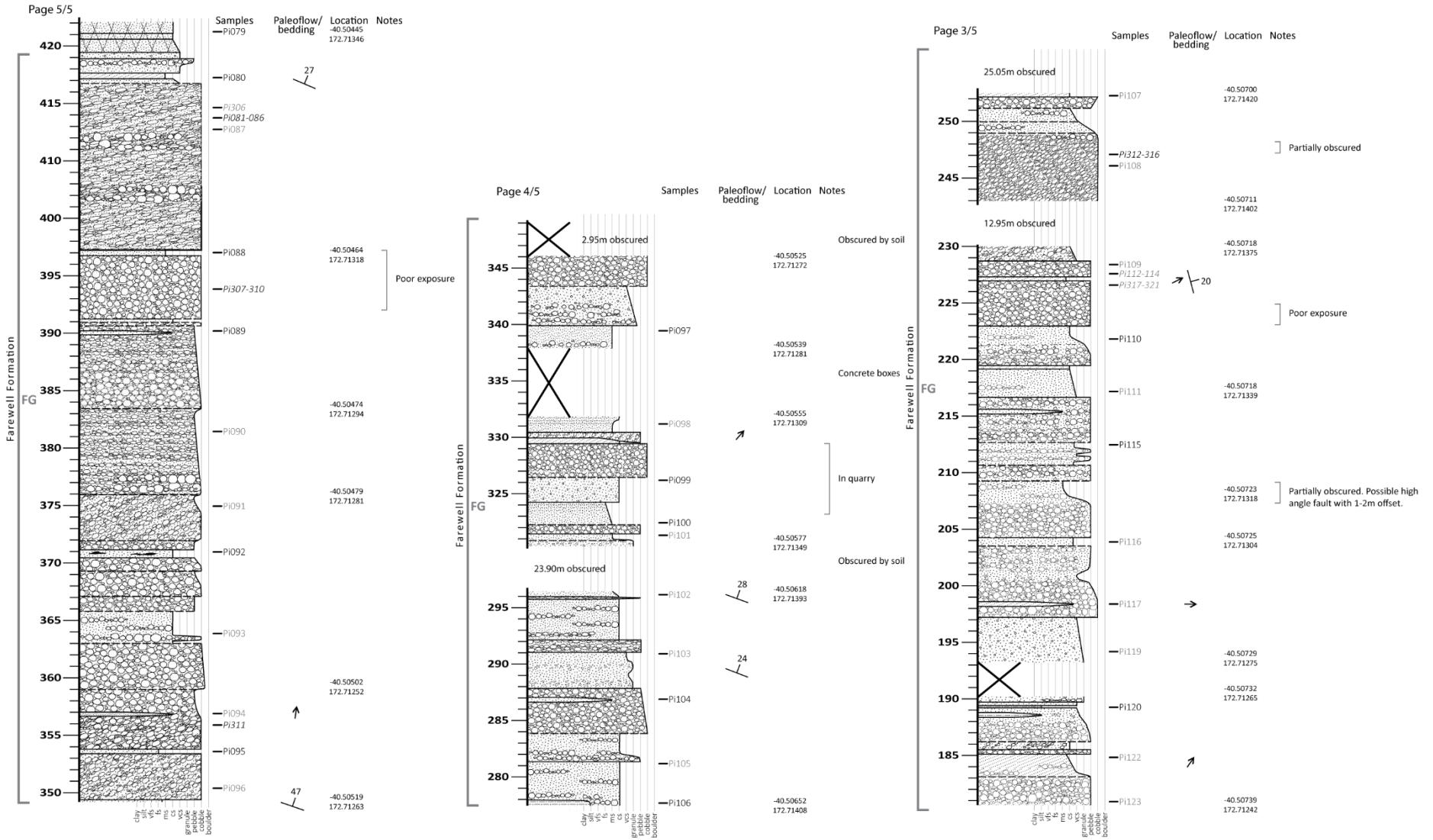
Page 5/5
Samples
Paleoflow/ bedding
Location
Notes
Pi079
-40.50445
172.71346
Pi080
27
Pi306
Pi081-086
Pi087
Pi088
-40.50464
172.71318
Poor exposure
Pi307-310
Pi089
-40.50474
172.71294
Pi090
Pi091
-40.50479
172.71281
Pi092
Pi093
-40.50502
172.71252
Pi094
Pi311
Pi095
Pi096
47
-40.50519
172.71263
Farewell Formation
FG
420
415
410
400
395
390
385
380
375
370
365
360
355
350
clay
silt
vfs
fs
ms
cs
vcs
granule
pebble
cobble
boulder
Page 4/5
Samples
Paleoflow/ bedding
Location
Notes
2.95m obscured
Obscured by soil
-40.50525
172.71272
Pi097
-40.50539
172.71281
Concrete boxes
Pi098
-40.50555
172.71309
Pi099
In quarry
Pi100
Pi101
-40.50577
172.71349
Obscured by soil
23.90m obscured
28
-40.50618
172.71393
Pi102
Pi103
24
Pi104
Pi105
Pi106
-40.50652
172.71408
Farewell Formation
FG
345
340
335
330
325
295
290
285
280
Page 3/5
Samples
Paleoflow/ bedding
Location
Notes
25.05m obscured
Pi107
-40.50700
172.71420
Partially obscured
Pi312-316
Pi108
-40.50711
172.71402
12.95m obscured
-40.50718
172.71375
Pi109
Pi112-114
Pi317-321
20
Poor exposure
Pi110
Pi111
-40.50718
172.71339
Pi115
-40.50723
172.71318
Partially obscured. Possible high angle fault with 1-2m offset.
Pi116
-40.50725
172.71304
Pi117
Pi119
-40.50729
172.71275
-40.50732
172.71265
Pi120
Pi122
Pi123
-40.50739
172.71242
Farewell Formation
FG
250
245
230
225
220
215
210
205
200
195
190
185
clay
silt
vfs
fs
ms
cs
vcs
granule
pebble
cobble
boulder

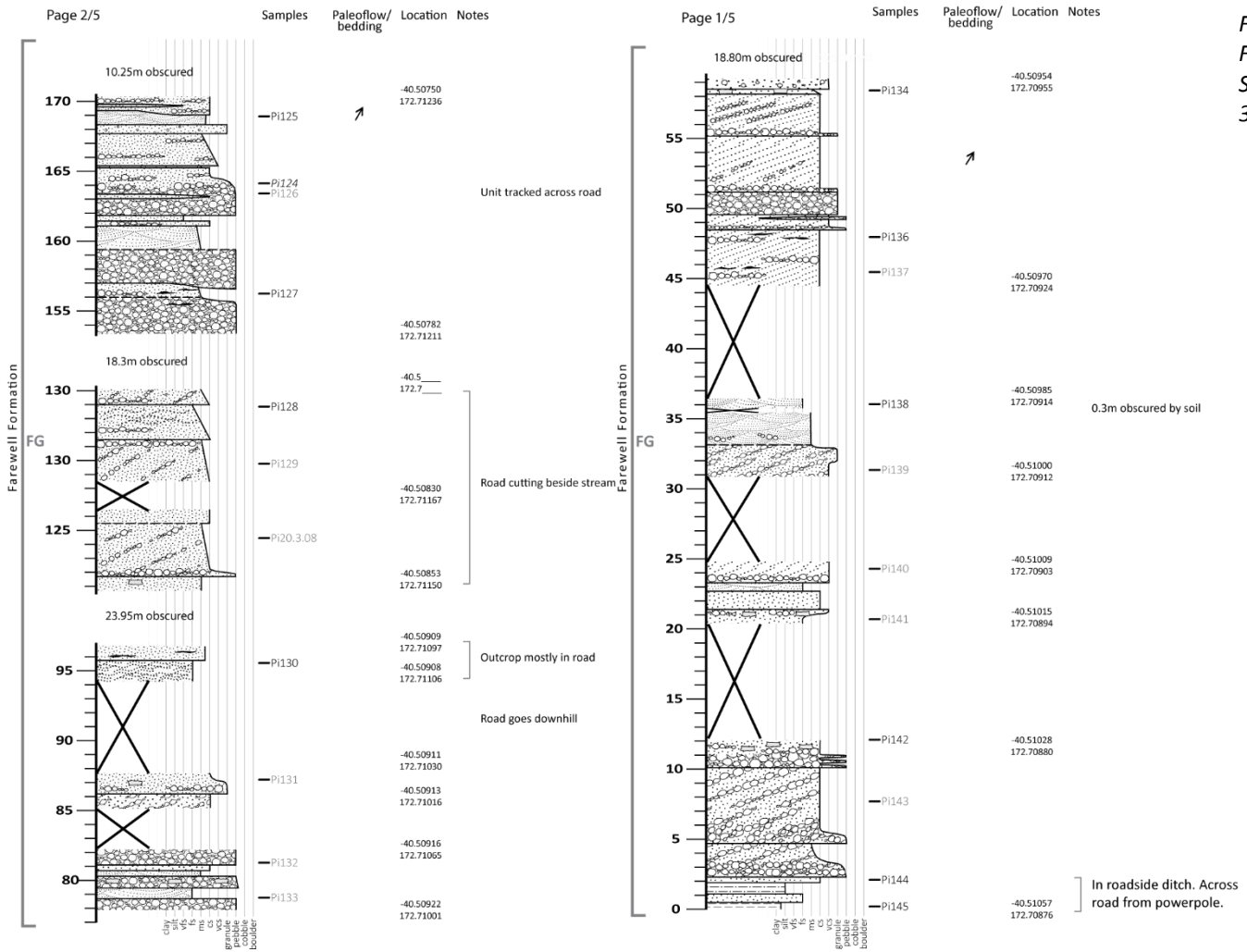

Fig. 3.19: Stratigraphic column of the Farewell Formation along the Pillar Point walking track. Section is gravelly braided association. See Fig. 3.5 for legend.

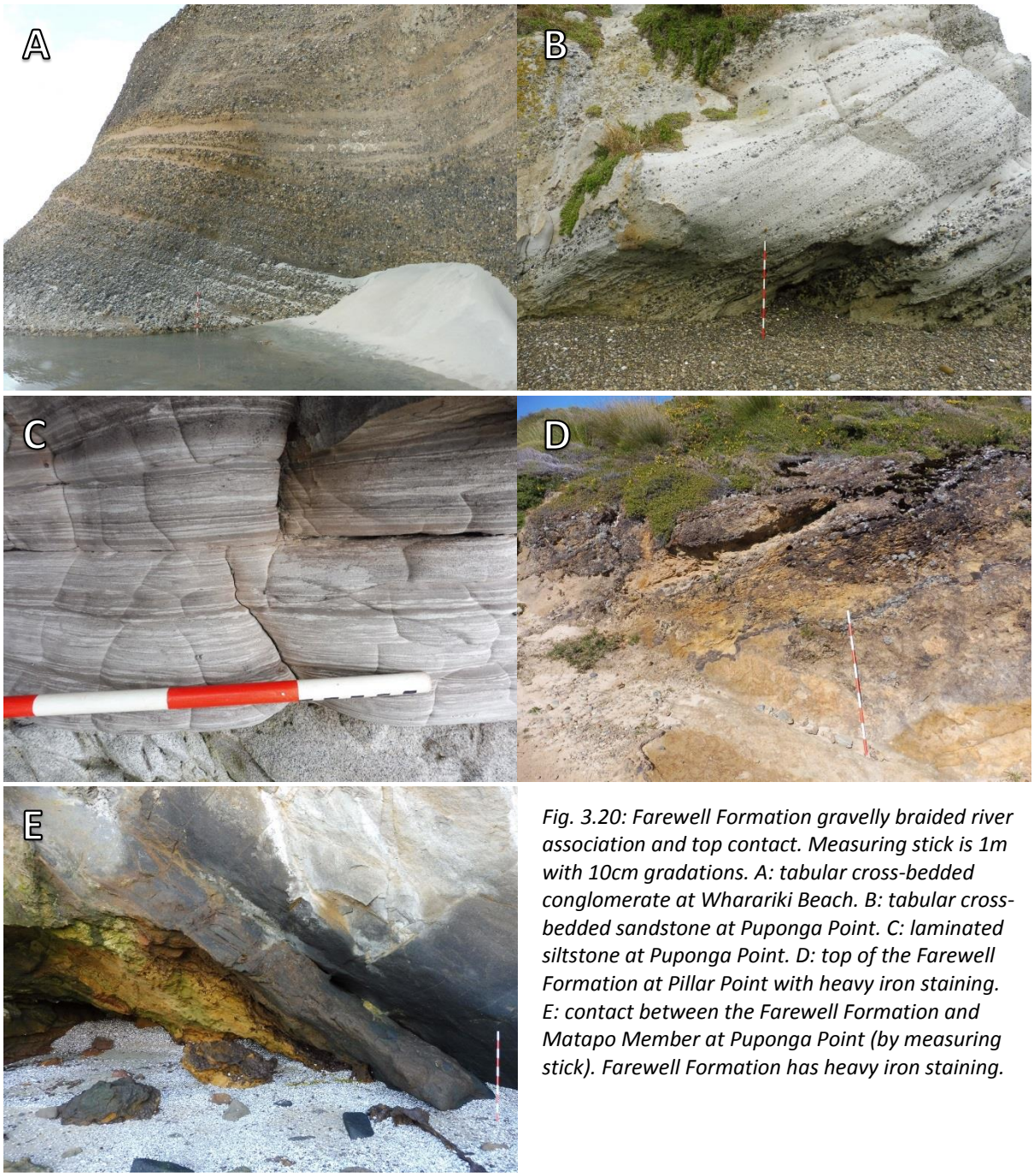

Fig. 3.20: Farewell Formation gravelly braided river association and top contact. Measuring stick is 1m with 10cm gradations. A: tabular cross-bedded conglomerate at Whararikí Beach. B: tabular cross-bedded sandstone at Puponga Point. C: laminated siltstone at Puponga Point. D: top of the Farewell Formation at Pillar Point with heavy iron staining. E: contact between the Farewell Formation and Matapo Member at Puponga Point (by measuring stick). Farewell Formation has heavy iron staining.

3.5.4 Upper contact of the Farewell Formation

The contact of the Farewell Formation with the overlying Matapo Member is well exposed at Puponga Point (Fig. 3.18E). The top of the Farewell Formation is also exposed at Pillar Point, although the Matapo Member (Otaraoa Formation) has been removed (Fig. 3.18D). The top 10-15m of the Farewell Formation is heavily iron stained (Figs. 3.18, 3.20D-E) increasing

towards the top contact. Iron oxides occur as cements, nodules and pans. The contact itself is sharp and planar on an outcrop scale (Fig. 3.20E).

3.6 Paleoflow

Paleoflow measurements from the North Cape and Farewell formations are shown in Fig. 3.21. In the Rakopi Formation outcrops in this study there were no paleoflow indicators that could be measured. Wizevich (1994) determined a northward paleoflow direction from imbrication in the Otimataura Conglomerate outcrops in the Marble Creek and Coal Creek areas.

The North Cape Formation shows west to north-northwest paleocurrent directions. At Pecks Point, the paleocurrent is directly perpendicular to the Wakamarama Fault, showing drainage away from the fault scarp. At Maori Point the paleoflow is toward the northwest, subperpendicular to the fault. Similarly, at Mangarakau the paleoflow is toward the north-northwest. These measurements are consistent with the north to northwest trend reported by Titheridge (1977) for the North Cape Formation, and reasonably consistent with Bal and

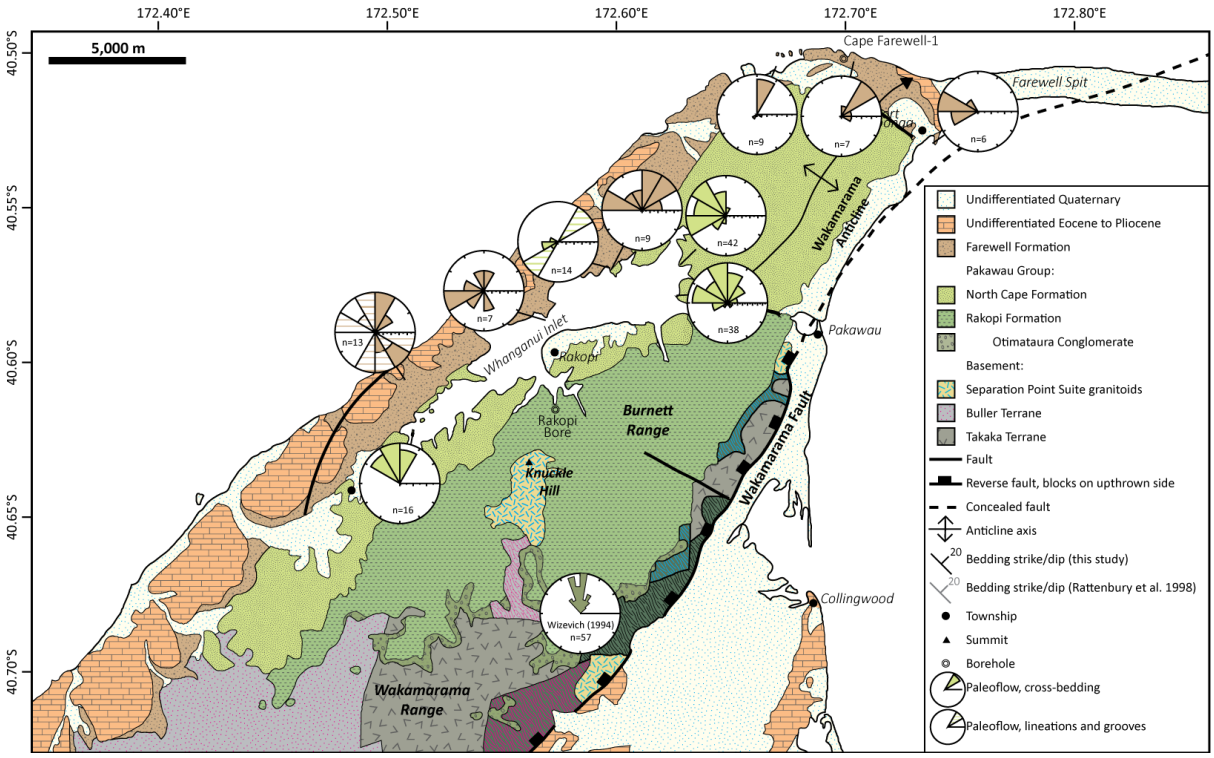

Fig. 3.21: Paleoflow directions from the Otimataura Conglomerate (data from Wizevich 1994), North Cape and Farewell formations.

Lewis (1994) who determined a north to northeast trend for the North Cape Formation in the southern Whanganui Inlet.

The Farewell Formation has variable paleocurrent directions. In the southern part of the outcrop, at Moki Point and Te Hapu Road, there is a broad range of paleoflow directions. This may be due to varying channel orientations. This supports the interpretation of the meandering river lithofacies association at Te Hapu Road as a meandering river.

The gravelly braided river association at Whararíki Beach and Pillar Point have paleoflow toward the northeast. This is parallel to the Wakamarama Fault, showing dominant drainage along the axis of the basin. By contrast, the paleoflow at Puponga is to the west, flowing subperpendicular away from the Wakamarama Fault. This shows there was still drainage from the material uplifted by the Wakamarama Fault. These measurements are consistent with those reported by Titheridge (1977) and Stark (1996).

3.7 Paleogeography

The Rakopi Formation is interpreted as fluvial and floodplain deposits formed on a low gradient coastal plain (Browne et al. 2008). The formation has similar lithofacies throughout its outcrop area and through the stratigraphic thickness. The floodplain and fluvial systems were therefore extensive.

The Otimataura Conglomerate is interpreted as deposits from alluvial fans draining directly off the Wakamarama Fault scarp (Fig. 3.22, Wizevich 1994). The Otimataura Conglomerate only occurs at the base of the Rakopi Formation, in the southern part of the field area and in the north in Cape Farewell-1 (Carter and Kintanar 1987; Rattenbury et al. 1998). It is thickest closer to the Wakamarama Fault in the Marble Creek-Otimataura Stream area. The Otimataura Conglomerate is absent in the Pakawau Bush Road region. The greater thickness in the south and the north suggests that these segments of the Wakamarama Fault had the most offset during this time (Fig. 3.22).

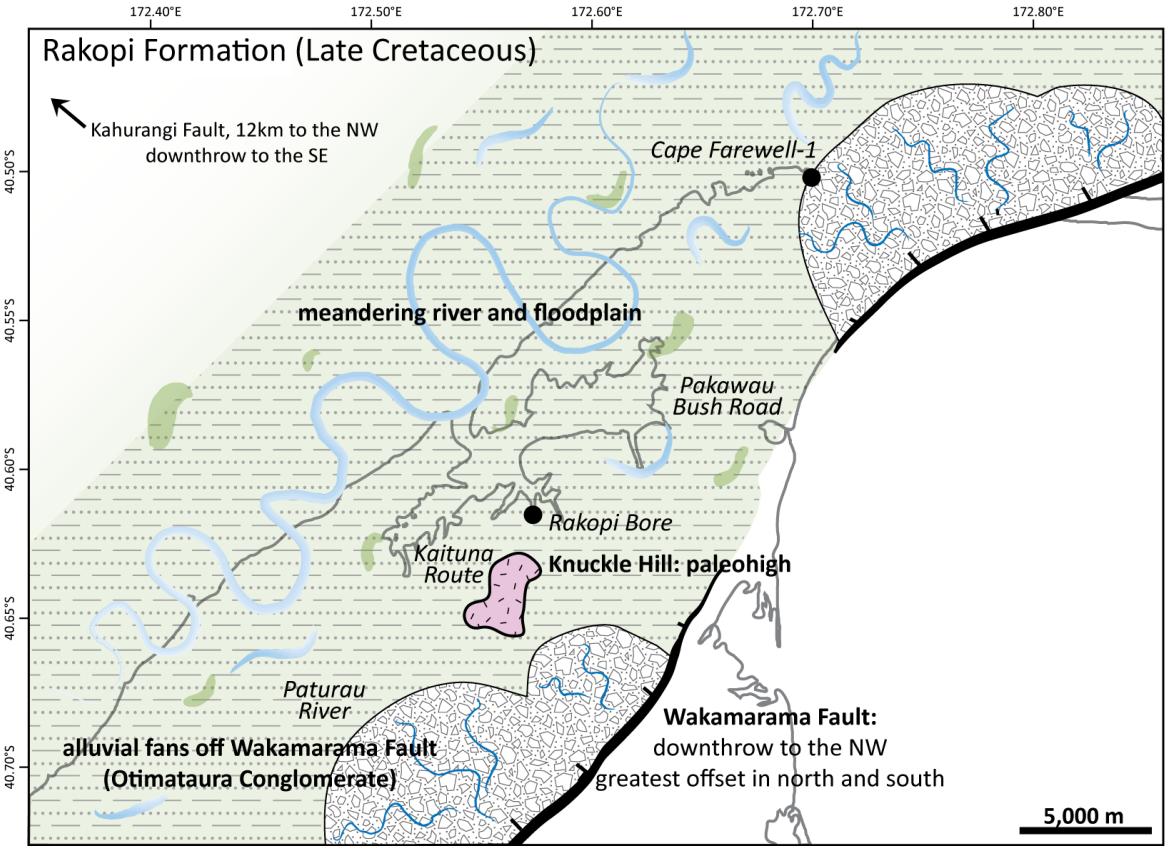

Fig. 3.22: Paleogeography of the Rakopi Formation constructed from outcrop sedimentology. Locations of key outcrops are labelled.

The North Cape Formation has a more complicated spatial and temporal lithofacies distribution (Fig. 3.23). The environment was shallow marine and coastal, with fan deltas prograding off the Wakamarama Fault into a marine embayment (Higgs et al. 2010). The depositional environments include high energy tidal channels on a delta front (lithofacies association A1), low energy intertidal and supratidal coastal deposits (A2), and fluvial delta top deposits (A3). There is usually a transition up the stratigraphy from the deeper water association A1, to the shallow water and coastal A2, to terrigenous A3. This shows coastlines prograding, suggesting the deltas were building outwards. The paleoflow data also shows dominant flow away from the Wakamarama Fault (Fig. 3.21), supporting the interpretation of fan deltas fed from the fault scarp.

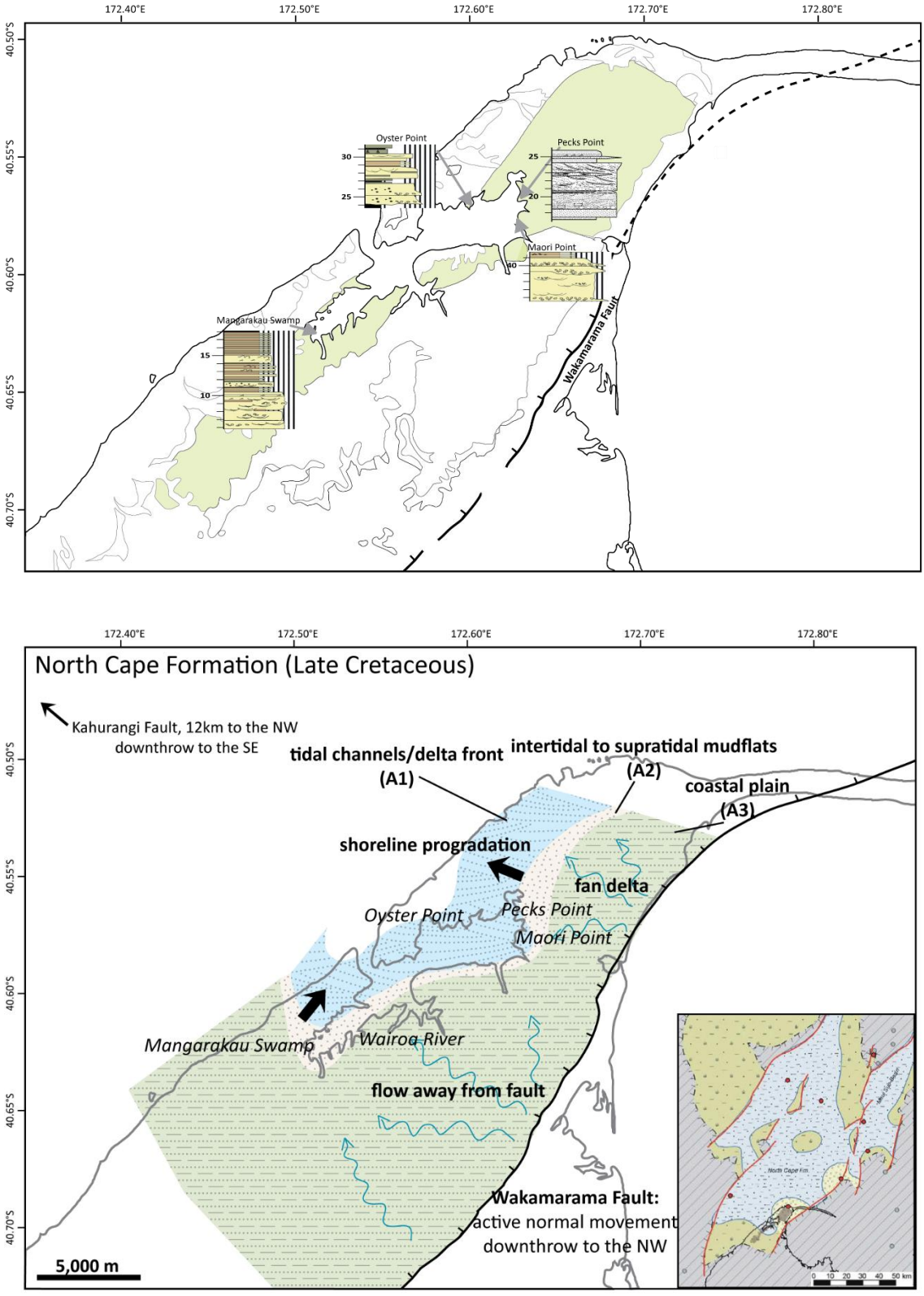

Fig. 3.23: Spatial variation in lithofacies association and local and regional paleogeography of the North Cape Formation. The first map shows sections of representative facies from the outcrops in this study. These sections were used to construct the paleogeographic map. Regional paleogeographic map inset from Strogen (2011).

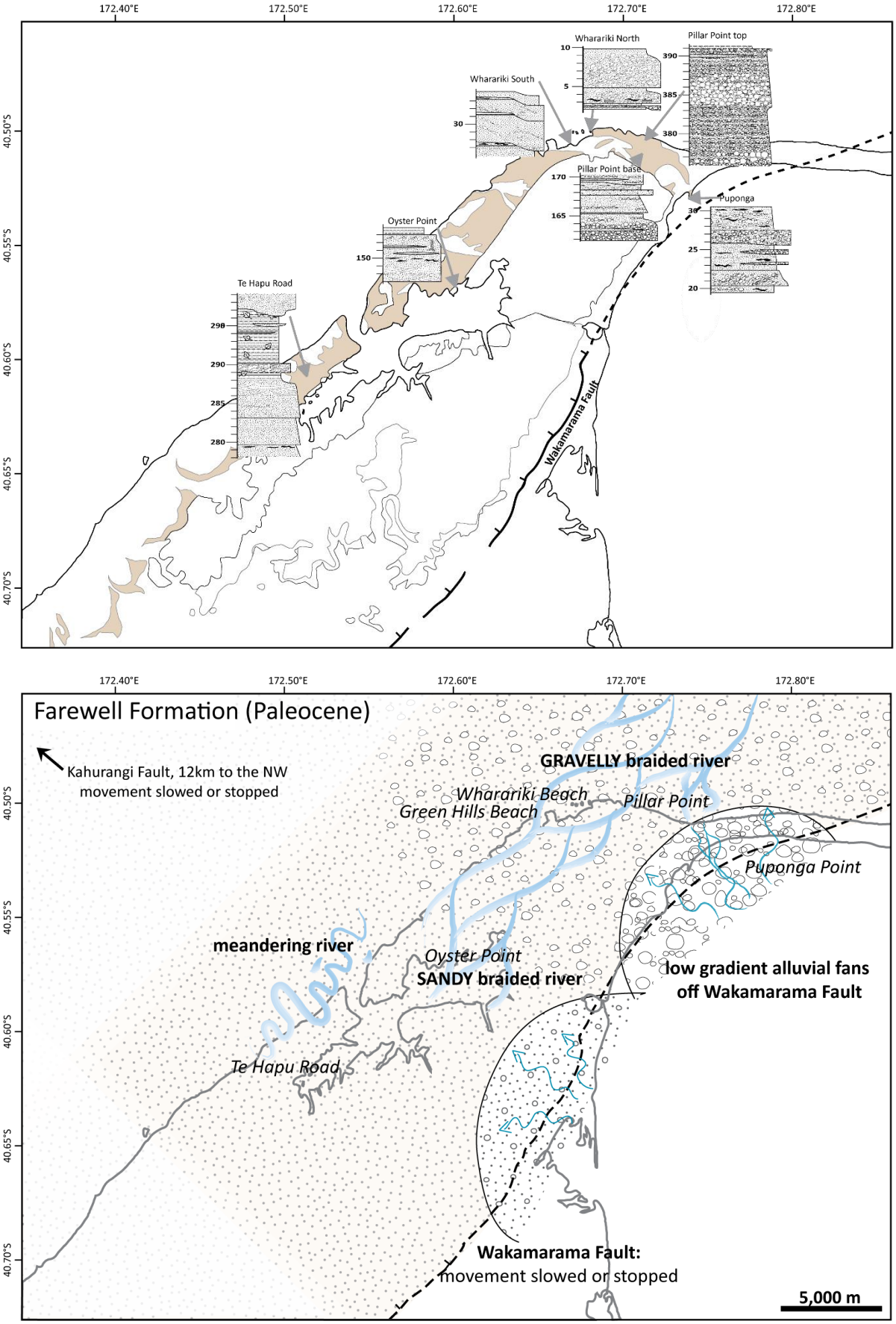

Fig. 3.24: Spatial variation in lithofacies association and paleogeography of the Farewell Formation.

The Farewell Formation is a terrigenous fluvial deposit, with a range of fluvial styles. The lithofacies associations have thicker mud units in the southwest, are sand-dominated in the central part of the field area, and are gravelly in the northeast (Fig. 3.24). The Farewell Formation also becomes more conglomeritic up the stratigraphy (Figs. 3.14, 3.18).

Most of the Farewell Formation is interpreted as braided river deposits, with grain size ranging from sand to gravel. The meandering river association, which has thicker mudstone units and sandstones in well-defined channels, only occurs at Te Hapu Road, the outcrop furthest from the Wakamarama Fault. This could be a smaller river system in the floodplain of the main braided river (Fig. 3.24). In the Kupe South field offshore, the Farewell Formation is also interpreted as an axial river system, with sandy channels in the centre of the Manaia half-graben and finer overbank deposits and smaller river systems towards the edges (Arnot 2017 personal communication). A similar model is appropriate for the Pakawau sub-basin.

The paleoflow data shows a strong component of axial drainage, with the paleoflow dominantly from the southeast (Fig. 3.21). At Puponga, flow is from the east, subperpendicular to the Wakamarama Fault. This demonstrates that although movement on the Wakamarama Fault had slowed or stopped by Paleocene time (Reilly et al. 2015), drainage was still occurring away from the uplifted footwall block. Low-gradient alluvial fans were likely to be developed feeding into the main basin (Fig. 3.24). This could explain the gravellier nature of the braided rivers in the north, if coarser gravels were being fed into the basin from the basin margins in the north.

3.8 Conclusions

The Rakopi Formation has two lithofacies associations: the coarse Otimataura Conglomerate, and finer grained interbedded silt, sand, and coal. The proposed environment was a low gradient coastal plain with meandering rivers on a floodplain setting, with these rivers having some marine influence. At the eastern margin alluvial fans were draining across the Wakamarama Fault.

The North Cape Formation has three lithofacies associations: A1 dominated by channelised, bidirectional trough cross-bedded sandstones with mud-drapes; A2 dominated by finely interbedded sandstones and siltstones; and A3 with sandstone, mudstone, and coal. These

deposits represent a marginal marine to coastal plain environment with fan deltas prograding into a marine embayment from the Wakamarama Fault.

The Farewell Formation has three lithofacies associations: a meandering river association with thick overbank mudstone deposits and sandstone in channels; a sandy braided river association with thick sandstone units with trough cross-bedding and complex stacked channels, and a gravelly braided river association with abundant cross-bedded conglomerates. The Farewell Formation is entirely fluvial and shows no evidence for marine influence. The paleoflow of the Farewell Formation shows dominantly axial flow, with some flow away from the Wakamarama Fault.

4. CONGLOMERATE COMPOSITION

4.1 Introduction

Conglomerate clasts are complete pieces of the original source material, which can be analysed by petrographic and geochemical techniques for direct comparison to potential source areas. The aim of this chapter is to describe the composition of the conglomerates of the Rakopi, North Cape, and Farewell formations and how this changes through the stratigraphy and across the outcrop region. The aim is to match the major clast types to basement or intrabasin sources in order to reconstruct drainage pathways. The petrography and geochemistry of the major clast types is described and compared to potential sources.

4.2 Methods

4.2.1 Clast count methods

At twenty-three locations, clast counts were undertaken on conglomerate beds with clasts larger than coarse pebble (32 mm diameter). Where possible, the count was done on the bedding surface of a unit. In cases where the bedding surface was not exposed, which was the majority of locations, clast counts were completed on cross-section exposures of a single bed, over less than 2 m of stratigraphy.

Before counting, each clast type in the conglomerate was noted. Representative samples from each clast type were collected for later thin section and geochemical analysis. To compare the conglomerate clast count results to the petrographic sandstone composition, a sandstone sample was collected for every site from a sandstone lens within the conglomerate if possible or from an adjacent bed. Sample locations and descriptions are included in Appendix B.

To make the clast count, a ruler was placed against the outcrop surface and clast types noted every 5 cm for coarse and very coarse pebble conglomerate sites, and every 10 cm for cobble conglomerate sites. Clasts less than 2 cm in diameter were counted as matrix. Where matrix was intersected this was noted. A total of at least 100 clasts were counted at each location. Clast count data is included in Appendix C.

4.2.2 Clast petrology methods

Sixty-seven clast samples representing a range of clast types were selected for thin sectioning. The granitoids and metasedimentary clasts were stained for K-feldspar using Na-cobaltinitrate stain on half of the thin section. Each clast thin section was described, including whole rock and mineral textures, and the modal mineralogy was estimated (Appendix D). On a selection of the granitoid clasts, a point count of 100 grains at 2 mm step length was conducted. The results of the point count were compared to the estimated mineralogy of the same thin section to validate the estimation (Appendix D).

4.2.3 Clast geochemistry methods

Approximately 30 g samples from the representative conglomerate clast samples were crushed to a powder with a tungsten carbide ring mill. Many of the clasts had a weathering rind and residual matrix cemented to them. Where the clasts were large enough, this was cut off with a rock saw. Smaller clasts were scrubbed to remove attached matrix and cement.

Twenty-seven crushed clast samples were analysed for major elements in the University of Canterbury X-ray fluorescence spectrometry (XRF) laboratory. The samples were prepared by oven drying and loss on ignition (LOI) was calculated by heating in a furnace. A split of the samples was prepared for major element analysis by adding a flux and ammonium nitrate to create a fusion bead. A Phillips PW 2400/00 x-ray spectrometer was used for the major element analysis. The raw geochemical data is included in Appendix E.

Due to lack of availability of University of Canterbury facilities, 78 clast samples, including the 27 analysed at the University of Canterbury, were sent to Spectrachem Ltd. for major and trace element analysis by XRF. For quality control, two crushed samples (Pu225, OP076) were split into two portions for separate analysis at the two laboratories in order to compare the two sets of results (Appendix F). Two granite basement samples from the Separation Point Suite at Knuckle Hill were also analysed.

Spectrachem Ltd. prepared the crushed samples by drying to 110°C, which was used as the reporting basis. LOI was calculated by ignition at 1000°C. For major element analysis, a lithium metaborate/tetraborate fused glass bead was prepared. For trace element analysis, a pressed powder briquette was made using 10% analytical-grade wax binder. A SRS3000

Siemens/Bruker x-ray fluorescence spectrometer was used for both major and trace element analysis. The Spectrachem laboratory has ISO17025 Certification (CRL Energy Ltd 2017; International Organization for Standardization 2017). The raw geochemical data is included in Appendix E.

4.3 Clast count results

The Otimataura Conglomerate member of the Rakopi Formation at the base of the Paturau River section is dominated by metasedimentary clasts (Figs. 4.1, 4.2). Vein quartz, volcanics, and chert are minor constituents of the upper two conglomerates. The clasts are subangular to angular, in contrast to the subrounded to rounded conglomerates of the North Cape and Farewell formations.

The North Cape Formation conglomerates are dominated by metasedimentary clasts, with minor granitoid clasts, vein quartz, volcanics, grey sedimentary clasts, and rare weathered granitoids, schist, and chert (Fig. 4.1). There are no strong spatial or stratigraphic trends.

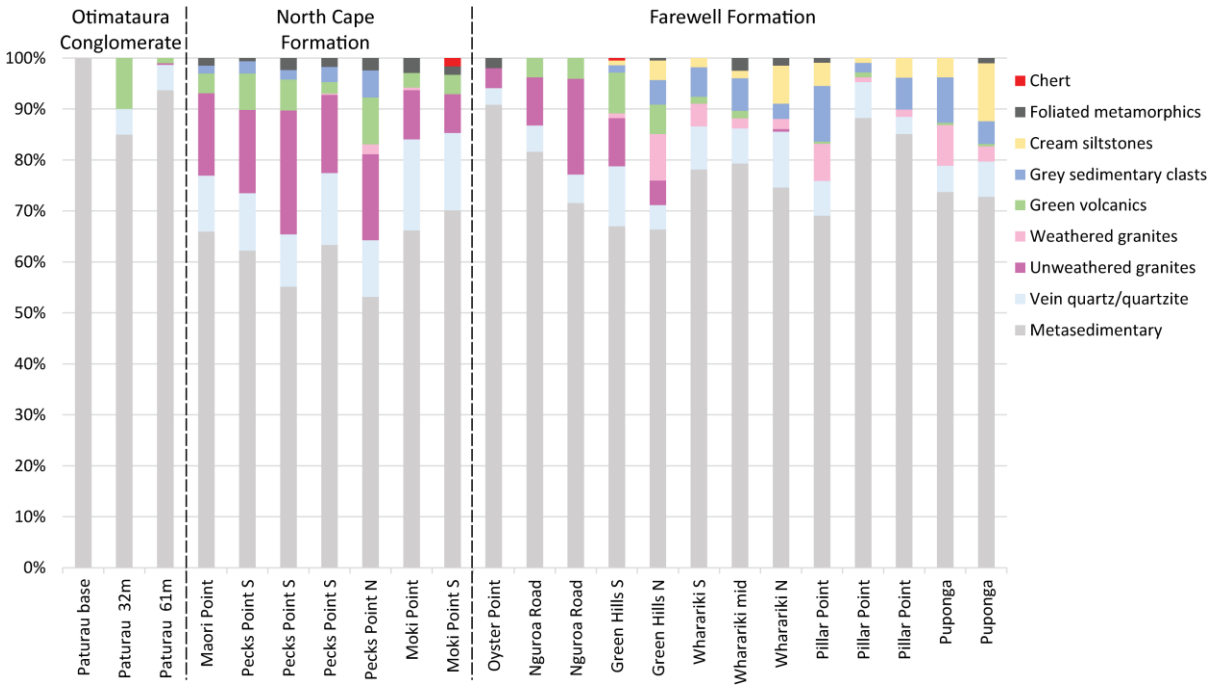

Fig. 4.1: Bar graph showing clast count results. Clast counts are organised into approximate stratigraphic position, with oldest conglomerates to the left.

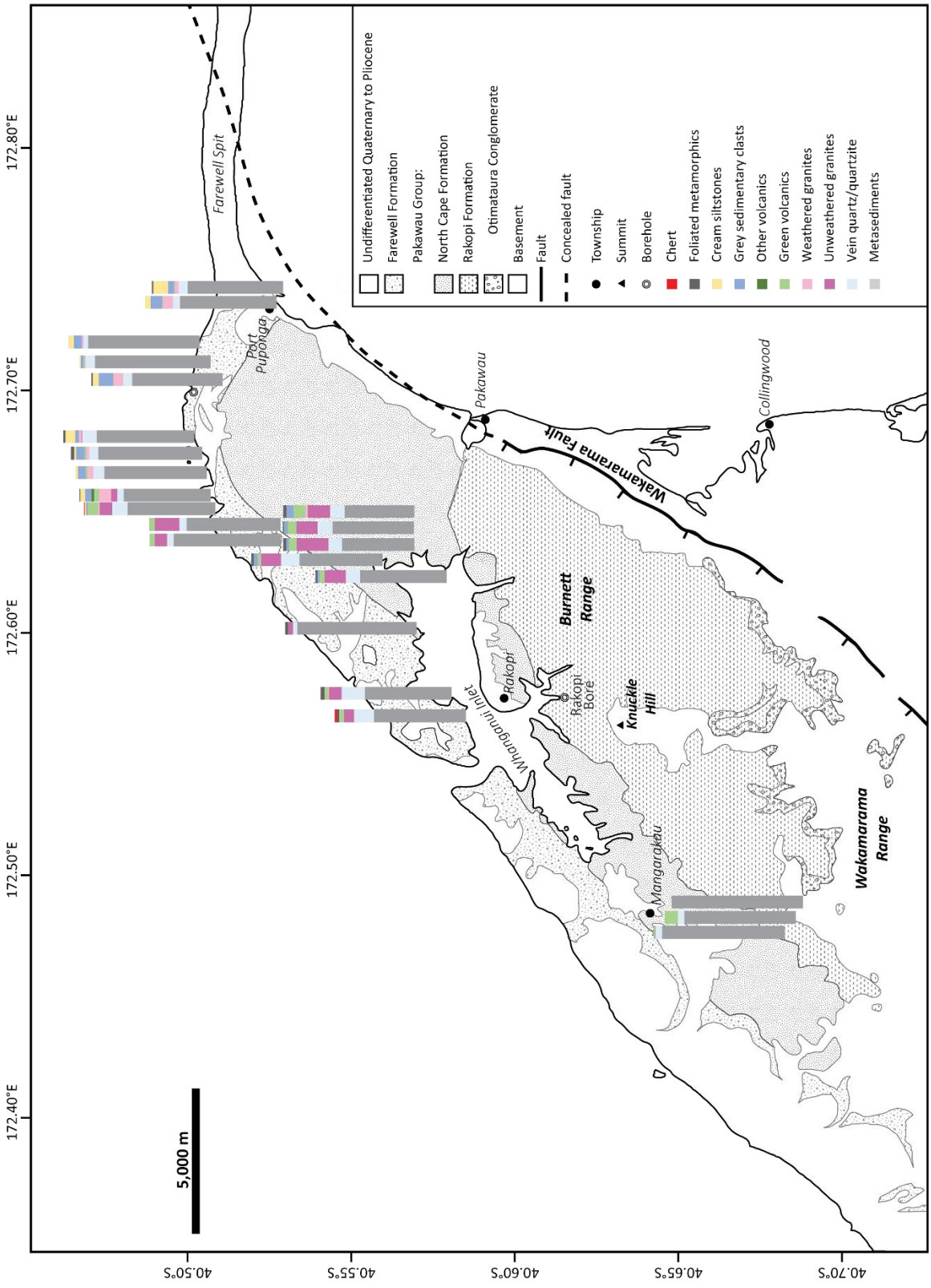

Fig. 4.2: Clast count results organised by outcrop location. Bottom of the bars is on the approximate outcrop location.

The Farewell Formation conglomerates are dominated by metasedimentary clasts with minor fresh and weathered granitoid clasts, vein quartz, volcanics, soft cream and grey fine sandstones to siltstones, and rare schist and chert (Fig. 4.1). The granitoids become more weathered towards the top of the formation and are almost entirely absent in some conglomerates in the Pillar Point, Whararikí Beach, and Green Hills Beach outcrops. Soft sedimentary clasts become more common towards the top of the Farewell Formation. The sedimentary clasts are either grey or cream in colour, moderately indurated, and typically siltstones. Cream sedimentary clasts are only present in the northern part of the field area (Fig. 4.2).

4.4 Metasedimentary clasts

Metasedimentary clasts are the dominant clast type in all of the studied conglomerates. In hand sample, they are well indurated very fine sandstone to siltstone, dominantly grey in colour, some are greenish-grey, red, and cream. The red and cream metasedimentary clasts were only observed in the Farewell Formation. Some metasedimentary clasts have quartz veins.

There are five potential metasedimentary basement sources in the northwest Nelson region. In the Buller Terrane, there is the Greenland Group and the more quartzose Golden Bay Group. The Greenland Group crops out further to the south than the Golden Bay Group, and in places the Golden Bay Group overlies the Greenland Group (Fig. 2.8) (Roser et al. 1996; Rattenbury et al. 1998; Nebel-Jacobsen et al. 2011). The Takaka Terrane comprises three compositionally distinct metasedimentary units. The Cambrian age sedimentary rocks of the Haupiri Group are the oldest, with a strong volcaniclastic signature (Fig. 4.3) (Roser et al. 1996; Münker and Cooper 1999). The overlying Cambrian to Ordovician Mount Patriarch and Mount Arthur groups are highly calcareous with less of a volcanic component (Roser et al. 1996). The Silurian to Devonian Ellis Group and Baton Formation are the most compositionally mature, being highly quartzose (Fig. 4.3) (Grindley 1980; Roser et al. 1996).

4.4.1 Metasedimentary clast petrology

The majority of the metasedimentary clasts are highly quartz-rich, plotting as quartzarenites and subfeldsarenites on a QFL diagram (Fig. 4.3). The clasts can be divided into four textural

groups. The majority of the samples are well-sorted very fine to fine sandstones with sutured quartz grain boundaries (Fig. 4.4A). These quartzarenites and subfeldsarenites contain quartz with undulose extinction, minor alkali feldspar with microcline twinning, minor plagioclase, chert lithics, opaques, detrital muscovite, and rare high birefringence heavy minerals.

Many of the samples are bimodal, with grain-supported very fine to fine sand in a silt matrix (Fig. 4.4B). The quartz grain boundaries are sutured. The composition and textures are similar to the well sorted sutured quartz sandstones above.

There is one very well sorted fine sandstone (Fig. 4.4C-D). The grains are sub-angular and have clay and red-brown opaques concentrated along the grain boundaries. This sample is a quartzarenite, with minor alkali feldspar. The “dirty” grain boundaries and retention of the original sedimentary textures and absence of metamorphic minerals suggest a very low-grade metamorphism. The quartz grains show very strong undulose extinction, indicating some strain.

There is one sample which shows a mosaic quartz texture (Fig. 4.4E). This sample is also a quartzarenite, with small interstitial crystals of alkali feldspar showing no twinning, and accessory muscovite and biotite.

The highly quartz-rich nature of the metasedimentary clasts means they are not derived from the Cambrian Takaka Terrane, as these are less mature sandstones with abundant volcanic lithics (Fig. 4.3) (Grindley 1980; Pound et al. 1993; Roser et al. 1996; Jongens 1997). From available data (Strong et al. 2016) the Baton Formation of the Devonian Takaka Terrane has similarly high lithic contents (Fig. 4.3), meaning it is an unlikely source.

The Greenland Group has a similar quartz content to the clast samples (Fig. 4.3). However, the Greenland Group has plagioclase feldspar not microcline, and polycrystalline quartz is present (Laird 1972). It also has a higher lithic content than the metasedimentary clasts (Fig. 4.3). This makes the Greenland Group an unlikely source.

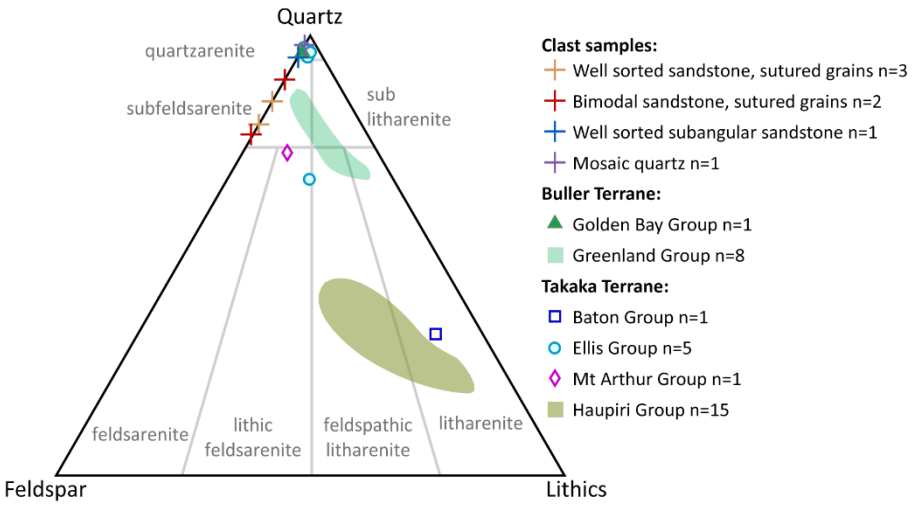

Fig. 4.3: Quartz-feldspar-lithics (QFL) diagram after Folk et al. (1970), showing composition of the metasedimentary clasts in the North Cape and Farewell formations compared to basement sources. Clasts are divided into their textural groups. Data source: Golden Bay Group Strong et al. (2016); Greenland Group Laird (1972); Baton Group Strong et al. (2016); Ellis Group original work from thin sections UC16743-UC16746, Strong et al. (2016); Mount Arthur Group Strong et al. (2016); Haupiri Group Pound (1993).

The remaining potential sandstones are the quartz-rich sandstone and quartzite of the Takaka Terrane Ellis Group (Hailes Quartzite and Fowler Formation), and the Buller Terrane Golden Bay Group. Very little literature is available on the petrology of the Takaka Terrane sedimentary units. The Hailes Quartzite and Wangapeka Formation are described by Grindley (1980) as "subangular quartz, minor albite, detrital muscovite, biotite, microcline, epidote, sphene, and accessory tourmaline, zircon, and Fe oxide" (p.20). Cooper (1965) describes the texture of the Hailes Quartzite as "rounded, even-sized quartz grains from 0.1 to 0.4 mm in diameter" (p.57). The metasedimentary clasts do not contain epidote, sphene, or tourmaline, and the feldspars are microcline not albite, and are typically finer than the medium sand grain size described by Cooper (1965). Thin sections of Ellis Group metasandstones from the University of Canterbury collection (C Anderson UC16744 – UC16748) have strongly undulose quartz with sutured boundaries similar to the metasedimentary clasts (Fig. 4.4F-H), have minor plagioclase, microcline, and chert lithics. They commonly have detrital muscovite and biotite, similar to the bimodal sandstone clasts (Fig. 4.4G-H). The overall texture and composition of these Ellis Group samples is similar to the well-sorted sandstone clasts with sutured quartz grains.

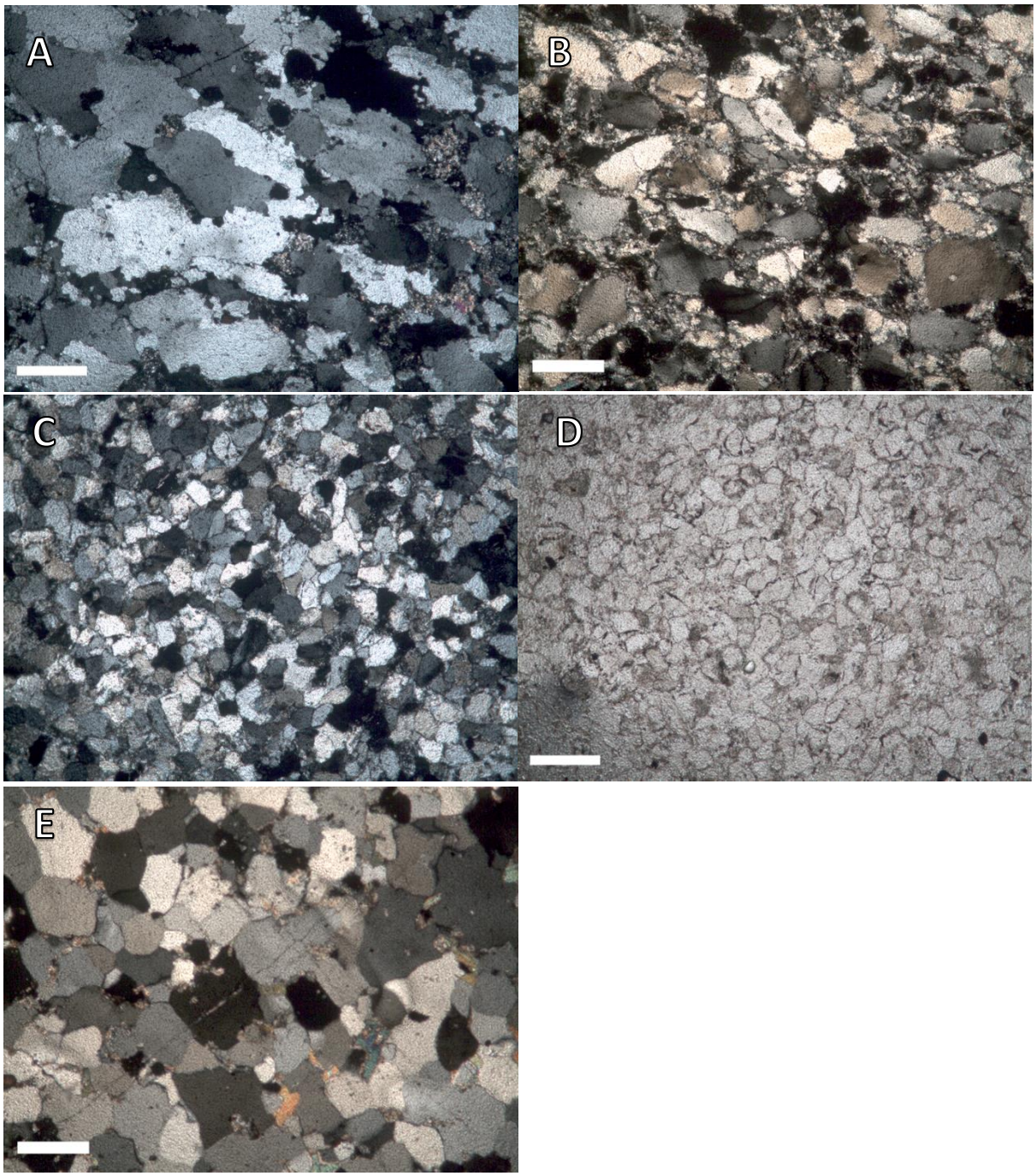

Fig. 4.4: Photomicrographs of metasedimentary clasts and basement sources. Scale bar is 200 μm. A: Wh285, clast with sutured quartz. B: Pu226, clast with sutured quartz in a silt matrix. C/D: Wh277.1 CPL/PPL, subangular very fine sandstone with dirty grain boundaries. E: MP037, clast with mosaic quartz texture.

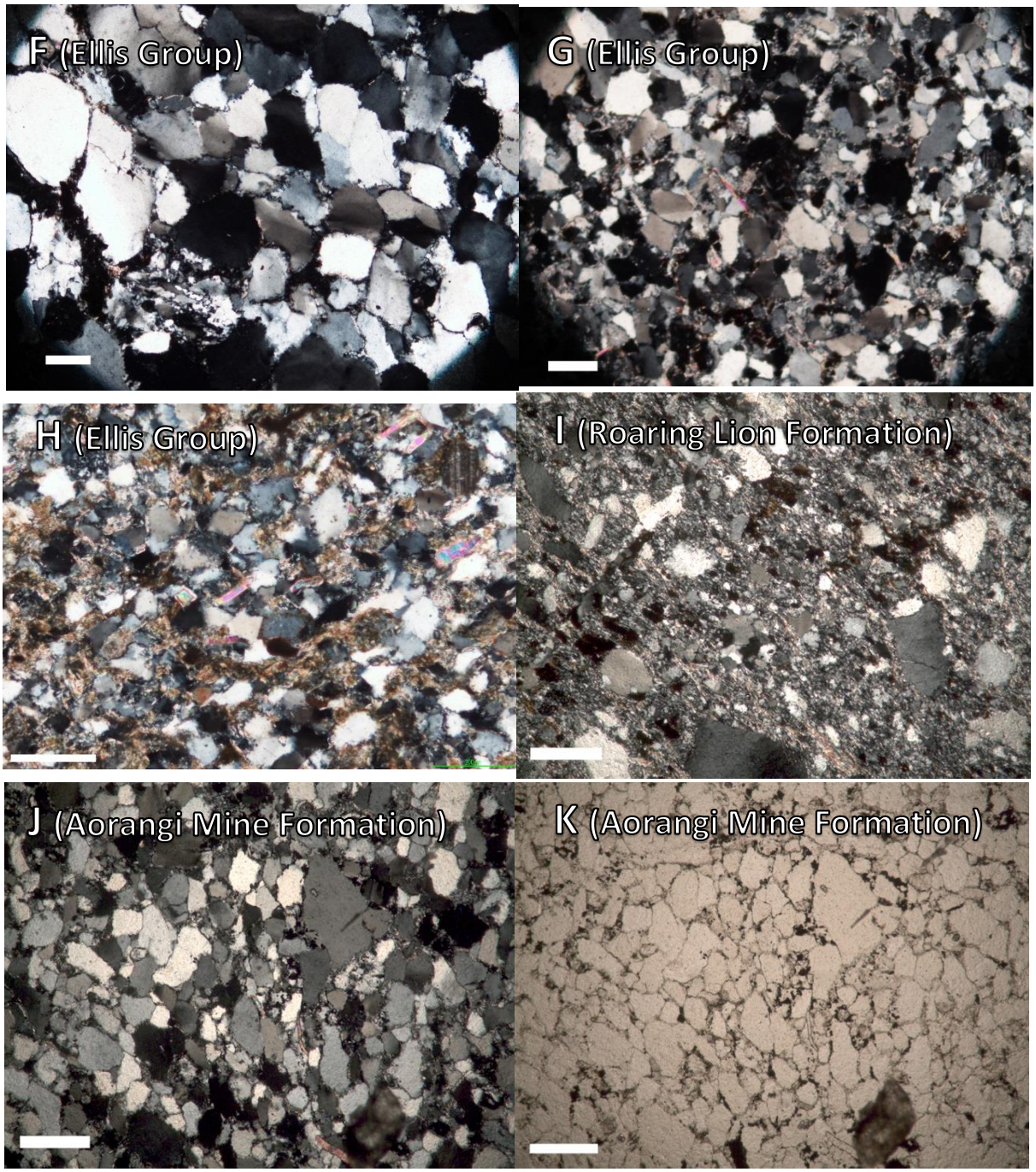

Fig. 4.4 cont.: Photomicrographs of metasedimentary clasts and basement sources. Scale bar is 200 μm. F: UC16743, sample from the Ellis Group, showing well-sorted texture, sutured quartz boundaries and strongly undulose extinction. Note textural similarity to A, Wh285. G: UC16744, sample from the Ellis Group, well-sorted fine sandstone with undulose quartz. H: UC16746, sample from the Ellis Group, very fine sandstone with muscovite and biotite matrix. I: RLF6 Harrison (1993), sample from Roaring Lion Formation of the Golden Bay Group showing very fine quartz grains in silt matrix with sutured boundaries. Note textural similarity to B, Pu226. J/K: LQ3A Harrison (1993), sample from Aorangi Mine Formation of the Golden Bay Group showing very fine, well sorted, angular quartz grains with dusty grain boundaries. Note textural similarity to C/D, Wh277.1.

The Golden Bay Group also exhibits similar composition and textures to the metasedimentary clasts. The Golden Bay Group Aorangi Mine Formation has a low degree of metamorphism, as shown by dusty grain boundaries (Fig. 4.4J-K) (Harrison 1993). This is very similar to the textures of the well sorted fine sandstone clast (Fig. 4.4C-D). Lithics in the Aorangi Mine Formation are chert (Burgess 1978; Harrison 1993). The Golden Bay Group Roaring Lion Formation and the Leslie Formation contain bimodal angular quartzarenites, similar in texture to the bimodal very fine sandstone clasts (Fig. 4.4I). However, feldspars in the Leslie Formation are albite (Harrison 1993).

4.4.2 Metasedimentary clast geochemistry

The source for the metasedimentary clasts is unlikely to be the Greenland Group, due to the clasts' high SiO_2 content (Fig. 4.5). The major element geochemistry of the samples fit best with the Takaka Terrane Ellis Group and the Mount Arthur and Mount Patriarch groups (Figs. 4.5, 4.6). As the basement data sets are small, a Buller Terrane Golden Bay Group source cannot be conclusively discounted for most of the clasts. Sample PP182 has much lower K_2O/Na_2O and higher F1 values than the Buller Terrane, and fits better with the Takaka Terrane (Figs. 4.5, 4.6).

The trace element geochemistry of the metasedimentary clasts is most similar to the Takaka Terrane Ellis, Mount Arthur, and Mount Patriarch groups (Fig. 4.7). The clasts have lower Ni concentrations than the Buller Terrane Golden Bay Group and have detectable Cr concentrations unlike the Golden Bay Group. (Fig. 4.7). Two samples, PP182 and Wh277.1 exhibit different trends to the rest of the clasts. Sample Wh277.1 has lower Ba, but still fits with the Ellis Group. Sample PP182 has higher V and significantly higher Sr than the other clasts. This trend fits better with the Mount Arthur and Mount Patriarch groups of the Takaka Terrane.

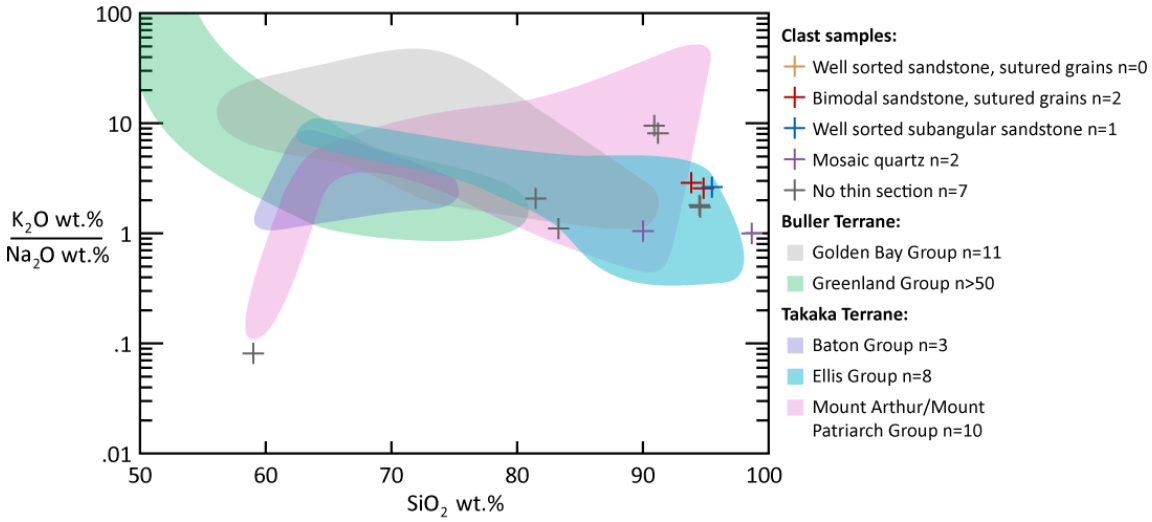

Fig. 4.5: Plot of K_2O/Na_2O against SiO_2, after Roser et al. (1996), comparing the major element geochemistry of the Takaka and Buller Terrane sedimentary and metasedimentary units to metasedimentary clasts.

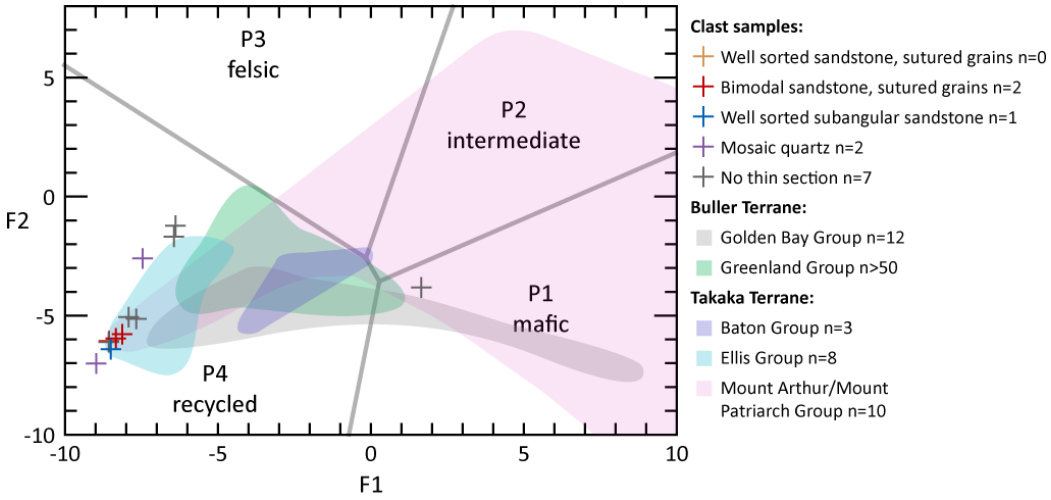

Fig. 4.6: Major element provenance discrimination plot (Roser and Korsch 1988) of metasedimentary clast samples compared to basement sources. Mount Arthur and Mount Patriarch Group have anomalously high F1 and F2 due to biogenic components increasing CaO.
$F1 = -1.773\ TiO_2 + 0.607\ Al_2O_3 + 0.76\ Fe_2O_3T - 1.5\ MgO + 0.616\ CaO + 0.509\ Na_2O - 1.224\ K_2O - 9.09$; $F2 = 0.445\ TiO_2 + 0.07\ Al_2O_3 - 0.25\ Fe_2O_3T - 1.142\ MgO + 0.438\ CaO + 1.475\ Na_2O + 1.426\ K_2O - 6.861$

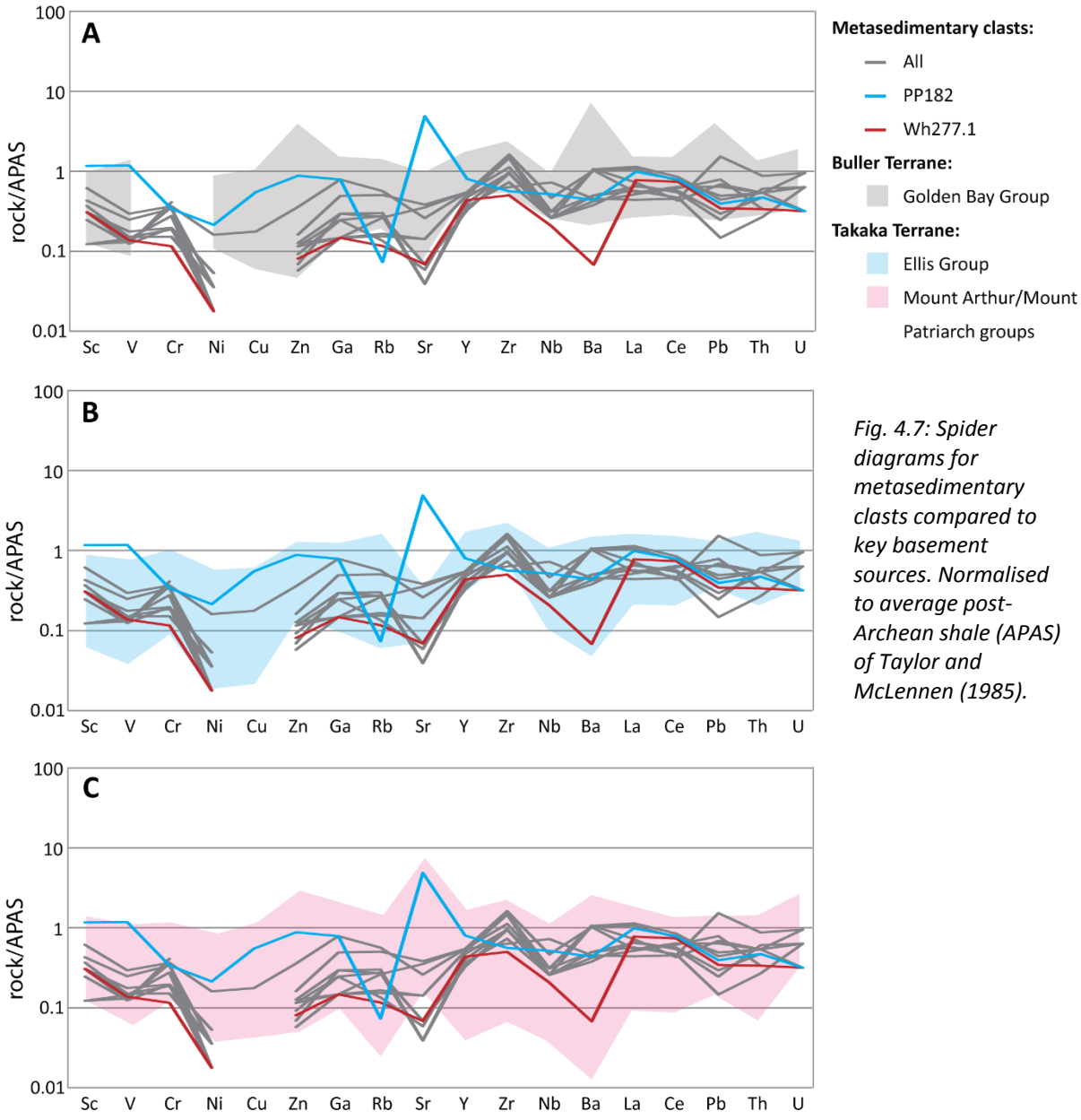

Fig. 4.7: Spider diagrams for metasedimentary clasts compared to key basement sources. Normalised to average post-Archean shale (APAS) of Taylor and McLennen (1985).

4.4.3 Provenance of metasedimentary clasts

The lack of volcanic lithics and high quartz content of the metasedimentary sandstones means they are unlikely to be from the Takaka Terrane Cambrian Haupiri Group and Mount Patriarch Group, or the Baton Formation. The clasts lack carbonates, making a Mount Arthur or Mount Patriarch Group source less likely. The petrographic textures of the clasts is similar to both the Buller Terrane Golden Bay Group and the Takaka Terrane Ellis Group. There is very little literature on the Ellis Group petrology, so the clasts cannot be definitively identified from the petrology alone.

The major and trace element geochemistry of the metasedimentary clasts is most similar to the Takaka Terrane. The majority overlap with the Ellis Group, while the geochemistry of sample PP182 indicate a Mount Arthur/Mount Patriarch source.

From the geochemical data, a Takaka Terrane Ellis Group provenance is preferred. However, more petrographic data from the upper Takaka Terrane is needed to definitively identify it as the metasedimentary clasts' source. Much of the Takaka Terrane basement east of the Wakamarama Fault is offshore in Golden Bay (Fig. 2.8) making comparison of the clasts to the likely Takaka Terrane source material particularly challenging.

4.5 Granitoid clasts

Granitoid clasts are the second most common clast type (Fig. 4.1). In hand sample they exhibit a variety of textures. Light coloured, equigranular granitoids are most common. Also present are porphyritic granitoids with pink feldspar phenocrysts approximately 10 mm long. Minor amounts of pink-coloured granites are present; the pink colour may possibly be a result of weathering. In the Green Hills Beach outcrop only, there are some weathered dark grey igneous clasts with lath-shaped feldspar phenocrysts 5-10 mm long.

There are two possible basement sources for the granitoid clasts. The first is the S-type Karamea Suite, which intrudes the Buller Terrane to the southwest of the field area (Fig. 2.8). The second is the I-type Separation Point Suite, which is part of the Median Batholith to the east and occurs in small plutons in the Golden Bay region such as at Knuckle Hill (Fig. 2.8). The Separation Point Suite is thought to underlie much of the Whanganui Inlet area (Tulloch and Mortimer 2017).

4.5.1 Granitoid clast petrology

In thin section, the granitoid clasts show a range of textures (Fig. 4.8). The majority are equigranular, medium-grained granitoids (Fig. 4.9A). Granitoids with this texture are generally less quartz-rich than the other clasts, plotting mostly as granites on a quartz-alkali feldspar-plagioclase diagram (Fig. 4.8). The alkali feldspars commonly have microcline twinning and perthitic texture (Fig. 4.9A). Some of the equigranular granites contain trace titanite (Fig. 4.9B), the only textural group to contain titanite. The equigranular granites contain minor interstitial muscovite and biotite (<3%).

Many of the granitoid clasts are porphyritic and foliated (Fig. 4.9C-D). The phenocrysts are coarse crystals of alkali feldspar, which have perthitic texture and microcline twinning. The medium grained groundmass is foliated, with the foliation shown by quartz ribbons and strings of muscovite and biotite. The quartz has strongly undulose extinction. The porphyritic foliated granitoids have more quartz than the equigranular granitoids, plotting mostly as granites and some as quartz-rich granitoids (Fig. 4.8). One sample is foliated, but not porphyritic. The mineralogy and texture of this sample is similar to the porphyritic foliated clasts.

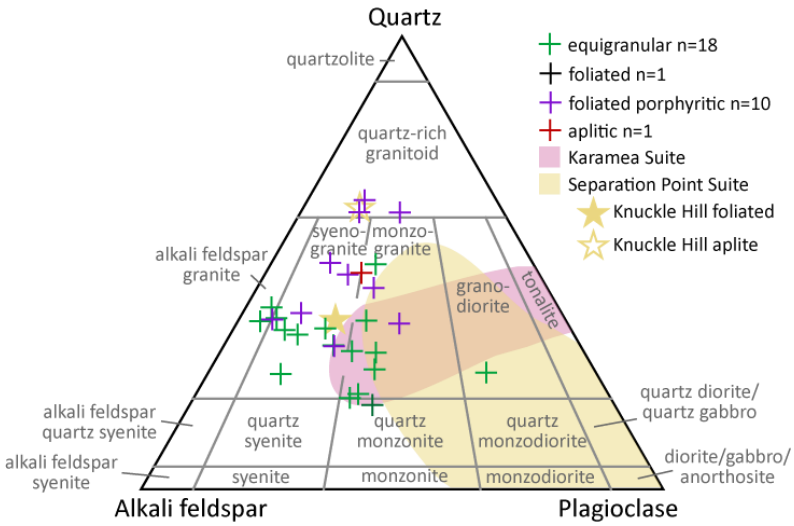

Fig. 4.8: Quartz-alkali feldspar-plagioclase IUGS classification of granitoid clast petrology (Le Maitre and International Union of Geological Sciences. Subcommission on the Systematics of Igneous 2004). Clasts are grouped based on the whole rock texture. Knuckle Hill data from this study, other basement data from Strong (2016).

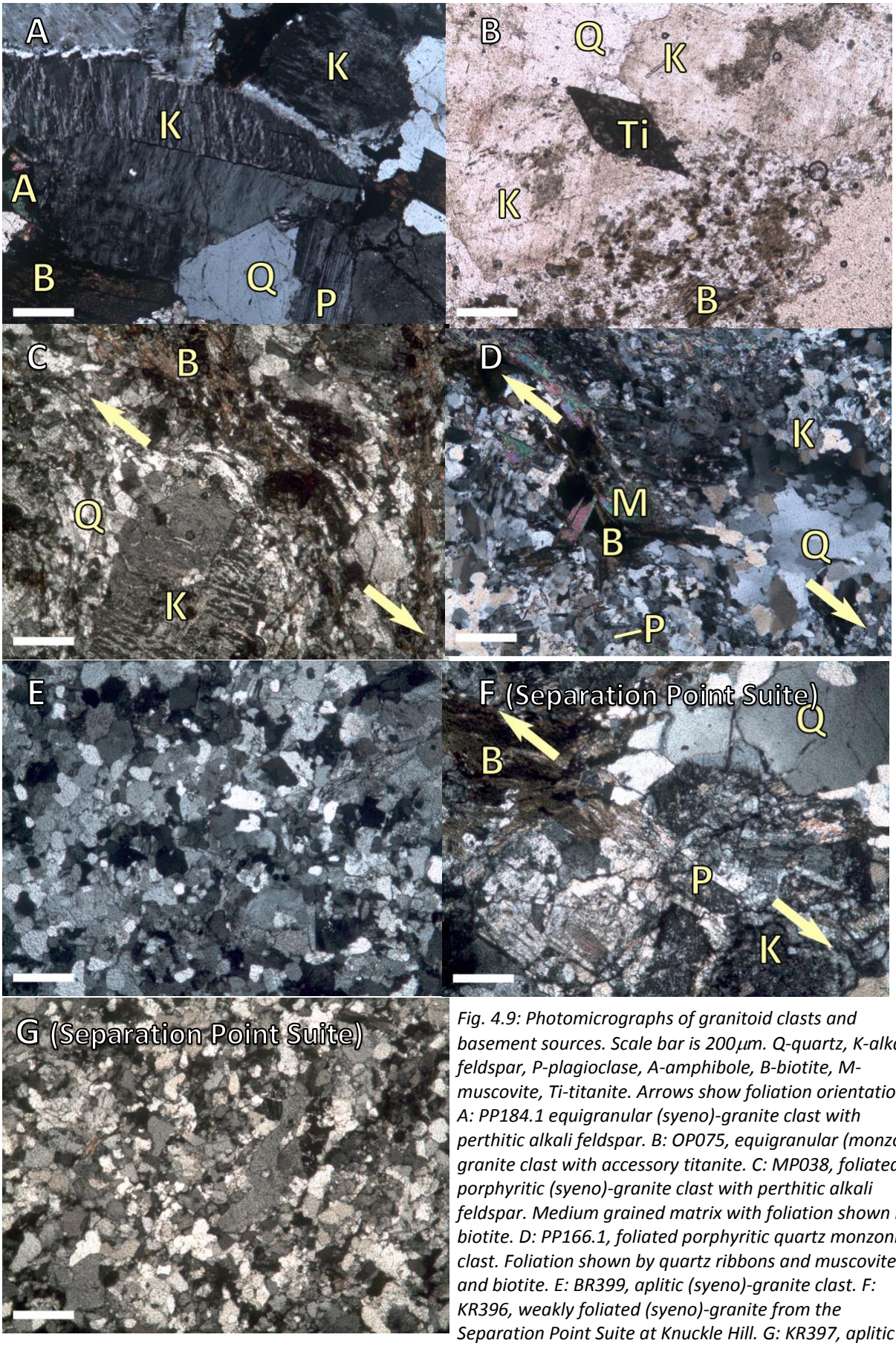

Fig. 4.9: Photomicrographs of granitoid clasts and basement sources. Scale bar is 200μm. Q-quartz, K-alkali feldspar, P-plagioclase, A-amphibole, B-biotite, M-muscovite, Ti-titanite. Arrows show foliation orientation. A: PP184.1 equigranular (syeno)-granite clast with perthitic alkali feldspar. B: OP075, equigranular (monzo)-granite clast with accessory titanite. C: MP038, foliated porphyritic (syeno)-granite clast with perthitic alkali feldspar. Medium grained matrix with foliation shown by biotite. D: PP166.1, foliated porphyritic quartz monzonite clast. Foliation shown by quartz ribbons and muscovite and biotite. E: BR399, aplitic (syeno)-granite clast. F: KR396, weakly foliated (syeno)-granite from the Separation Point Suite at Knuckle Hill. G: KR397, aplitic quartz-rich granitoid from aplitic veins in the Separation Point Suite at Knuckle Hill.

There is one sample with an aplitic texture. It is a fine to medium grained, equigranular granite (Figs. 4.8, 4.9E). The alkali feldspar has myrmekitic texture, and there is minor muscovite.

The granitoid clasts do not match the modal mineralogy previously recorded in either the Karamea Suite or the Separation Point Suite (Fig. 4.8). The presence of alkali feldspar granites is more suggestive of an A-type affinity (Whalen et al. 1987; Eby 1992; Tulloch 2017). However, the Separation Point Suite may include a wider range of compositions than shown in Fig. 4.8. Hutton (1995) reported that the Separation Point Suite contains syenogranites on the western margin of the Median Batholith. The granite sample collected in this study from the Separation Point Suite at Knuckle Hill is more plagioclase-depleted than is typical for the Separation Point Suite (Fig. 4.8). The Knuckle Hill granite also has a weakly foliated texture (Fig. 4.9F), consistent with the foliated granitoid clasts. The granite at Knuckle Hill is intruded by veins of aplite (Fig. 4.9E), which is more quartz-rich than the host granite (Fig. 4.8). This is a possible source for the aplitic clasts. Accessory titanite, as seen in some clasts, is also common in the Separation Point Suite, but not the Karamea Suite (Tulloch 1983; Muir et al. 1995).

4.5.2 Granitoid clast geochemistry

On a total alkali silica (TAS) diagram, the unweathered granitoids plot as granites and one syenite sample (Fig. 4.10), which is consistent with the petrology. In the weathered samples, K_2O and Na_2O are depleted. This is typical in weathered granites, where CaO and Na_2O are depleted due to the removal of plagioclase before more stable orthoclase (Harriss and Adams 1966; Middelburg et al. 1988). The dark igneous clast from Green Hills Beach plots as a gabbro diorite, although its high LOI (8.01 wt.%) indicates that it has been affected by weathering. The low SiO_2 content of 49.5 wt.% is still suggestive of a more mafic source feeding the Green Hills Beach conglomerate, such as a mafic end-member of the Separation Point Suite.

A ternary diagram of Na_2O, CaO, and K_2O was used by Tulloch (1983) to distinguish Karamea Suite and Separation Point Suite granitoids (Fig. 4.11). The granitoid clasts plot mostly in the area of overlap between the two suites. There are two samples from Maori Point with lower K_2O than the rest. These clearly plot in the Separation Point Suite field and are similar to the Knuckle Hill intrusion. In hand sample, the Maori Point clasts are medium grained aplites, similar to the aplite veins that cut the Knuckle Hill intrusion.

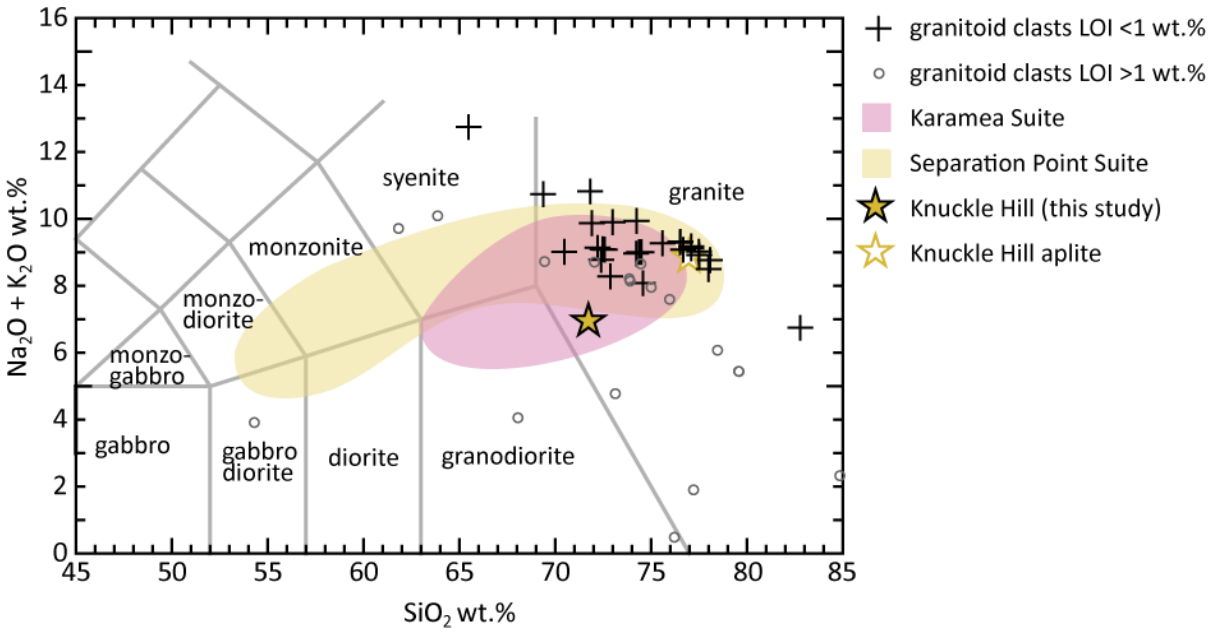

Fig. 4.10: Total alkali silica (TAS) diagram for granitoid clasts (Le Maitre 1989). *Samples with high LOI are likely to be affected by weathering and alteration.*

For analysis of the trace element geochemistry, only granitoid clast samples with LOI below 1.0 wt.% were plotted on a chondrite normalised spider diagram (Sun and McDonough 1989), as samples with higher LOI are likely to have been affected by weathering and alteration. The samples were grouped according to distinguishing geochemical characteristics (Figs. 4.12-4.15).

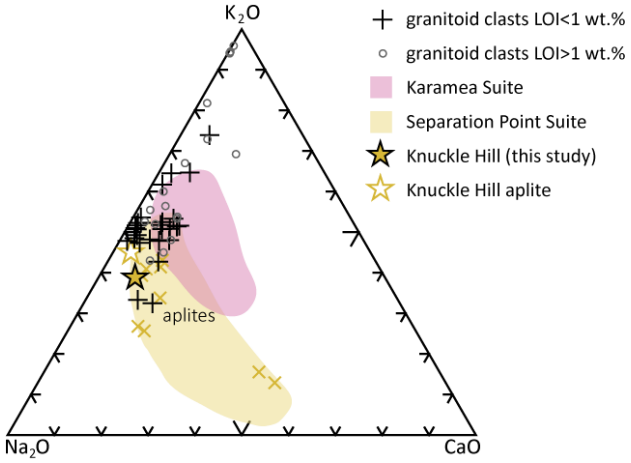

Fig. 4.11: Ternary diagram of major element geochemistry for the granitoid clast samples compared to potential basement sources.

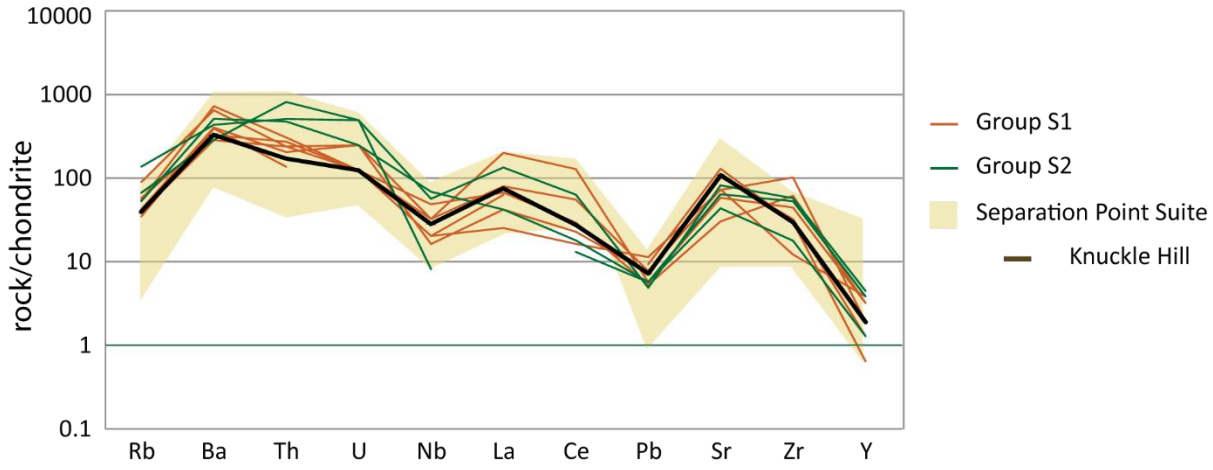

Fig. 4.12: Chondrite normalised spider diagram of granitoid clasts with geochemistry similar to the Separation Point Suite. Chondrite data from Sun and McDonough (1989).

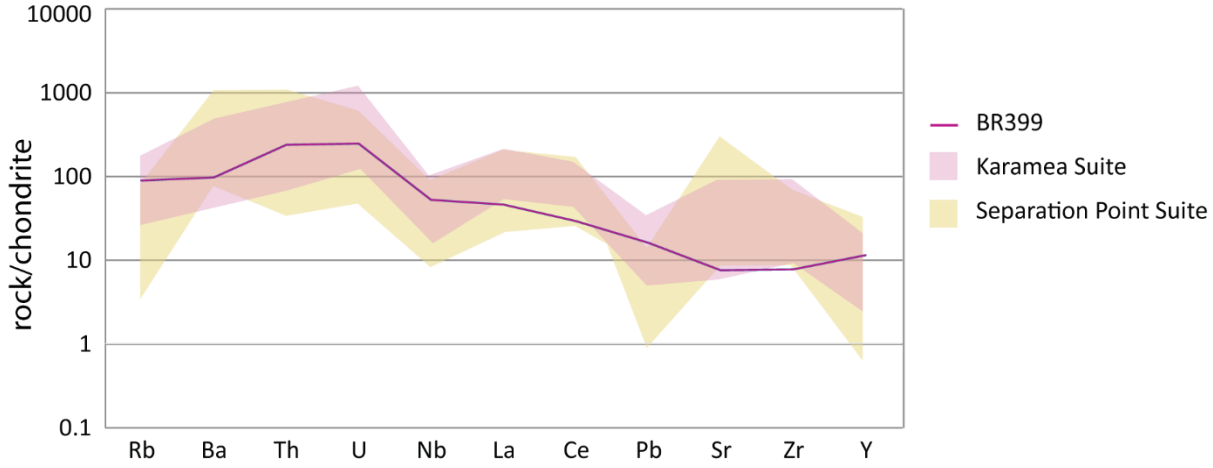

Fig. 4.13: Chondrite normalised spider diagram of granitoid clast BR399 compared to the Karamea and Separation Point suites. Chondrite data from Sun and McDonough (1989).

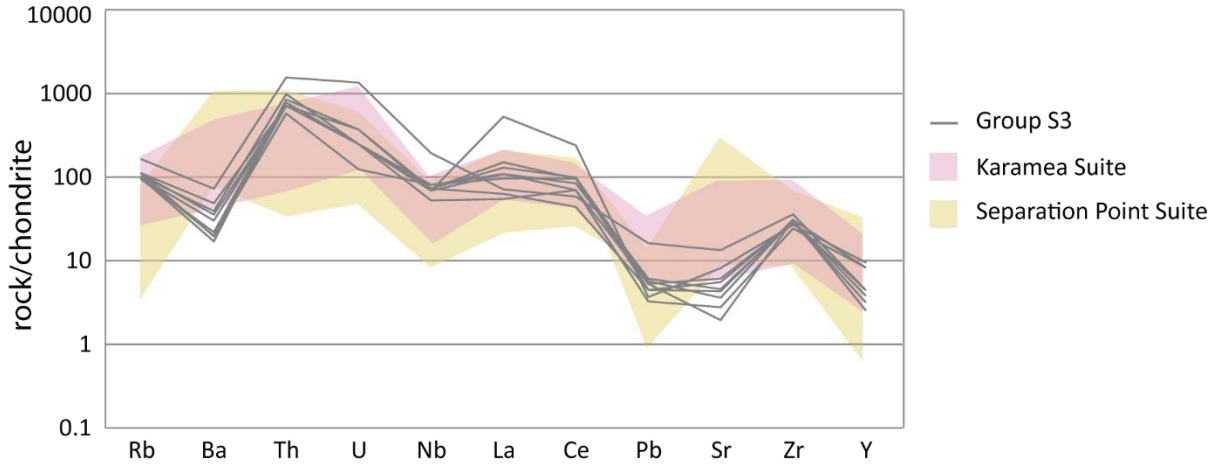

Fig. 4.14: Chondrite normalised spider diagram of granitoid clasts in group S3 compared to the Karamea and Separation Point Suite. Chondrite data from Sun and McDonough (1989).

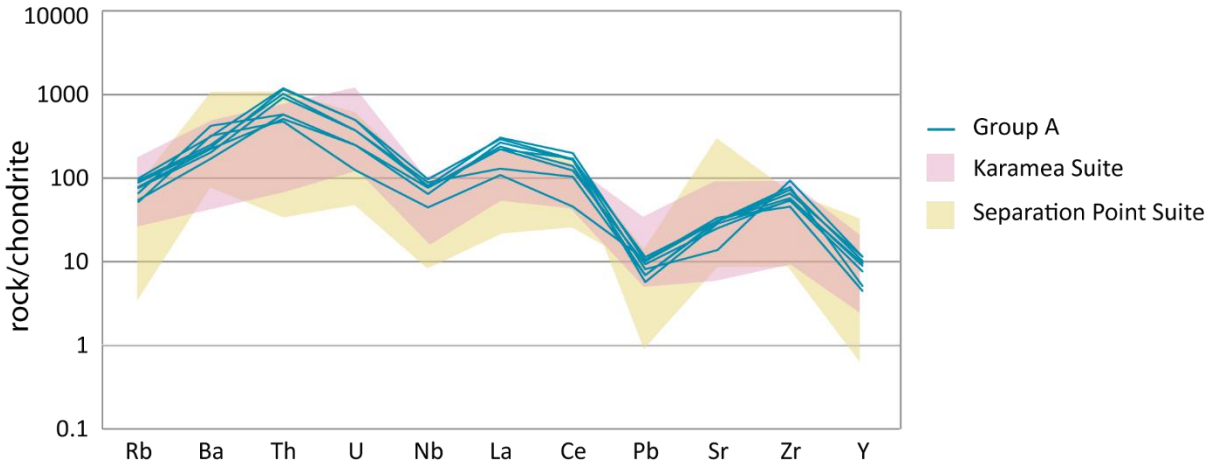

Fig. 4.15: Chondrite normalised spider diagram of granitoid clasts with "A-type" chemistry compared to the Karamea and Separation Point Suite. Chondrite data from Sun and McDonough (1989).

Group S1 granitoid clasts are characterised by high Ba and Sr, moderate Th, and low Nb and Y (Fig. 4.12). These samples best match the trace element geochemistry of the Separation Point Suite, which has peaks in Sr, Ba, and Th. The aplite samples identified in the CaO-Na_2O-K_2O ternary diagram (Fig. 4.11) have a trace element trend almost identical to a Knuckle Hill sample, strongly suggesting that these aplites were sourced from Knuckle Hill or a similar intrusion. Group S2 has higher Rb, Th and U than Group S1, but is otherwise similar (Fig. 4.12). These samples are also likely to be from the Separation Point Suite.

Sample BR399 does not fit the other groups. It lacks strong peaks, with a smooth trend (Fig. 4.13). In terms of trace elements, between the Separation Point and Karamea suites, it fits the Karamea Suite best.

Group S3 is characterised by very low Ba and Sr; high Th, La and Ce; and moderately high Nb (Fig. 4.14). These samples do not fit either the Karamea Suite or the Separation Point Suite well, particularly with regard to the low Ba and Sr. The trace element trend is similar to that for a A-type granites, which have low Ba and Sr, and high Th and La (Winter 2014; Tulloch 2017 personal communication). However, the high field strength element (HFSE) concentration is lower than is typical for an A-type granite (Fig. 4.16) (Whalen et al. 1987). Alternatively, the trace element trends in group S3 may be a result of high degrees of fractional crystallisation. In highly fractionated granites Ba, Sr, Zr, and the transition metals are depleted while U and Nb are enriched (Chappell and White 1992). This is consistent with the trace element trend seen in Fig. 4.14. The group S3 clasts also have the highest SiO_2 and

lowest Al_2O_3 and $Fe_2O_3^T$ of the clasts (Fig. 4.17), further suggesting these clasts are highly fractionated I- or S-type granites rather than A-type.

Group S3 is most likely to be a highly fractionated variant of the Separation Point Suite. The Separation Point Suite includes a wide range of compositions, including very silica-rich end-members (Fig. 4.10). One pluton, just north of the Te Waikoropupū Springs, has high SiO_2 contents of 74.53 – 74.97 wt.% (Strong et al. 2016); is depleted in Ba and Sr; and enriched in Th, U, and Nb similar to the S3 group samples (Fig. 4.18). S3 samples have relatively low aluminium saturation index (ASI) values of 1.02 – 1.08, which is consistent with the metaluminous to weakly metaluminous nature of the Separation Point Suite (Fig. 4.19) (Muir et al. 1995). One of the three thin sections from the S3 group clasts (Wh273) has large titanite crystals, a characteristic accessory mineral of the Separation Point Suite (Tulloch 1983; Muir et al. 1995).

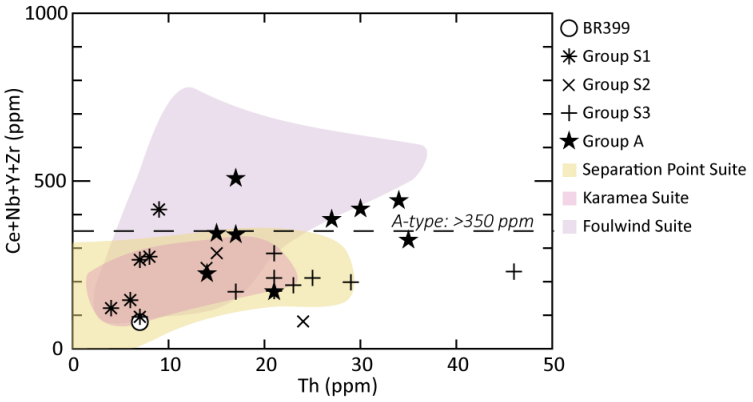

Fig. 4.16: Bivariate plot of total HFSE against Th, for granitoid clasts with LOI <1 wt.% compared to Separation Point, Karamea, and Foulwind suites.

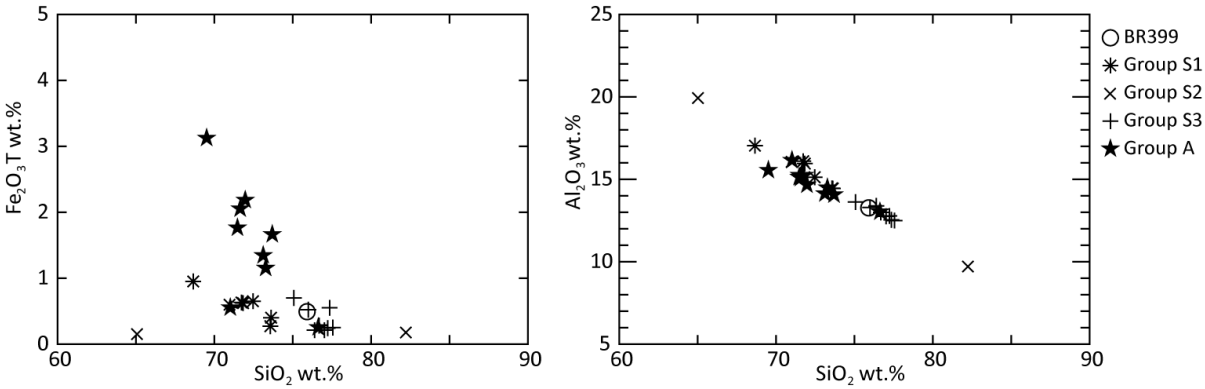

Fig. 4.17: Bivariate plots showing variation of total Fe_2O_3 and Al_2O_3 with SiO_2 for granitoid clasts with LOI <1 wt.%. Samples are grouped according to their trace element trends (see Figs. 4.12-4.15).

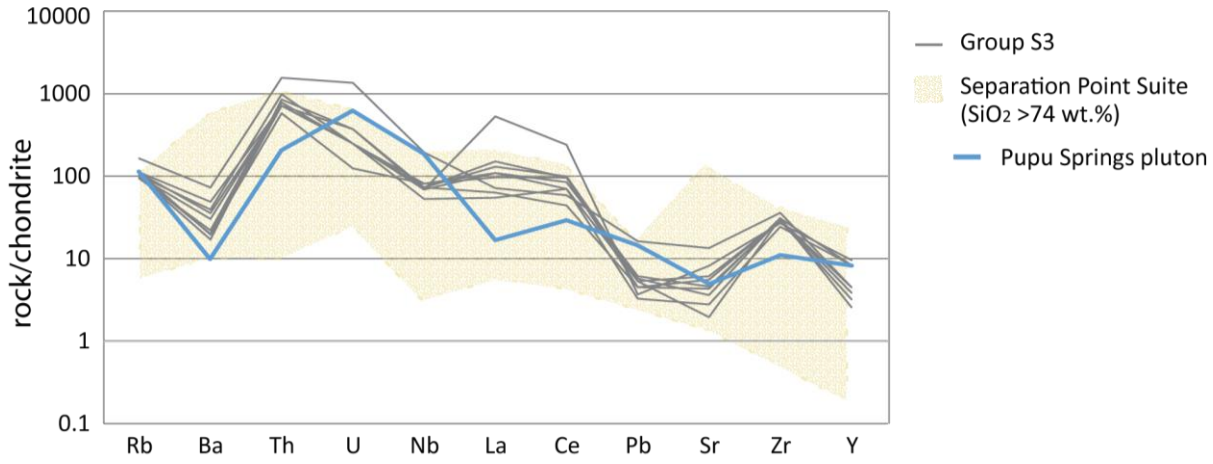

Fig. 4.18: Chondrite normalised spider diagram of granitoid clasts in group S3, interpreted as highly fractionated granites, compared to granites with high SiO_2 from the Separation Point Suite, and to the Separation Point Suite pluton just north of the Te Waikoropupū Springs. Chondrite data from Sun and McDonough (1989).

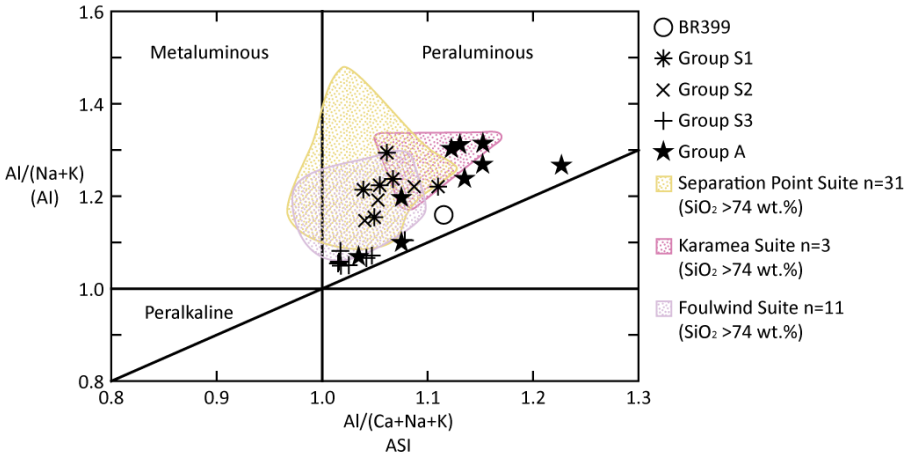

Fig. 4.19: Alkali index and aluminium saturation index (Shand 1947) for granitoid clast samples with LOI <1 wt.% compared to high silica granites from the Karamea, Separation Point, and Foulwind suites.

Group A clasts are characterised by peaks at Th, La, Ce, and Zr (Fig. 4.15). These do not fit either the Karamea Suite or Separation Point Suite trace element trends, particularly the high La and Ce (Fig. 4.15). Unlike group S3, they are unlikely to be fractionated granites, as indicated by the lower SiO_2 and higher Al_2O_3, $Fe_2O_3^T$, Sr, and Ba (Figs. 4.15, 4.17).

The high Th, La, Ce, and Zr seen in group A are typical of A-type granites (Whalen et al. 1987; Winter 2014; Tulloch 2017). These granites have elevated HFSE, with total Ce+Nb+Y+Zr between 169 and 507 ppm, covering the >350 ppm boundary used for defining A-type granites (Whalen et al. 1987). This suggests that the group A granitoids are weakly A-type.

The A-type Foulwind Suite has similar trace element concentrations to the A group clasts (Fig. 4.20). The Foulwind Suite only outcrops near Westport, 160km to the SSW of the North Cape and Farewell formation outcrop. It is unlikely that conglomerate clasts were transported this

distance, assuming the present-day basement geometry is the same as at the time of deposition. However, A-type granites grouped into the Foulwind Suite are present in offshore wells Toropuihi-1, North-Tasman-1, and Motueka-1 (Fig. 2.8) (Tulloch and Mortimer 2017).

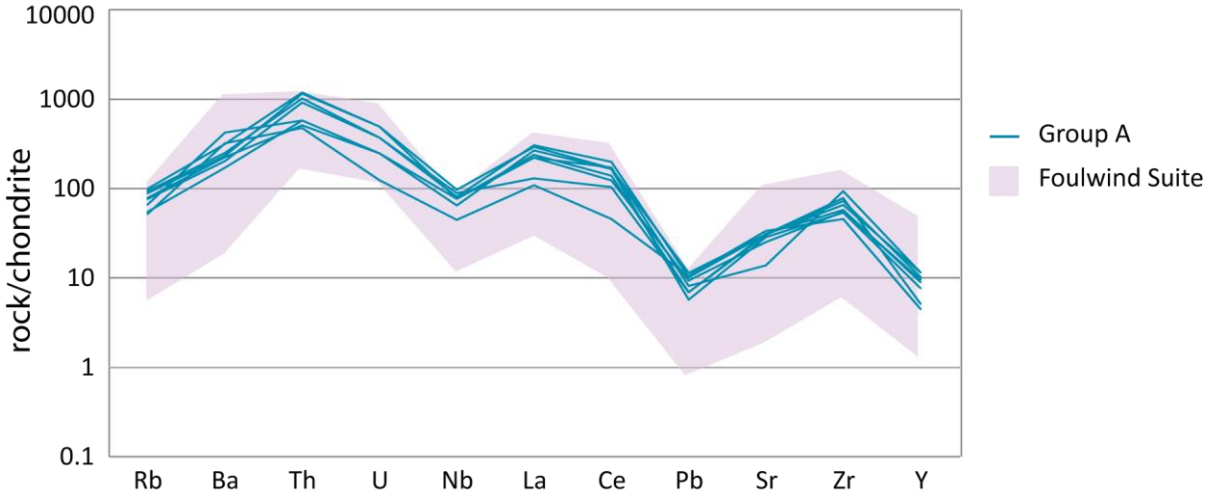

Fig. 4.20: Chondrite normalised spider diagram of granitoid clasts in group A, which have "A-type" chemistry, compared to the Foulwind Suite. Chondrite data from Sun and McDonough (1989).

4.5.3 Provenance of granitoid clasts

The granitoid clasts are from a variety of sources. There is both petrographic and geochemical evidence for Separation Point Suite input, shown by the presence of titanite, foliated granites and aplite similar to Knuckle Hill, and from the major and trace element geochemistry. One sample is typed back to a Karamea Suite source.

A large proportion of the granites do not fit with the petrology or geochemistry of either the I-type Separation Point Suite or the S-type Karamea Suite. Instead, they are more plagioclase poor than typical, and have trace element trends more typical for A-type granites. A-type granites also tend to be more plagioclase-poor (Whalen et al. 1987; Eby 1992; Tulloch 2017). A-type granites are not known onshore in or near to the North Cape and Farewell Formation outcrop area. However, wells offshore including Toropuihi-1, Motueka-1, and North Tasman-1 all intersected A-type granites, grouped with the Foulwind Suite (Fig. 2.8). These granites have a geochemistry and petrography similar to the clasts in the field area. The granite from well Motueka-1 contains accessory green biotite and titanite, and the granite from Toropuihi-1 contains mesoperthitic alkali feldspar (Cooper and Tulloch 1992; Mortimer et al. 1997).

The A-type granite source for the clasts may also be from a granite that has been completely unroofed and is no longer exposed. A-type granites are commonly associated with rifting (Winter 2014), so it is possible that the granite was emplaced and exposed during rifting from Gondwana, in a similar manner to the Paparoa Core Complex of Westland (Laird and Bradshaw 2004). Adams et al. (2017) found anomalously young zircons (81 ± 2 and 84 ± 2 Ma) in a Rakopi Formation sandstone from the Paturau River and speculated that these zircons were derived from rift-related magmatism. The A-type granitoid clasts may be derived from the same magmatic activity as these zircons.

Granite clasts with similar A-type chemistry are also found in conglomerates of the Late Cretaceous to Paleocene Paparoa Coal Measures in the Greymouth Basin (Steadman 2017). It is possible that this basin was also fed by a rift-related granitoid or by an A-type granite offshore.

The only granitoid clast from the Rakopi Formation is sample BR399, taken from the Pakawau Bush Road outcrop. This sample has a trace element signature that is distinct from all the other clast samples, suggesting that the Rakopi Formation was fed from a different source than the younger formations. The granite most closely corresponds to the Karamea Suite, tentatively suggesting axial drainage. Alternatively, BR399 may be from a granite that was entirely eroded away during Rakopi Formation time.

The North Cape Formation contains a mixture of S1/S2, S3, and A groups (Table 4.1). Group S1/S2 is only found in North Cape Formation outcrops in the northeast Whanganui Inlet. This group is likely to be derived from the Separation Point Suite, such as Knuckle Hill. The presence of these granites suggests drainage from local sources, for example fan deltas draining the Wakamarama Fault scarp.

Table 4.1: Comparison of granitoid clast trace element composition between sedimentary formations.

Trace element group	*Potential source*	*Rakopi Formation number (% formation clasts)*	*North Cape number*	*Farewell number*
A	Foulwind Suite, other A-type granite	0 (0%)	6 (32%)	3 (50%)
S1/S2	Separation Point Suite	0 (0%)	9 (47%)	0 (0%)
S3	Highly fractionated Separation Point Suite	0 (0%)	4 (21%)	3 (50%)
BR399	Karamea Suite?	1 (100%)	0 (0%)	0 (0%)

The less felsic Separation Point Suite granites, similar to those at Knuckle Hill, are absent in the Farewell Formation (Table 4.1). The Separation Point Suite outcrop may have been buried by the time of Farewell Formation deposition, or the catchments feeding the Farewell Formation may not have drained any Separation Point Suite outcrops.

4.6 Volcanic clasts

Volcanic clasts are a minor constituent of the conglomerates in both the North Cape and Farewell formations but are absent in the basal Otimataura Conglomerate of the Rakopi Formation in the Paturau River. In hand sample these clasts are green in colour and may have white (feldspar), green or black (amphibole) tabular phenocrysts 0.5-5 mm long.

There are two possible sources for the volcanic clasts: Cambrian Takaka Terrane Devil River Volcanics and volcaniclastic Haupiri Group conglomerates; or syn-sedimentary volcanism. Late Cretaceous and Paleocene rift-related and intraplate volcanism is recorded in Zealandia basins, including the Greymouth Basin (Bishop DJ 1992; Steadman 2017), Canterbury Basin (Wilding et al. 1971; Weaver and Pankhurst 1991), and Great South Basin (Sahoo et al. 2014). In Marlborough, basanite dykes of the Tapuaenuku Volcanics are Late Cretaceous to early Tertiary in age, and the alkaline mafic to ultramafic Lookout Volcanics have been dated to 98 Ma (Grapes et al. 1992; McCoy-West et al. 2010). In the northern Taranaki Basin, volcanics intruding and interbedded with the North Cape and Rakopi formations were intersected by Romney-1 (Anadarko New Zealand Taranaki Company 2015). The rift-related and intraplate Cretaceous and Paleocene volcanics of other Zealandia basins are generally basaltic with an ocean island basalt (OIB) geochemical signature (Baker et al. 1994; Jongens 1997; Nicholson and Black 2004). Syn-sedimentary volcanics should therefore be readily distinguishable from the Takaka Terrane by their OIB signature, as the Takaka Terrane volcanics are arc-related and do not have an OIB source (Münker and Cooper 1999; Münker 2000).

4.6.1 Petrology of volcanic clasts

All of the volcanic clasts collected show alteration, although the primary volcanic textures are preserved. From the estimated primary mineralogy, the majority of the clasts are andesites and basalts with minor rhyolite (Fig. 4.21). The majority of the volcanic clasts are porphyritic, with some showing weak flow-banding (Fig. 4.22A). The phenocrysts show a range of

compositions. The most common is plagioclase (Fig. 4.21), which may be almost unaltered with original polysynthetic twinning, or range towards completely replaced by albite, zeolites, and sericite. Alkali feldspar is less common and is usually sericitised. Amphiboles are common, their original habit is diagnostic, but they are almost always replaced by chlorite and opaques (Fig. 4.22B). Quartz is present in some samples, and usually shows resorption and embayments. Clinopyroxene was only found in sample MP040.4, here the centre of the crystal is unaltered, and the rim is replaced by chlorite (Fig. 4.22B).

In the majority of the samples the groundmass is very fine-grained sericite, chlorite, albite, opaques, zoisite, and/or quartz. In some samples, microlites are present (Fig. 4.22A). Some samples have a fine-grained groundmass of interlocking plagioclase, biotite, chlorite, and opaques (Fig. 4.22D).

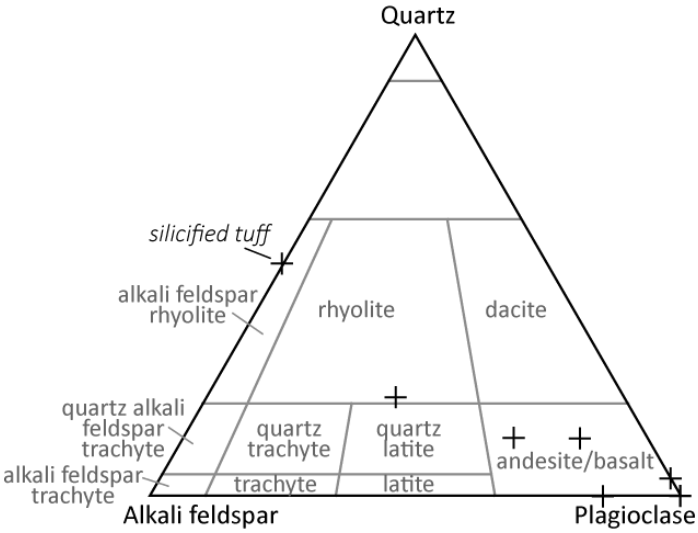

Fig. 4.21: Volcanic QAP diagram for the volcanic clasts, after Le Maitre (2004). Modal mineralogy was estimated from the phenocryst composition.

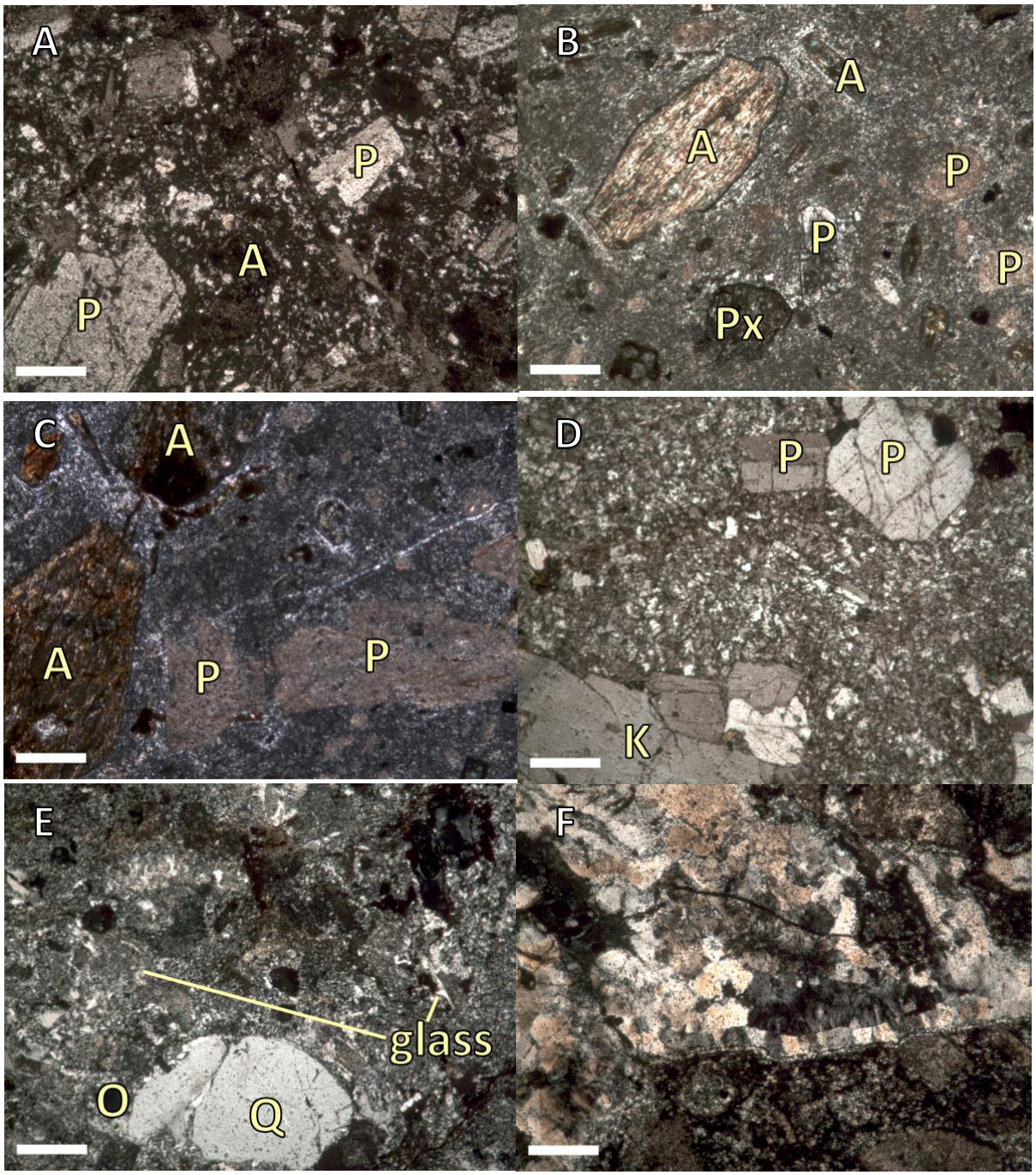

Fig. 4.22: Photomicrographs of volcanic clasts and basement sources. Scale bar is 200μm. Q-quartz, K-alkali feldspar, P-plagioclase, A-amphibole, Px-pyroxene, O-opaques. A: Wh276.1, porphyritic volcanic clast with weak flow banding (bottom left to top right). B: MP040.4, porphyritic volcanic clast with amphibole phenocrysts replaced by chlorite, diagnosed by their characteristic six-sided habit. Darker, equant phenocrysts are interpreted as pyroxene pseudomorphs. C: MP040.4, porphyritic volcanic clast with amphibole phenocrysts replaced by chlorite (left), and plagioclase phenocryst replaced by sericite and zeolites (tabular shapes in bottom right). D: OP074, volcanic porphyritic clast with plagioclase and alkali feldspar phenocrysts in a fine-grained crystalline groundmass. E: MP040.3, silicified tuff clast. Embayed quartz crystal (bottom middle). Matrix has silicified, cuspate glass shards. F: MP040.3, quartz-filled void in silicified tuff clast.

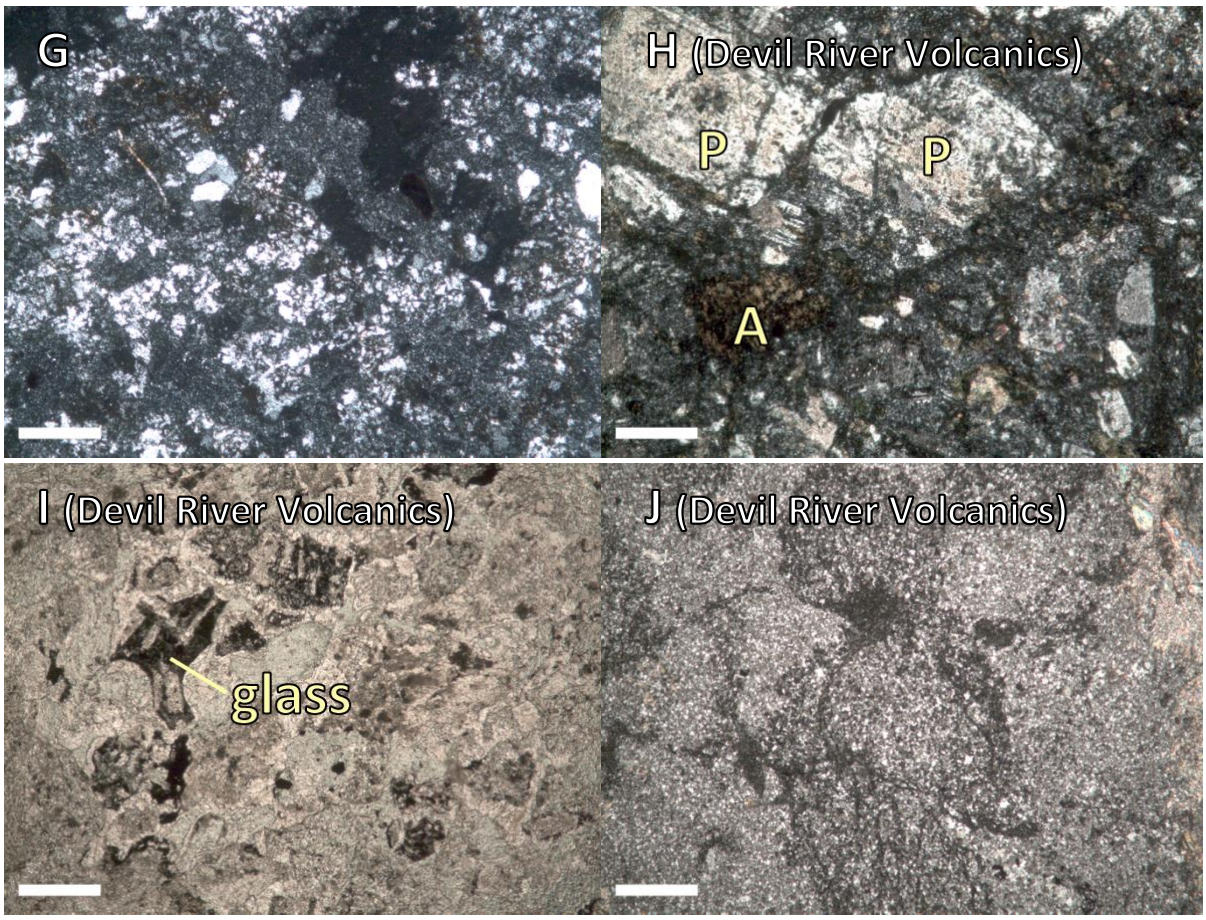

Fig. 4.22 cont. G: Pi307.1, highly silicified volcanic clast, where groundmass and phenocrysts are almost entirely replaced by quartz, albite, sericite, and zoisite. H: DRM12 Maclean (1994), sample from the Devil River Volcanics showing porphyritic volcanic textures. Phenocrysts are albitised plagioclase (white) and amphibole replaced by chlorite (dark brown). Note textural similarity to A-D. I: DRM17 Maclean (1994), PPL, silicified tuff sample with cuspate glass shards from the Devil River Volcanics. J: DRM 124, Maclean (1994), silicified sample creating chert from the Devil River Volcanics.

Sample MP040.3 is a highly altered tuff (Fig. 4.22E-F). This has embayed quartz grains, silicified glass shards, and sericitised feldspars. Two other porphyritic volcanic samples are highly silicified (Fig. 4.22G). These contain fine grained quartz, albite, sericite, and zoisite, with tabular shapes suggesting feldspar phenocrysts. Vesicles and fractures in these samples are filled with quartz (Fig. 4.22F).

Alteration of the volcanics could have occurred at the time of volcanism, as a result of metasomatism related to the volcanism, or metamorphism during the burial and uplift of the volcanics; or alteration could have occurred during diagenesis of the conglomerates. The conglomerate matrix, sandstones, and other clasts do not have this degree of alteration, so the alteration is likely to be related to metasomatism or metamorphism of the volcanics.

The Takaka Terrane Devil River Volcanics show extensive very low to low-grade metamorphism, with a mineral assemblage of albite + chlorite ± carbonate ± quartz ± epidote ± prehnite ± pumpellyite ± actinolite ± sericite ± (clino)zoisite ± stilpnomelane (Münker and Cooper 1999). The primary volcanic textures are usually preserved (Fig. 4.22H) (Maclean 1994; Münker and Cooper 1999). The volcanics are generally andesitic to basaltic in composition, but include tuffs, and silicified volcanics creating cherts (Fig. 4.22I-J) (Maclean 1994). This is consistent with the mineralogy and textures seen in the volcanic clasts.

4.6.2 Geochemistry of volcanic clasts

Due to the highly altered nature of the volcanic clasts, the major element geochemistry is not reliable. On a conventional TAS discrimination diagram, the samples all plot as rhyolites and dacites, which contradicts the petrology (Figs. 4.21, 4.23A). On a discrimination diagram using immobile trace elements (Fig. 4.23B) the volcanics are classified as mostly rhyolites, rhyodacite/dacites and trachyandesites, with some subalkaline basalts and alkaline basalts. This is still more felsic than the plagioclase and amphibole-dominated mineral assemblage would suggest. It is also more felsic than the Devil River Volcanics and Lockett Conglomerate. This may be because the samples have undergone further alteration during erosion from the source, transport, and diagenesis.

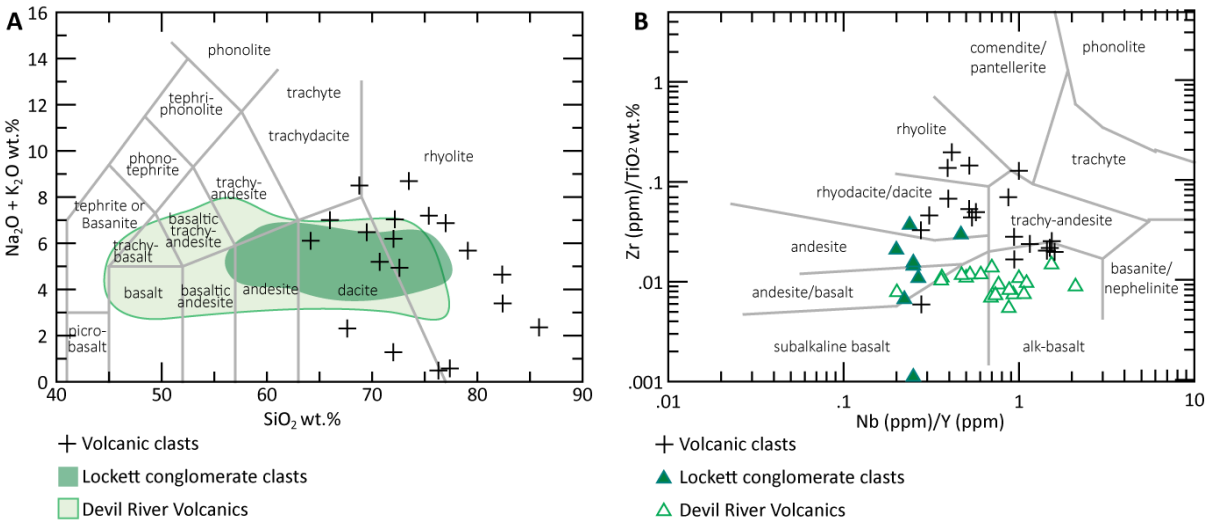

Fig. 4.23: Classification of volcanic clasts and Takaka Terrane volcanics and volcaniclastics by A: major element geochemistry TAS diagram after Le Maitre (1989); and B: immobile trace element discrimination diagram after Winchester and Floyd (1977).

The majority of the samples plot as calc-alkaline, similar to the volcanic clasts in the Lockett Conglomerate and some of the Devil River Volcanics (Fig. 4.24). Calc-alkaline compositions are usually restricted to island-arc settings (Winter 2014).

The trace element data shows an island-arc signature. The data do not equal 1 when normalised to N-MORB (Fig. 4.25), nor does it exhibit the trend on the N-MORB normalised diagram typical of an OIB, with large iron lithophiles and high field strength elements increasing smoothly with increasing incompatibility (Winter 2014). The samples are therefore most likely to be from an island-arc setting and their trace element trends are consistent with those of the arc-related Takaka Terrane volcanics (Fig. 4.25).

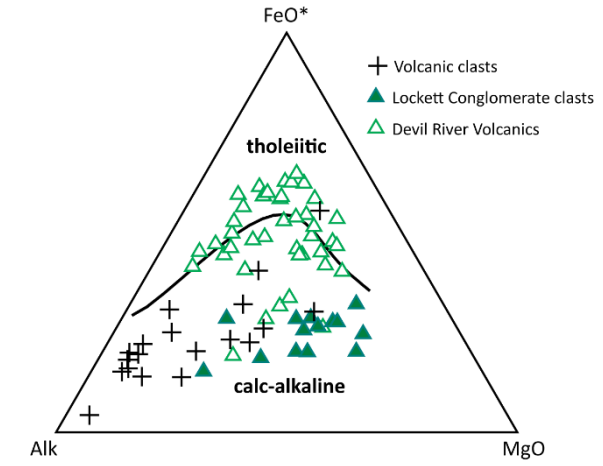

Fig. 4.24: Tholeiitic vs. calc-alkaline discrimination diagram after Irvine and Baragar (1971). Takaka Terrane volcanics and volcaniclastics are compared to the clast samples.

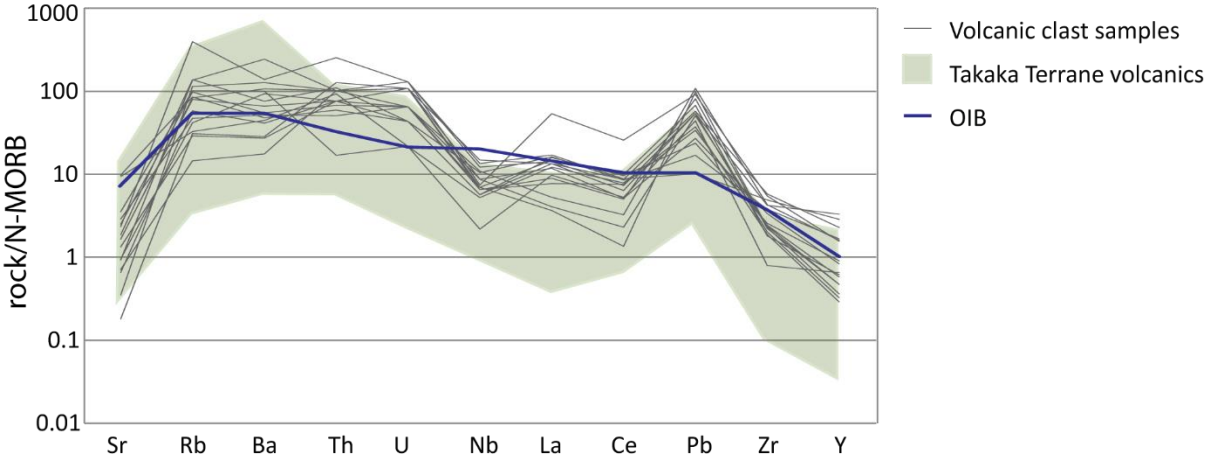

Fig. 4.25: N-MORB normalised spider diagram for all available trace elements of volcanic clasts compared to Takaka Terrane volcanics and to average OIB. Element order after Pearce (1984), N-MORB and OIB data from Sun and McDonough (1989).

4.6.3 Provenance of volcanic clasts

The major and trace element geochemistry of the volcanic clasts is consistent with an island-arc source for the volcanics. This means they are more likely to come from the Takaka Terrane volcanics than from a rift-related Paleocene or Late Cretaceous source. The petrographic textures of the samples are similar to the Takaka Terrane Devil River Volcanics, the samples have a similar degree of very low to low grade metamorphism. The Takaka Terrane is therefore the most likely source for the volcanic clasts.

4.7 Other clasts

The conglomerates also contain vein quartz, chert, schist, and cream and grey siltstones. The metasedimentary clasts often have small quartz veins, so the vein quartz clasts are likely to be eroded out of veins in the metasedimentary source. Similarly, chert is a component of both the Golden Bay Group and the Takaka Terrane, so is likely to be sourced from one or both of these units (Cooper 1979, 1989; Harrison 1993; Rattenbury et al. 1998).

The North Cape and Farewell formation conglomerates have a minor schist component. These clasts are small and weathered, so were difficult to sample. One sample, OP073, was collected and thin sectioned. This schist is fine grained and strongly foliated, with a mineral assemblage of quartz, biotite, opaques, minor alkali feldspar, and feldspars altered to clay (Fig. 4.26A). There are several schists in the region, including the Bay Schist, Onekaka Schist, Wakamarama Schist, and Waingaro Schist. The Bay Schist contains quartz + albite + muscovite ± chlorite ±

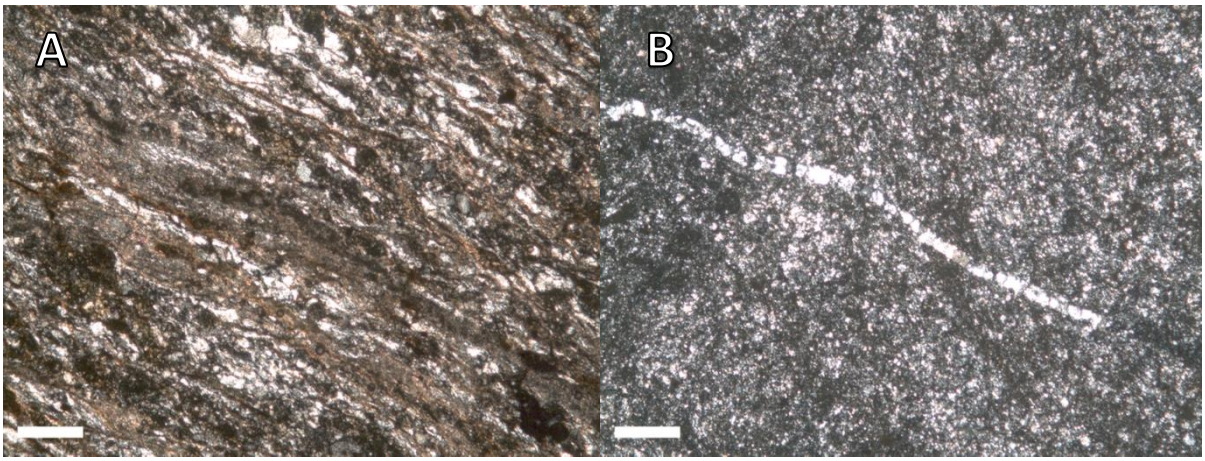

Fig. 4.26: Photomicrographs of other clast types. Scale bar is 200μm. A: OP073, schist clast with foliated quartz, biotite, clays. B: Pu227.1 cream sedimentary clast with fine silt quartz and clay matrix. Vein in centre filled with quartz.

biotite ± graphite ± garnet ± calcite (Bishop 1971); the Onekaka Schist contains siliceous quartz + albite/oligoclase + biotite + muscovite + oxide + sphene ± calcite ± stauralite (Grindley 1980); the Wakamarama Schist is weakly foliated and contains albite + quartz ± epidote ± biotite ± muscovite ± chlorite ± calcite ± actinolite ± hornblende ± sphene ± iron oxide (Bishop 1971); and the Waingaro greenschist contains quartz + albite + muscovite + chlorite + calcite + sphene + epidote (Rattenbury et al. 1998). The schist clast is unlikely to be the Waingaro Schist as it lacks chlorite and calcite. The clast is strongly foliated so is unlikely to be the Wakamarama Schist. The Onekaka Schist or the Bay Schist are therefore the most likely sources for the schist clast.

The North Cape and Farewell formations contain two types of sedimentary clasts. In the North Cape Formation, there are moderately indurated grey siltstones. No samples were collected, as the clasts were small and eroded flat to the outcrop surface. The clasts were similar in grain size, colour, angularity, shape, and induration to siltstone rip-up clasts in the sandstone units. This, combined with the weaker induration compared to the metasedimentary basement, suggests that they are intrabasinal clasts.

In the Farewell Formation in the northern part of the field area there are cream siltstones (Fig. 4.2). The cream siltstone in thin section is very fine silt sized quartz, brown opaques and clays (Fig. 4.26B). There are sparse, coarse silt sized, sub-rounded to sub-angular, quartz grains in the matrix. One sample is cut by very thin quartz veins (Fig.4.26B). The veins suggest these are not intrabasinal clasts but instead have a longer burial and metamorphic history. The trace element trends of these clasts are most similar to the Takaka Terrane metasedimentary units (Fig. 4.27).

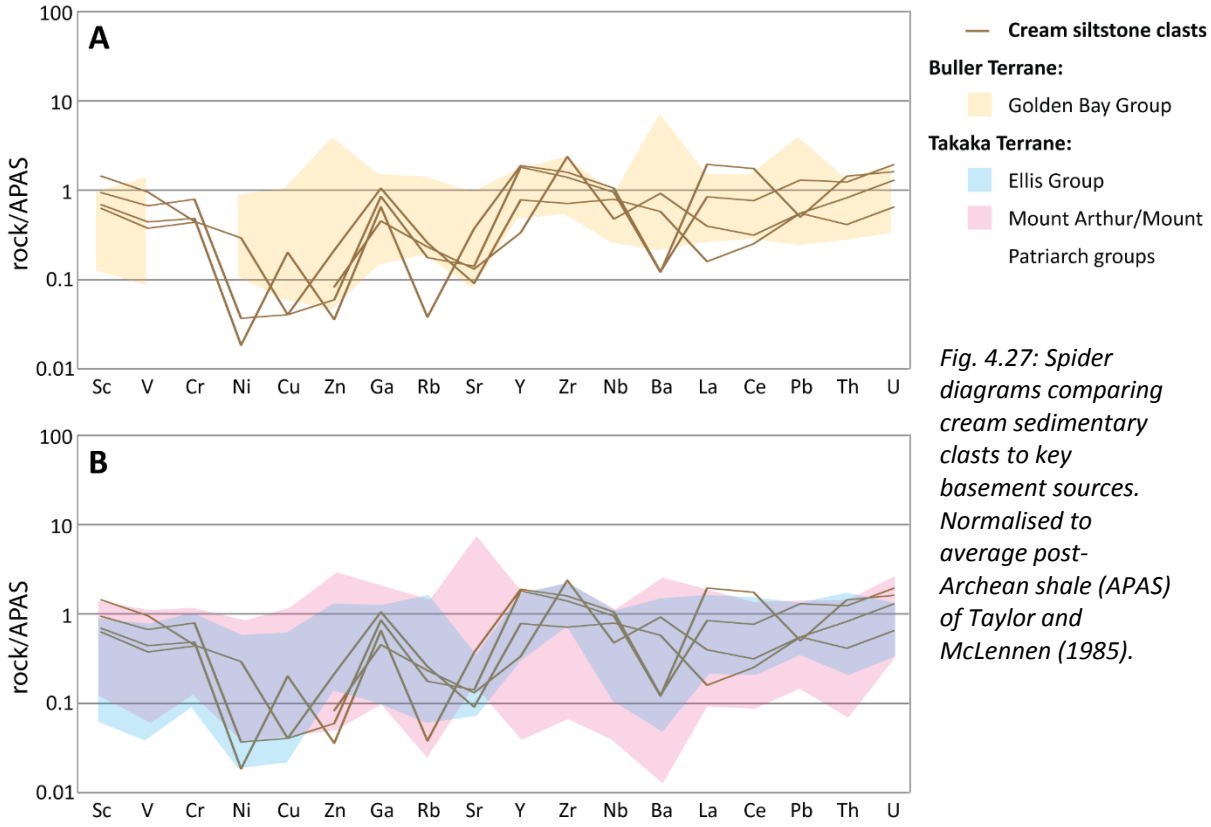

Fig. 4.27: Spider diagrams comparing cream sedimentary clasts to key basement sources. Normalised to average post-Archean shale (APAS) of Taylor and McLennen (1985).

4.8 Conglomerate provenance

The Rakopi Formation Otimataura Conglomerate in the Paturau River is dominated by metasedimentary clasts (Fig. 2.1). No samples of these clasts were collected as the outcrop was surrounded by deep water; so either a Takaka Terrane provenance or a Golden Bay Group (the underlying basement) provenance is possible (Fig. 4.28A). The overall monomictic nature of the conglomerate suggests a single point source, such as a fan supplying the conglomerate. The presence of minor volcanic clasts in the upper conglomerates suggests a Takaka Terrane source.

The North Cape Formation conglomerates are dominated by clasts from the upper Takaka Terrane Ellis Group, with minor granites from both the Separation Point Suite and an undocumented A-type granite, and minor Takaka Terrane volcanics. This reflects a mix of both distal and local sources (Fig. 4.28B). The volcanic units of the Takaka Terrane outcrop to the south, showing transport of these clasts along the basin axis. The Takaka Terrane metasedimentary units and the Separation Point Suite clasts were fed into the basin from the east, the uplifted fault scarp. During North Cape Formation time, sediments were therefore

fed into the basin both from the southwest along the axis, and from local areas on the Wakamarama Fault scarp.

The Farewell Formation has a similar mix of clasts to the North Cape Formation, with Takaka Terrane metasedimentary clasts still dominant. Takaka Terrane volcanics were still present, suggesting a mixture of drainage from material uplifted by the Wakamarama Fault and flow along the basin axis (Fig. 4.28C).

Among the fresh and weathered granitoid clast samples collected from the Farewell Formation, no low silica Separation Point Suite granites were found. This suggests that the less felsic Separation Point Suite outcrop was either buried, or transport directions had shifted away from this outcrop. The granitoid clasts also become more weathered towards the top of the Farewell Formation (Fig. 4.1). Granitoids are almost absent towards the top of the Farewell Formation at Pillar Point, possibly because the granites have completely weathered to sand. The increased clast weathering suggests that the clasts have a higher residence time in the fluvial system and more exposure to weathering agents, or there was more in situ weathering of the granitoid source area, or some combination of both. As the granite clasts become more weathered, the volcanic clasts also decrease in abundance. This is probably the same effect as the unstable volcanic glass, feldspars, amphiboles, and pyroxenes are weathered and removed.

Increased weathering could be affected by changing climatic conditions. The Rakopi Formation at Pakawau Bush Road is inferred to have been deposited in a cool to mild temperate climate with mean annual temperatures of 12 – 16°C, interpreted from the fossil leaf assemblage (Kennedy 2003). The Farewell Formation at Pillar Point was deposited in cooler conditions (6 – 9°C), but with slightly higher rainfall (Kennedy 2003). Cooler temperatures in the Paleocene would have been less favourable to weathering reactions, although a wetter climate would have been more favourable. Overall, the subtle change in climate does not account for the strong increase in weathered material in the Farewell Formation. The increased sediment residence time and increased basement weathering is instead likely to be the result of the slowing or cessation of movement on the Wakamarama Fault decreasing the rate of erosion and transportation.

The Farewell Formation has cream siltstones, probably from the Takaka Terrane, only in the northern outcrop area. Their absence in the southern outcrop area could be due to a source

feeding them into the basin in the north (Fig. 4.28). This shows that although the Wakamarama Fault may have slowed, it was still influencing drainage through Farewell Formation time.

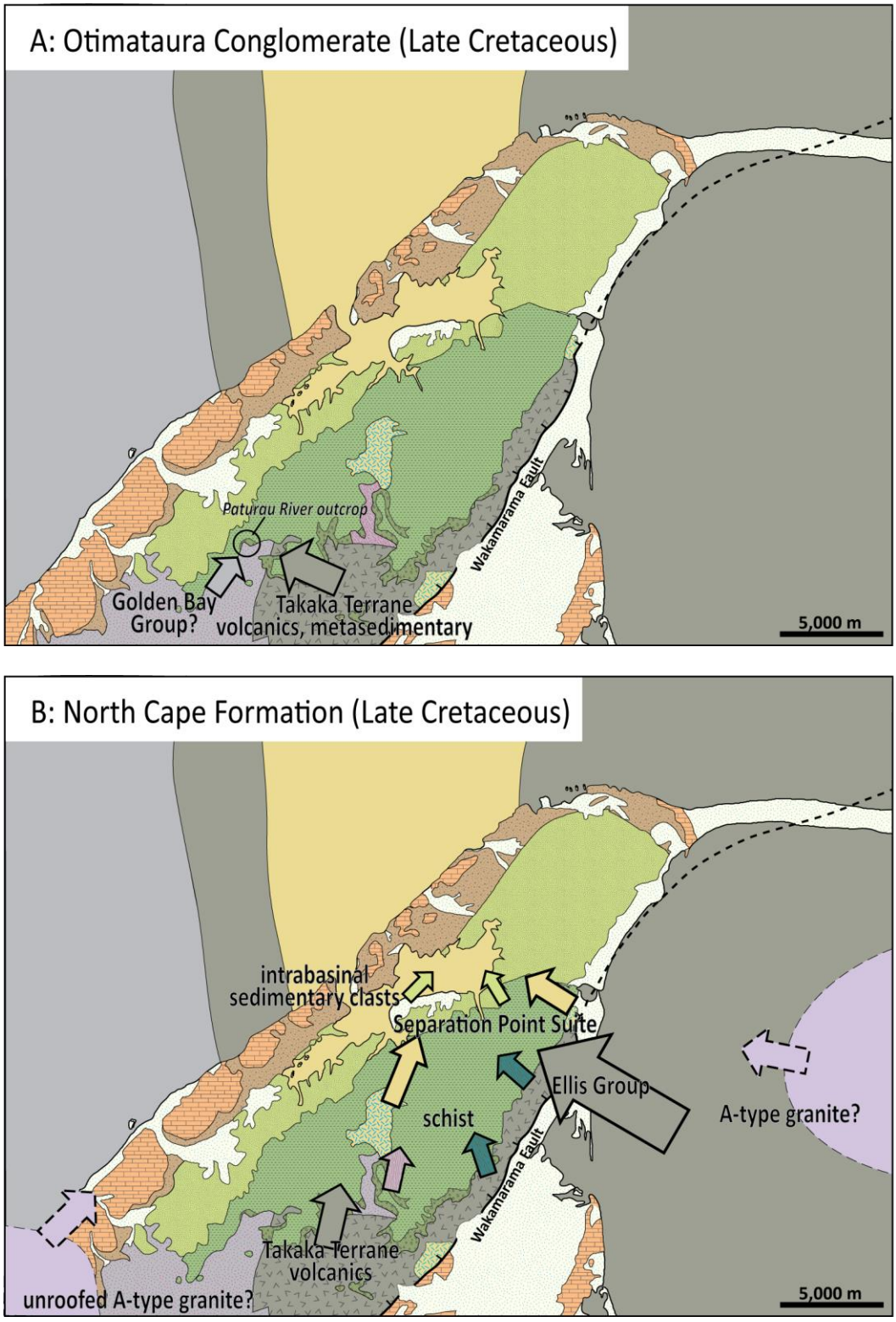

Fig. 4.28 cont.

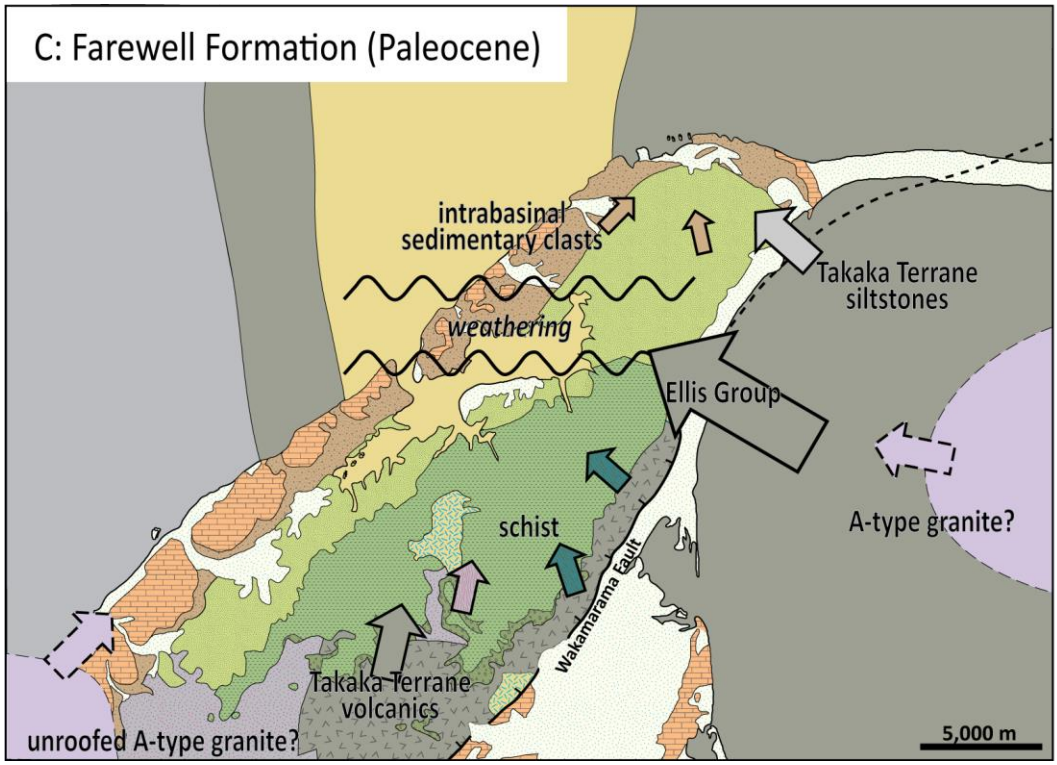

Fig. 4.28: maps showing schematic transport pathways of conglomerate clasts from basement sources to conglomerates for each of the Otimataura Conglomerate (A), North Cape Formation (B), and Farewell Formation (C). See Fig. 2.3 for full legend.

5. Sandstone Petrology

5.1 Introduction

The aim of this chapter is to describe the composition of Rakopi, North Cape, and Farewell Formation sandstones by petrographic analysis. Stratigraphic trends are described, and related to changes in provenance, depositional processes, and diagenesis.

The detrital sandstone composition and volume of authigenic and detrital minerals is one of the major factors determining reservoir potential of sandstones in the Taranaki Basin (Higgs et al. 2010). This outcrop study contributes to understanding how the Late Cretaceous and Paleocene sandstone composition changes in response to provenance and diagenesis, and the effects on the reservoir potential of these sandstones.

5.2 Methods

One-hundred and seven sandstone samples were selected for thin sectioning, covering as much of the stratigraphy as possible and including a range of lithofacies associations. Medium-grained sandstones were chosen where possible. Sandstones pieces approximately 30 mm by 20 mm were impregnated with clear epoxy resin and made into thin sections.

Of these thin sections, 43 were stained with both Na-cobaltinitrate to identify alkali feldspar and K-rhodizonate to identify plagioclase. Half of the thin section was left unstained to enable description of the sandstone without the stain obscuring details. It was found that the pink K-rhodizonate stain was also staining alkali feldspars (for example, feldspars with microcline twinning), and the yellow Na-cobaltinitrate stain was not visible. In this case, alkali feldspars were differentiated from plagioclase by the presence of simple and microcline twinning, and perthite and myrmekitic textures. The remaining 64 sandstones were stained with only Na-cobaltinitrate following the method of Lewis and McConchie (1994). In these samples alkali feldspar was identified by the stain and plagioclase was distinguished by the lack of yellow stain and presence of textures that distinguish it from quartz, such as polysynthetic twinning, cleavage, and alteration.

Each sample was point counted using a PELCON Automatic Point Counter. Five-hundred point counts were made on the stained portion of the thin sections. The spacing between each grid point was set to larger than the maximum grain size, to avoid counting the same grain multiple times (Van der Plas and Tobi 1965; Neilson and Brockman 1977). Where this was not practicable, for example in sandstones that had a few granules or pebbles, the grid spacing was set to be larger than the majority of the grains. The raw point count data is included in Appendix G.

5.3 Composition and texture of Rakopi Formation sandstones

The Rakopi Formation sandstones (excluding the Otimataura Conglomerate) are feldsarenites and lithic feldsarenites with dominantly sedimentary lithics (Fig. 5.1). The Rakopi Formation sandstones are generally moderately to well sorted, and subrounded to subangular (Fig. 5.2C). The matrix is clay and silt.

Samples from the Otimataura Conglomerate in the Paturau River (PR200) and the samples on Pakawau Bush Road closest to the Wakamarama Fault (BR408, BR409, BR412) have distinctly different compositions to the rest of the Rakopi Formation samples. The Pakawau Bush Road are therefore grouped with the Otimataura Conglomerate and interpreted as a sandy equivalent to the conglomerate. The Otimataura Conglomerate samples have high lithic contents, plotting as litharenites and a sub-litharenite. The lithics in the Paturau River (PR200) are dominated by schist (Fig. 5.2A). The lithics in the Pakawau Bush Road samples are entirely sedimentary (Fig. 5.2C).

The Pakawau Bush Road Otimataura Conglomerate samples have only poor to moderate sorting and are subangular to angular. Sample BR408 is bimodal, with coarse sand grains in a silt to very fine sand matrix. In contrast, the Paturau River Otimataura Conglomerate sample (PR200) is moderately sorted and subangular (Fig. 5.2A). This sample shows evidence of compaction, with schist grains deformed around quartz grains.

These results are consistent with Wizevich (1992) and Browne et al. (2008), who found that the Rakopi Formation was dominated by lithic feldsarenites, and the Otimataura Conglomerate was litharenites, with lithic compositions dependant on the local basement.

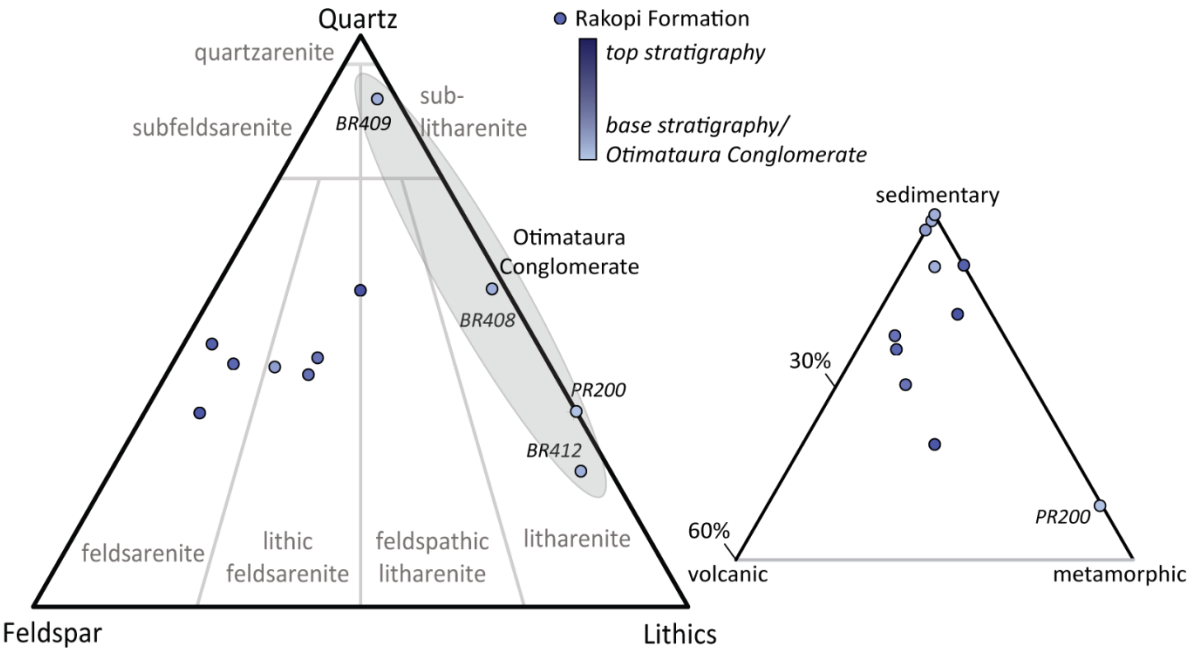

Fig. 5.1: Quartz-feldspar-lithic (QFL) diagram after Folk et al. 1970 showing overall composition of the Rakopi Formation samples, and the lithic composition. Points are shaded according to the approximate stratigraphic position of the samples.

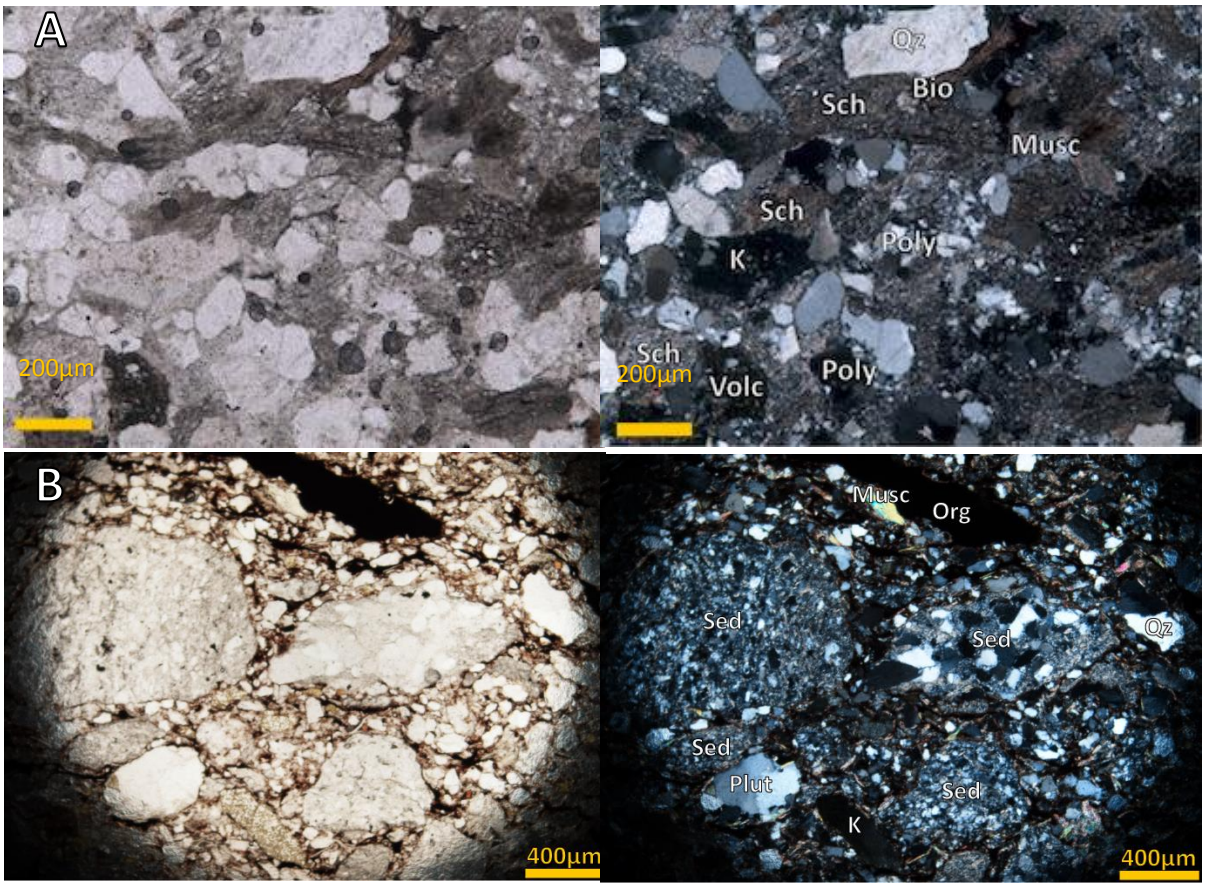

Fig. 5.2 cont.

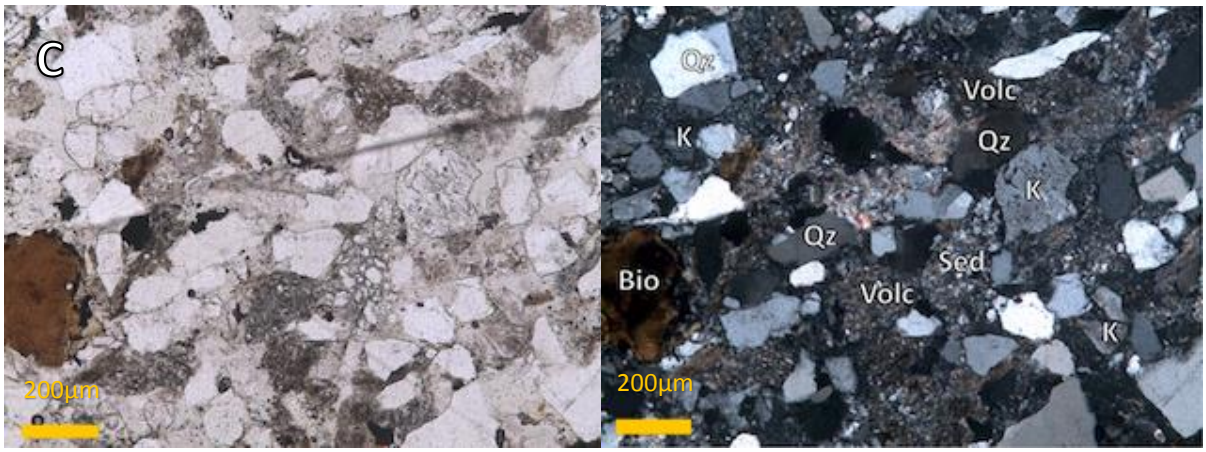

Fig. 5.2: Photomicrographs showing typical composition and textures of the Otimataura Conglomerate and the Rakopi Formation. A: PR200 PPL (left) and CPL (right) of same view of thin section, Otimataura Conglomerate in the Paturau River with schist lithics. B: BR408 PPL (left) and CPL (right) of same view, Otimataura Conglomerate equivalent sandstone from the Pakawau Bush Road, with sedimentary lithics in a silt, clay, and organic-rich matrix. Grain outlines are visible in the PPL view. C: PR199 PPL (left) and CPL (right) of same view, Rakopi Formation sandstone from the Paturau River showing typical moderately sorted, subangular texture.
Qz: quartz; Poly: polycrystalline quartz; K: alkali feldspar; Bio: biotite; Musc: muscovite; Sed: sedimentary lithics; Volc: volcanic lithics; Sch: schist lithics.

5.4 Composition and texture of North Cape Formation sandstones

The majority of the North Cape Formation sandstones are feldsarenites and lithic feldsarenites, with minor feldspathic litharenites (Fig. 5.3). Three very coarse sandstones (MP339, PP296, PP295) have more lithics than the other sandstones due to their larger grain size (Fig. 5.4). The lithics in the North Cape Formation are dominated by sedimentary grains, with some volcanics and minor metamorphic schist. There are no strong stratigraphic or spatial trends.

The North Cape Formation sandstones are moderately to very well sorted and have subrounded to subangular grains. The sandstone matrix includes void space, silt and minor clay, iron oxide, and rare organics. Sedimentary lithics may be deformed to make a pseudomatrix. The iron oxide is the main cement and occurs along grain boundaries (Fig. 5.5). There is more void space in sandstones from lithofacies association A1 compared to A2 and A3 sandstones. The North Cape Formation has more void space overall than either the Rakopi or Farewell formations.

The results from this study are consistent with the findings of Higgs et al. (2010), who found that the North Cape Formation sandstones are a mixture of feldsarenites and lithic feldsarenites in the Whanganui Inlet outcrops. Stark (1996) found that the North Cape varies

laterally in composition with lithic feldsarenites in the south and north of the Whanganui Inlet, and feldspathic litharenites in the centre of the Whanganui Inlet at Moki Point. This trend was not observed in this study.

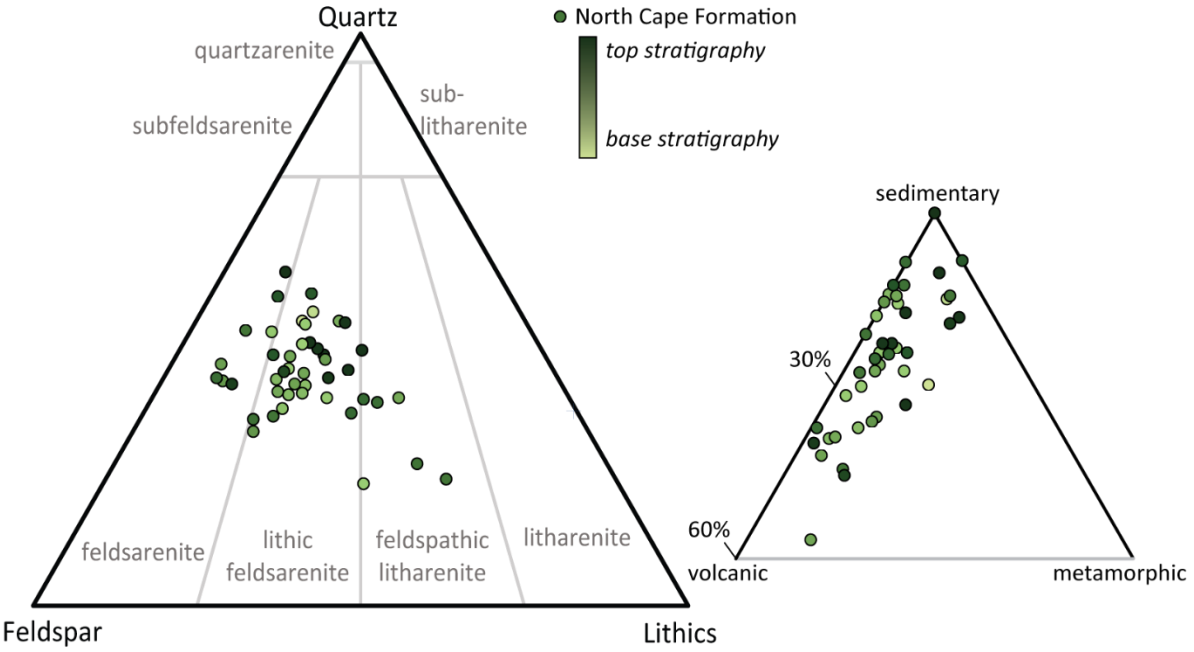

Fig. 5.3: QFL diagram after Folk et al. (1970) showing overall composition of the North Cape Formation samples, and the lithic composition. Points are shaded according to the approximate stratigraphic position of the samples.

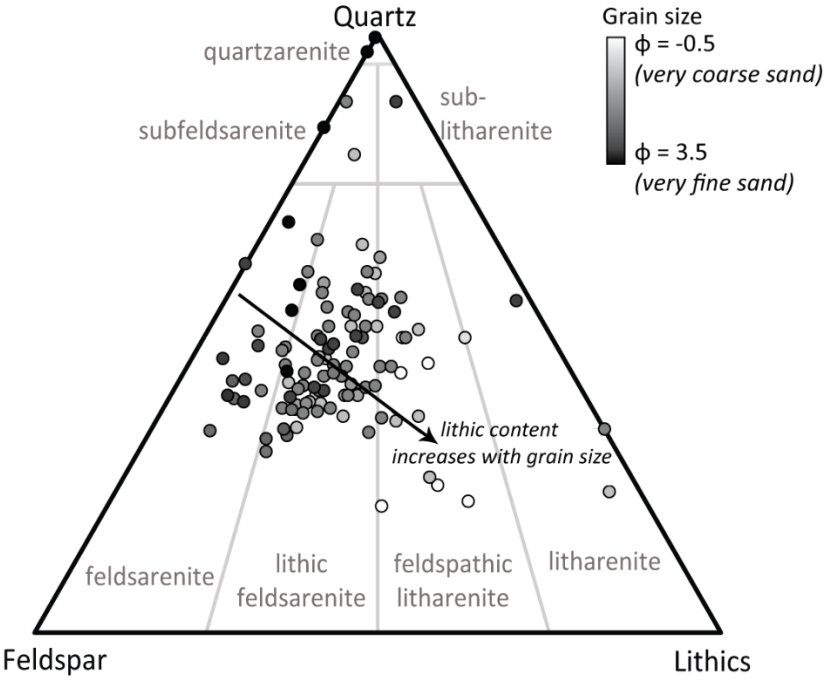

Fig. 5.4: QFL diagram after Folk et al. (1970) composition of all Pakawau Group and Farewell Formation sandstone samples in this study, with points shaded according to the sample grain size.

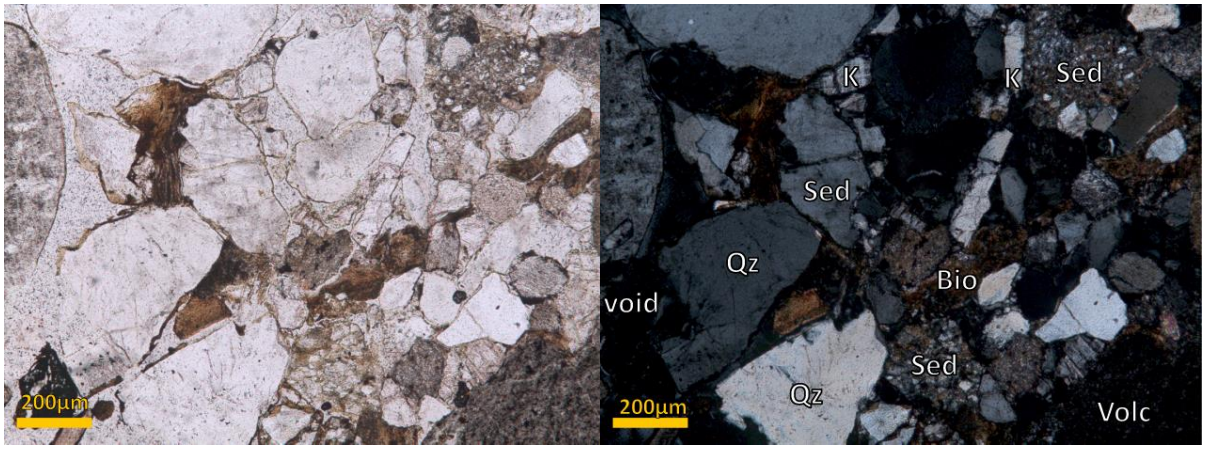

Fig. 5.5: photomicrographs showing typical composition and textures of the North Cape Formation (PP190). PPL on left, CPL on right of same view of thin section.
Qz: quartz; Poly: polycrystalline quartz; K: alkali feldspar; Bio: biotite; Musc: muscovite; Sed: sedimentary lithics; Volc: volcanic lithics; Sch: schist lithics. Scale bar is 200µm.

5.5 Composition and texture of Farewell Formation sandstones

The Farewell Formation is dominated by lithic feldsarenites with minor feldsarenites and feldspathic litharenites (Fig. 5.6). There is a strong temporal trend, with the sandstones becoming more quartzose up the stratigraphy. The two samples taken from the heavily iron-stained sandstone just below the top contact of the Farewell Formation (Pi079 and Pu221) are very quartzose, plotting as subfeldsarenites. The lithic composition also changes through the Farewell Formation. At the base, it is similar to the North Cape Formation with a mix of dominantly sedimentary lithics, some volcanics, and minor metamorphics (Fig. 5.6). Sedimentary lithics become more abundant upward through the Farewell Formation.

The Farewell Formation sandstones are moderately sorted and subangular to subrounded. The matrix is silt, with minor clay and voids. Minor iron oxide cements may coat grain boundaries. The top two samples from the Farewell Formation are rounded and well-sorted, with abundant iron oxide cement and minor to moderate glauconite (Fig. 5.7).

The results are consistent with a study of the offshore Farewell Formation by Higgs and King (2017), who found that the Farewell Formation is slightly more quartzose than the North Cape Formation, and has a mean feldsarenite composition. Titheridge (1977) also found that the Farewell Formation sandstones are feldsarenites. Stark (1996) described two feldsarenite Farewell Formation samples, six feldspathic litharenites and four litharenites. From visual estimation of Stark's (1996) thin sections, they have approximately the same composition as the samples in this study. Stark's (1996) anomalous results may be from incorrect

identification of clay and silt matrix as lithics, and/or misidentification of feldspars as quartz as the thin sections are not stained.

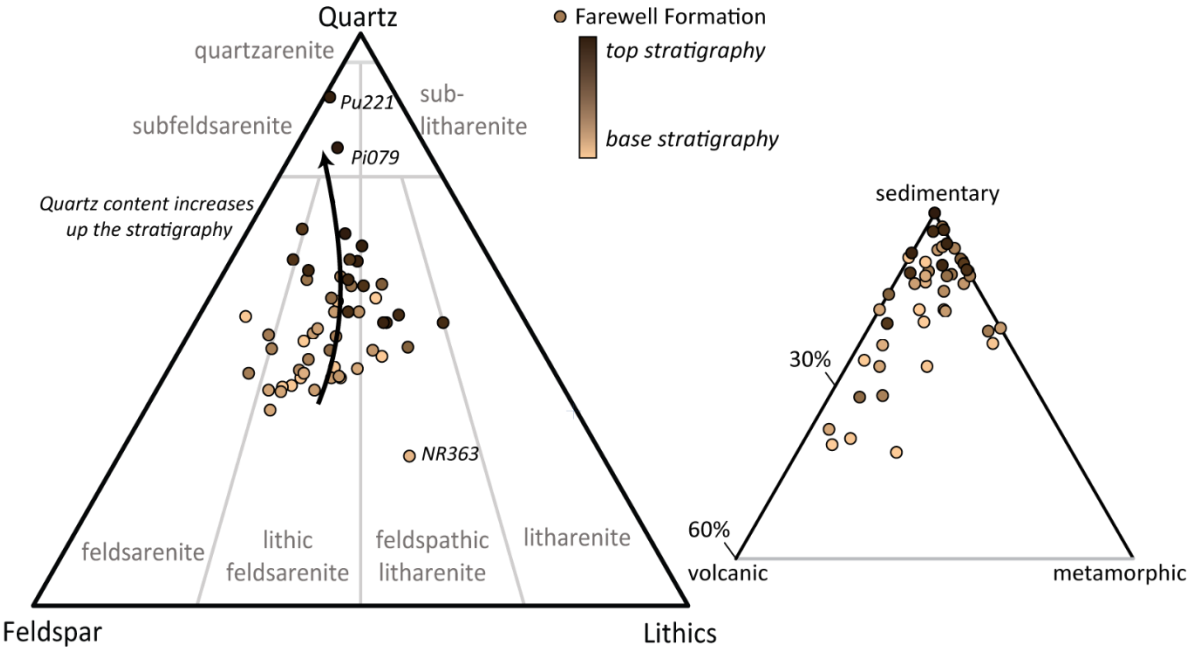

Fig. 5.6: QFL diagram after Folk et al. 1970 showing overall composition of the Farewell Formation samples, and the lithic composition. Points are shaded according to the approximate stratigraphic position of the samples.

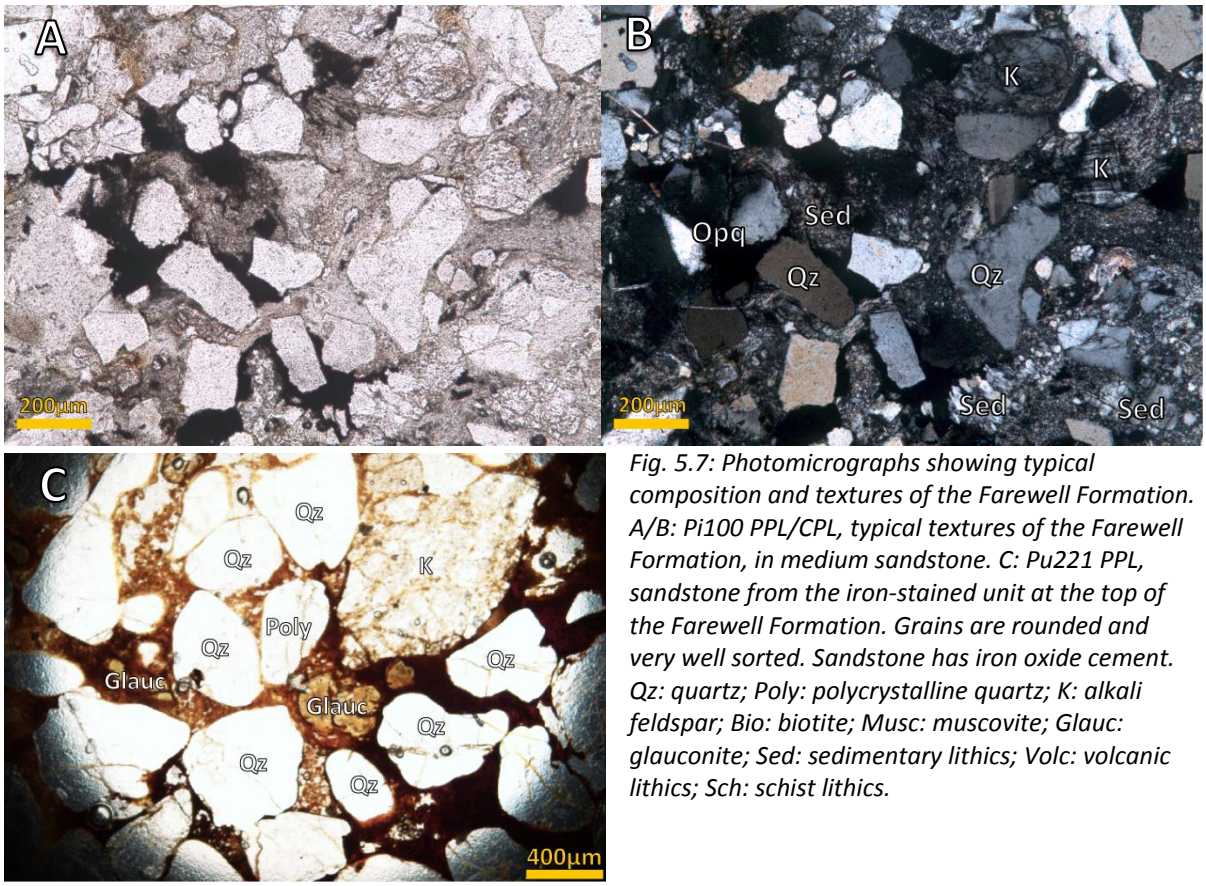

Fig. 5.7: Photomicrographs showing typical composition and textures of the Farewell Formation. A/B: Pi100 PPL/CPL, typical textures of the Farewell Formation, in medium sandstone. C: Pu221 PPL, sandstone from the iron-stained unit at the top of the Farewell Formation. Grains are rounded and very well sorted. Sandstone has iron oxide cement. Qz: quartz; Poly: polycrystalline quartz; K: alkali feldspar; Bio: biotite; Musc: muscovite; Glauc: glauconite; Sed: sedimentary lithics; Volc: volcanic lithics; Sch: schist lithics.

5.6 Description of grain types

5.6.1 Quartz

Quartz grains show low relief and birefringence, and is differentiated from feldspars by its lack of cleavage, twinning, alteration, and staining from both the Na-cobaltinitrate and K-rhodizonate stains. Quartz morphologies include quartz with straight extinction, undulose extinction, and polycrystalline quartz (more than three crystals, all of which are quartz) (Fig. 5.8). Fine grained polycrystalline quartz (individual grains <0.01 mm) is classified here as chert. The coarser polycrystalline quartz commonly shows strong undulose extinction. In some cases, the polycrystalline quartz shows a bladed morphology (Fig. 5.9A).

The quartz grains are dominated by a mixture of undulose and straight extinction, which does not vary across the stratigraphy (Fig. 5.8). On the provenance discrimination plot of Basu et al. (1975), this mixture of quartz types plots as “low rank metamorphic” and “middle and upper rank metamorphic” (Fig. 5.8). The metasedimentary and metamorphic sources in the Buller and Takaka terranes are mostly low-grade metamorphic (chlorite and biotite zone). This distribution therefore likely represents a mixture of mostly low-grade metamorphic sources, with some plutonic sources contributing non-undulatory quartz.

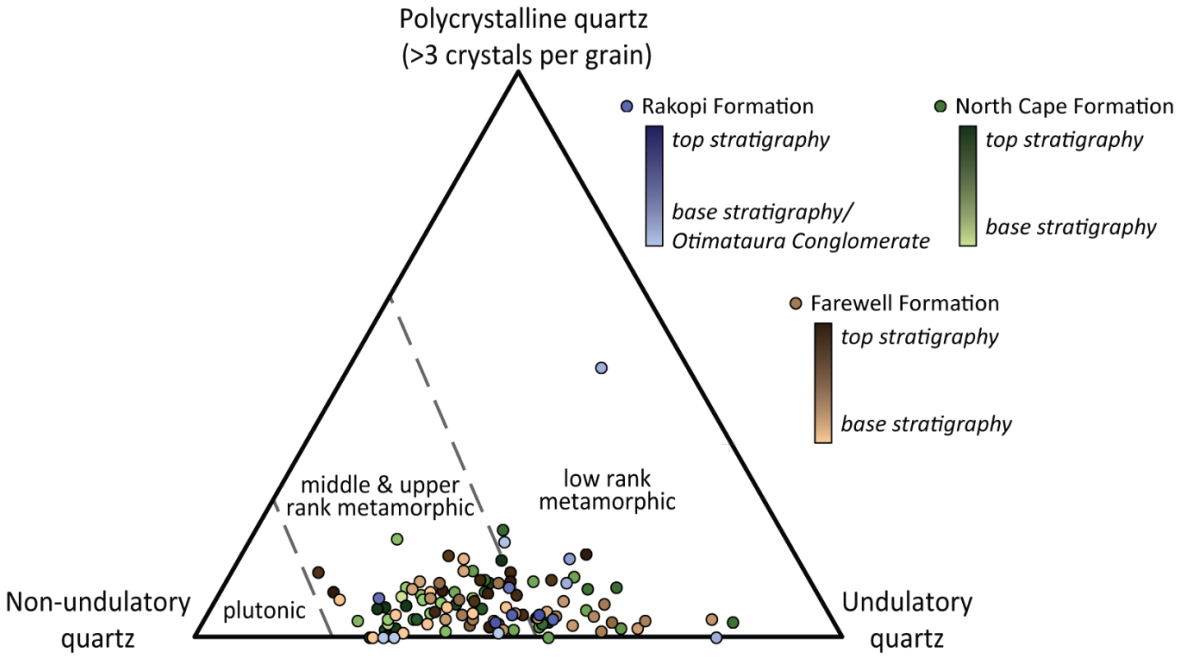

Fig. 5.8: quartz provenance discrimination plot after Basu et al. (1975). Data points are shaded according to approximate stratigraphic position.

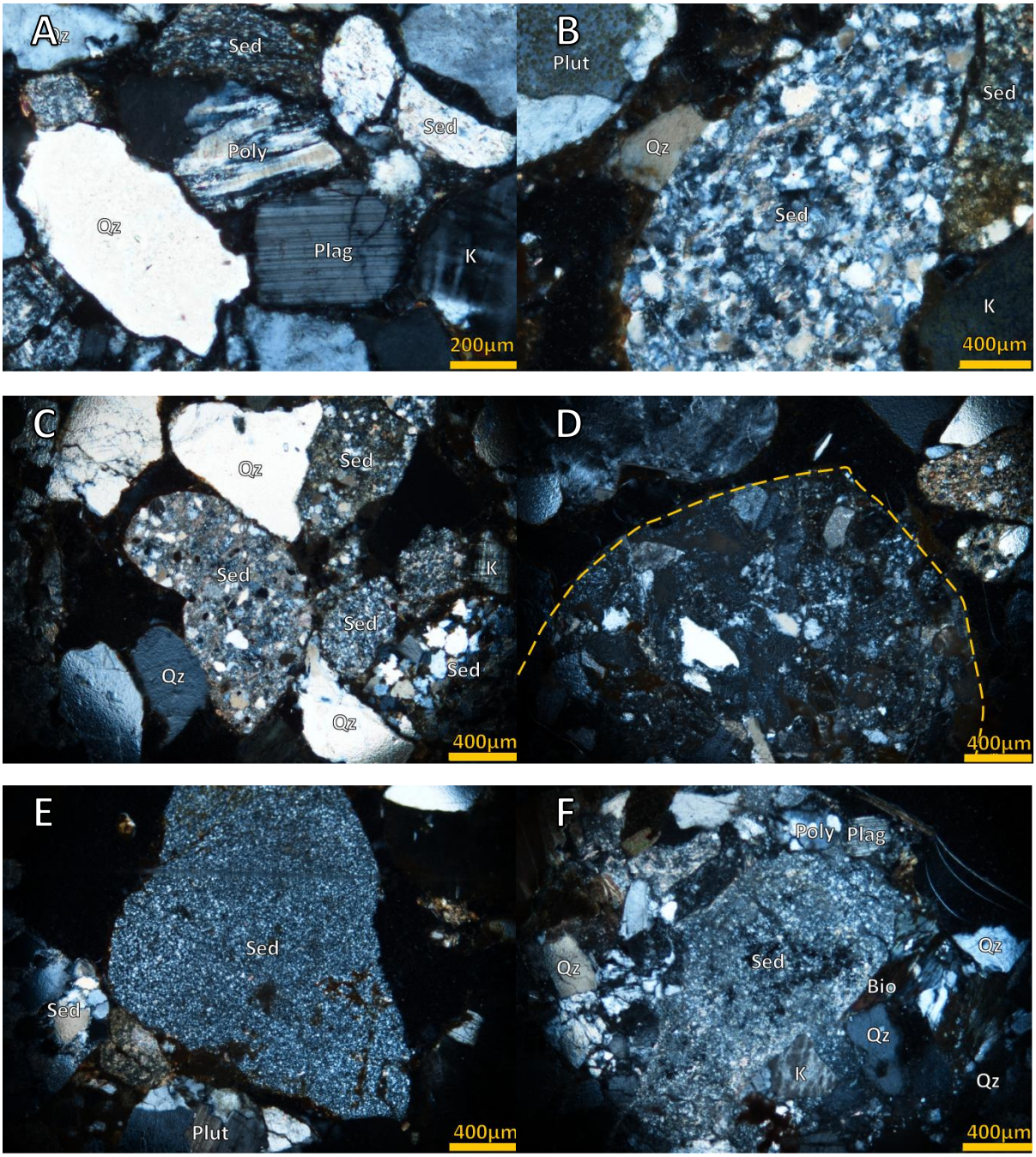

Fig. 5.9: Photomicrographs showing grain types in the Rakopi, North Cape, and Farewell formations. A: PP144 CPL, showing polycrystalline quartz grin with bladed morphology. B: PP296 CPL, metasedimentary grain (centre). Plutonic grain in top left has interlocking alkali-feldspar and quartz. C: PP296 CPL, metasedimentary grains with moderate sorting (centre). D: PP296 CPL, very fine sandstone lithic (outlined), with quartz, feldspar, and lithic grains. E: PP296 CPL, quartzose siltstone lithic (centre). F: Wh269 CPL, siltstone lithic with high birefringent clay minerals.
Qz: quartz; Poly: polycrystalline quartz; K: alkali feldspar; Bio: biotite; Sed: sedimentary lithics; Volc: volcanic lithics; Plut: plutonic lithics.

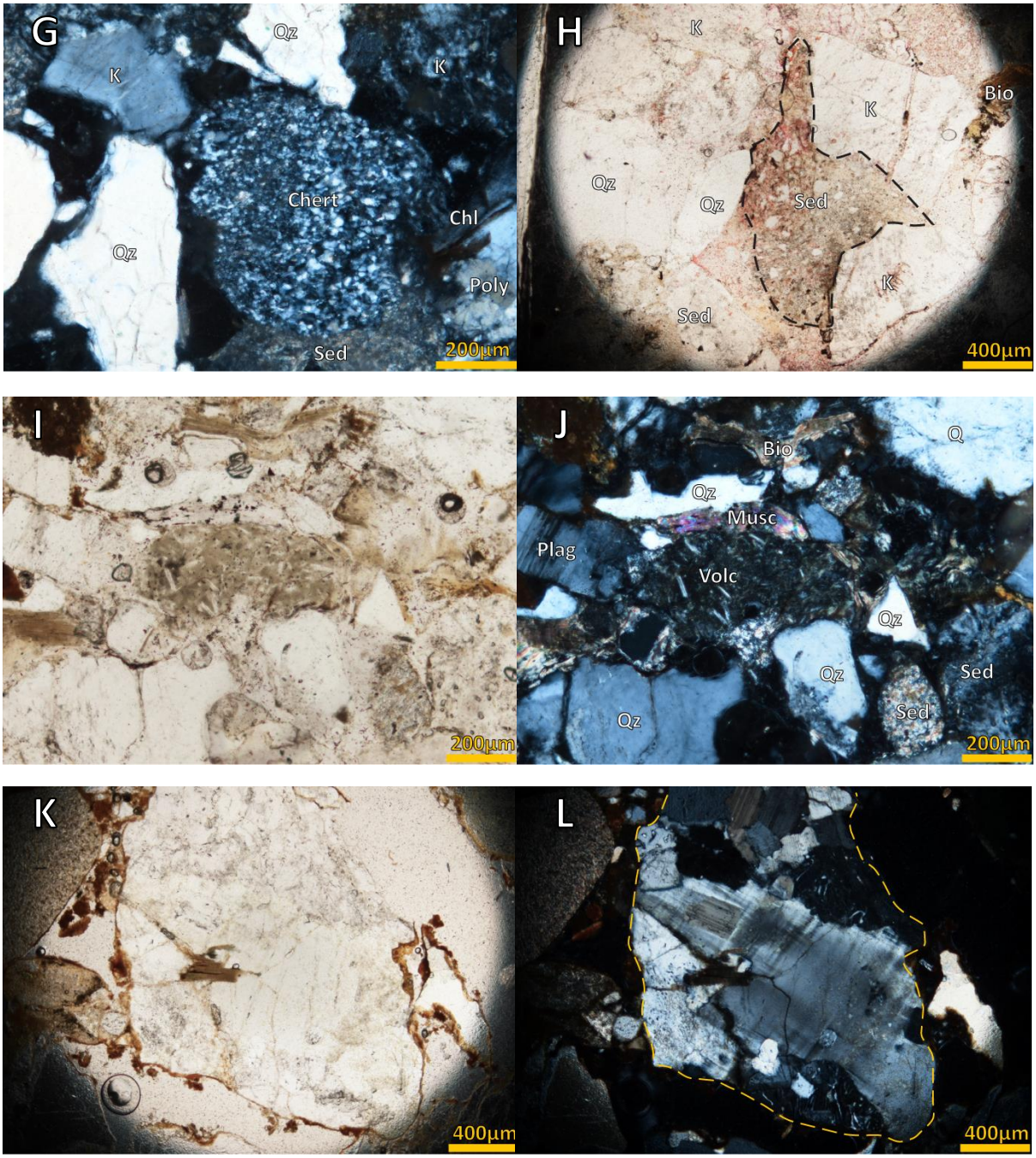

Fig. 5.9 cont.: Photomicrographs showing grain types in the Rakopi, North Cape, and Farewell formations. G: Wh269 CPL, chert lithic. H: OP069 PPL, sedimentary lithic (outlined) deformed around adjacent quartz and feldspar grains forming a pseudomatrix. I/J: PP144 PPL/CPL, volcanic lithic (centre) with plagioclase laths. K/L: PP296 PPL/CPL, plutonic grain (centre, outlined) with interlocking crystals of microcline feldspar, plagioclase, quartz, and biotite.
Qz: quartz; Poly: polycrystalline quartz; K: alkali feldspar; Bio: biotite; Musc: muscovite; Sed: sedimentary lithics; Volc: volcanic lithics; Plut: plutonic lithics.

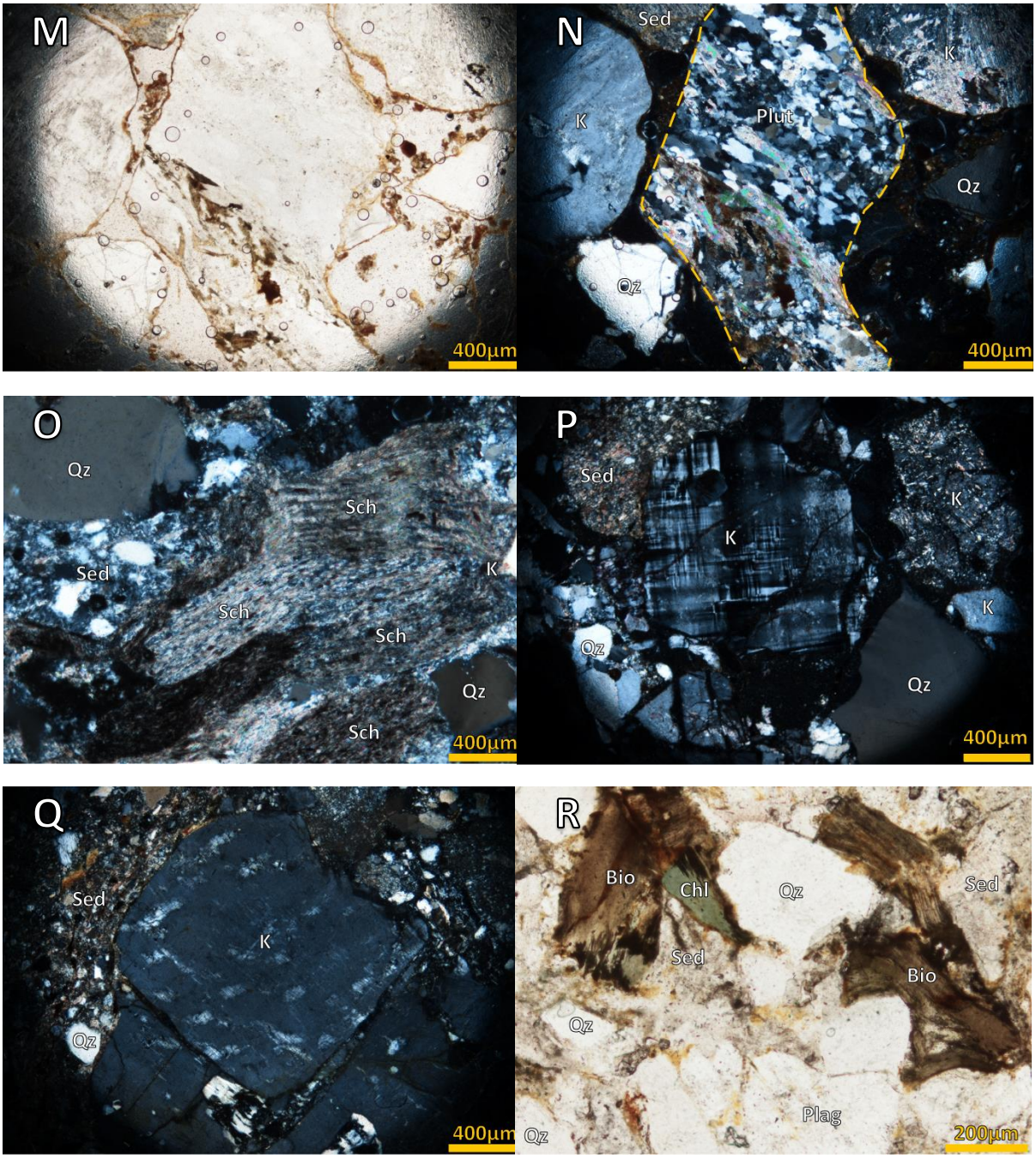

Fig. 5.9 cont.: Photomicrographs showing grain types in the Rakopi, North Cape, and Farewell formations. M/N: PP296 PPL/CPL, foliated plutonic grain (centre, outlined) with interlocking crystals of quartz, feldspar, and muscovite and biotite showing foliation. O: PR200 CPL, schist lithics in Otimataura Conglomerate sandstone. P: OP069 CPL, alkali feldspar (centre) showing microcline twinning. Q: OP061 CPL, alkali feldspar grain with perthite texture. R: Wh244 PPL, green-brown biotite partially altered to clays, and chlorite.
Qz: quartz; Poly: polycrystalline quartz; K: alkali feldspar; Bio: biotite; Chl: chlorite; Sed: sedimentary lithics; Volc: volcanic lithics; Plut: plutonic lithics, Sch: schist lithic.

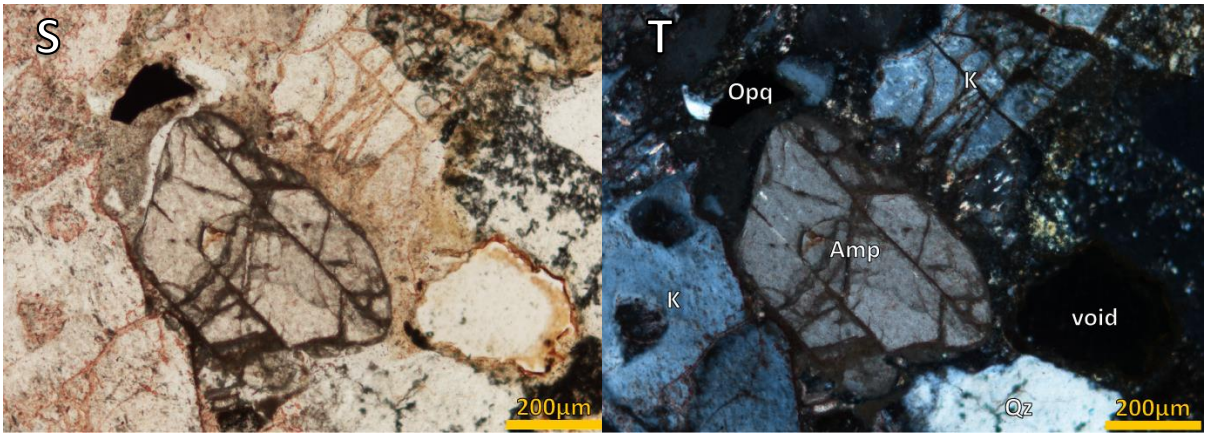

Fig. 5.9 cont.: Photomicrographs showing grain types in the Rakopi, North Cape, and Farewell formations. S/T: OP069 PPL/CPL, amphibole grain with green-brown colour, high first order interference colours, high relief.
Qz: quartz; Poly: polycrystalline quartz; K: alkali feldspar; Amp: amphibole; Bio: biotite; Chl: chlorite; Sed: sedimentary lithics; Volc: volcanic lithics; Plut: plutonic lithics.

5.6.2 Lithics

The Rakopi, North Cape, and Farewell formations have a variety of lithic types, including sedimentary and metasedimentary lithics, schist, and volcanic and plutonic lithics (Fig. 5.10). Metasedimentary and sedimentary lithics are dominant in almost all of the samples, with volcanic and plutonic lithics, and minor schist. The basal Otimataura Conglomerate of the Rakopi Formation is dominated by schistose lithics in the Paturau River, and by sedimentary lithics in the Pakawau Bush Road outcrops. Volcanic and plutonic lithics become less common towards the top of the Farewell Formation. These trends mirror those seen in the conglomerate clast count results (Fig. 4.1).

The "metasedimentary" lithics are those that show evidence for high burial depths and significant compaction, such as sutured boundaries on quartz grains, strained quartz, and quartz overgrowths. The metasedimentary lithics are quartzose, with minor alkali feldspar, and small muscovite grains on grain boundaries (Fig. 5.9B). The lithics may be cut by thin quartz veins. These lithics have similar composition and textures to the metasedimentary conglomerate clasts, which are most likely from the Ellis Group of the Takaka Terrane.

Some siltstone grains do not have sutured grain boundaries and highly strained quartz. These are usually quartz-dominated and are often moderately sorted with subangular quartz in a fine silt matrix (Fig. 5.9C). The quartz siltstones are unlikely to be intrabasinal, as they are

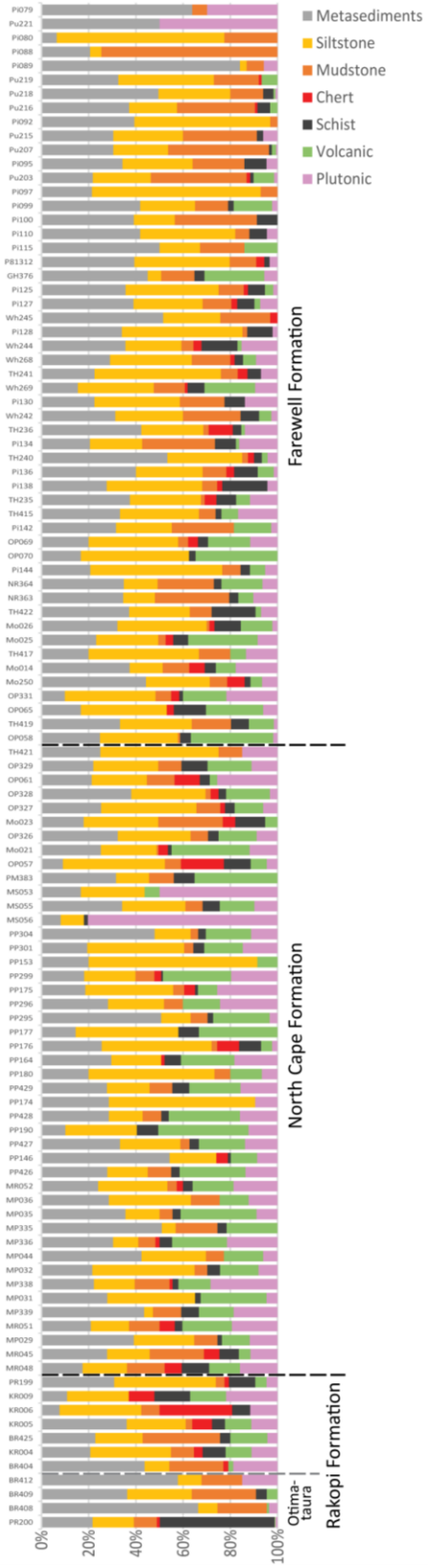

Fig. 5.10: Composition of lithics in sandstone samples organised into stratigraphic position.

significantly more quartzose than the Pakawau Group and Farewell Formation. Both the upper Takaka Terrane (Baton and Ellis groups) and the Golden Bay Group of the Buller Terrane are highly quartzose, either are possible sources due to their similar petrology (Section 4.4.1)

There are also rare siltstone lithics which have quartz, feldspar and sedimentary lithics in similar proportions to the Pakawau Group and Farewell Formation (Fig. 5.9D). These are therefore likely to be intrabasinal clasts.

When point-counting, the very fine siltstone to mudstone lithics were classified as either "quartz-dominated" or "high birefringent mineral dominated". The quartz-dominated mudstones are matrix-supported, with very fine silt quartz grains in a mud matrix (Fig. 5.9E). These grains may have small quartz veins. The high birefringent mineral dominated very fine siltstones to mudstones are distinguished by a prevalence of grains with second to third order interference colours, possibly clay minerals such as illite (Fig. 5.9F). These mudstones are typically better sorted than the quartz-dominated mudstones. Because they are fine-grained, it is difficult to identify a source for these lithics. They are also difficult to distinguish from the devitrified glass seen in the Takaka Terrane volcanics and the volcanic clasts in the conglomerates.

Chert is a very minor grain type. It is here defined as being 100% siliceous (i.e. unable to see internal crystal boundaries in plane-polarised light as all crystals have the same relief) and has a grain-size of fine to very fine silt (Fig. 5.9G). Chert occurs as lithics, veins and beds in

the Golden Bay Group (Harrison 1993), and as clasts and nodules in the Takaka Terrane (Grindley 1980; Rattenbury et al. 1998).

Volcanic lithics are common in the Rakopi and North Cape formations, becoming less abundant in the Farewell Formation. The volcanic lithics have devitrified and altered glass, which is green-brown in plane-polarised light, and may be black in cross-polarised light, or altered to very fine grained high birefringent clay minerals (Fig. 5.9I-J). The volcanics may have phenocrysts, usually of plagioclase, which may also be altered and replaced. The volcanic lithics are likely to be from the Takaka Terrane Devil River Volcanics.

Plutonic lithics are grains which have more than one interlocking crystal of different minerals (e.g. quartz, feldspar, biotite, and/or muscovite) (Fig. 5.9K-L). Some plutonic grains show foliation (Fig. 5.9M-N). The quartz may have straight or undulose extinction. Plutonic lithics are more common in the coarser sandstones.

Foliated metamorphics are a moderately common lithic type. They are usually finely foliated, and often heavily altered to clays. They may have fine-grained muscovite, biotite, and quartz which define the foliation (Fig. 5.9O).

5.6.3 Feldspar

Alkali feldspars were dominant over plagioclase in all samples (Fig. 5.11). Microcline twinning is the dominant texture in the alkali feldspars in both the Pakawau Group and the Farewell Formation (Fig. 5.9P). Perthitic textures are common (Fig. 5.9Q), as well as mild to strong alteration, typically to sericite, and rare myrmekite.

Plagioclase feldspars commonly showed strong polysynthetic twinning (Fig. 5.9A, J), and occasionally deformation twinning. They are commonly altered, more strongly than alkali feldspars in the same sample.

The feldspars are most likely to be derived from the plutonic sources in the region. The Takaka and Buller Terrane metasedimentary rocks are highly quartzose, and thus unable to supply large amounts of feldspar. The Takaka Terrane volcanics and volcaniclastics are typically altered, so the feldspars are not as fresh as those seen in the sandstones.

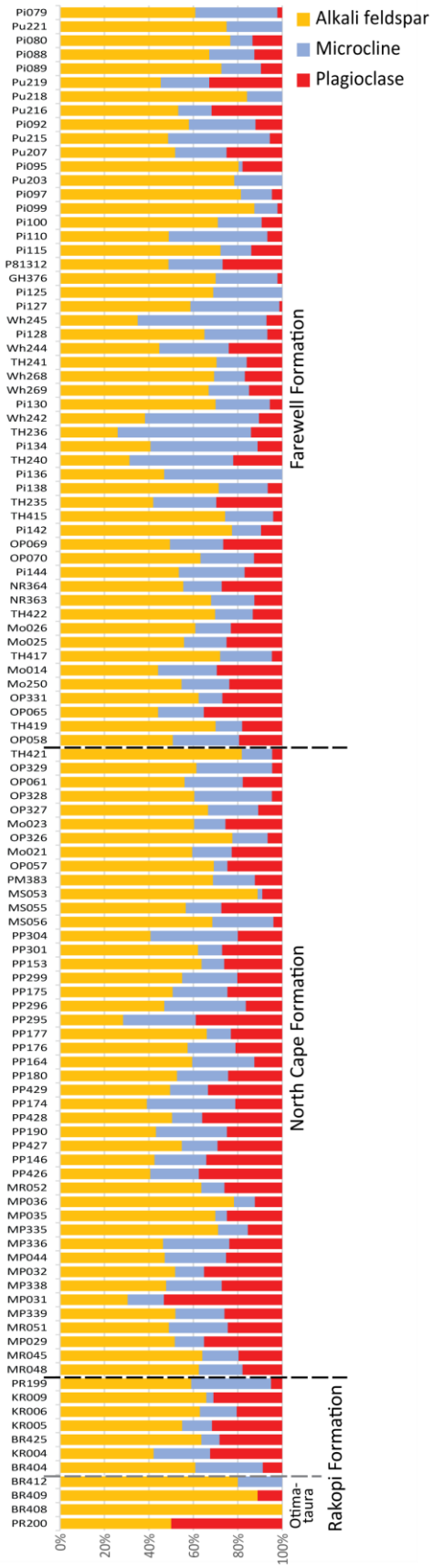

Fig. 5.11: Feldspar content of sandstone samples organised into stratigraphic position.

Apart from in the Otimataura Conglomerate, the relative proportion of microcline, other alkali feldspars, and plagioclase is consistent throughout the Rakopi, North Cape, and Farewell formations (Fig. 5.11). This suggests the feldspar source(s) are not changing. The total feldspar content does not change through the stratigraphy, apart from the top of the Farewell Formation where the feldspar content decreases slightly (Fig. 5.6). This fits with trends seen in the sandstone lithics and in the conglomerates where plutonic sources become less significant at the top of the Farewell Formation. The Otimataura Conglomerate samples from both the Paturau River and Pakawau Bush Road have very little feldspar, but these few are dominated by alkali feldspars.

5.6.4 Micas

Biotite is the most common mica type, followed by muscovite (Fig. 5.12). The biotite is green-brown in colour and shows moderate to very strong pleochroism (Fig. 5.9R). It may be partially altered to clays. Chlorite is rare in thin sections, and where present typically replaces biotite. Biotite and muscovite grains are commonly aligned along bedding and may be deformed around less labile grains. Muscovite grains are typically smaller than biotite.

The micas are most likely to be derived from a plutonic source. There are schists and metasedimentary rocks containing micas in northwest Nelson, however these are finer grained than the micas observed in the sandstones (Harrison 1993; Rattenbury et al. 1998).

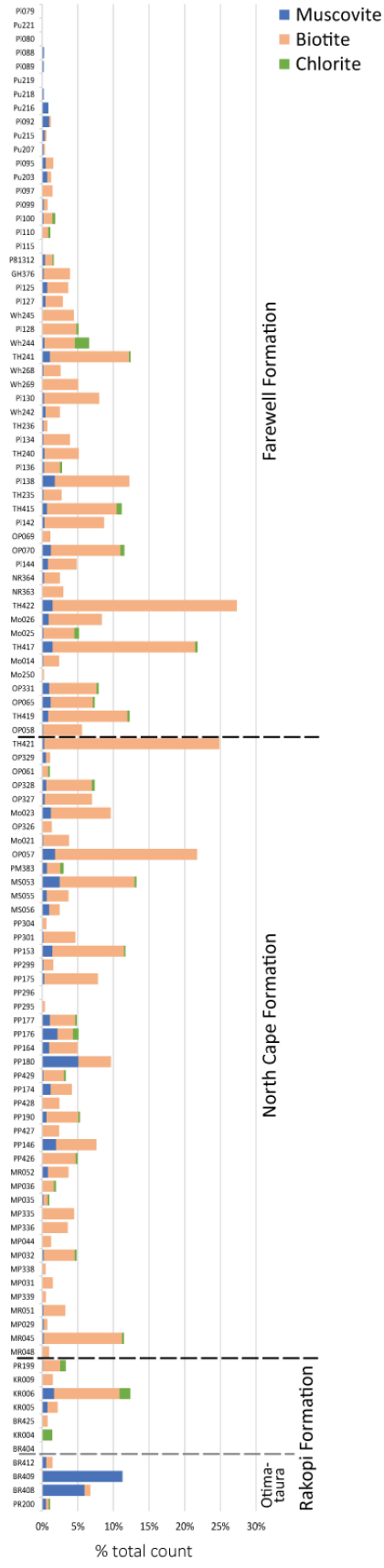

Fig. 5.12: Mica content of sandstone samples organised into stratigraphic position.

Biotite and muscovite are accessory minerals in both the Separation Point and Karamea suites, although the Karamea Suite has red-brown biotite compared to green-brown in the Separation Point Suite (Tulloch 1983; Muir et al. 1995). Chlorite, green-brown biotite, and muscovite are all observed in the conglomerate granitoid clasts.

The total mica content in the sandstone is variable, ranging from <1% of the total grains to 27%. The variability is likely due to highly localised variation in mica concentration between beds. The mica concentration does decrease towards the top of the Farewell Formation (Fig. 5.12), suggesting that granitoid sources became less significant.

5.6.5 Heavy minerals and opaques

Minerals including amphibole, pyroxene, and olivine are rare in the samples. Where present, the crystals are small and altered. They are distinguished by their high relief and birefringence. Amphiboles are pale green with weak pleochroism, have 60°/120° cleavage, and sometimes have a subhedral, elongated hexagonal shape (Fig. 5.9S-T). Orthopyroxene is greenish yellow, non-pleochroic, has 90° cleavage, and has high first to low second order interference colours.

There are several possible sources for the amphiboles, pyroxenes, and olivine. Phenocrysts of amphibole, pyroxene, and olivine occur in the Takaka Terrane Devil River Volcanics (Maclean 1994; Münker and Cooper 1999). Hornblende is an accessory mineral in the Separation Point Suite and is a rare accessory mineral in the Karamea Suite (Tulloch 1983; Muir et al. 1995). Hornblende also occurs in the Wakamarama Schist (Rattenbury et al. 1998).

Opaque minerals show a range of morphologies. Detrital opaque minerals are rare, and are typically completely opaque, subhedral, equant grains. Secondary red-brown semi-opaque minerals can occur as equant grains, but are commonly present filling interstitial spaces, concentrated along bedding surfaces, or in fractures.

5.7 Sandstone provenance

The Rakopi, North Cape, and Farewell Formation samples all plot in the recycled orogenic and dissected arc fields of Dickinson et al.'s (1983) provenance discrimination plot (Fig. 5.13). This is consistent with the mixture of metasedimentary, plutonic, and volcanic basement terranes (recycled orogen). The plot may be skewed towards a "dissected arc" setting because of the input of volcanic lithics from the Takaka Terrane, and feldspars from the Separation Point Suite and other plutonic sources.

The Otimataura Conglomerate reflects local sources. The schist in the Paturau River sample is likely to be sourced from the Waingaro Schist of the Takaka Terrane, which outcrops several kilometres to the east of the Paturau River outcrop (Fig. 2.8). The basement does not outcrop in the Pakawau Bush Road region (Rattenbury et al. 1998), although it is likely to be the upper sedimentary units of the Takaka Terrane, a likely source for the sedimentary lithics (Fig. 2.8). The micas in the Pakawau Bush Road samples are dominated by muscovite, derived either from a metamorphic or metasedimentary source, or from a muscovite-rich granitoid.

The Rakopi (excluding Otimataura Conglomerate), North Cape, and lower Farewell Formation sandstones are lithic feldsarenites and feldsarenites, reflecting a mix of sources. The lithics in both formations are a mixture of plutonic, volcanic, sedimentary and metasedimentary grains, likely to be from the Separation Point Suite and/or Karamea Suite, the Takaka Terrane volcanics, and Buller and Takaka Terrane metasedimentary and sedimentary units. Plutonic and metasedimentary sources are also suggested by quartz grains with both straight and undulose extinction. Minor muscovite and biotite is likely to be derived from plutonic sources.

The Farewell Formation changes composition up the stratigraphy. The upper ~250 m has increasing quartz content, decreasing volcanic and plutonic lithics, and decreasing mica content. This suggests that the metasedimentary sources become more dominant towards the end of Farewell Formation time. This is consistent with the conglomerate clast count data,

which shows that granitoid clasts became more weathered and less abundant in the conglomerates towards the top of the Farewell Formation (Fig. 4.1). The granitoid sources may become less important because the drainage pathways shifted or the granitoid source was buried, or it may be because there was greater alteration at the surface reducing feldspars and micas to clays.

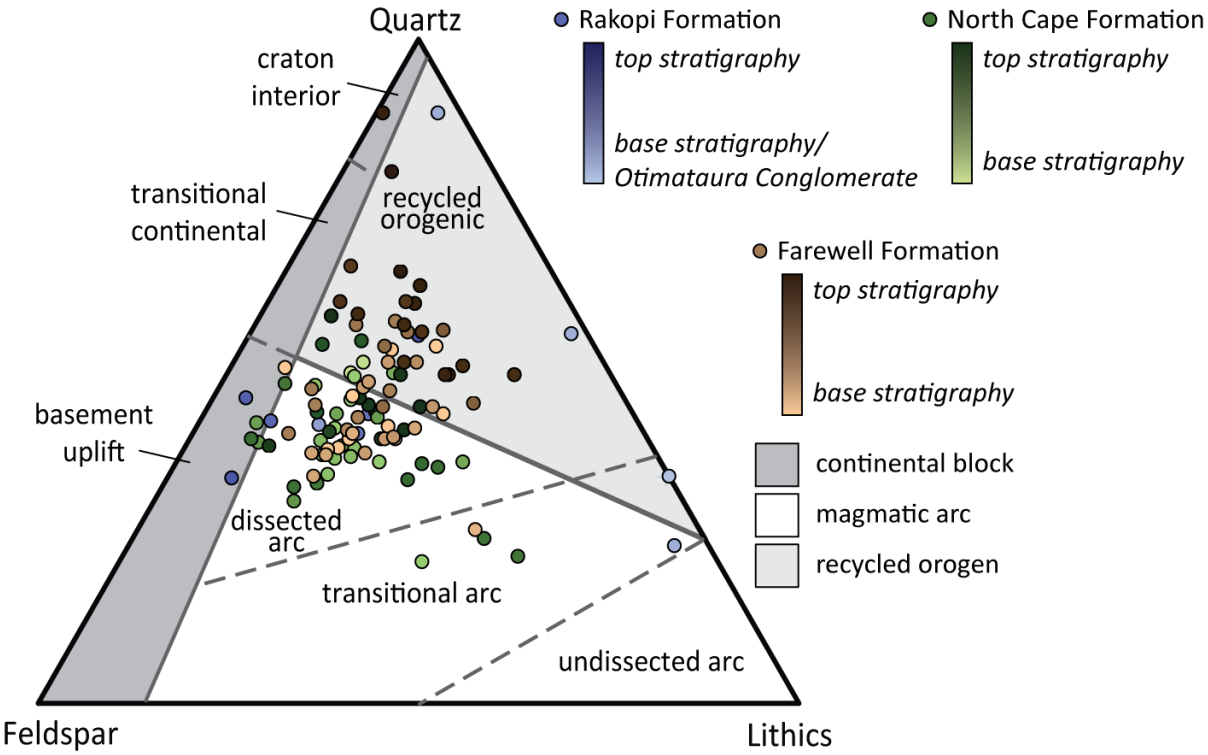

Fig. 5.13: sandstone provenance discrimination diagram after Dickinson et al. (1983). Note that this diagram is intended for medium sandstones, coarse and very coarse sandstones are enriched in lithics and fine and very fine sandstones are depleted.

5.8 Petrographic indicators of depositional setting

Browne et al. (2008) reported that the top of the Rakopi Formation contains minor glauconite, up to 2.4% in one sample. In this study, trace glauconite (up to 1.1%) was observed in Rakopi samples from the Kaituna Route northwest of Knuckle Hill, and from sample PR199 from near the top of the Paturau River section (Fig. 5.14). Glauconite is absent in the Otimataura Conglomerate sample from the Paturau River, and from all the basal Rakopi Formation samples along the Pakawau Bush Road.

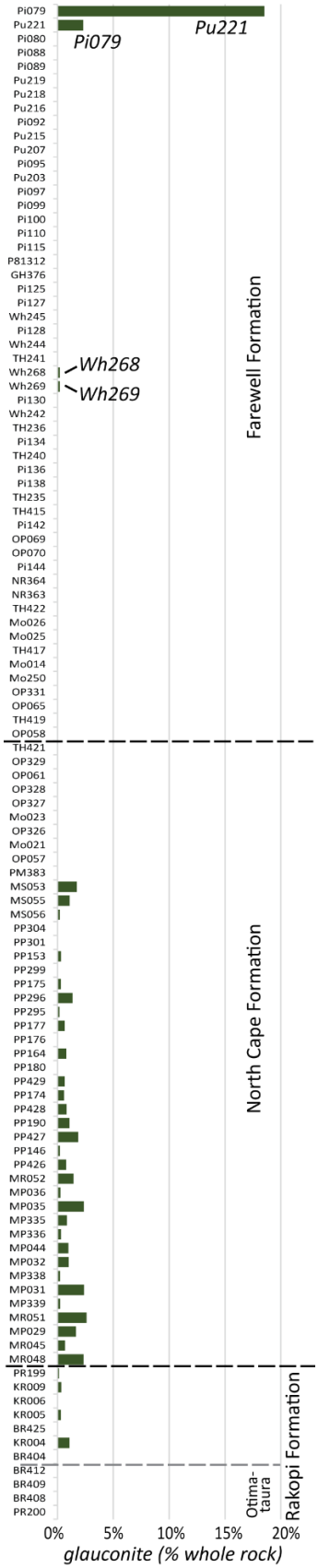

Fig. 5.14: Glauconite content of sandstone samples organised into stratigraphic position.

Glauconite in the Rakopi Formation was interpreted by Browne et al. (2008) as deposits from episodic marine incursions across the low-gradient coastal plain. Browne et al. (2008) also observed dinoflagellate cysts and high sulfur content in the Rakopi coals, further suggesting a marine influence. However, there are no sedimentological indicators of a paralic or marine environment. Alternative sources for the glauconite include reworking of older glauconitic units, or the glauconite and dinoflagellates were introduced by aeolian processes. None of the older units in the region contain glauconite, so this is not the source. Airborne contamination of sedimentary units by older, reworked, diatoms has been demonstrated in the Antarctic Sirius Group (Burckle and Potter 1996). A similar mechanism could be applied to the Rakopi Formation, where glauconite grains and dinoflagellates are picked up off an exposed shore platform or tidal mudflats and transported inland. High sulfur contents in the coal could be explained by very early diagenetic influence from sulfate-rich marine water.

Both explanations for the presence of glauconite require that the coastline was relatively close. This is consistent with the overall transgressive setting as the Rakopi Formation transitions into the marginal marine North Cape Formation.

The North Cape Formation contains minor glauconite (up to 2.6%) in all lithofacies associations (Figs. 5.14, 5.15A/B). Glauconite formation commonly occurs on the continental shelf and slope (Reineck and Singh 1980). It has also been shown to form in marginal marine and paralic environments at

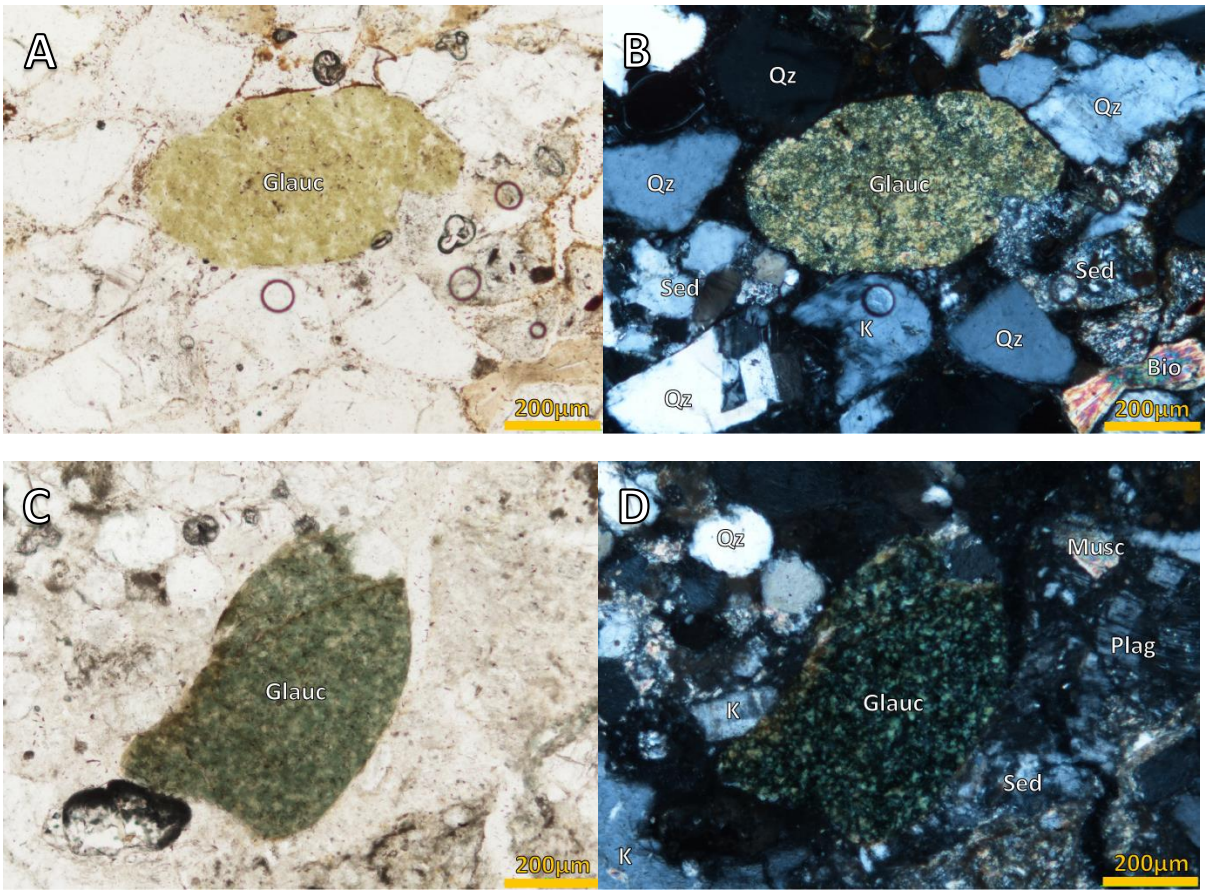

Fig. 5.15: Photomicrographs of glauconite in the North Cape and Farewell formations. Qz: quartz; K: alkali feldspar; Bio: biotite; Glauc: glauconite; Sed: sedimentary lithics.
A/B: PP144 PPL/CPL, pale green glauconite grain in the North Cape Formation. C/D: Wh269 PPL/CPL, glauconite grain in the Farewell Formation.

water depths from less than 10 m to intertidal, despite high energy and high sedimentation rates (Chafetz and Reid 2000). The glauconite in the tidal shallow marine North Cape Formation may have been transported from the shelf by marine currents or have formed in situ. The glauconite in the terrestrial lithofacies association A3 may have been transported inland by a marine incursion across the shallow coastal/delta plain, or by aeolian processes.

The majority of the Farewell Formation sandstones have no glauconite, which is consistent with the fluvial interpretation discussed in Chapter 3. However, there are two samples from Whariki Beach, approximately half-way through the Farewell Formation, which have a few grains of emerald green glauconite (Wh268 and Wh269, 0.2% glauconite in both samples) (Figs. 5.14, 5.15C/D). The samples both come from the same unit in the gravelly braided river association, a planar cross-bedded conglomerate and pebbly sandstone. As for the Rakopi Formation, the glauconite could be interpreted as reworked glauconite from an older unit, glauconite transported by aeolian processes, or glauconite from a marine incursion. There is

no glauconite in the basement lithologies, however it may be reworked from the older North Cape or Rakopi formations.

The two samples from the iron stained unit at the top of the Farewell Formation (Pi079 and Pu221) have a distinctly different composition and texture to the rest of the Farewell Formation. These sandstones are well rounded and well sorted with abundant iron oxide cement. Sample Pi079 has abundant glauconite (19%), and Pu221 has moderate glauconite (2%). The glauconite suggests that these are marine or marine-influenced sedimentary rocks. The high degree of rounding and sorting is also suggestive of highly reworked coastal or shelf deposits. The iron-stained unit therefore represents the marine transgression at the end of Farewell Formation time, prior to the unconformity with the marine Matapo (greensand) Member.

5.9 Conclusion

The North Cape and Rakopi formations (excluding the Otimataura Conglomerate) are a mix of feldsarenites and lithic feldsarenites. There are no spatial or stratigraphic trends within these formations. These sandstones are moderately to very well sorted with subangular to subrounded grains. The lithics are dominated by metasedimentary siltstones, as well as siltstones, mudstones, chert, volcanics, plutonic grains, and minor schist. The feldspars are dominated by alkali feldspar, commonly with perthitic textures. There is moderate to abundant mica, which is mostly biotite. Heavy minerals are rare.

The Otimataura Conglomerate of the Rakopi Formation has a different composition to the rest of the Pakawau Group. The sandstones have a higher proportion of lithics, plotting as litharenites. The lithics in the Paturau River section are schists, and the Pakawau Bush Road outcrops have sedimentary lithics. The micas in the Pakawau Bush Road are dominated by muscovite.

The lower Farewell Formation is similar in composition to the Rakopi and North Cape formations. The composition changes up the Farewell Formation stratigraphy, becoming more quartzose. Plutonic and volcanic lithics become less common up the stratigraphy, and the total mica content decreases. Two sandstones from the top, iron-stained, unit of the

Farewell Formation are highly quartzose, with minor to abundant glauconite, and rounded, well-sorted grains.

The Otimataura Conglomerate has a local provenance, with lithic compositions reflecting the local basement. The Rakopi, North Cape, and Farewell Formation sandstones have a mixed provenance of metasedimentary and sedimentary siltstones and mudstones (Buller and/or Takaka Terrane), plutonic sources (Separation Point Suite), volcanics (Takaka Terrane), and schist (Buller and/or Takaka Terrane). Metasedimentary and sedimentary sources become more dominant towards the top of the Farewell Formation, possibly due to shifting drainage pathways, burial of some basement outcrops, or because surface alteration removed more readily altered material including the volcanics rocks and plutonic feldspars.

6. SEDIMENTARY GEOCHEMISTRY

6.1 Introduction

The aim of this chapter is to use the whole rock chemical composition of sedimentary samples from the Rakopi, North Cape, and Farewell formations to investigate stratigraphic changes in provenance, depositional environment, and diagenesis. Geochemical analysis is useful for mudstones too fine to be analysed by petrographic techniques. Mudstones in sand and gravel-dominated lithologies represent a more homogenous mix of source areas and may include more distal sources (McLennan et al. 1993). In this chapter, the geochemical interpretations are validated by comparison to petrographic interpretations from the sandstones.

6.2 Methods

In this study, 51 sedimentary samples were selected and sent for analysis at the Chemostrat Ltd. laboratory, United Kingdom. Those samples were chosen to represent the full range of the stratigraphy and lithofacies associations recorded as part of this thesis. Samples with a variety of grain sizes were selected and these range from claystones to very coarse sandstones, with a fine sandstone average. Uncrushed, 50 g samples were sent to the Chemostrat UK laboratory for processing. Samples were prepared there by flux fusion. The major elements and S and Sc were analysed using a iCAP 7000 Series inductively coupled plasma optical emission spectrometer (ICP-OES). Thirty-four trace elements and REEs were analysed using a Thermo Scientific XSERIES 2 inductively coupled plasma mass spectrometer (ICP-MS). The Chemostrat laboratory has ISO9001:2008 Certification (International Organization for Standardization 2015; Origin Analytical 2018). The raw geochemical data is included in Appendix H.

Six additional sedimentary samples were crushed using a tungsten carbide ring mill and sent to Spectrachem Ltd. for X-ray Fluorescence (XRF) analysis. Three of the samples were included to cover additional outcrops. Three samples were sent to both Spectrachem and Chemostrat to ensure that the results from both laboratories were comparable (Appendix F). Methods from the Spectrachem Ltd. laboratory are described in Section 4.2.3.

6.3 Geochemical indicators of paleoenvironment

6.3.1 Marine indicators

The sedimentology of the North Cape Formation indicates a marginal marine environment (Section 3.4), as does the presence of glauconite in North Cape Formation sandstones. The marine influence clearly shows in the sedimentary whole rock geochemistry; North Cape sedimentary rocks have elevated P_2O_5 concentrations of 0.02 – 0.27 wt.%, and S of 78.74 – 874.51 ppm (Fig. 6.1). Both elements are associated with marine settings (Reineck and Singh 1980).

Terrestrial lithofacies association A3 (coastal plain/meandering river deposits, Section 3.4) are expected to have the least marine influence of the North Cape Formation samples. In thin section, the association A3 sandstones contain glauconite in similar concentrations to the shallow marine and estuarine A1 and A2 lithofacies. However, the P_2O_5 and S concentration is lower in samples from lithofacies A3 (0.06 – 0.11 wt.% and 78.74 – 85.67 ppm respectively) (Fig. 6.1), suggesting that these geochemical indicators are more sensitive to the degree of marine influence than petrographic indicators (presence of glauconite).

In contrast to the North Cape Formation, the Farewell Formation has low P_2O_5 and S concentrations of 0.01 and 0.06 wt.% and 22.43 – 182.14 ppm respectively (Fig. 6.1), excluding the two samples from the iron-stained unit at the top of the formation. This confirms the terrestrial interpretation from the sedimentology and petrographic data (Sections 3.4 and 5.8).

The Rakopi Formation has minor glauconite in some sandstone samples (Fig. 6.1). It also has elevated P_2O_5 concentrations, although the S concentration is low. P_2O_5 may be introduced to the system in detrital phosphate minerals in a similar manner to the glauconite (Section 5.8). S may be included in the North Cape Formation due to sulfates in marine pore fluids very early in diagenesis, a mechanism which is not applicable in the freshwater Rakopi Formation.

Several studies have suggested that other trace elements and REEs including Cr, Cu, Ga, Ni, V, and the Zr/Hf ratio are elevated in marine deposits (Ernst 1970; Reineck and Singh 1980).

However, in this study no correlation was found between these parameters and sedimentological and petrographic indicators of marine influence.

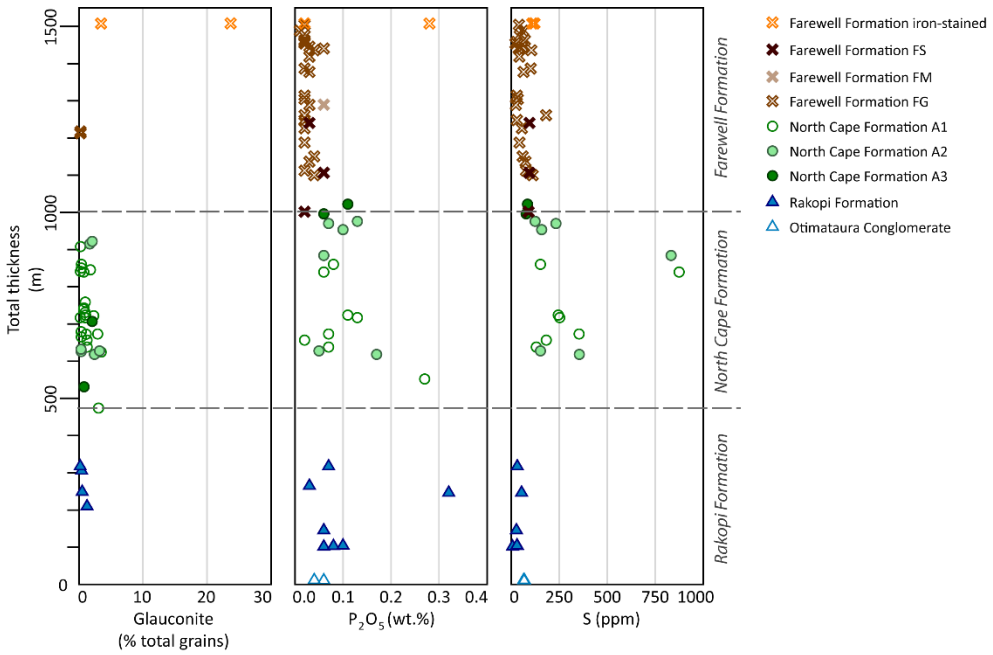

Fig. 6.1: Stratigraphic variation in petrographic marine indicators (glauconite concentration from point-count results) and whole-rock geochemistry marine indicators (P_2O_5 and S). Samples are depicted by their stratigraphic position within their respective formations (thickness in metres), not by age. Stratigraphic position was calculated from measured stratigraphic columns, outcrop locations, and bedding orientation.

6.3.2 Reducing conditions

Ni, Co, and V have all been suggested in the literature as indicators of reducing depositional environments (Ernst 1970). These three elements are all positively correlated in the samples from this study (Fig. 6.2), showing that they are being controlled by the same process. S concentration is also often elevated in reducing environments, as sulfide minerals are more readily precipitated (Ernst 1970). Ni, Co, and V have higher concentrations in the Rakopi Formation, lithofacies association A2 and A3 of the North Cape Formation, and in some samples from the Farewell Formation (Fig. 6.3).

Reducing environments are associated with systems rich in organic matter and where water and air circulation is restricted (Berner 1981). It is reasonable to expect reducing conditions to develop in the coastal plain and coal mires of the Rakopi Formation, estuary and coastal plain/swamps of the North Cape Formation (associations A2 and A3 respectively), and in abandoned channels and overbank deposits of the Farewell Formation rivers.

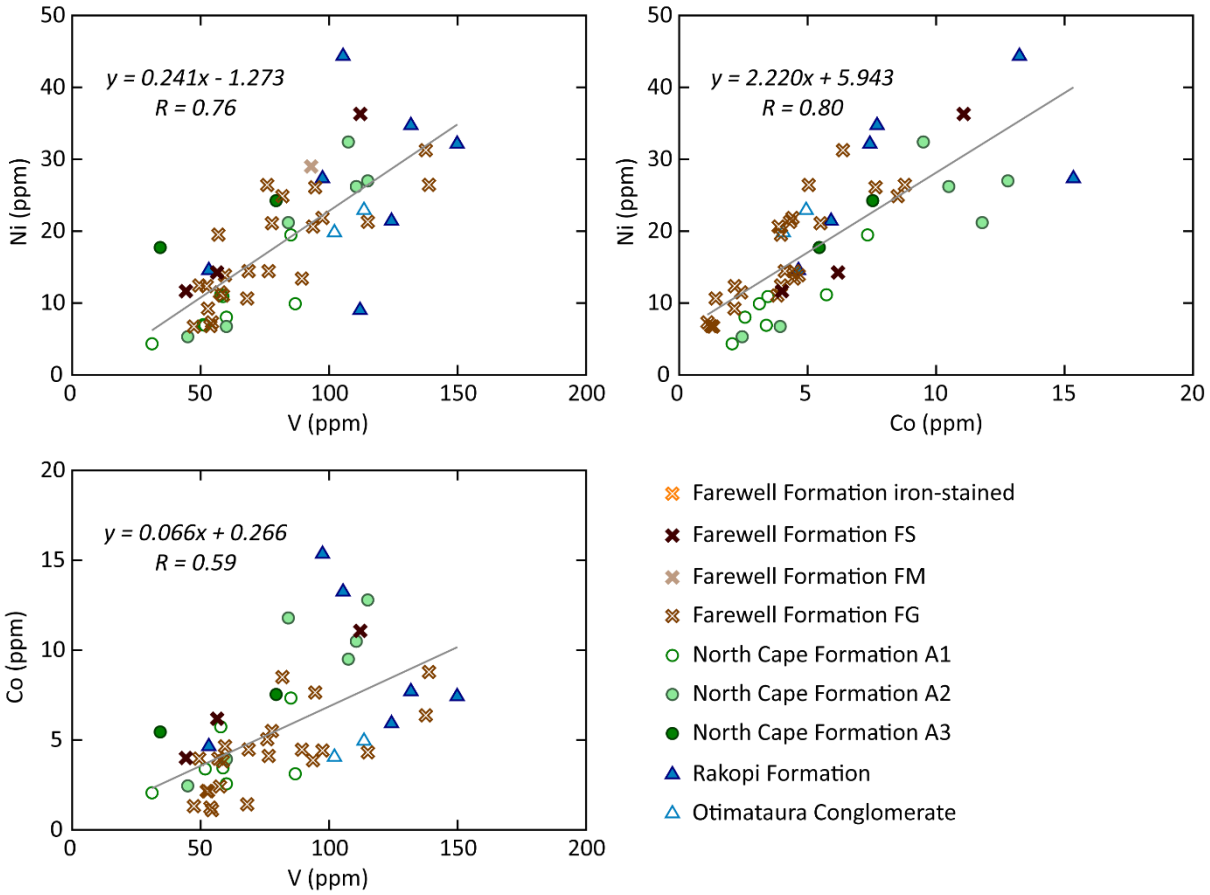

Fig. 6.2: bivariate plots showing correlation between Ni, Co, and V, elements associated with reducing depositional environments.

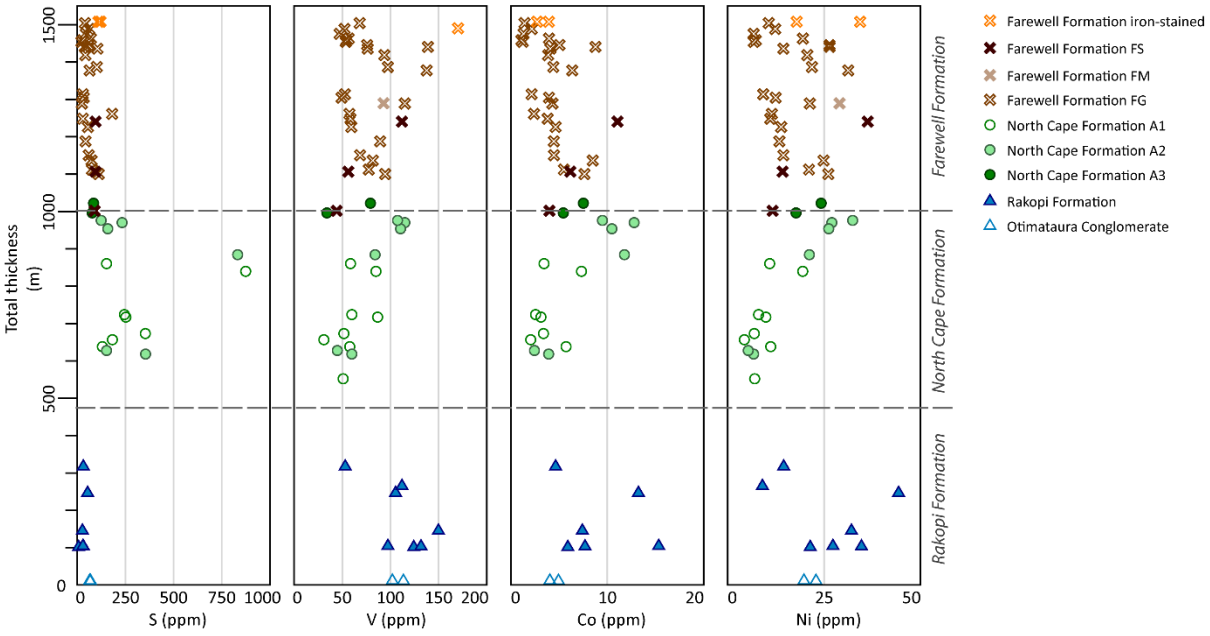

Fig. 6.3: stratigraphic variation in potential geochemical indicators of reducing environments.

6.4 Clay geochemistry

The chemical index of alteration (CIA) was proposed by Nesbitt and Young (1982) as a geochemical indicator of the amount of weathering sediments have undergone. The CIA works on the principle that as feldspars are weathered to clays the ratio of non-mobile aluminium to mobile alkalis increases:

$$CIA = [Al_2O_3/(Al_2O_3 + CaO^* + Na_2O + K_2O)] \times 100$$

Similarly, the ratio of Rb to Sr can also be used as an indicator for weathering, as Rb^+ is more readily bonded with clay exchange sites in illite and smectite clays than smaller Sr^{2+} (McLennan et al. 1993; Ratcliffe et al. 2010).

Both the CIA and Rb/Sr can be affected by grain size, as finer sedimentary rocks have higher proportions of detrital clays (Fig. 6.4). They are also affected by diagenetic formation of clay minerals (López et al. 2005). High carbonate concentration can anomalously lower the CIA, as the ratio works on the assumption that the majority of CaO is in plagioclase. This effect is observed in sample MR050 from the North Cape Formation at Mangarakau River, which has CaO = 21.23 wt.% and CIA = 26.4, likely as a result of calcite cements similar to those observed by Higgs et al. (2010) in North Cape Formation sandstones at Mangarakau Swamp.

The CIA values from the Farewell Formation increase up the stratigraphy (Fig. 6.5). This is consistent with the petrographic data, where the proportion of clay in the matrix increases up the stratigraphy, and the relative proportion of quartz increases as lithics and other minerals are altered to clays. From x-ray diffraction (XRD) analysis of the clay-sized matrix in the Farewell Formation, Stark (1996) found that the matrix was composed of kaolinite, mica, chlorite, and chert cement. Kaolinite was also observed as an alteration product of feldspars, lithics, and micas. The ratio of Ga to Rb is a suggested indicator of the ratio of kaolinite to illite/smectite (Ratcliffe et al. 2010). Ga/Rb increases up the stratigraphy in the Farewell Formation (Fig. 6.5), suggesting it is a good indicator of kaolinite concentration. In contrast, Rb/Sr does not increase up the stratigraphy as kaolinite does not have cation exchange sites and does not bond Rb^+ (Tucker 1991).

The North Cape Formation has consistent quartz contents throughout, and slightly increasing clay matrix up the stratigraphy (Fig. 6.5). There is a strong trend in the North Cape Formation for the CIA and Rb/Sr to increase up the stratigraphy (with younging), and this trend continues

upward into the Farewell Formation. This may be due to increasing amounts of weathering up the stratigraphy, in which case, CIA and Rb/Sr are more sensitive indicators of changing clay content than petrographic data alone.

The Rakopi Formation has high CIA, extremely high Rb/Sr, and moderate to high proportions of clay in the matrix (Fig. 6.5). These values are consistent for samples from both the Paturau River and the Kaituna Route, suggesting a stratigraphic rather than spatial trend. Ga/Rb is low, suggesting that the clays are illite and/or smectite rather than kaolinite. The Rakopi Formation is not as quartzose as the Farewell Formation, suggesting that the clays are not a result of alteration of detrital grains. The high CIA in the Rakopi Formation is therefore likely to be due to diagenetic illitization. Illite/smectite cements were observed in Rakopi Formation sandstones by Browne et al. (2008), although their composition was not confirmed by XRD or scanning electron microscope analysis.

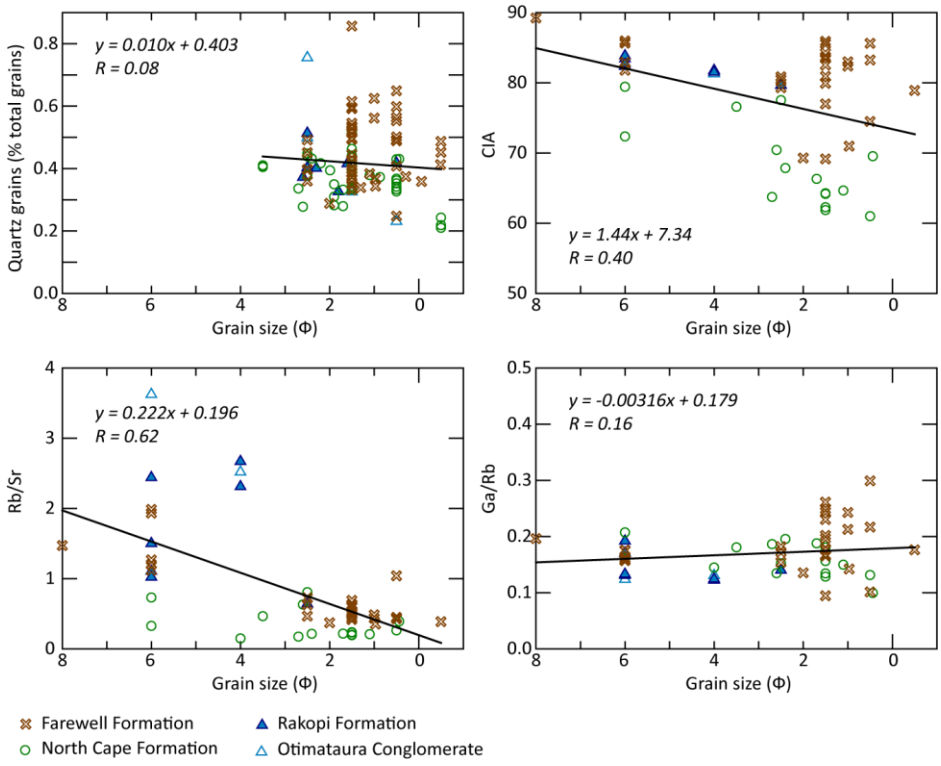

Fig. 6.4: Relationship between sediment grain-size and petrographic and geochemical indicators of clay concentration and composition.

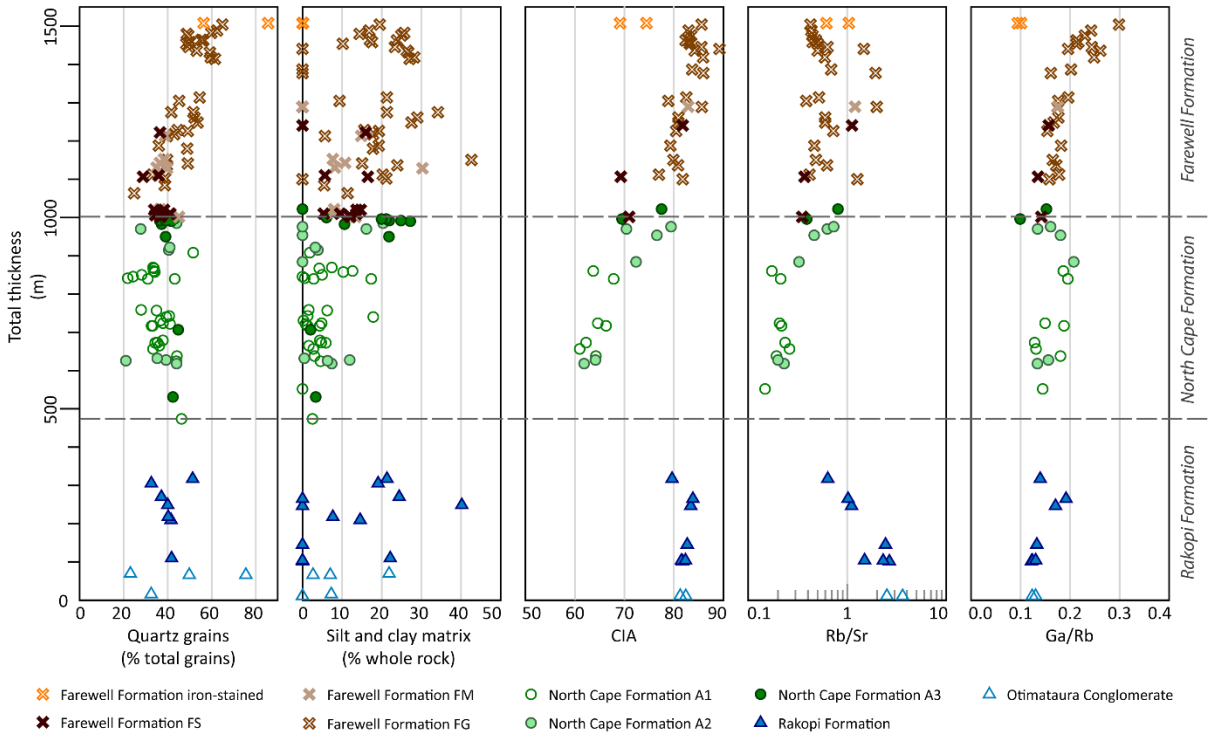

Fig. 6.5: Stratigraphic variation in clay composition from point count results and whole-rock geochemical indicators.

6.5 Sediment provenance

On the major element provenance discrimination plot of Roser and Korsch (1988) the sedimentary samples plot as having a mixture of recycled orogenic and felsic igneous provenance (Fig. 6.6). This suggests a mixture of Takaka and/or Buller Terrane quartzose metasedimentary sources (recycled orogenic) and granitic sources (felsic igneous).

The North Cape Formation has significantly higher F2 values than the Rakopi or Farewell formations, suggesting granitic sources were more significant during North Cape Formation deposition (Fig. 6.6, 6.7). This is confirmed by both the lithic composition, which shows that plutonic lithics are more common in the North Cape Formation, and the conglomerate clast counts which show more granitoid clasts in the North Cape Formation compared to the Farewell Formation (Fig. 6.7). The plutonic signature in the North Cape Formation is at least partly due to the formation having the least amount of weathering and diagenetic alteration, as plutonic lithics are more readily altered than the quartzose metasedimentary lithics.

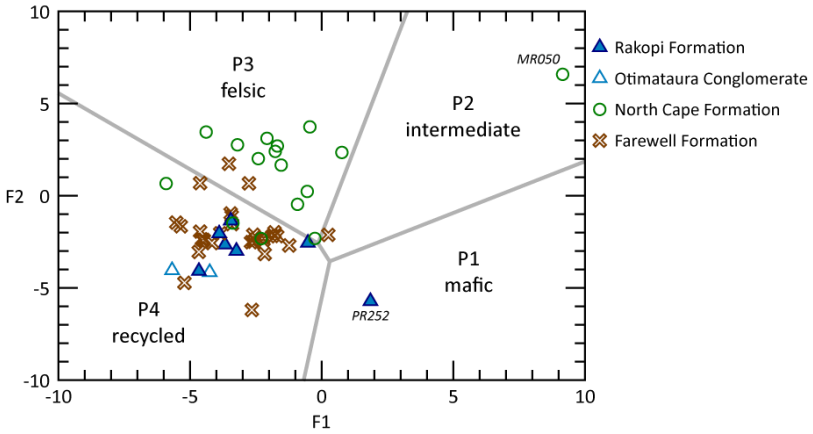

Fig. 6.6: Major element provenance discrimination plot (Roser & Korsch 1988) *of sedimentary samples.*
F1 = − 1.773 TiO_2 + 0.607 Al_2O_3 + 0.76 Fe_2O_3T −1.5 MgO + 0.616 CaO + 0.509 Na_2O − 1.224 K_2O − 9.09; F2 = 0.445 TiO_2 + 0.07 Al_2O_3 − 0.25 Fe_2O_3T − 1.142 MgO + 0.438 CaO + 1.475 Na_2O + 1.426 K_2O − 6.861

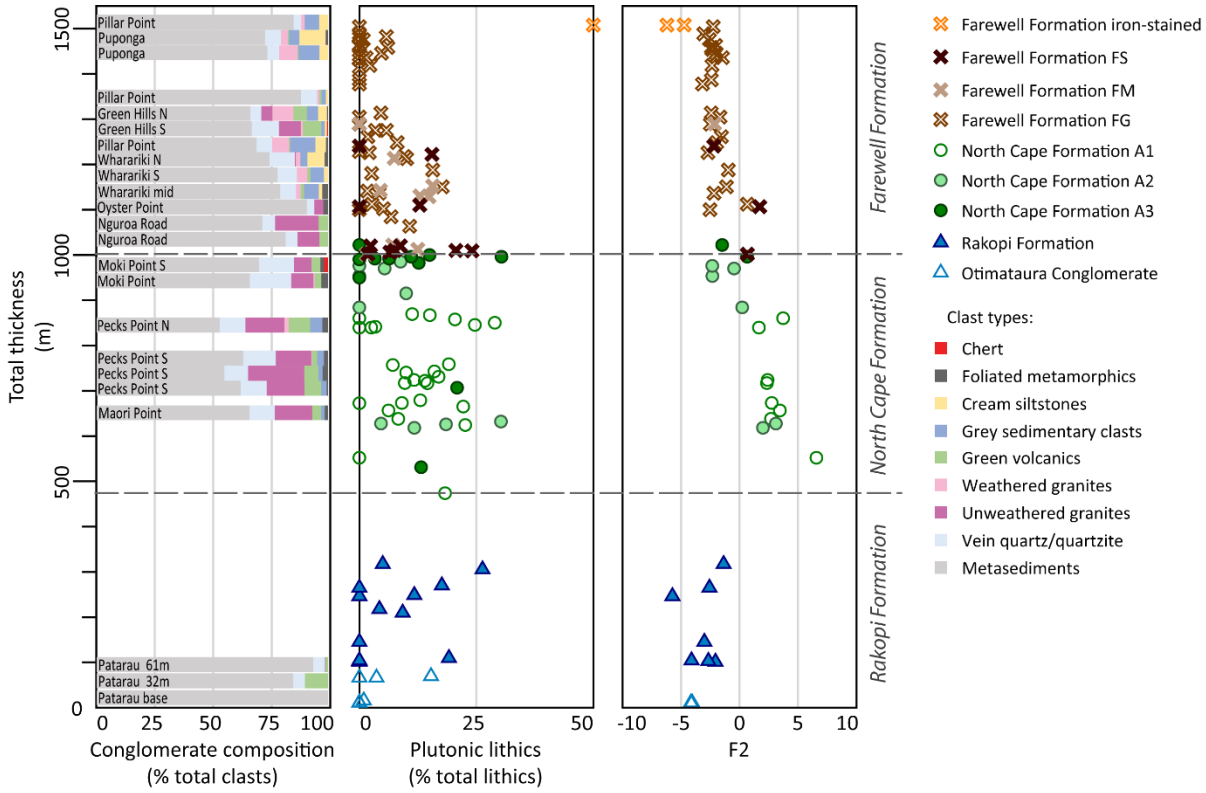

Fig. 6.7: Stratigraphic variation in plutonic provenance from clast count results, lithic composition from point count results, and whole-rock geochemistry. See Fig. 6.6 for definition of F2.

6.5.1 Feldspar composition

Na_2O and CaO can be used as indicators of plagioclase, whereas K_2O is an indicator of alkali feldspars (Ratcliffe et al. 2010). The North Cape Formation has significantly higher Na_2O and CaO concentrations, reflecting the higher abundance of plagioclase (Figs. 6.8, 6.9). The Na_2O and CaO concentration decreases up the stratigraphy through the North Cape Formation and the lower Farewell Formation. This trend is also observed in the offshore Taranaki Basin,

where the Farewell Formation becomes more alkali feldspar-dominated towards the top (Higgs and King 2017).

The changing feldspar composition through the North Cape and Farewell formations could be a result of weathering or of changing provenance. Plagioclase feldspars are the most susceptible to alteration, so will be removed from the system first (Bhatia and Crook 1986). The decreasing plagioclase content could reflect increasing weathering through North Cape time into the Farewell Formation. Alternatively, a plagioclase-rich source such as a granitoid, may have been more significant at the start of North Cape Formation time.

The Rakopi Formation has higher K_2O concentrations (Figs. 6.8, 6.9). This is likely to be due to diagenetic input of illite discussed above (Section 6.4).

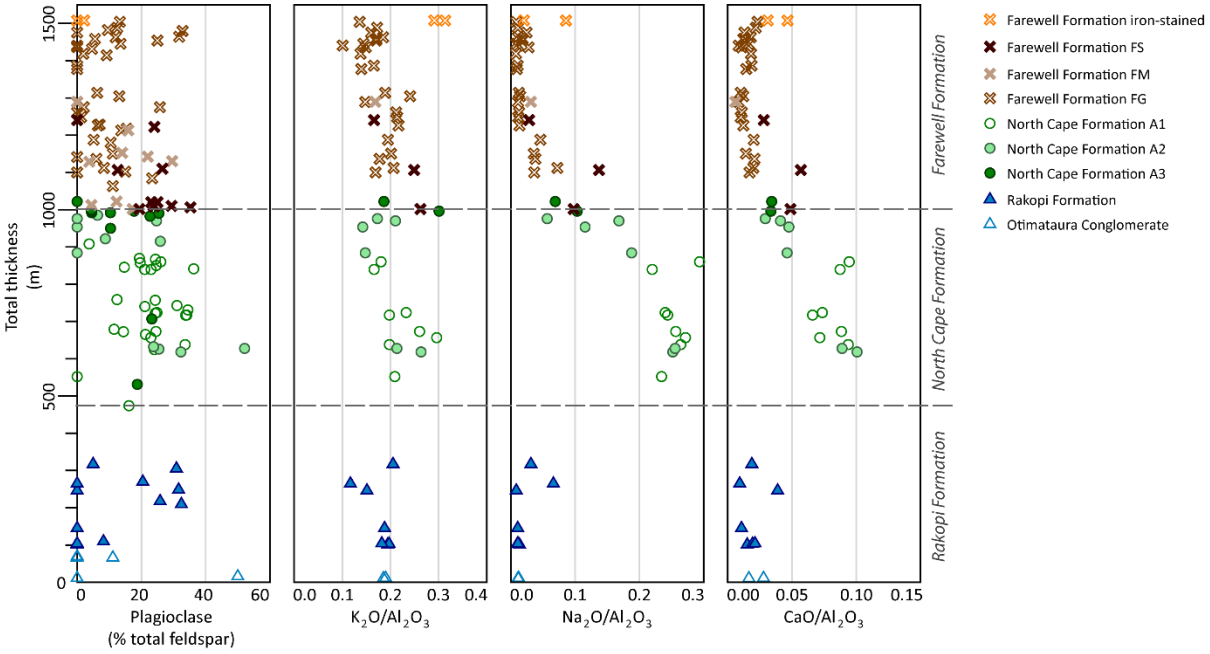

Fig. 6.8: Stratigraphic variation in feldspar concentration from point count results, and whole-rock geochemical indicators. The alkalis are normalised to Al_2O_3 wt. % to reduce the signal from grain-size and/or clays.

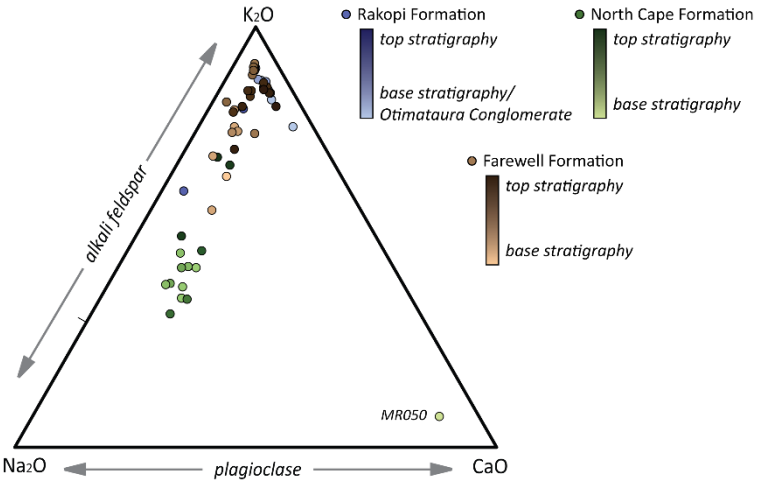

Fig. 6.9: Stratigraphic variation in feldspar composition from whole-rock geochemistry.

6.5.2 Heavy minerals

Some sandstone samples contain very minor quantities of heavy minerals, including amphibole, pyroxene, titanite, and opaques. As the heavy minerals are a very small proportion of the sandstones, the petrographic results were not sensitive enough to be definitive (Fig. 6.11). The whole rock geochemistry can instead be used as an indicator of heavy mineral composition.

Zr and Hf are well-established indicators of zircon concentration (Winter 2014). These elements are very strongly correlated in the samples (R = 0.99) in a ratio very similar to that in granitic zircons (Fig. 6.10), suggesting the concentration of both elements is controlled by zircon. In the samples, there is a weak negative relationship between increasing grain size and Zr concentration. Zircons can be concentrated in finer sediments due to hydraulic sorting (Garzanti et al. 2010), although the weak relationship here shows that grain size is not the only variable (Fig. 6.10). Zircon is commonly associated with recycled sedimentary or metasedimentary sources, as it is stable in sedimentary systems for considerable periods of time (McLennan et al. 1993). In the northwest Nelson region, the presence of zircon is therefore likely to indicate a metasedimentary basement source, rather than the plutonic or volcanic sources.

Zr is slightly enriched in the Rakopi Formation compared to the North Cape and Farewell formations (Fig. 6.11). The Zr concentration increases slightly up through the North Cape Formation and decreases slightly through the Farewell Formation. This suggests that metasedimentary sources are more significant in the upper North Cape Formation and lower

Farewell Formation. Alternatively, zircon may be concentrated in these formations due to weathering, as zircon is resistant to alteration.

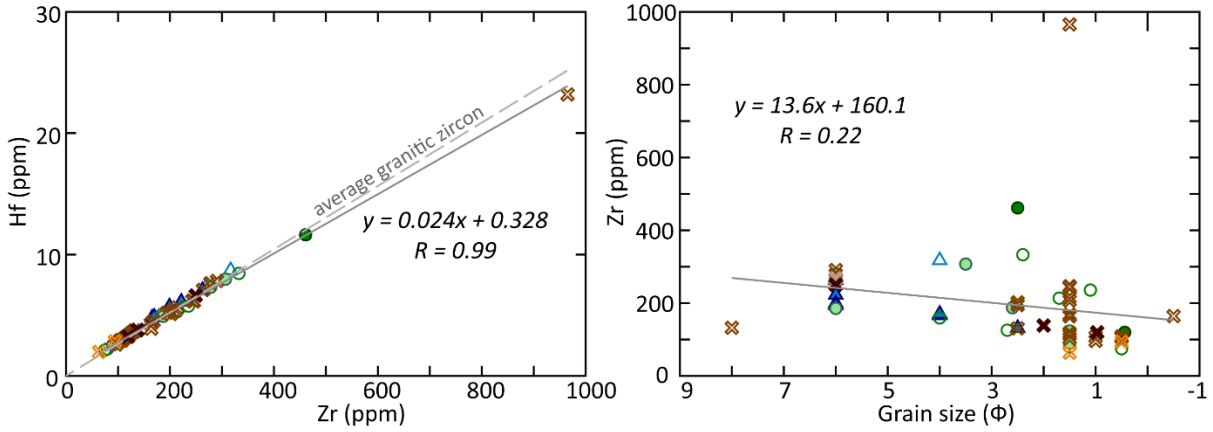

Fig. 6.10: Relationship between Hf and Zr concentration in samples compared to average granitic zircon (Wang et al. 2010), indicating the presence of zircon, and effect of grain size on zircon concentration.

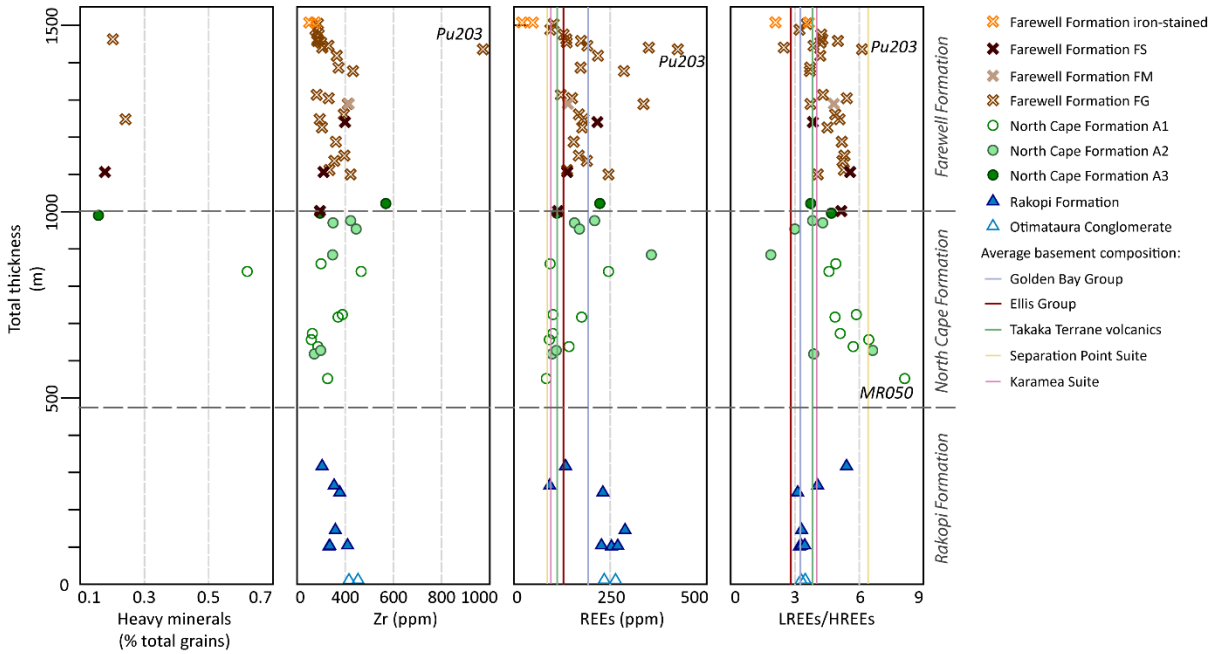

Fig. 6.11: Stratigraphic variation in heavy mineral concentration from point count results, and key geochemical indicators. The average composition of likely basement sources is also plotted, data from Strong et al. (2016).

The rare earth elements (REEs) are incorporated in heavy minerals including garnet, olivine, pyroxene, amphibole, titanite, and apatite (McLennan et al. 1993; Ratcliffe et al. 2010; Winter 2014). There are a number of variables controlling heavy mineral and REE concentration. The heavy minerals are concentrated in finer sediments (Fig. 6.12). REEs can also be concentrated by surface weathering processes (McLennan et al. 1993), in these samples there is a moderate relationship (R = 0.44) between CIA and REE concentration (Fig. 6.12). Finally, sediment provenance also controls heavy minerals and REEs. The less stable minerals such as olivine,

pyroxene, and amphibole are supplied from igneous or metamorphic sources, while the more stable minerals may be concentrated by sediment recycling in the same manner as zircon (Bhatia and Crook 1986; McLennan et al. 1993). In the samples from this study, there is a moderately strong relationship between Zr and REE concentration (R = 0.63, Fig. 6.12), suggesting it is the more stable minerals including zircon controlling REE concentration.

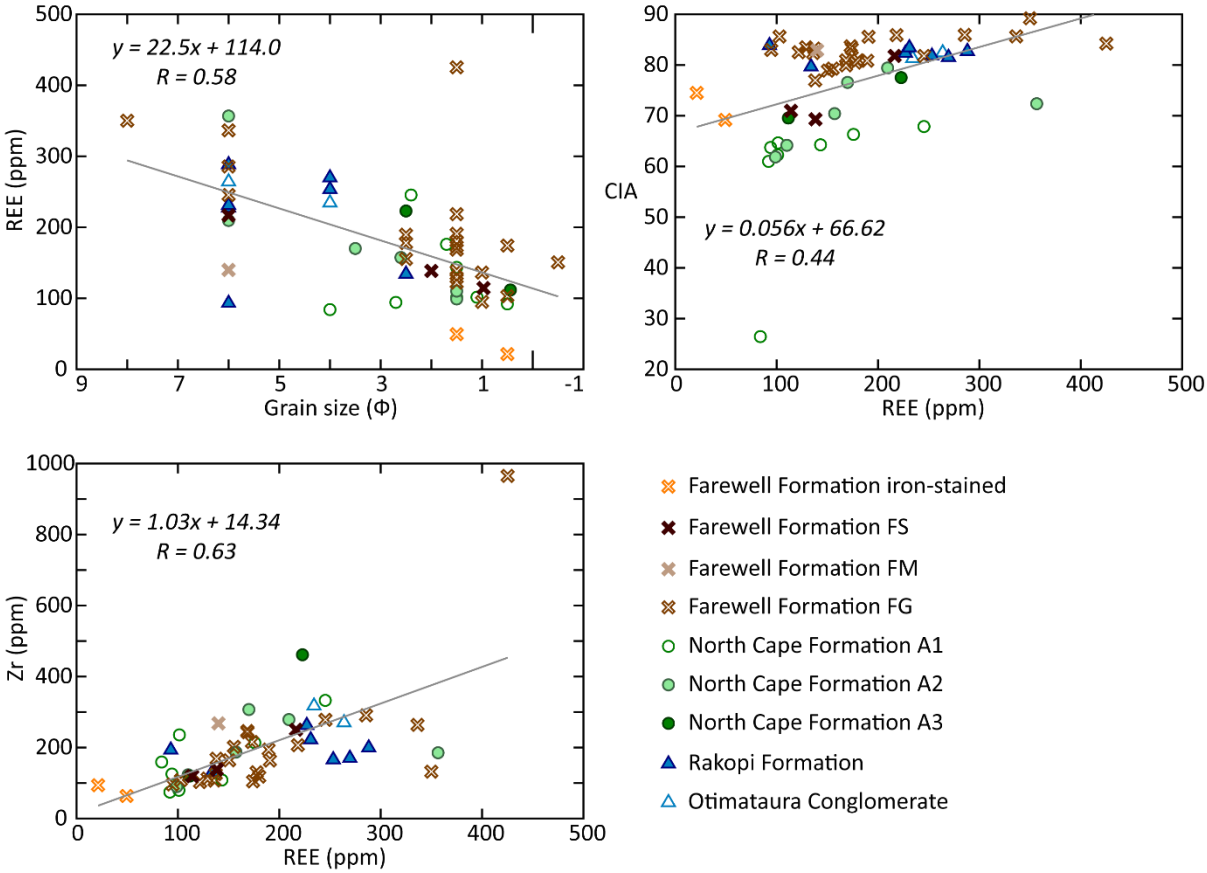

Fig. 6.12: Factors influencing REE concentration, including sediment grain size, weathering (using CIA as an indicator of weathering), and relationship between zircon concentration (Zr) and REEs.

The total REE concentration is high in the lower Rakopi Formation and Otimataura Conglomerate, decreasing towards the top of the formation (Fig. 6.11). The North Cape Formation has lower REE concentrations, with a slight increase in concentration up the stratigraphy. The REE concentration in the Farewell Formation is similar to the North Cape Formation. In the top ~150 m of the Farewell Formation the REE concentration decreases sharply. This suggests that metasedimentary sources are more significant in the Rakopi and Farewell Formation. The REEs may also be indicating greater weathering, which has the effect of concentrating the stable heavy minerals.

The ratio of light REEs (LREEs) and heavy REEs (HREEs) is dependent on the type of heavy minerals. LREEs are typically associated with more felsic sources whereas the HREEs are associated with more mafic sources (Bhatia and Crook 1986; McLennan et al. 1993; López et al. 2005). In the basement in northwest Nelson, LREEs are more enriched in the Separation Point Suite, whereas HREEs are more enriched in the Karamea Suite, Takaka Terrane volcanics, and Takaka Terrane Ellis Group and Buller Terrane Golden Bay Group (Fig. 6.11).

The Rakopi Formation is depleted in LREEs, becoming more enriched towards the top of the Formation (Fig. 6.11). The North Cape Formation is enriched in LREEs, which decrease towards the top of the formation. The Farewell Formation is consistently depleted in LREEs. This suggests that more felsic or continental sources such as the Separation Point Suite became more significant part-way through Rakopi Formation time and were most significant around the start of North Cape Formation time. Felsic sources were less important in the Farewell Formation. This may be because weathering and alteration was removing the less stable plutonic component of the sediments.

Sample Pu203 from near the top of the Farewell Formation is a clear outlier in the REE and zircon plots (Fig. 6.11). It is highly enriched in Zr, Hf and the LREEs. This may be because it is a tuff, or has additional volcanic material, likely with a felsic to intermediate composition due to the enrichment of LREEs compared to HREEs. However, there is no petrographic evidence of glass shards or other fresh volcanic material. The petrography does show that the sample has more detrital opaque minerals than is typical, more iron oxide cement, and has small amounts of pyroxene, although in quantities too small to be included in the point count (Fig.

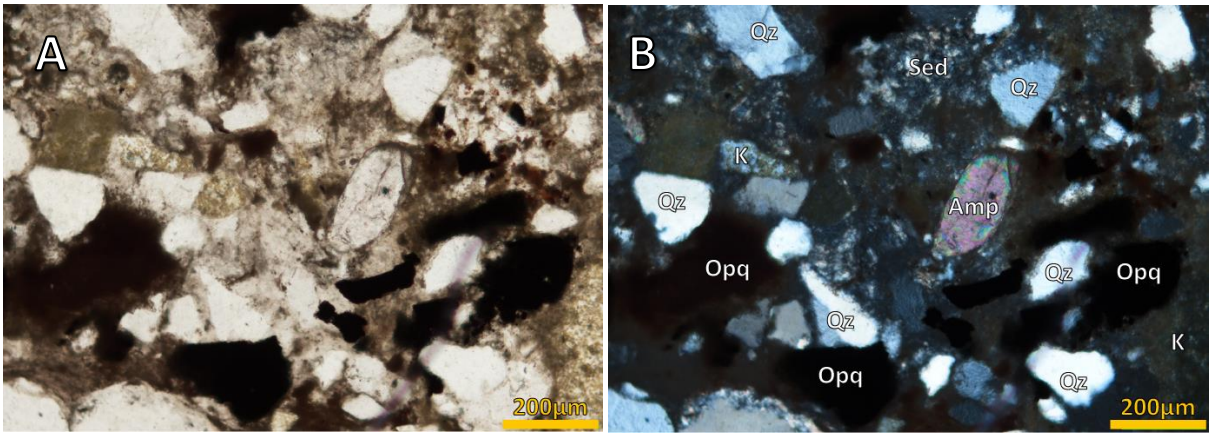

Fig. 6.13: Photomicrographs of sample Pu203, showing opaque minerals, iron oxide cement, and detrital amphibole.
Qz: quartz; K: alkali feldspar; Amp: amphibole; Opq: opaque; Sed: sedimentary lithic.

6.13). Heavy minerals, especially very dense minerals such as monazite and zircon, can be concentrated in fluvial systems due to localised entrainment effects (Irvine and Baragar 1971). This is a likely explanation for the unusual chemistry of sample Pu203.

6.6 Geochemical petrofacies

From the geochemical parameters discussed above, the Late Cretaceous and Paleocene succession in northwest Nelson can be divided into six geochemically unique petrofacies (Fig. 6.14). This chemostratigraphic technique is particularly relevant for bores where there is no outcrop (Ratcliffe et al. 2007; Ratcliffe et al. 2010; Craigie et al. 2016). Here, the outcrop geochemistry is a useful analogue for wells in the Taranaki Basin, where the chemostratigraphy has been investigated in the Kupe South field (Chemostrat Ltd. 2017).

From the base of the stratigraphy (oldest) to the top (youngest), the petrofacies identified here are:

- P1: Petrofacies 1 (P1) at the base of the stratigraphy is characterised by high CIA (81 - 83), high Rb/Sr (1.5 – 3.6), high REE (227 – 288 ppm), and low LREE/HREE (3.2 – 3.5).
- P2: Also has high CIA (80 – 84), but lower Rb/Sr than P1 (0.6 – 1.1), low REE concentrations (93 – 231 ppm) and moderate LREE/HREE (3.1 – 5.4).
- P3: is characterised by low CIA (26 – 79) and Rb/Sr (0.1 – 0.8), high S (79 – 875 ppm), high Na_2O (Na_2O/ Al_2O_3 = 0.06 to 0.29), and high LREE/HREE (1.9 – 8.1).
- P4: has high CIA (69 – 86), moderate Rb/Sr (0.4 – 2.0), moderate REEs (114 – 336 ppm) and moderate LREE/HREE (3.7 – 5.6).
- P5: has high CIA (82 – 89), slightly lower Rb/Sr than P4 (0.4 – 1.5), high Ga/Rb (0.2 -0.3), and low REEs (95 – 425ppm).
- P6: defined by only two samples. These have low CIA (69, 64) and low Ga/Rb (0.09, 0.10). Not shown in Fig. 6.14, they also have high SiO_2 (83, 83 wt.%) and Fe_2O_3 (3.8, 7.5 wt./%).

The boundaries of the petrofacies are consistent with the formation contacts (Table 6.1). P1 and P2 are part of the Rakopi Formation, P1 includes the Otimataura Conglomerate. The geochemistry of P1 and P2 is partly due to diagenetic effects with the formation of illite at the greater burial depths. There is a shift in provenance between P1 and P2, indicated by the

change in REE composition and concentration. This may reflect a change from the localised sources feeding the Otimataura Conglomerate, to more regional drainage.

P3 overlaps with the North Cape Formation, with geochemistry affected by both depositional environment and provenance. P3 has elevated S and P_2O_5, likely as a result of marine influence during deposition. A more felsic, igneous provenance for this petrofacies is also suggested by the higher Na_2O (plagioclase) and LREEs relative to HREEs.

P4 – P6 overlap with the Farewell Formation. Unlike the North Cape Formation, there is little to no marine influence, as shown by low S concentration. P4 and P5 have higher clay contents, shown by the high CIA. In P5, Rb/Sr decreases while Ga/Rb increases, showing that the clay composition becomes dominated by kaolinite, most likely due to weathering. The P6 samples come from the iron-stained unit at the top of the Farewell Formation, these samples have abundant iron oxide cements likely causing the high Fe_2O_3 concentration and are more quartzose than the rest of the Farewell Formation.

Table 6.1: Summary of petrofacies from sandstone and mudstone whole-rock geochemistry, with additional petrographic features, and equivalent formations.

Petrofacies	*Formation*	*Age*	*Depositional environment*	*Distinguishing geochemical features*	*Petrographic features*	*Comments and interpretation*
P1	Rakopi (Otimataura Conglomerate)	Late Cretaceous	Alluvial fans/ coastal plain	high CIA (81-83) high Rb/Sr (1.5 -3.6) high REE (227-288 ppm) low LREE/HREE (3.2–3.5)	High lithics in lowest samples Moderate clay matrix	Diagenetic illite clays
P2	Rakopi	Late Cretaceous	Coastal plain	high CIA (80–84) lower Rb/Sr than P1 (0.6–1.1) low REE concentrations (93–231 ppm) moderate LREE/HREE (3.1–5.4)	Rare glauconite Moderate clay matrix	Diagenetic illite clays
P3	North Cape	Late Cretaceous	Coastal plain/estuary	low CIA (26–79) low Rb/Sr (0.1–0.8) high S (79–875 ppm) high Na_2O (Na_2O/ Al_2O_3 = 0.06 to 0.29) high LREE/HREE (1.9–8.1)	Low clay matrix Minor glauconite High plutonic lithics High plagioclase	Greater plutonic provenance likely Marine influence during deposition/ very early diagenesis
P4	Lower Farewell	Paleocene	Meandering/ braided river	high CIA (69 – 86) moderate Rb/Sr (0.4–2.0) moderate REEs (114–336 ppm) moderate LREE/HREE (3.7–5.6)	Increasing quartz content Increasing sedimentary lithics Higher clay matrix	Sedimentary provenance increases in influence up the stratigraphy
P5	Upper Farewell	Paleocene	Braided river	high CIA (82–89) slightly lower Rb/Sr than P4 (0.4–1.5) high Ga/Rb (0.2-0.3) low REEs (95-425 ppm)	High quartz Sedimentary lithics dominant High clay matrix	Sedimentary/ metasedimentary provenance likely. Weathering to kaolinite clays
P6	Top Farewell	Paleocene	Marine	low CIA (69, 64) low Ga/Rb (0.09, 0.10) high SiO_2 (83, 83 wt.%) and Fe_2O_3 (3.8, 7.5 wt.%)	Minor to moderate glauconite High quartz Abundant iron oxide cement Rounded, well sorted	Reworked deposits from marine regression at top of Farewell

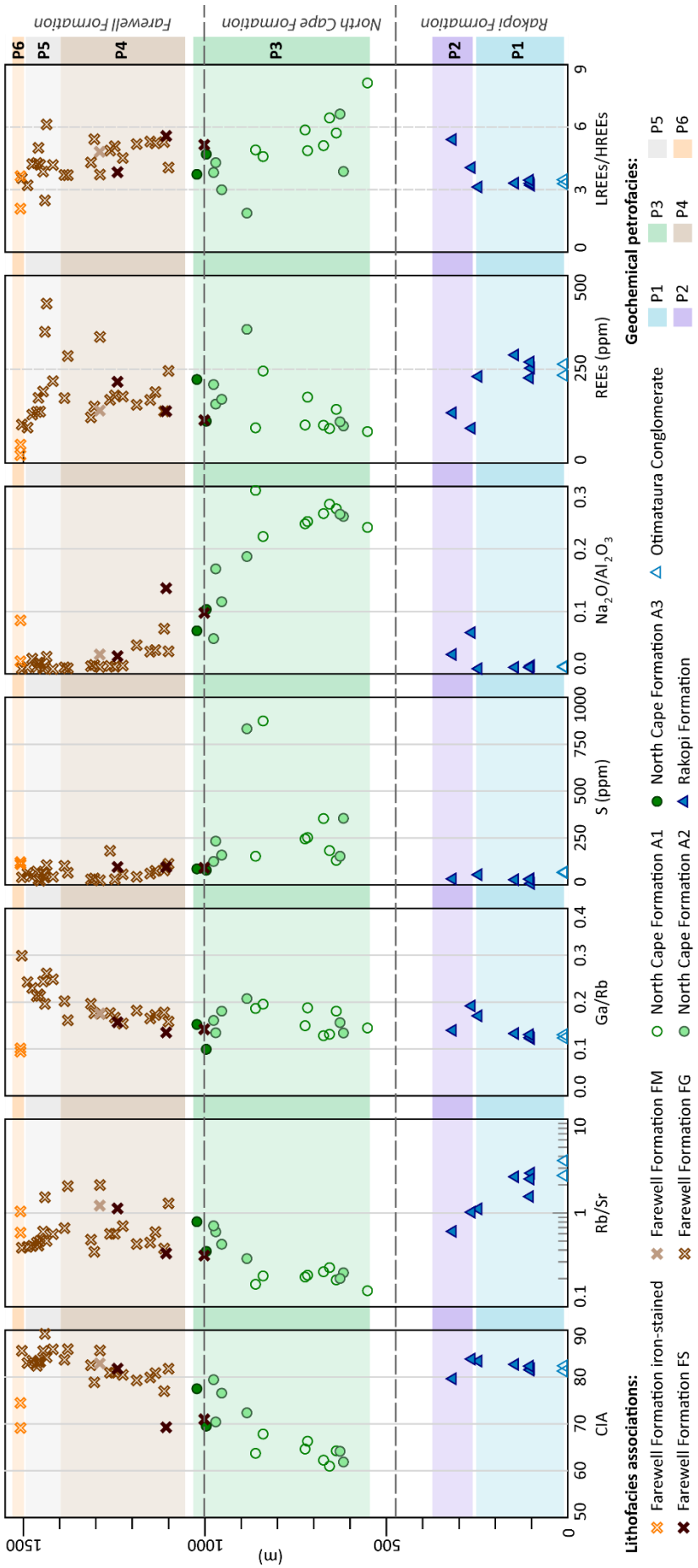

Fig. 6.14: Stratigraphic variations in whole-rock geochemistry of the Rakopi, North Cape and Farewell formations. The succession is divided into geochemical petrofacies based on their geochemistry.

6.7 Conclusion

The whole-rock geochemistry is a useful indicator of paleoenvironment. There is a strong correlation between S and P_2O_5 and marginal marine lithofacies in the North Cape Formation. Ni, Co, and V are possible indicators of reducing environments, with higher concentrations of these elements in estuarine and swampy lithofacies.

The clay content and composition of the sedimentary rocks can be effectively investigated by whole-rock geochemistry. The Rakopi Formation has high CIA and Rb/Sr values suggesting the presence of illite, likely diagenetic. The North Cape Formation has little clays overall, but the clay content increases through the stratigraphy as shown by the CIA and Rb/Sr. The Farewell Formation has high kaolinite content, shown by the CIA and Ga/Rb. This is likely to be a result of surface weathering at the time of deposition.

The Rakopi and Farewell formations are dominated by metasedimentary sources. This is shown by the major element geochemistry (F2 values), low plagioclase contents (Na_2O and CaO), higher concentration of zircon and heavy minerals, and relative depletion of LREEs. A felsic igneous source such as the Separation Point Suite becomes more significant at the end of Rakopi Formation time, when the F2 values, plagioclase content, and LREE concentration increase, and peaks at the start of North Cape Formation time. This felsic source becomes less important through the North Cape Formation. The change in composition may either be because the provenance changed, or due to increasing weathering and diagenetic alteration removing unstable plutonic material.

This understanding of how the depositional environment, diagenetic processes and provenance affect the whole-rock geochemistry is applicable to the Pakawau Group and Farewell Formation in the offshore Taranaki Basin, where the composition of cores and cuttings could be used for environmental and provenance interpretations.

7. Conclusions and implications

The aim of this research was to investigate the provenance of the only outcrops of Taranaki Basin Late Cretaceous and Paleocene sedimentary rocks, found in northwest Nelson. The research focused on how the provenance of the Late Cretaceous Rakopi and North Cape formations and the Paleocene Farewell Formation changed through time. One aim was to use the provenance to inform the paleogeography, in the context of sedimentological field studies. The paleogeographic models are a useful tool for understanding Zealandia's changing tectonic regime as it shifted from rifting during the Late Cretaceous to a passive margin in the Paleocene. The paleogeography and provenance are also important for the Taranaki Basin, as these factors influence the location and quality of petroleum source, reservoir, and seal lithologies.

7.1 Paleogeography

The Rakopi Formation was deposited by a fluvial system, with meandering rivers and floodplains on a coastal plain (Fig. 7.1). The Rakopi Formation is composed of interbedded sandstones, rare conglomerates, siltstones, carbonaceous mudstones, and coals, often in fining upwards cycles. This facies progression is typical of meandering river and floodplain deposits.

The Rakopi Formation (excluding the Otimataura Conglomerate) has a mixed provenance of metasedimentary, plutonic, volcanic, and schistose sources, shown by the sandstone composition and geochemistry. The granitoid pebble collected from the Rakopi Formation has a composition that fits best with the Karamea Suite, possibly indicating some material was fed from the south along the basin axis. In the sandstones, the presence of Takaka Terrane volcanic lithics and schist, as well as possible Separation Point Suite and Takaka metasedimentary lithics, indicating a large amount of material was derived from drainage of areas to the southeast that had been uplifted by the Wakamarama Fault (Fig. 7.1).

A marine influence in the Rakopi Formation is suggested by minor glauconite in the sandstones, and elevated P_2O_5 in the sandstones and mudstones. This marine influence may have been from periodic marine incursions across the low gradient coastal plain, as suggested by Browne et al. (2008), although there is no sedimentological evidence for a marine setting.

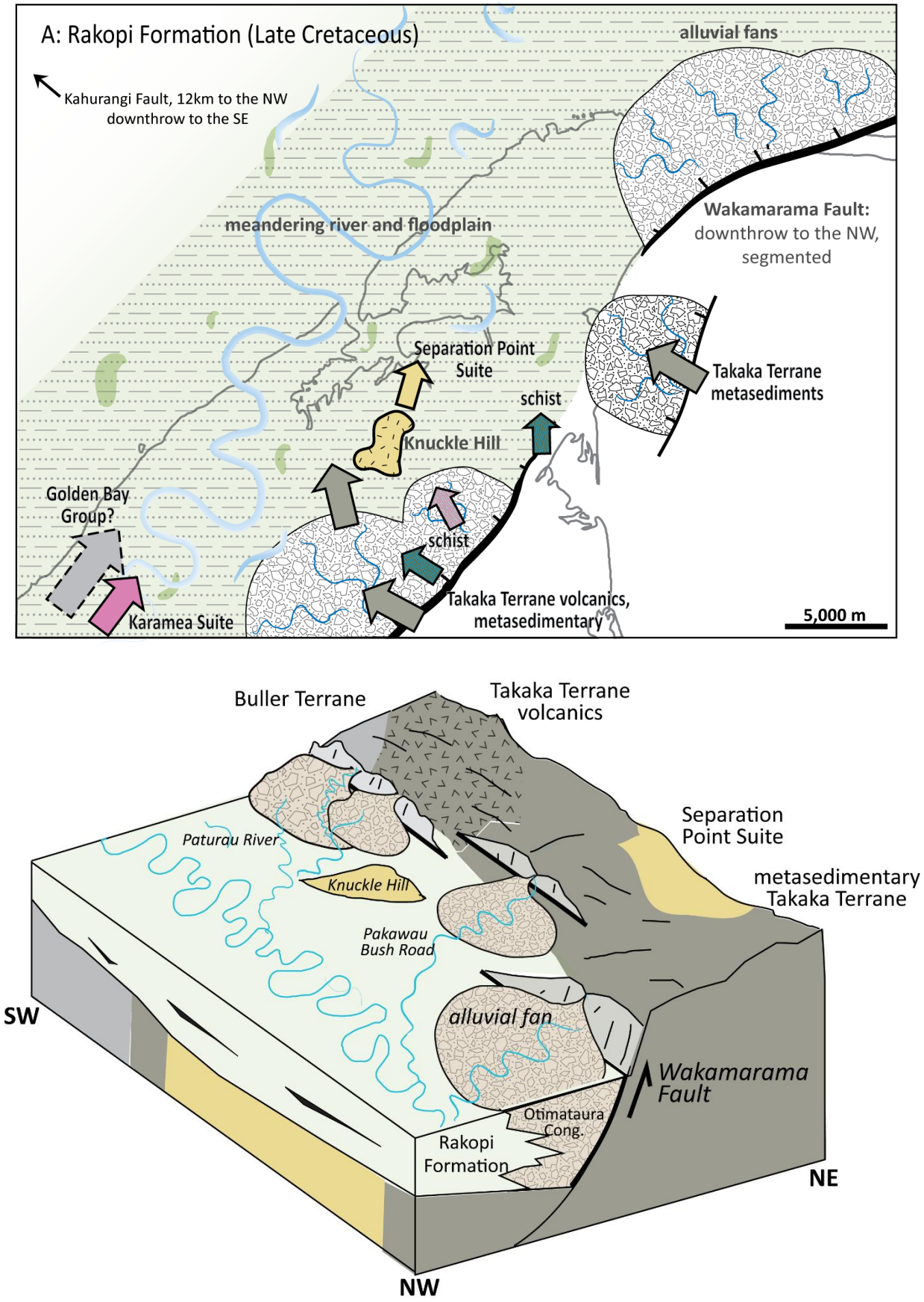

Fig. 7.1: Paleogeography, provenance and structure of the Rakopi Formation during the Late Cretaceous

Alternatively, glauconite and phosphatic minerals may have been transported inland by aeolian processes.

The basal Otimataura Conglomerate of the Rakopi Formation is interpreted to be alluvial fans fed from the Wakamarama Fault. The Otimataura Conglomerate in the Paturau River contains subangular matrix supported conglomerates, a typical texture of fans fed by mixed stream flow and debris flow. The provenance of the Otimataura Conglomerate also suggests an alluvial fan setting; the composition of the sandstones and conglomerates reflects the local basement rather than a mix of sources. The variability in thickness of the Otimataura Conglomerate suggests different rates of movement on the Wakamarama Fault, most likely devided into fault segments. The Pakawau Bush Road sandstones have a sedimentary provenance, but the sand grain size suggest this outcrop is the base of a fan from a fault segment further east of the modern Wakamarama Fault (Fig. 7.1).

The sedimentology of the North Cape Formation indicates a marginal marine, estuarine, and paralic environment (Chapter 3). There are three main lithofacies associations: bidirectional trough cross-bedded sandstones with mud drapes, conglomerates, and siltstones deposited in sub-tidal channels; thinly interbedded fine sandstones and siltstones with bidirectional ripples passing upwards into mudstones and thin coal beds deposited in tidal mudflats and coastal mires; and sandstones, mudstones, and thicker coal beds deposited in meandering rivers and floodplains. The distribution of these lithofacies associations and the paleocurrent measurements indicate that these environments were part of deltas and fan-deltas prograding from the Wakamarama Fault into a shallow marine embayment (Fig. 7.2). The marine influence is evident in the petrology and geochemistry (Chapter 5, 6), with minor glauconite in the sandstones, and elevated S and P_2O_5 in the sandstones and mudstones, particularly those of the tidal lithofacies associations.

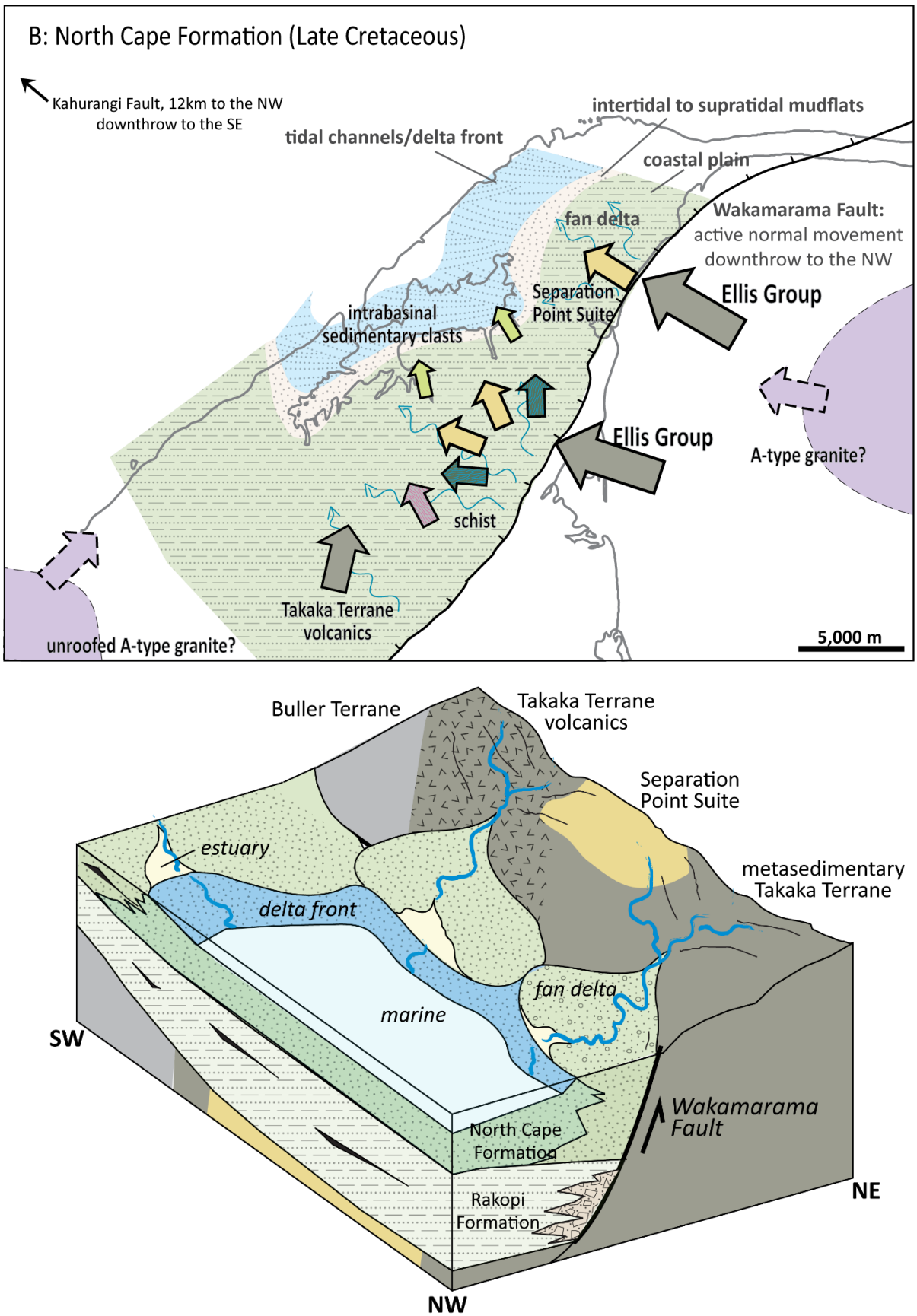

Fig. 7.2: Paleogeography, provenance and structure of the North Cape Formation during the Late Cretaceous

The provenance of the North Cape Formation supports the interpretation of fan deltas sourced from southeast of the Wakamarama Fault (Fig. 7.2). The provenance is dominated by metasedimentary sources, most likely the younger Takaka Terrane (Ellis Group), with granitoids from the Separation Point Suite and a previously undocumented A-type granite, Takaka Terrane volcanics, and schist. The geochemistry of the sandstones and mudstones suggest that the North Cape Formation has a greater proportion of granitoid sources than either the Rakopi Formation or Farewell Formation, possibly due North Cape Formation outcrops being closer to the Separation Point Suite outcrop. Overall, the provenance of the North Cape Formation supports sedimentological data indicating a southeast to northwest paleoflow that drained the uplifted material southeast of the Wakamarama Fault.

Wizevich (1992) and Stark (1996) described both temporal and spatial trends in the composition of the Pakawau Group. In this study, the Otimataura Conglomerate and sandstone equivalents at the base of the Rakopi Formation were shown to have distinctly different compositions from the rest of the Pakawau Group, plotting as litharenites with spatially variable lithic compositions. Within the remaining Rakopi and North Cape formations no strong spatial trends were found.

The Farewell Formation is interpreted as being entirely fluvial (Chapter 3). In the southwest of the field area it comprises channelised sandstones in thick carbonaceous mudstones that are interpreted as sandy meandering river deposits. In the central part of the field area trough cross-bedded sandstones in complex stacked channels capped by thin siltstones are interpreted as sandy braided river deposits. In the north, thick conglomerates with sandstones and rare siltstones are interpreted as gravelly braided rivers. As well as spatial variation, there is a stratigraphic transition from sand-dominated to gravel-dominated braided rivers between the lower and the upper Farewell Formation. The meandering rivers may represent smaller streams in the main floodplains of the braided river system. The spatial and stratigraphic transition from sandy braided rivers to gravelly braided rivers may represent a change in energy levels, or a change in the grain size of the source material. The paleoflow data suggests an alluvial fan was feeding the northern part of the field area, possibly supplying gravel to the system (Fig. 7.3). Takaka Terrane siltstone clasts are present in the northern part of the field area, also indicating an alluvial fan draining highlands in the northeast.

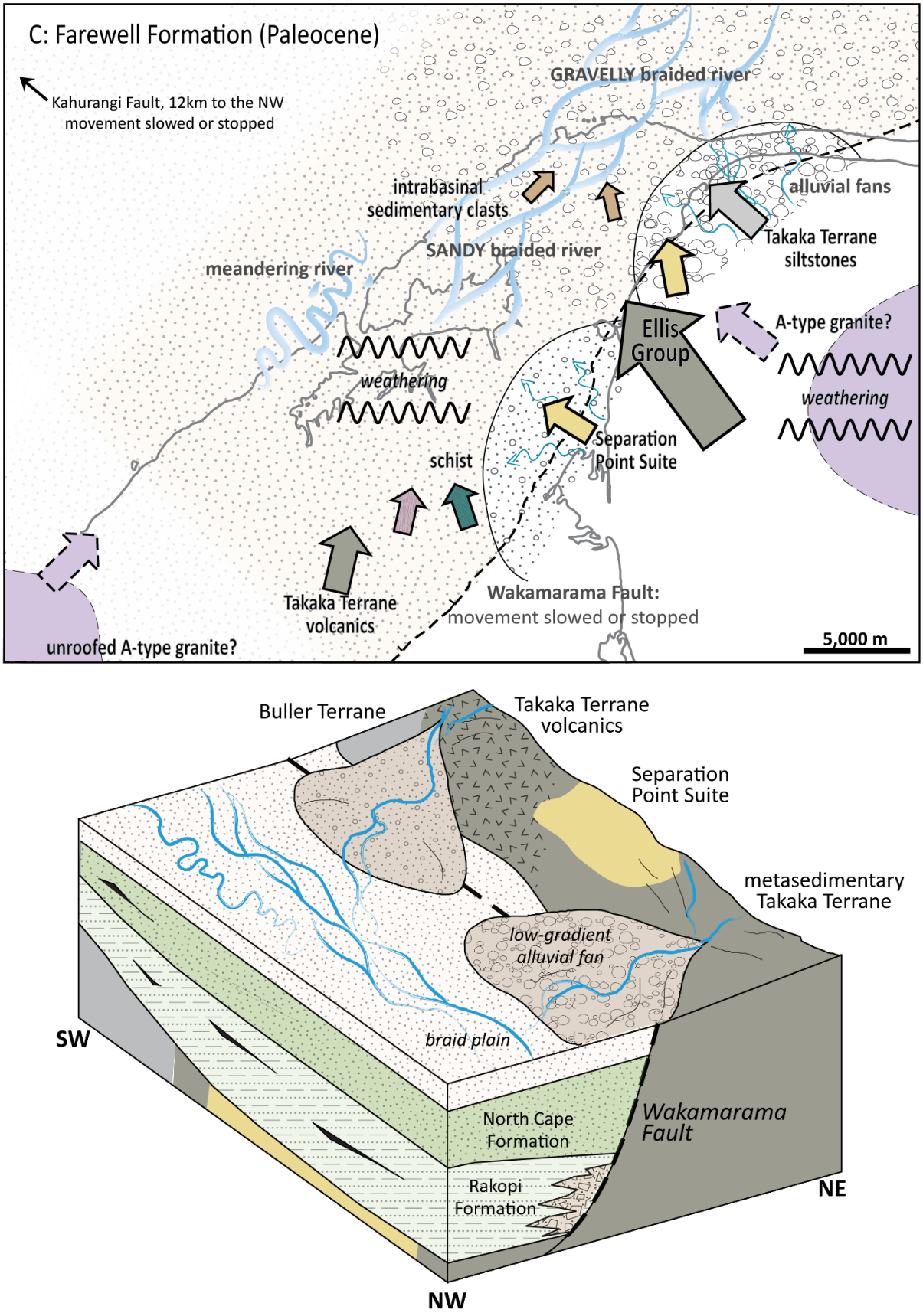

Fig. 7.3: Paleogeography, provenance and structure of the Farewell Formation during the Paleocene.

The provenance of the Farewell Formation is dominated by metasedimentary material, likely from the Takaka Terrane. Other conglomerate sources are high-silica Separation Point Suite granitoids, an A-type granitoid, Takaka Terrane volcanics, Takaka Terrane siltstones, and schist. This indicates that although the rate of uplift along the Wakamarama Fault had slowed, material was still being supplied from east of the fault, rather than from along the basin axis to the southwest. The sedimentary geochemistry, sandstone petrology, and conglomerate clast counts show that a metasedimentary provenance is more significant in the Farewell Formation compared to the North Cape Formation and becomes more dominant towards the top of the Farewell Formation. Low silica Separation Point Suite granitoids were not found in the Farewell Formation conglomerates, suggesting the catchments feeding the Farewell Formation had shifted away from this source.

Stark (1996) argued that there is no evidence for alluvial fans flowing perpendicular to the Wakamarama Faults, as he measured only paleoflow directions parallel to the Wakamarama Fault and observed slightly finer grain sizes closer to the fault. In this study, the gravelly braided river association was found close to the fault at Puponga Point, and paleoflow measurements perpendicular to the fault were also recorded. Variations in the proportion of sandstone beds within the gravelly braided river association are accounted for by the high spatial variability observed in braided river environments. The provenance data show that the majority of the material was fed from the Takaka Terrane east of the Wakamarama Fault, indicating drainage from the footwall block.

The Farewell Formation sediments become more weathered towards the top of the formation. The granitoid and volcanic conglomerate clasts are increasingly weathered, the sandstones become more quartzose, and kaolinite clays become more abundant. Weathering at least partially accounts for the increased prevalence of metasedimentary sources as the less stable granitoid and volcanic components are weathered to clays. Weathering in the Farewell Formation is observed across the Taranaki Basin, Larmer (1998) reported kaolinite likely related to pedogenesis in the Farewell Formation, and Higgs and King (2017) reported increasing sediment maturity in the Farewell Formation.

7.2 Tectonic setting

One aim of this project was to use the provenance and paleogeographic interpretations of the Rakopi, North Cape, and Farewell formations to investigate the tectonic setting of the southern Taranaki Basin as rifting initiated and propagated in the Late Cretaceous, and then ceased and transitioned to a passive margin setting in the Paleocene. The northwest Nelson outcrops are useful for studying the adjacent Wakamarama Fault, which developed in response to rifting in the Late Cretaceous.

The Rakopi Formation and Otimataura Conglomerate were the first sedimentary units deposited in the incipient Pakawau Sub-basin during the Late Cretaceous. The Wakamarama Fault was initially segmented, as suggested by the variation in thickness, location, and composition of the Otimataura Conglomerate, in comparison to the present-day location of the fault and basement lithologies. The mechanism of normal-fault development where small faults form to accommodate extension, propagate and then combine, is well-established in the literature (Peacock and Sanderson 1991; Gawthorpe and Leeder 2000; Young et al. 2001; Henstra et al. 2015; Fossen and Rotevatn 2016).

By North Cape Formation time (Late Cretaceous) the Wakamarama Fault was highly active. Rifting had progressed enough that the majority of the graben was shallow marine, as indicated by tidal lithofacies and the presence of glauconite, S, and P_2O_5 in the sandstones and mudstones. The paleoflow and provenance indicate that drainage was perpendicular to subperpendicular to the Wakamarama Fault, in which case uplift was controlling sedimentation in the basin.

Lamb et al. (2016) suggested that there was significant sinistral offset on the Alpine Fault in the Late Cretaceous. Thrasher (1990) and King and Thrasher (1996) also suggest strike-slip movement in the southern and central Taranaki Basin in the Late Cretaceous as a mechanism for extension. Similarly, transtension has been proposed as the mechanism for Late Cretaceous to Paleocene extension in the Greymouth Basin (Bishop DJ 1992; Cody 2015). However, Reilly et al. (2015) found no evidence of strike-slip movement seismic reflection studies in the offshore southern Taranaki Basin. From this research, there is no evidence of strike-slip faulting in the Pakawau sub-basin or on the Wakamarama Fault. The provenance of the Pakawau Group and Farewell Formation is the basement material east of the

Wakamarama Fault, it has not been offset as would be expected if there was lateral movement along the fault. The provenance also does not change up the Pakawau Group stratigraphy, as would be expected if the source material southeast of the fault was being moved laterally.

By Farewell Formation time (Paleocene), movement on the Wakamarama Fault had slowed or stopped. In the upper part of the Farewell Formation, the granitoid and volcanic conglomerate clasts become more weathered, the sandstones become more quartzose, and the CIA and Ga/Rb of the sandstones and mudstones increases indicating the formation of kaolinite clays. This is interpreted to be caused by enhanced weathering of the sediments and basement source during erosion, transport and deposition. This may be partly due to changing climate, as the Paleocene was slightly wetter than the Late Cretaceous in the Pakawau sub-basin, although it was also cooler (Kennedy 2003). The major control on weathering of the sediments is likely to be the rate of erosion of the basement and the residence time of sediments in the fluvial system, both of which are affected by the rate of uplift and faulting. Uplift on the Wakamarama Fault is therefore likely to have slowed or stopped in the Paleocene. In other parts of the offshore Taranaki Basin the Pakawau Group and Farewell Formation become more compositionally mature upsection (Higgs and King 2017), suggesting that increasing weathering as rifting ceased in Paleocene was widespread.

Although the Wakamarama Fault was not uplifting new material in the Paleocene, there was still topography with highlands to the southeast of the Wakamarama Fault (Fig. 7.3). These highlands were drained by alluvial fans, as shown by the presence of Takaka Terrane clasts and coarser material north of the Whanganui Inlet.

Rift-related magmatism from the Late Cretaceous and Paleocene is recorded around Zealandia. To the south of the Pakawau sub-basin is the Paparoa Metamorphic Core Complex and associated mid-Cretaceous intrusives, which developed in the mid-Cretaceous as a result the initial break-up of Gondwana (Tulloch and Kimbrough 1989; Sagar and Palin 2011). Volcanism due to Late Cretaceous and Paleocene rifting is observed in the Great South Basin, Canterbury Basin, Greymouth Basin, Marlborough, and in the northern Taranaki Basin (Wilding et al. 1971; Weaver and Pankhurst 1991; Bishop DJ 1992; Grapes et al. 1992; Sahoo et al. 2014; Rad and Anadarko New Zealand Taranaki Company 2015). Adams et al. (2017) found Late Cretaceous (81 ± 2, 84 ± 2 Ma) detrital zircons in Rakopi Formation sandstones in

the Paturau River, and suggested they were from rift-related magmatism. In this study, there was no evidence from the conglomerates, sandstone petrology, or sandstone or mudstone geochemistry of syn-sedimentary volcanism in the Pakawau Group or Farewell Formation. However, many of the granitoid conglomerate clasts were from an A-type granitoid which does not outcrop in the northwest Nelson region. A-type granitoids are commonly associated with rifting (Winter 2014), this A-type granitoid may have been emplaced and unroofed during the extension of the continental crust in the early Late Cretaceous. The granitoid may be Late Cretaceous in age, accounting for the young zircons, although further dating and investigation of the A-type granitoid clasts are necessary to confirm this hypothesis. Alternatively, the A-type granitoid may be an unknown subcrop of an older granitoid such as the Foulwind Suite.

7.3 Implications for petroleum systems

The Rakopi, North Cape, and Farewell formations are important producing and potential source and reservoir units in the Taranaki Basin. One aim of this research was to relate the composition of these formations to the petroleum system, as previous work has shown that the composition of these formations strongly controls their reservoir potential (Higgs et al. 2010).

The presence and composition of clay minerals has been shown to be a main factor in the reservoir potential of Taranaki Basin sedimentary rocks (Higgs et al. 2010). In this study, whole-rock geochemistry has been shown to be an effective measure of clay composition (Chapter 6). The Rakopi Formation has a high proportion of diagenetic illite. In the wider Taranaki Basin, sedimentary units buried to a similar depth to the northwest Nelson Rakopi outcrops (~3000 m, Browne et al. 2008) could therefore be expected to have significant diagenetic clays.

The North Cape Formation has the lowest clay content of the three formations, and thus has a greater reservoir potential. It also has better sorted sandstones than either the Rakopi or Farewell formations, due to the coastal depositional processes. Joyce (2018) showed that North Cape Formation sandstones in the Whanganui Inlet had porosities of 7 – 46% and permeability of 0.33 – 545.05 mD, confirming that it has good reservoir potential. However,

the North Cape Formation sandstones are dominantly lithic feldsarenites, with a high proportion of relatively unstable components such as feldspars and igneous lithics. At greater burial depths in the Taranaki Basin these components will be readily compacted and chemically altered, affecting the porosity and permeability of reservoir sandstones.

The Farewell Formation is a reservoir unit in the wider Taranaki Basin. It is more quartzose than the Pakawau Group, suggesting it has better reservoir potential. It has more kaolinite clays in the upper formation, as a result of weathering, which may decrease the reservoir potential. Kaolinite clays are likely to be observed across the Taranaki Basin, as normal faulting ceased across the basin in the Paleocene.

From the whole-rock geochemistry, samples from the Pakawau Group and Farewell Formation were divided into six compositionally distinct petrofacies (Chapter 6). The petrofacies aligned well with the formation contacts, and the composition was shown to relate well to depositional and provenance trends established from the sandstone petrology and conglomerate composition. This technique and the understanding of how provenance, diagenesis, and depositional environment affects sedimentary geochemistry established in this study would be an effective tool for samples from wells in the Taranaki Basin. Many of the wells in the Pakawau sub-basin do not have core (for example, Cape Farewell-1 and Fresne-1), but the geochemical techniques could be applied to cuttings.

7.4 Future work

The same provenance techniques used in this study could be expanded into wells in the Taranaki Basin. Petrology and whole-rock geochemistry have been shown here to be effective tools for diagnosing depositional environment, clay composition, and provenance. Now that the relationship between these factors and the composition of the Pakawau Group and Farewell Formation are better known, these techniques could be applied to cuttings and core. The understanding of how the mineralogy of the sandstones affects their whole-rock chemistry established here could also be applied to cuttings and core.

The relationships between sediment composition and reservoir potential hypothesised above should be tested with porosity and permeability testing on samples from the northwest Nelson outcrops.

A previously unknown A-type granitoid has been identified in the conglomerate clasts of the North Cape and Farewell formations. This should be further characterised by dating and analysing the REE chemistry of the clasts. Further work is also needed on the composition of the younger Takaka Terrane sedimentary rocks, very little literature was available to compare the metasedimentary conglomerate clasts in this study to the Takaka Terrane basement.

Further work is needed on the Otimataura Conglomerate. The most accessible outcrops were included in this study, however more clast samples and sandstone should be collected from other outcrops in the Burnett Range.

7.5 Contributions

The Farewell Formation had been briefly described and interpreted as a fluvial deposit by Suggate (1956), Titheridge (1977), and Rattenbury et al. (1998). Here, five new detailed stratigraphic columns from the Whanganui Inlet and Cape Farewell regions are presented. The lithofacies association scheme of Stark (1996) has been revised to include the Farewell Formation outcrops on the north-western coast of the Whanganui Inlet, which were interpreted as North Cape Formation by Stark (1996), as well as previously undocumented outcrops on Te Hapu Road. Three overarching lithofacies associations are proposed: a sandy meandering river association, a sandy braided river association, and a gravelly braided river association.

This study presented the first petrographic and geochemical analyses of conglomerate clasts from the North Cape and Farewell formations. The metasedimentary clasts have previously been interpreted as Buller Terrane clasts, derived from rivers draining the southwest along the basin axis (Stark 1996). However, it has been shown from their geochemistry that these clasts are dominantly from the Takaka Terrane, east of the outcrops. From geochemical analysis of the granitoid clasts, a new A-type granitoid was identified, as well as a highly fractionated end-member of the Separation Point Suite.

The paleogeographic models of the Rakopi and North Cape Formation presented by Strogen (2011) and the depositional models for these formations discussed by Browne et al. (2008), Higgs et al. (2010), and Joyce (2018) have been confirmed by outcrop descriptions and additional stratigraphic columns for the North Cape Formation at Pecks Point, and by the

provenance data. The dominantly Takaka Terrane provenance confirms the interpretation of fans and fan deltas draining material uplifted by the Wakamarama Fault.

A new paleogeographic model for the Farewell Formation has been proposed. Stark (1996) argued that all drainage occurred along the basin axis, and there were no alluvial fans flowing from the footwall. However, this study suggests it has a Takaka Terrane provenance requiring drainage to be from the east, rather than from the southwest as suggested by Stark (1996). Alluvial fans are also suggested by east to west paleoflow measurements close to the fault at Puponga, and by the presence of coarser material and Takaka Terrane siltstone clasts in the northern part of the field area likely fed from a fan.

Increasing weathering of the Farewell Formation conglomerate clasts was noted by Suggate (1956), who described increasingly leached greywacke and granite pebbles. In this research, weathering and removal of the granitoid and volcanic conglomerate clasts were observed in the upper Farewell Formation. Increasing weathering of the Farewell Formation sandstones and mudstones was also demonstrated by the increasing proportion of quartz and stable quartzose metasedimentary lithics, and by the increasing chemical index of alteration and Ga/Rb showing the formation of kaolinite clays.

The whole-rock geochemistry of the Rakopi, North Cape, and Farewell formations has not been previously studied. It has been shown here to be a useful tool for diagnosing depositional environment (S and P_2O_5 for marine settings), clay content and composition (CIA, Rb/Sr, and Ga/Rb), and provenance (Na_2O and CaO for plagioclase, Zr, REEs). These principles could be applied to the offshore Taranaki Basin.

REFERENCES

Adams CJ, Campbell HJ, Mortimer N, Griffin WL. 2017. Perspectives on Cretaceous Gondwana break-up from detrital zircon provenance of southern Zealandia sandstones. Geological Magazine. 154(04):661-682.

Anadarko New Zealand Taranaki Company. 2015. PEP 38451 Romney-1 Well Completion Report. NZP&M, Ministry of Business, Innovation & Employment (MBIE), New Zealand Unpublished Petroleum Report PR4951.

Bache F, Mortimer N, Sutherland R, Collot J, Rouillard P, Stagpoole V, Nicol A. 2014. Seismic stratigraphic record of transition from Mesozoic subduction to continental breakup in the Zealandia sector of eastern Gondwana. Gondwana Research. 26(3-4):1060-1078.

Baker JA, Gamble JA, Graham IJ. 1994. The age, geology, and geochemistry of the Tapuaenuku Igneous Complex, Marlborough, New Zealand. New Zealand Journal of Geology and Geophysics. 37(3):249-268.

Bal AA. 1992. Estuarine to fluvial transition: the Cretaceous/Tertiary "Puponga" Coal Measures in the Pakawau Group, northwest Nelson [BSc Hons]. Christchurch, New Zealand: University of Canterbury.

Bal AA. 1994. Cessation of Tasman Sea spreading recorded as a sequence boundary. In: van der Lingen GJ, Swanson KM, Muir RJ, editors. Evolution of the Tasman Sea Basin. Rotterdam, Netherlands: A. A. Balkema; p. 105-117.

Bal AA, Lewis DW. 1994. A Cretaceous - early Tertiary macrotidal estuarine-fluvial succession: Puponga Coal Measures in Whanganui Inlet, onshore Pakawau Sub-basin, northwest Nelson, New Zealand. New Zealand Journal of Geology and Geophysics. 37(3):287-307.

Basu A, Young SWSLJ, Suttner LJ, James WC, Mack GH. 1975. Re-evaluation of the use of undulatory extinction and polycrystallinity in detrital quartz for provenance interpretation. Journal of Sedimentary Research. 45(4):873-882.

Berner RA. 1981. A new geochemical classification of sedimentary environments. SEPM Journal of Sedimentary Research. 51(2):359-365.

Bhatia MR, Crook KaW. 1986. Trace element characteristics of greywackes and tectonic setting discrimination of sedimentary basins. Contributions to Mineralogy & Petrology. 92:181-193.

Bishop DG. 1971. Geological map of New Zealand sheet S1, S3 & pt.S4: Farewell-Collingwood, scale 1:63,360. Wellington: Department of Scientific and Industrial Research.

Bishop DJ. 1992. Extensional tectonism and magmatism during the middle Cretaceous to Paleocene, North Westland, New Zealand. New Zealand Journal of Geology and Geophysics. 35(1):81-91.

Blair TC, McPherson JG. 1994. Alluvial fans and their natural distinction from rivers based on morphology, hydraulic processes, sedimentary processes, and facies assemblages. Journal of Sedimentary Research. A64(3):450-489.

Blair TC, McPherson JG. 2009. Processes and forms of alluvial fans. In: Parsons AJ, Abrahams AD, editors. Geomorphology of Desert Environments. 2nd ed. Netherlands: Springer Science + Business Media B. V.; p. 413-467.

Bridge JS, Lunt IA. 2006. Depositional models of braided rivers. Braided Rivers: Process, Deposits, Ecology and Management.11-50.

Browne GH. 2009. First New Zealand record of probable dinosaur footprints from the Late Cretaceous North Cape Formation, northwest Nelson. New Zealand Journal of Geology and Geophysics. 52(4):367-377.

Browne GH, Kennedy EM, Constable RM, Raine JI, Crouch EM, Sykes R. 2008. An outcrop-based study of the economically significant Late Cretaceous Rakopi Formation, northwest Nelson, Taranaki Basin, New Zealand. New Zealand Journal of Geology and Geophysics. 51(4):295-315.

Bull S, Strogen DP, Seebeck H, Zhu H, Hill MG, Arnot MJ, Kroeger KF. 2016. Seismic reflection interpretation, static modelling and velocity modelling of the southern Taranaki Basin (4D Taranaki Project). GNS Science Report 2016/02.

Burckle LH, Potter N. 1996. Pliocene-Pleistocene diatoms in Paleozoic and Mesozoic sedimentary and igneous rocks from Antarctica: A Sirius problem solved. Geology. 24:235-238.

Burgess AW. 1978. Gold mineralization at the Golden Blocks gold field [MSc]. Christchurch, New Zealand: University of Canterbury.

Bussell MR. 1985. Report following geological mapping of the Pakawau Group in Westhaven Inlet, northwest Nelson. Ministry of Economic Development New Zealand Unpublished Coal Report CR1571.

Carter M, Kintanar ERL. 1987. Cape Farewell-1 Well Completion Report PPL 38119. Ministry of Economic Development New Zealand Unpublished Petroleum Report PR1234.

Chafetz HS, Reid A. 2000. Syndepositional shallow-water precipitation of glauconitic minerals. Sedimentary Geology. 136(1-2):29-42.

Chappell BW, White AJR. 1992. I- and S-type granites in the Lachlan Fold Belt. Transactions of the Royal Society of Edinburgh: Earth Sciences. 83:1-26.

Chemostrat Ltd. 2017. Chemostratigraphy of six wells from the Kupe PML of the Manaia Graben, Southern Taranaki Basin, Offshore New Zealand (Redacted Version). NZP&M, Ministry of Business, Innovation & Employment (MBIE), New Zealand Unpublished Petroleum Report PR5500.

Cody E-NO. 2015. Sedimentology and hydrocarbon potential of the Paparoa Coal Measures lacustrine mudstones [MSc]. Christchurch, New Zealand: University of Canterbury.

Cooper RA. 1965. Lower Paleozoic rocks between Upper Takaka and Riwaka, North-West Nelson. New Zealand Journal of Geology and Geophysics. 8(1):49-61.

Cooper RA. 1979. Lower Palaeozoic rocks of New Zealand. Journal of the Royal Society of New Zealand. 9(1):29-84.

Cooper RA. 1989. Early Paleozoic terranes of New Zealand. Journal of the Royal Society of New Zealand. 19(1):73-112.

Cooper RA, Tulloch AJ. 1992. Early Palaeozoic terranes in New Zealand and their relationship to the Lachlan Fold Belt. Tectonophysics. 214:129-144.

Craigie NW, Breuer P, Khidir A. 2016. Chemostratigraphy and biostratigraphy of Devonian, Carboniferous and Permian sediments encountered in eastern Saudi Arabia: An integrated approach to reservoir correlation. Marine and Petroleum Geology. 72:156-178.

CRL Energy Ltd. 2017. SpectraChem Quality Assurance. [accessed 2018 10 April]. https://www.crl.co.nz/spectrachem-quality-assurance.

Dickinson WR, Beard LS, Brakenridge GR, Erjavec JL, Ferguson RC, Inman KF, Knepp RA, Lindberg FA, Ryberg PT. 1983. Provenance of North American Phanerozoic sandstones in relation to tectonic setting. Geological Society of America Bulletin. 94:222-235.

Eby GN. 1992. Chemical subdivision of the A-type granitoids: Petrogenetic and tectonic implications. Geology. 20(7):641

Ernst W. 1970. Methods in geochemistry and geophysics. Amsterdam, London, New York: Elsevier Publishing Company.

Folk RL, Andrews PB, Lewis DW. 1970. Detrital sedimentary rock classification and nomenclature for use in New Zealand. New Zealand Journal of Geology and Geophysics. 13(4):937-968.

Fossen H, Rotevatn A. 2016. Fault linkage and relay structures in extensional settings-A review. Earth-Science Reviews. 154:14-28.

Garzanti E. 1986. Source rock versus sedimentary control on the mineralogy of deltaic volcanic arenites (Upper Triassic, northern Italy). Journal of Sedimentary Petrology. 56(2):267-275.

Garzanti E, Andò S, France-Lanord C, Vezzoli G, Censi P, Galy V, Najman Y. 2010. Mineralogical and chemical variability of fluvial sediments. 1. Bedload sand (Ganga-Brahmaputra, Bangladesh). Earth and Planetary Science Letters. 299(3-4):368-381.

Gawthorpe RL, Leeder MR. 2000. Tectono-sedimentary evolution of active extensional basins. Basin Research. 12:195-218.s

Godin PD. 1991. Fining-upward cycles in the sandy braided-river deposits of the Westwater Canyon Member (Upper Jurassic), Morrison Formation, New Mexico. Sedimentary Geology. 70(1):61-82.

Grapes RH, Lamb SH, Adams CJ. 1992. K-Ar ages of basanitic dikes, Awatere Valley, Marlborough, New Zealand. New Zealand Journal of Geology and Geophysics. 35(4):415-419.

Grindley GW. 1980. Geological map of New Zealand 1:63 360, sheet S23 Cobb. New Zealand Geological Survey, Department of Scientific and Industrial Research.

Harrison IS. 1993. The structure of the Buller Terrane west of the Anatoki Thrust, upper Cobb Valley, northwest Nelson, New Zealand [MSc]. Christchurch, New Zealand: University of Canterbury.

Harriss RC, Adams JAS. 1966. Geochemical and mineralogical studies on the weathering of granitic rocks. American Journal of Science. 264:146-173.

Henstra GA, Rotevatn A, Gawthorpe RL, Ravnås R. 2015. Evolution of a major segmented normal fault during multiphase rifting: The origin of plan-view zigzag geometry. Journal of Structural Geology. 74:45-63.

Higgs KE, Arnot MJ, Browne GH, Kennedy EM. 2010. Reservoir potential of Late Cretaceous terrestrial to shallow marine sandstones, Taranaki Basin, New Zealand. Marine and Petroleum Geology. 27(9):1849-1871.

Higgs KE, King PR. 2017. Taranaki reservoirs: sandstone provenance and sediment pathways through time with implications for reservoir quality. 2nd New Zealand Petroleum Geoscience Workshop. Lower Hutt, New Zealand.

Hutton PR. 1995. A structural study of the Separation Point Batholith: emplacement mechanisms and the tectonic regime [MSc]. Christchurch, New Zealand: University of Canterbury.

International Organization for Standardization. 2015. ISO 9001:2015(en) Quality management systems — Requirements. [accessed 2018 20 April]. https://www.iso.org/obp/ui/#iso:std:iso:9001:ed-5:v1:en.

International Organization for Standardization. 2017. ISO/IEC 17025:2017(en) General requirements for the competence of testing and calibration laboratories. [accessed 2018 20 April]. https://www.iso.org/obp/ui/#iso:std:iso-iec:17025:ed-3:v1:en.

Irvine TN, Baragar WRA. 1971. A guide to the chemical classification of the common volcanic rocks. Canadian Journal of Earth Sciences. 8(5):523-548.

Johnsson MR. 1993. The system controlling the composition of clastic sediments. In: Johnsson MR, Basu A, editors. Boulder, Colorado: Geological Society of America Special Paper 284; p. 1-19.

Jongens R. 1997. The Anatoki Fault and structure of the adjacent Buller and Takaka Terrane rocks, northwest Nelson, New Zealand [PhD]. Christchurch, New Zealand: University of Canterbury.

Joyce R. 2018. Assessment of paleo-depositional environments and reservoir potential of the Late Cretaceous North Cape Formation, Nelson, New Zealand [MSc]. Christchurch, New Zealand: University of Canterbury.

Kennedy EM. 2003. Late Cretaceous and Paleocene terrestrial climates of New Zealand: Leaf fossil evidence from South Island assemblages. New Zealand Journal of Geology and Geophysics. 46(2):295-306.

Killops SD, Woolhouse AD, Weston RJ, Cook RA. 1994. A Geochemical Appraisal of Oil Generation in the Taranaki Basin, New Zealand. AAPG Bulletin. 78(10):1560-1585.

King PR, Thrasher GP. 1996. Cretaceous-Cenozoic geology and petroleum systems of the Taranaki Basin, New Zealand. Lower Hutt, New Zealand: Institute of Geological & Nuclear Sciences Limited.

Laird MG. 1972. Sedimentology of the Greenland Group in the Paparoa Range, West Coast, South Island. New Zealand Journal of Geology and Geophysics. 15(3):372-393.

Laird MG. 1981. The Late Mesozoic fragmentation of the New Zealand segment of Gondwana. In: Cresswell MM, Vella P, editors. Gondwana Five: proceedings of the Fifth International

Gondwana Symposium, Wellington, February 1980. Rotterdam, Netherlands: A. A. Balkema; p. 311-318.

Laird MG, Bradshaw JD. 2004. The Break-up of a Long-term Relationship: the Cretaceous Separation of New Zealand from Gondwana. Gondwana Research. 7(1):273-286.

Lamb S, Mortimer N, Smith E, Turner G. 2016. Focusing of relative plate motion at a continental transform fault: Cenozoic dextral displacement >700 km on New Zealand's Alpine Fault, reversing >225 km of Late Cretaceous sinistral motion. Geochemistry, Geophysics, Geosystems. 17:1197-1213.

Larmer MP. 1998. Clay minerals in mudstones of the Taranaki Basin, New Zealand. Institute of Geological & Nuclear Sciences science report 1998/26.

Le Maitre RW, International Union of Geological Sciences. Subcommission on the Systematics of Igneous R. 2004. Igneous rocks: a classification and glossary of terms : recommendations of the International Union of Geological Sciences, Subcommission on the Systematics of Igneous Rocks. 2nd ed. Cambridge: Cambridge University Press.

Lewis DW, McConchie D. 1994. Analytical Sedimentology. New York: Chapman & Hall.

López JMG, Bauluz B, Fernández-Nieto C, Oliete AY. 2005. Factors controlling the trace-element distribution in fine-grained rocks: The Albian kaolinite-rich deposits of the Oliete Basin (NE Spain). Chemical Geology. 214:1-19.

Lunt IA, Sambrook Smith GH, Best JL, Ashworth PJ, Lane SN, Simpson CJ. 2013. Deposits of the sandy braided South Saskatchewan river: Implications for the use of modern analogs in reconstructing channel dimensions in reservoir characterization. AAPG Bulletin. 97(4):553-576.

Macaire JJ. 1986. Sequence of polycyclic soils formed on plio-quaternary alluvial deposits in South-Western Paris basin (France). Paleoecological significance. Catena. 13(1-2):29-46.

Maclean DR. 1994. The geology and geochemistry of the Cambrian Devil River Volcanics, Anatoki Range, northwest Nelson [MSc]. Christchurch, New Zealand: University of Canterbury.

McCoy-West AJ, Baker JA, Faure K, Wysoczanski R. 2010. Petrogenesis and origins of mid-Cretaceous continental intraplate volcanism in Marlborough, New Zealand: Implications for the long-lived HIMU magmatic mega-province of the SW Pacific. Journal of Petrology. 51(10):2003-2045.

McLennan SM, Hemming S, McDaniel DK, Hanson GN. 1993. Geochemical approaches to sedimentation, provenance, and tectonics. Geological Society of America Special Paper. 284:21-40.

Miall AD. 2010. Chapter 6, Alluvial deposits. In: James NP, Dalrymple RW, editors. Facies Models 4. Newfoundland: Geological Association of Canada; p. 105-138.

Middelburg JJ, Van Der Weijden CH, Woittiez JRW. 1988. Chemical processes affecting the mobility of major, minor and trace elements during weathering of granitic rocks. Chemical Geology. 68(3-4):253-273.

Mortimer N. 2004. New Zealand's Geological Foundations. Gondwana Research. 7(1):261-272.

Mortimer N, Rattenbury MS, King PR, Bland KJ, Barrell DJA, Bache F, Begg JG, Campbell HJ, Cox SC, Crampton JS et al. 2014. High-level stratigraphic scheme for New Zealand rocks. New Zealand Journal of Geology and Geophysics. 57(4):402-419.

Mortimer N, Tulloch AJ, Ireland TR. 1997. Basement geology of Taranaki and Wanganui Basins, New Zealand. New Zealand Journal of Geology and Geophysics. 40(2):223-236.

Mortimer N, Tulloch AJ, Spark RN, Walker NW, Ladley E, Allibone A, Kimbrough DL. 1999. Overview of the Median Batholith, New Zealand: a new interpretation of the geology of the Median Tectonic Zone and adjacent rocks. Journal of African Earth Sciences. 29(1):257-268.

Muir RJ, Weaver SD, Bradshaw JD, Eby GN, Evans JA. 1995. The Cretaceous Separation Point batholith, New Zealand: granitoid magmas formed by melting of mafic lithosphere. Journal of the Geological Society, London. 152:689-701.

Münker C. 2000. The isotope and trace element budget of the Cambrian Devil River arc system, New Zealand: Identification of four source components. Journal of Petrology. 41(6):759-788.

Münker C, Cooper RA. 1999. The Cambrian arc complex of the Takaka Terrane, New Zealand: An integrated stratigraphical, paleontological and geochemical approach. New Zealand Journal of Geology and Geophysics. 42(3):415-445.

Nebel-Jacobsen Y, Münker C, Nebel O, Mezger K. 2011. Precambrian sources of Early Paleozoic SE Gondwana sediments as deduced from combined Lu–Hf and U–Pb systematics of detrital zircons, Takaka and Buller terrane, South Island, New Zealand. Gondwana Research. 20:427-442.

Neilson MJ, Brockman GF. 1977. The error associated with point-counting. American Mineralogist. 62:1238-1244.

Nicholson KN, Black PM. 2004. Cretaceous to early Tertiary basaltic volcanism in the Far North of New Zealand: Geochemical associations and their tectonic significance. New Zealand Journal of Geology and Geophysics. 47(3):437-446.

NZ Aquitaine Petroleum Ltd. 1976. Well completion report Fresne-1. Ministry of Economic Development New Zealand PR674.

Ongley M, Macpherson EO. 1923. The geology and mineral resources of the Collingwood Subdivision, Karamea Division. New Zealand Geological Survey Bulletin. 25:52.

Origin Analytical. 2018. ICP-MS, ICP-OES & LA-ICP-MS. [accessed 2018 10 April]. https://originanalytical.com/process/icp-ms-icp-oes/.

PBE. 2017. Petroleum Basin Explorer 3.0. Institute of Geology and Nuclear Sciences; [accessed 2018 February]. https://data.gns.cri.nz/dataportal/.

Peacock DCP, Sanderson DJ. 1991. Displacements, segment linkage and relay ramps in normal fault zones. Journal of Structural Geology. 13(6):721-733.

Pearce Ja, Harris NBW, Tindle AG. 1984. Trace element distribution diagrams for the tectonic interpretation of granitic rocks. Journal of Petrology. 25(4):956-983.

Pound KS, Cooper RA, Grapes RH, Stedman H. 1993. Northwest Nelson - basement geology. Wellington, New Zealand: Geologial Society of New Zealand Miscellaneous Publication 79B; p. 75-146.

Rad F, Anadarko New Zealand Taranaki Company. 2015. PEP 38451 Romney-1 Well Completion Report.

Ratcliffe KT, Morgan AC, Ritcey DH, A. EC. 2007. Whole-rock geochemistry and heavy mineral analysis as petroleum exploration tools in the Bowser and Sustut basins, British Columbia, Canada. Bulletin of Canadian Petroleum Geology. 55(4):320-336.

Ratcliffe KT, Wright AM, Montgomery P, Palfrey A, Vonk A, Vermeulen J, Barrett M. 2010. Application of chemostratigraphy to the Mungaroo Formation, the Gorgon Field, offshore northwest Australia. APPEA Journal. 50th Anniversary Issue:371-386.

Rattenbury MS, Cooper RA, Johnston MR, Forsyth PJ compilers. ss1998. Geology of the Nelson area. Institute of Geological & Nuclear Sciences 1:250 000 geological map 9. 1 sheet + 67 p. Lower Hutt, New Zealand: Institute of Geological & Nuclear Sciences Limited.

Reilly C, Nicol A, Walsh JJ, Seebeck H. 2015. Evolution of faulting and plate boundary deformation in the Southern Taranaki Basin, New Zealand. Tectonophysics. 651:1-18.

Reineck HE, Singh IB. 1980. Depositional sedimentary environments, with reference to terrigenous clastics. 2nd ed. Berlin, Heidelberg, New York: Springer-Verlag.

Roncaglia L, Morgans HG, Fohrmann M, Crundwell MP, Milner M. 2013. Well log stratigraphy in the central and southern offshore area of the Taranaki Basin, New Zealand. GNS Science Report 2013/27.

Roser BP, Cooper Ra, Nathan S, Tulloch AJ. 1996. Reconnaissance sandstone geochemistry, provenance, and tectonic setting of the lower Paleozoic terranes of the West Coast and Nelson, New Zealand. New Zealand Journal of Geology and Geophysics. 39(1):1-16.

Roser BP, Korsch RJ. 1988. Provenance signatures of sandstone-mudstone suites determined using discriminant function analysis of major-element data. Chemical Geology. 67(1-2):119-139.

Sagar MW, Palin JM. 2011. Emplacement, metamorphism, deformation and affiliation of mid-Cretaceous orthogneiss from the Paparoa Metamorphic Core Complex lower-plate, Charleston, New Zealand. New Zealand Journal of Geology and Geophysics. 54(3):273-289.

Sahoo TR, King PR, Bland KJ, Strogen DP, Sykes R, Bache F. 2014. Tectono-sedimentary evolution and source rock distribution of the mid to Late Cretaceous succession in Great South Basin, New Zealand. APPEA Journal.259-274.

Savage KM, de Cesero P, Potter PE. 1988. Mineralogic maturity of modern sand along a high-energy tropical coast: Baixada de Jacarepaguá, Rio de Janeiro, Brazil. Journal of South American Earth Sciences. 1(4):317-328.

Shand JS. 1947. Eruptive rocks. New York: John Wiley & Sons, Inc.

Smale D. 1996. Petrographic summaries of Taranaki petroleum reports. Lower Hutt, New Zealand: Institute of Geological and Nuclear Sciences science report 96/1.

Stallard AR. 1994. An investigation of the geology and tectonics of the Bay Schist in the context of the Buller Terrane-Takaka Terrane boundary [MSc]. Christchurch, New Zealand: University of Canterbury.

Stark CJ. 1996. Interpretation of some Paleocene fluvial sediments from the upper Pakawau and Kapuni Groups, Pakawau Sub-Basin, north-west Nelson [MSc]. Christchurch, New Zealand: University of Canterbury.

Steadman RD. 2017. Provenance and porosity analysis of the Greymouth Basin, New Zealand [MSc]. Christchurch, New Zealand: University of Canterbury.

Strogen DP. 2011. Updated paleogeographic maps for the Taranaki Basin and surrounds. Lower Hutt, New Zealand: GNS Science Report 2010/53. 9780478198010.

Strogen DP, Seebeck H, Nicol A, King PR, Cret E. 2017. Two-phase Cretaceous – Paleocene rifting in the Taranaki Basin region, New Zealand; implications for Gondwana break-up. Journal of the Geological Society.

Strong DT, Turnbull RE, Haubrock SN, Mortimer N. 2016. Petlab: New Zealand's national rock catalogue and geoanalytical database. New Zealand Journal of Geology and Geophysics. 59(3):475-481.

Suggate RP. 1956. Puponga Coalfield. New Zealand Journal of Science and Technology. 37(5):539-559.

Sun Ss, McDonough WF. 1989. Chemical and isotopic systematics of oceanic basalts: implications for mantle composition and processes. Geological Society, London, Special Publications. 42(1):313-345.

Thrasher GP. 1990. Tectonics of the Taranaki Rift. 1989 New Zealand Petroleum Conference Proceedings. Wellington, New Zealand: Petroleum and Geothermal Unit, Energy and Resources Division, Ministry of Commerce; p. 124-133.

Thrasher GP. 1992. Late Cretaceous geology of Taranaki Basin, New Zealand [PhD]. Wellington, New Zealand: Victoria University of Wellington.

Titheridge DG. 1977. Stratigraphy and sedimentology of the upper Pakawau and lower Westhaven Groups (Upper Cretaceous - Oligocene), northwest Nelson [MSc]. Christchurch, New Zealand: University of Canterbury.

Tucker ME. 1991. Sedimentary Petrology: an introduction to the origin of sedimentary rocks. 2nd ed. Oxford: Blackwell Scientific Publications.

Tulloch AJ. 1983. Granitoid rocks of New Zealand - A brief review. Memoir of the Geological Society of America: Circum-Pacific plate tectonics. 159:5-20.

Tulloch AJ, Kimbrough DL. 1989. The Paparoa Metamorphic Core Complex, New Zealand: Cretaceous extension associated with fragmentation of the Pacific margin of Gondwana. Tectonics. 8(6):1217-1234.

Tulloch AJ, Mortimer N. 2017. New basement map of Taranaki Basin. 2nd New Zealand Petroleum Geoscience Workshop. Lower Hutt, New Zealand.

Tulloch AJ, Rabone SDC. 1993. Mo-bearing granodiorite porphyry plutons of the Early Cretaceous Separation Point Suite, west Nelson, New Zealand Downloaded. New Zealand Journal of Geology and Geophysics. 36:401-408.

Turnbull RE, Size WB, Tulloch AJ, Christie AB. 2017. The ultramafic–intermediate Riwaka Complex, New Zealand: summary of the petrology, geochemistry and related Ni–Cu–PGE mineralisation. New Zealand Journal of Geology and Geophysics.1-26.

Turnbull RE, Tulloch AJ, Ramezani J. 2013. Zetland Diorite, Karamea Batholith, west Nelson: field relationships, geochemistry and geochronology demonstrate links to the Carboniferous Tobin Suite. New Zealand Journal of Geology and Geophysics. 56(2):83-99.

Van der Plas L, Tobi AC. 1965. A chart for judging the reliability of point counting results. American Journal of Science. 263:87-90.

van Oyen FH, Branger J. 1970. Cook-1 well completion report. Ministry of Economic Development New Zealand unpublished petroleum report PR513.

Wang X, Griffin WL, Chen J. 2010. Hf contents and Zr/Hf ratios in granitic zircons. Geochemical Journal. 44:65-72.

Weaver SD, Pankhurst RJ. 1991. A precise Rb-Sr age for the Mandamus Igneous Complex, North Canterbury, and regional tectonic implications. New Zealand Journal of Geology and Geophysics. 34(3):341-345.

Wellman HW. 1950. Geology of Sheets 51,2,3 (Farewell, Kahurangi, and Collingwood), with an outline of the geology of northwest Nelson and Westland. Unpublished manuscript held at the Institute of Geological and Nuclear Sciences library Lower Hutt, New Zealand.

Whalen JB, Currie KL, Chappell BW. 1987. A-type granites: geochemical characteristics, discrimination and petrogenesis. Contributions to Mineralogy and Petrology. 95(4):407-419.

Wilding A, Sweetman LAD, BP Shell Aquitaine Todd Petroleum Developments Ltd. 1971. Endeavour-1 Well Completion Report. Ministry of Economic Development New Zealand Unpublished Petroleum Report PR303.

Winchester JA, Floyd PA. 1977. Geochemical discrimination of different magma series and their differentiation products using immobile elements. Chemical Geology. 20:325-343.

Winter JD. 2014. Principles of igneous and metamorphic petrology. 2nd ed. Harlow, Essex: Pearson Education Limited.

Wizevich MC. 1992. Petrography of sandstones in the Pakawau Basin, northwest Nelson. In: Nobes DC, editor. Geological Society of New Zealand and New Zealand Geophysical Society Joint Annual Conference. University of Canterbury, Christchurch, New Zealand; p. 164-164.

Wizevich MC. 1994. Sedimentary evolution of the onshore Pakawau Subbasin: rift sediments of the Taranaki Basin deposited during Tasman Sea spreading. In: Van der Lingen GJ, Swanson KM, Muir RJ, editors. Evolution of the Tasman Sea Basin. Rotterdam, Netherlands: A.A. Balkema; p. 83-104.

Wizevich MC, Thrasher GP, Bussell MR, Wilson GJ, Collen JD. 1992. Evidence for marine deposition in the Late Cretaceous Pakawau Group, northwest Nelson. New Zealand Journal of Geology and Geophysics. 35(3):363-369.

Wright AJ, Cooper RA, Simes JE. 1994. Cambrian and Ordovician faunas and stratigraphy, Mt Patriarch, New Zealand. New Zealand Journal of Geology and Geophysics. 37(4):437-476.

Young MJ, Gawthorpe RL, Hardy S. 2001. Growth and linkage of a segmented normal fault zone; the Late Jurassic Murchison-Statfjord North Fault, northern North Sea. Journal of Structural Geology. 23:1933-1952.

APPENDIX A: RAKOPI BORE LOG

Table A.1: driller's log of the Rakopi Bore (also "Bassett's Bore"), drilled in 1915, from Wellman (1950), with depth converted to metres for Fig. 3.3.

Driller's description	*Depth, Suggate (1950)*	*Depth (m)*	*Unit thickness (m)*
Surface debris	70 ft	21.3	21.34
Sandstone with thin bands of hard blue marl and traces of coal	93 ft	28.3	7.01
Conglomerate	103 ft	31.4	3.05
Sandstone	109 ft 6 in	33.4	1.98
Carbonaceous matter with hard coal	110 ft 6 in	33.7	0.30
Sandstone	118 ft	36.0	2.29
Coal	118 ft 3 in	36.0	0.08
Sandstone	132 ft	40.2	4.19
Coal	132 ft 2 in	40.3	0.05
Sandstone and fine grit	150 ft	45.7	5.44
Coal	150 ft 1 in	45.7	0.03
Sandstone	163 ft	49.7	3.94
Coal	163 ft 10 in	49.9	0.25
Sandstone	174 ft	53.0	3.10
Coal	175 ft	53.3	0.30
Sandstone	185 ft	56.4	3.05
Coal	185 ft 5 in	56.5	0.13
Sandstone	192 ft	58.5	2.01
Coal	193 ft 4 in	58.9	0.41
Sandstone	206 ft	62.8	3.86
Coal	206 ft 5 in	62.9	0.13
Sandstone	213 ft	64.9	2.01
Coal	214 ft	65.2	0.30
Sandstone	243 ft	74.1	8.84
Sandstone with carb. Matter and traces of coal	270 ft	82.3	8.23
Coal	270 ft 2 in	82.3	0.05
Dirt band	270 ft 8 in	82.5	0.15
Coal	272 ft 3 in	83.0	0.48
Dirt band	272 ft 10 in	83.2	0.18
Coal	273 ft	83.2	0.05
Carbonaceous matter with traces of coal	280 ft	85.3	2.13
Sandstone	300 ft	91.4	6.10
Coal	300 ft 5 in	91.6	0.13
Sandstone free from marl etc.	315 ft	96.0	4.44
Coal	315 ft 3 in	96.1	0.08
Sandstone	315 ft 9 in	96.2	0.15
Coal	316 ft	96.3	0.08
Sandstone	330 ft	100.6	4.27
Carbonaceous matter	330 ft 6 in	100.7	0.15
Sandstone	343 ft	104.5	3.81
Conglomerate	353 ft	107.6	3.05
Coal	353 ft 6 in	107.7	0.15
Carbonaceous matter	356 ft	108.5	0.76
Coal	356 ft 3 in	108.6	0.08
Sandstone	365 ft	111.3	2.67
Coaly matter	366 ft	111.6	0.30
Sandstone	382 ft	116.4	4.88
Coaly matter	383 ft	116.7	0.30
Sandstone	397 ft	121.0	4.27

Driller's description	*Depth, Suggate (1950)*	*Depth (m)*	*Unit thickness (m)*
Coal	397 ft 9 in	121.2	0.23
Stone	399 ft	121.6	0.38
Coal	399 ft 3 in	121.7	0.08
Sandstone	422 ft	128.6	6.93
Coal (hard)	423 ft 2 in	129.0	0.36
Sandstone	432 ft	131.7	2.69
Coal	432 ft 7 in	131.9	0.18
Sandstone	441 ft	134.4	2.57
Conglomerate with quartz pebbles	442 ft	134.7	0.30
Grey sandstone	442 ft 4 in	134.8	0.10
Pebble bed	443 ft 4 in	135.1	0.30
Carbonaceous matter	448 ft	136.6	1.42
Coal	448 ft 7 in	136.7	0.18
Sandstone	457 ft	139.3	2.57
Coal	457 ft 5 in	139.4	0.13
Sandstone, mudstone, and carbonaceous matter	480 ft	146.3	6.88
Coal	480 ft 6 in	146.5	0.15
Sandstone	488 ft	148.7	2.29
Coal	488 ft 5 in	148.9	0.13
Sandstone	517 ft	157.6	8.71
Sandstone with bands of hard marl or mudstone	524 ft	159.7	2.13
Coal	525 ft	160.0	0.30
Sandstone	526 ft	160.3	0.30
Coal	526 ft 6 in	160.5	0.15
Sandstone	531 ft	161.8	1.37
Coal`	531 ft 10 in	162.1	0.25
Sandstone	546 ft	166.4	4.32
Coal	546 ft 5 in	166.5	0.13
Sandstone	560 ft	170.7	4.14
Coal	560 ft 5 in	170.8	0.13
Sandstone	560 ft 8 in	170.9	0.08
Coal	561 ft 6 in	171.1	0.25
Sandstone	565 ft	172.2	1.07
Fine grit merging into conglomerate with quartz pebbles	575 ft	175.3	3.05
Hard dark sandstone	578 ft	176.2	0.91
Coal	578 ft 4 in	176.3	0.10
Sandstone	597 ft	182.0	5.69
Coaly matter	601 ft	183.2	1.22
Sandstone with hard marl	630 ft	192.0	8.84
Coaly matter	632 ft	192.6	0.61
Quartz grit (as in Westport Coalfield but finer)	650 ft	198.1	5.49
Finer grit (carbonaceous band at 650 ft)	673 ft	205.1	7.01
Coal	673 ft 4 in	205.2	0.10
Sandstone	685 ft	208.8	3.56
Coal	685 ft 3 in	208.9	0.08
Sandstone	716 ft	218.2	9.37
Fine grits (gradually coarser with depth)	734 ft	223.7	5.49
Pebble bed (no core)	740 ft	225.6	1.83
Sandstone	744 ft	226.8	1.22
Coal	744 ft 10 in	227.0	0.25
Sandstone (with plant fossils)	761 ft	232.0	4.93
Coal	761 ft 8 in	232.2	0.20
Sandstone	763 ft	232.6	0.41
Coal	763 ft 10 in	232.8	0.25
Sandstone	778 ft	237.1	4.32

Driller's description	*Depth, Suggate (1950)*	*Depth (m)*	*Unit thickness (m)*
Coal	778 ft 6 in	237.3	0.15
Sandstone	786 ft	239.6	2.29
Coal	786 ft 4 in	239.7	0.10
Sandstone and fireclay	787 ft	239.9	0.20
Coal	788 ft 2 in	240.2	0.36
Sandstone and fireclay	790 ft	240.8	0.56
Coal	790 ft 6 in	240.9	0.15
Sandstone and fireclay	790 ft 9 in	241.0	0.08
Coal	791 ft 1 in	241.1	0.10
Sandstone and fireclay	793 ft	241.7	0.58
Coal	793 ft 5 in	241.8	0.13
Sandstone and fireclay	795 ft 3 in	242.4	0.56
Coal	795 ft 9 in	242.5	0.15
Sandstone	806 ft	245.7	3.12
Coarse grey sandstone	815 ft	248.4	2.74
Fine grit with conglomerate bands	831 ft	253.3	4.88
Coarse conglomerate	840 ft	256.0	2.74
Carbonaceous shale	840 ft 6 in	256.2	0.15
Coal	840 ft 10 in	256.3	0.10
Sandstone	850 ft	259.1	2.79
Coal	850 ft 8 in	259.3	0.20
Sandsrone (laminated and micaceous)	872 ft	265.8	6.50
Coal	872 ft 4 in	265.9	0.10
Sandstone (grey and dark) and mudstone	883 ft	269.1	3.25
Sandstone and fine grit	899 ft	274.0	4.88
Micaceous mudstone	906 ft	276.1	2.13
Coal	906 ft 4 in	276.3	0.10
Sandstone (grey and dark)	921 ft	280.7	4.47
Mudstone	924 ft	281.6	0.91
Coal	925 ft 4 in	282.0	0.41
Mudstone	926 ft	282.2	0.20
Coal	926 ft 4 in	282.3	0.10
Fireclay	926 ft 10 in	282.5	0.15
Coal	927 ft 1 in	282.6	0.08
Mudstone	930 ft 6 in	283.6	1.04
Coaly matter	931 ft	283.8	0.15
Mudstone	936 ft	285.3	1.52
Coal	936 ft 4 in	285.4	0.10
Grey sandstone, mudstone below	946 ft	288.3	2.95
Coal	946 ft 4 in	288.4	0.10
Alternating mudstone and micaceous sandstone	958 ft	292.0	3.56
Coal	958 ft 3 in	292.1	0.08
Mudstone and micaceous sandstone	973 ft	296.6	4.50
Carbonaceous matter	973 ft 6 in	296.7	0.15
Mudstone, etc.	975 ft	297.2	0.46
Fine grit merging into conglomerate	995 ft	303.3	6.10
Coal	995 ft 2 in	303.3	0.05
Fireclay	995 ft 3 in	303.4	0.03
Mudstone with sandstone and fine grit	1020 ft	310.9	7.54
Coal	1020 ft 3 in	311.0	0.08
Mudstone, sandstone, and fine grit	1036 ft	315.8	4.80
Coal	1036 ft 6 in	315.9	0.15
Mudstone, sandstone, and fine grit	1050 ft	320.0	4.11
Coal	1050 ft 4 in	320.1	0.10
Sandstone	1054 ft	321.3	1.12

Driller's description	*Depth, Suggate (1950)*	*Depth (m)*	*Unit thickness (m)*
Grit	1060 ft	323.1	1.83
Sandstone	1064 ft	324.3	1.22
Grit	1070 ft	326.1	1.83
Mudstone, sandstone, and fine grit	1090 ft	332.2	6.10
Coal	1090 ft 2 in	332.3	0.05
Mudstone with thin sandstones and fine grits	1100 ft	335.3	3.00
Coal	1100 ft 10 in	335.5	0.25
black shale	1101 ft 4 in	335.7	0.15
Mudstone and fine grit	1107 ft	337.4	1.73
Coal	1107 ft 4 in	337.5	0.10
Coaly matter	1108 ft	337.7	0.20
Black shale	1108 ft 4 in	337.8	0.10
Mudstone	1108 ft 10 in	338.0	0.15
Coal	1109 ft 6 in	338.2	0.20
Mudstone	1114 ft	339.5	1.37
Coal	1114 ft 4 in	339.6	0.10
Mudstone, sandstone, and grit	1120 ft	341.4	1.73
Sandstone merging into grit	1130 ft	344.4	3.05
Mudstone	1140 ft	347.5	3.05
Grit and conglomerate	1145 ft	349.0	1.52
Mudstone and sandstone	1180 ft	359.7	10.67
Grit and mudstone	1184 ft	360.9	1.22
Coal	1184 ft 3 in	361.0	0.08
Grey sandstone	1193 ft	363.6	2.67
Coal	1193 ft 6 in	363.8	0.15
Sandstone and mudstone	1213 ft	369.7	5.94
Coal	1213 ft 3 in	369.8	0.08
Sandsrone and mudstone	1221 ft	372.2	2.36
Indurated fireclay	1229 ft	374.6	2.44
Semi-coarse grit	1250 ft	381.0	6.40
Carbonaceous matter (coal, fireclay, etc.)	1255 ft	382.5	1.52
Sandstone	1260 ft	384.0	1.52
Coal	1260 ft 4 in	384.1	0.10
Grit	1262 ft 6 in	384.8	0.66
Sandstone	1263 ft	385.0	0.15
Coal	1263 ft 3 in	385.0	0.08
Mudstone	1267 ft	386.2	1.14
Grit	1269 ft 2 in	386.8	0.66
Shale	1269 ft 6 in	386.9	0.10
Coal, fireclay, etc.	1271 ft 2 in	387.5	0.51
Mudstone?	1271 ft 9 in	387.6	0.18
Coal	1272 ft	387.7	0.08
Mudstone	1276 ft	388.9	1.22
Grit and mudstone mixed	1277 ft	389.2	0.30
Mudstone	1295 ft	394.7	5.49
Grit	1299 ft	395.9	1.22
Sandstone	1302 ft	396.8	0.91
Coal	1302 ft 4 in	397.0	0.10
Sandstone`	1304 ft	397.5	0.51
Mudstone	1306 ft	398.1	0.61
Coal	1306 ft 5 in	398.2	0.13
Coarse grit	1309 ft	399.0	0.79
Coal	1309 ft 2 in	399.0	0.05
Sandstone?	1309 ft 10 in	399.2	0.20
Coal	1310 ft	399.3	0.05

Driller's description	*Depth, Suggate (1950)*	*Depth (m)*	*Unit thickness (m)*
Mudstone	1317 ft	401.4	2.13
Sandstone	1325 ft	403.9	2.44
Grit	1326 ft	404.2	0.30
Sandstone	1327 ft	404.5	0.30
Stony coal	1327 ft 10 in	404.7	0.25
Mudstone	1332 ft	406.0	1.27
Stony coal	1332 ft 8 in	406.2	0.20
Mudstone	1336 ft	407.2	1.02
Coal	1337 ft	407.5	0.30
Sandstone	1340 ft	408.4	0.91
Grits and carbonaceous matter	1360 ft	414.5	6.10
Grits and carbonaceous matter with fireclay	1370 ft	417.6	3.05
Grits and carbonaceous matter with coal streaks and occasional thin bands of sandstone	1416 ft	431.6	14.02
Grits with large quartz pebbles and quartzite gradually merging into granite	1420 ft	432.8	1.22
Granite (increasing hardness with depth)	1440 ft	438.9	6.10

APPENDIX B: SAMPLE DATA

Table B.1: all samples used in this study, with locations, latitude and longitude (WGS 84), whether samples are conglomerate clasts or sedimentary (sed), outcrop lithofacies and lithofacies associations, thin section and geochemical analyses completed.

Sample	Unit	Location	Latitude (WGS 84 °S)	Longitude (WGS 84 °E)	Elevation (m)	Sample type	Field description	Calculated thickness from basement (m)	Lithofacies	Lithofacies association	Thin section Y/N	Thin section stain	Geochem laboratory	Petrofacies	Notes
BR399	Rakopi Formation	Pakawau Bush Rd	40.58566	172.66643		Clast	granite: light, equigranular		Gm	R	Y	None	Spectrachem		
BR404	Rakopi Formation	Pakawau Bush Rd	40.58566	172.66643		Sed	medium sandstone	109.4	Sm	R	Y	None			
BR408	Rakopi Formation	Pakawau Bush Rd	40.58646	172.67024		Sed	carbonaceous medium sandstone	66	Sm	R	Y	None			
BR409	Rakopi Formation	Pakawau Bush Rd	40.58636	172.67017		Sed	carbonaceous fine sandstone	66.1	Sm	R	Y	None			
BR412	Rakopi Formation	Pakawau Bush Rd	40.58557	172.66942		Sed	coarse sandstone	69.3	Sm	R	Y	None			
BR425	Rakopi Formation	Pakawau Bush Rd	40.58339	172.65678		Sed	medium sandstone	217.4	Sm	R	Y	None			
GH376	Farewell Formation	Green Hills Beach	40.50666	172.65492		Sed	medium sandstone	1275	St	FG	Y	None			
GH379	Farewell Formation	Green Hills Beach	40.50677	172.65497		Clast	dark igneous w/ white xtls		Gm	FG	Y	None	Spectrachem		
GH380	Farewell Formation	Green Hills Beach	40.50677	172.65497		Clast	Green crystalline clast, white phenocrysts		Gm	FG	N		Spectrachem		
GH381	Farewell Formation	Green Hills Beach	40.50677	172.65497		Clast	granite: light, equigranular		Gm	FG	N		Spectrachem		
GH382	Farewell Formation	Green Hills Beach	40.50838	172.65042		Clast	fine white igneous, black xtls		Gm	FG	Y	None	Spectrachem		
GH383	Farewell Formation	Green Hills Beach	40.50838	172.65042		Clast	basalt?		Gm	FG	Y	None	Spectrachem		
KR001	Rakopi Formation	Kaituna Route	40.63303	172.54628		Sed	siltstone	264.7	HI	R	N		Spectrachem	P2	
KR004	Rakopi Formation	Kaituna Route	40.62569	172.54549		Sed		209.6	Sw	R	Y	Plag/Kspar			
KR005	Rakopi Formation	Kaituna Route	40.62255	172.54660		Sed		248.3	Sw	R	Y	Plag/Kspar			
KR006	Rakopi Formation	Kaituna Route	40.62112	172.54668		Sed		269.6	St	R	Y	Plag/Kspar			
KR009	Rakopi Formation	Kaituna Route	40.61741	172.54915		Sed		305	St	R	Y	Plag/Kspar			
KR392	Bay Schist	Kaituna Route	40.65759	172.55209	320	BASEMENT	Schist				Y	None			
KR393	Bay Schist	Kaituna Route	40.65759	172.55209	320	BASEMENT	Schist				Y	None			
KR394	Bay Schist	Kaituna Route	40.65759	172.55209	320	BASEMENT	Schist				Y	None			
KR395	Bay Schist	Kaituna Route	40.65728	172.55205		BASEMENT	Schist				Y	None			
KR396	Separation Point Suite	Kaituna Route	40.63631	172.55757		BASEMENT	granite: dark, non-foliated, equigranular				Y	None	Spectrachem		
KR397	Separation Point Suite	Kaituna Route	40.63631	172.55757		BASEMENT	granite: light, no biotite, equigranular				Y	None	Spectrachem		
Mo014	Farewell Formation	Moki Point S	40.58466	172.56274		Sed	coarse sandstone	1010	St	FS	Y	Plag/Kspar			
Mo017	Farewell Formation?	Moki Point S				Clast	Vein quartz		Gm	FS	Y	None	Spectrachem, UC		
Mo021	North Cape Formation	Moki Point	40.58200	172.57254		Sed	coarse sandstone	982.4	St	A3	Y	Plag/K-spar			
Mo023	North Cape Formation	Moki Point	40.58123	172.57260		Sed	sandstone	990	Sl	A3	Y	Plag/K-spar			
Mo025	Farewell Formation	Moki Point N	40.57930	172.56987		Sed	sandstone	1020	Sm	FS	Y	Plag/K-spar			
Mo026	Farewell Formation	Moki Point N	40.57837	172.57002		Sed	sandstone	1020	St	FS	Y	Plag/K-spar			
Mo027	North Cape Formation	Moki Point	40.58139	172.57295		Clast	granite: red		Gm	A3	N		Spectrachem		
Mo028	North Cape Formation	Moki Point	40.58139	172.57295		Clast	grey metasedimentary		Gm	A3	N		Spectrachem		
Mo250	Farewell Formation	Moki Point S				Sed	very coarse sandstone	1010	Gm	FS	Y	Plag/K-spar			
MP029	North Cape Formation	Maori Point	40.58115	172.62813		Sed	medium sandstone	618	St	A2	Y	K-spar	Chemostrat	P3	

Sample	Unit	Location	Latitude (WGS 84 °S)	Longitude (WGS 84 °E)	Elevation (m)	Sample type	Field description	Calculated thickness from basement (m)	Lithofacies	Lithofacies association	Thin section Y/N	Thin section stain	Geochem laboratory	Petrofacies	Notes
MP031	North Cape Formation	Maori Point	40.58082	172.62744		Sed	sandstone	627.5	Sw	A2	Y	K-spar	Chemostrat	P3	
MP032	North Cape Formation	Maori Point	40.58088	172.62671		Sed	sandstone	638	St	A1	Y	K-spar	Chemostrat	P3	
MP035	North Cape Formation	Maori Point	40.57991	172.62515		Sed	medium to coarse sandstone	673	St	A1	Y	K-spar	Chemostrat	P3	
MP036	North Cape Formation	Maori Point	40.57964	172.62457		Sed	sandstone	679	St	A1	Y	K-spar			
MP037	North Cape Formation	Maori Point	40.58039	172.62572		Clast	grey metasedimentary		Gm	A1	Y	None	Spectrachem, UC		
MP038	North Cape Formation	Maori Point	40.58039	172.62572		Clast	granite: dark		Gm	A1	Y	None	Spectrachem, UC		
MP039	North Cape Formation	Maori Point	40.58039	172.62572		Clast	granite: light		Gm	A1	N		Spectrachem		
MP040.1	North Cape Formation	Maori Point	40.58039	172.62572		Clast	Green volcanic (?) clast		Gm	A1	Y	None	Spectrachem		
MP040.2	North Cape Formation	Maori Point	40.58039	172.62572		Clast	Green volcanic (?) clast		Gm	A1	Y	None	Spectrachem		
MP040.3	North Cape Formation	Maori Point	40.58039	172.62572		Clast	Green volcanic (?) clast		Gm	A1	Y	None	Spectrachem		
MP040.4	North Cape Formation	Maori Point	40.58039	172.62572		Clast	Green volcanic (?) clast		Gm	A1	Y	None	Spectrachem		
MP044	North Cape Formation	Maori Point	40.58039	172.62572		Sed	sandstone	656.5	St	A1	Y	Kspar	Chemostrat	P3	
MP335	North Cape Formation	Maori Point	40.57981	172.62508		Sed	sandstone	672.5	St	A1	Y	None			
MP336	North Cape Formation	Maori Point	40.58022	172.62521		Sed	sandstone	665	Sp	A1	Y	None			
MP338	North Cape Formation	Maori Point	40.58098	172.62718		Sed	sandstone	632	St	A2	Y	None			
MP339	North Cape Formation	Maori Point	40.58105	172.62782		Sed	sandstone	625.7	Sw	A2	Y	None			
MP342	North Cape Formation	Maori Point	40.48044	172.62569		Clast	granite: light, equigranular		Gm	A1	Y	None			
MP343	North Cape Formation	Maori Point	40.48044	172.62569		Clast	granite: light, equigranular		Gm	A1	N		Spectrachem		
MP352	North Cape Formation	Maori Point	40.48044	172.62569		Clast	Green crystalline clast, black phenocrysts		Gm	A1	Y	None			
MP354	North Cape Formation	Maori Point	40.48044	172.62569		Clast	Green crystalline clast?		Gm	A1	Y	None			
MP355	North Cape Formation	Maori Point	40.48044	172.62569		Clast	granite: light, equigranular		Gm	A1	Y	None			
MP356	North Cape Formation	Maori Point	40.48044	172.62569		Clast	granite: light, equigranular		Gm	A1	Y	None	Spectrachem		
MR045	North Cape Formation	Mangarakau River	40.63892	172.52156		Sed		530.9	S	A3	Y	Kspar			
MR048	North Cape Formation	Mangarakau River	40.63692	172.52058		Sed		473.6	St	A1	Y	Kspar			
MR050	North Cape Formation	Mangarakau River	40.63690	172.51756		Sed	carbonaceous siltstone to very fine sandstone	551.9	St	A1	N		Spectrachem	P3	
MR051	North Cape Formation	Mangarakau River	40.63378	172.51807		Sed		624.4	St	A1	Y	K-spar			
MR052	North Cape Formation	Mangarakau River	40.63080	172.51698		Sed		706.7	St	A3	Y	K-spar			
MS053	North Cape Formation	Mangarakau Swamp	40.62236	172.51351		Sed		922	Hl	A2	Y	K-spar			
MS055	North Cape Formation	Mangarakau Swamp	40.62243	172.51366		Sed	fine sandstone	915.2	St	A2	Y	K-spar			
MS056	North Cape Formation	Mangarakau Swamp	40.62424	172.51216		Sed	coarse sandstone	908	St	A1	Y	K-spar			
NR363	Farewell Formation	Nguroa Road	40.53416	172.63860		Sed	medium sandstone	1063.4	St	FG	Y	None			
NR364	Farewell Formation	Nguroa Road	40.53508	172.63934		Sed	medium sandstone	1084.4	St	FG	Y	None			
NR366	Farewell Formation	Nguroa Road	40.53508	172.63934		Clast	granite: light, equigranular		Gp	FG	N		Spectrachem		
NR367	Farewell Formation	Nguroa Road	40.53508	172.63934		Clast	granite: light, equigranular		Gp	FG	N				
NR368	Farewell Formation	Nguroa Road	40.53508	172.63934		Clast	granite: dark, non-foliated, porphyritic		Gp	FG	Y	None	Spectrachem		
NR369	Farewell Formation	Nguroa Road	40.53508	172.63934		Clast	granite: dark, non-foliated, porphyritic		Gp	FG	N				
NR370	Farewell Formation	Nguroa Road	40.53508	172.63934		Clast	Green crystalline clast		Gp	FG	Y	None	Spectrachem		

Sample	Unit	Location	Latitude (WGS 84 °S)	Longitude (WGS 84 °E)	Elevation (m)	Sample type	Field description	Calculated thickness from basement (m)	Lithofacies	Lithofacies association	Thin section Y/N	Thin section stain	Geochem laboratory	Petrofacies	Notes
NR372	Farewell Formation	Nguroa Road	40.53508	172.63934		Clast	Green crystalline clast, white phenocrysts		Gp	FG	Y	None			
OP057	North Cape Formation	Oyster Point	40.57153	172.59999		Sed	fine sandstone	970	HI	A2	Y	Plag/K-spar	Chemostrat	P3	
OP058	Farewell Formation	Oyster Point	40.57021	172.59891		Sed	sandstone	1001.5	Gm	FS	Y	Plag/K-spar	Chemostrat	P4	
OP059	North Cape Formation	Oyster Point	40.57036	172.59875		Sed	fine sandstone	1021.9	St	A3	N		Chemostrat	P3	
OP061	North Cape Formation	Oyster Point	40.57072	172.59903		Sed	sandstone	996	Sm	A3	Y	Plag/K-spar	Chemostrat	P3	
OP063	North Cape Formation	Oyster Point	40.57109	172.59926		Sed	siltstone	975.8	Sw	A2	N		Chemostrat	P3	
OP064	North Cape Formation	Oyster Point	40.57127	172.59962		Sed	very fine sandstone	953.4	Mc	A2	N		Chemostrat	P3	
OP065	Farewell Formation	Oyster Point	40.57005	172.59868		Sed	medium sandstone	1006	St	FS	Y	Plag/K-spar			
OP067	Farewell Formation	Oyster Point	40.56845	172.59706		Sed	siltstone	1240.3	HI	FS	N		Chemostrat	P4	
OP069	Farewell Formation	Oyster Point	40.56826	172.59499		Sed		1110	St	FS	Y	Plag/K-spar			
OP070	Farewell Formation	Oyster Point	40.56842	172.59563		Sed	carbonaceous siltstone	1106.3	Sm	FS	Y	Plag/K-spar	Chemostrat	P4	
OP071	Farewell Formation	Oyster Point	40.56664	172.59700	46	Clast	granite: dark		Gm	FG	N		Spectrachem, UC		
OP072	Farewell Formation	Oyster Point	40.56664	172.59700	46	Clast	Foliated granite		Gm	FG	Y	None	Spectrachem, UC		
OP073	Farewell Formation	Oyster Point	40.56664	172.59700	46	Clast	Schist/foliated metamorphics		Gm	FG	Y	None			
OP074	Farewell Formation	Oyster Point	40.56664	172.59700	46	Clast	Green crystalline clast		Gm	FG	Y	None			
OP075	Farewell Formation	Oyster Point	40.56664	172.59700	46	Clast	granite: light		Gm	FG	Y	None	Spectrachem, UC		
OP076	Farewell Formation	Oyster Point	40.56664	172.59700	46	Clast	grey metasedimentary		Gm	FG	N		Spectrachem, UC		2 duplicates submitted to geochem
OP326	North Cape Formation	Oyster Point	40.57111	172.59909		Sed	medium sandstone	985	Sw	A2	Y	K-spar			
OP327	North Cape Formation	Oyster Point	40.57107	172.59872		Sed	medium sandstone	992	St	A3	Y	K-spar			
OP328	North Cape Formation	Oyster Point	40.57100	172.59885		Sed	fine to medium sandstone	992	St	A3	Y	K-spar			
OP329	North Cape Formation	Oyster Point	40.57074	172.59900		Sed	medium sandstone	996	Sm	A3	Y	K-spar			
OP331	Farewell Formation	Oyster Point	40.57003	172.59854		Sed	fine to medium sandstone	1009	St	FS	Y	K-spar			
Pi079	Farewell Formation	Pillar Point	40.50451	172.71342	147	Sed	coarse sandstone, iron staining	1508.3	Si	FI	Y	Plag/K-spar	Chemostrat	P6	Outcrop is iron stained
Pi080	Farewell Formation	Pillar Point	40.50455	172.71336	143	Sed	medium sandstone	1504.3	Sp	FG	Y	Plag/K-spar	Chemostrat	P5	
Pi083	Farewell Formation	Pillar Point	40.50459	172.71326	142	Clast	Cream soft sediment		Gm	FG	N		Spectrachem		2 duplicates submitted to geochem
Pi085	Farewell Formation	Pillar Point	40.50459	172.71326	142	Clast	White soft sediment (weathered granite?)		Gm	FG	N		Spectrachem		
Pi088	Farewell Formation	Pillar Point	40.50467	172.71317	138	Sed	medium sandstone	1488.8	Sm	FG	Y	Plag/K-spar	Chemostrat	P5	
Pi089	Farewell Formation	Pillar Point	40.50471	172.71304	137	Sed	coarse sandstone	1482.5	Gm	FG	Y	Plag/K-spar			
Pi092	Farewell Formation	Pillar Point	40.50481	172.71266	136	Sed	coarse sandstone	1463.1	Sm	FG	Y	Plag/K-spar	Chemostrat	P5	Minor weathering
Pi095	Farewell Formation	Pillar Point	40.50512	172.71260	128	Sed	fine sandstone	1445.6	Sm	FG	Y	K-spar	Chemostrat	P5	
Pi097	Farewell Formation	Pillar Point	40.50534	172.71281	120	Sed	medium sandstone	1431.5	St	FG	Y	Plag/K-spar			
Pi099	Farewell Formation	Pillar Point	40.50569	172.71336	118	Sed	medium sandstone	1418.6	Sm	FG	Y	None	Chemostrat	P5	
Pi100	Farewell Formation	Pillar Point	40.50575	172.71347	119	Sed		1414.4	Sm	FG	Y	Plag/K-spar			
Pi104	Farewell Formation	Pillar Point	40.50637	172.71396		Sed	medium sandstone	1386.7	St	FG	N		Chemostrat	P4	
Pi106	Farewell Formation	Pillar Point	40.50651	172.71414	100	Sed	siltstone	1377.5	M	FG	N		Chemostrat, Spectrachem	P4	
Pi110	Farewell Formation	Pillar Point	40.50717	172.71358	89	Sed	medium to coarse sandstone	1313.7	Sm	FG	Y	K-spar	Chemostrat	P4	
Pi115	Farewell Formation	Pillar Point	40.50721	172.71327	86	Sed	very coase sandstone	1304.4	Sh	FG	Y	K-spar	Chemostrat	P4	

Sample	Unit	Location	Latitude (WGS 84 °S)	Longitude (WGS 84 °E)	Elevation (m)	Sample type	Field description	Calculated thickness from basement (m)	Lithofacies	Lithofacies association	Thin section Y/N	Thin section stain	Geochem laboratory	Petrofacies	Notes
Pi120	Farewell Formation	Pillar Point	40.50731	172.71268	77	Sed	carbonaceous siltstone	1289	Sw	FG	N		Chemostrat	P4	
Pi124.1	Farewell Formation	Pillar Point	40.50760	172.71212	71	Clast	Cream metasediment		Gm	FG	N		Spectrachem		
Pi124.2	Farewell Formation	Pillar Point	40.50760	172.71212	71	Clast	Cream metasediment		Gm	FG	N		Spectrachem		
Pi125	Farewell Formation	Pillar Point	40.50750	172.71233	71	Sed		1261	St	FG	Y	K-spar	Chemostrat	P4	
Pi127	Farewell Formation	Pillar Point	40.50778	172.71213	68	Sed	medium to coarse sandstone	1248.2	Sm	FG	Y	K-spar	Chemostrat	P4	
Pi128	Farewell Formation	Pillar Point	40.50806	172.71181	65	Sed	medium sandstone	1225.9	St	FG	Y	K-spar	Chemostrat	P4	
Pi130	Farewell Formation	Pillar Point	40.50835	172.71167	64	Sed	medium sandstone	1187.6	Sw	FG	Y	K-spar	Chemostrat	P4	
Pi134	Farewell Formation	Pillar Point	40.50952	172.70952	78	Sed	medium sandstone	1150.5	Sm	FG	Y	K-spar	Chemostrat	P4	
Pi136	Farewell Formation	Pillar Point	40.50962	172.70930	77	Sed		1141.1	Sp	FG	Y	K-spar			
Pi138	Farewell Formation	Pillar Point	40.50984	172.70914	70	Sed	fine to medium sandstone	1136.1	St	FG	Y	K-spar	Chemostrat	P4	
Pi142	Farewell Formation	Pillar Point	40.51028	172.70879	69	Sed	medium sandstone	1112.1	Sm	FG	Y	K-spar	Chemostrat	P4	
Pi144	Farewell Formation	Pillar Point	40.51048	172.70868	67	Sed		1102.1	Sm	FG	Y	K-spar			
Pi145	Farewell Formation	Pillar Point	40.51056	172.70876	67	Sed	carbonaceous siltstone	1100	Ml	FG	N		Chemostrat	P4	
Pi306	Farewell Formation	Pillar Point	40.50459	172.71326		Clast	weathered granite: cream		Gm	FG	Y	None	Spectrachem		
Pi307.1	Farewell Formation	Pillar Point	40.50471	172.71303		Clast	Green crystalline clast		Gm	FG	Y	None	Spectrachem		
Pi307.2	Farewell Formation	Pillar Point	40.50471	172.71303		Clast	Green crystalline clast		Gm	FG	Y	None	Spectrachem		
Pi307.3	Farewell Formation	Pillar Point	40.50471	172.71303		Clast	Green crystalline clast		Gm	FG	Y	None	Spectrachem		
Pi311	Farewell Formation	Pillar Point	40.50497	172.71251		Clast	weathered granite: white		Gm	FG	Y	None			
Pi312.1	Farewell Formation	Pillar Point	40.50701	172.71416		Clast	weathered granite: white		Gm	FG	Y	None	Spectrachem		
Pi314	Farewell Formation	Pillar Point	40.50701	172.71416		Clast	weathered granite: porphyritic		Gm	FG	Y	None			
PM388	North Cape?	Puponga Mine track	40.51951	172.71123		Sed	fine to medium sandstone	950	Sm	A3	Y	None			
PP146	North Cape Formation	Pecks Point S	40.57292	172.63373		Sed	sandstone	717	St	A1	Y	Plag/K-spar	Chemostrat	P3	
PP147.1	North Cape Formation	Pecks Point S	40.57292	172.63373		Clast	granite: light		Gm	A1	N		Spectrachem		
PP147.2	North Cape Formation	Pecks Point S	40.57292	172.63373		Clast	granite: light		Gm	A1	Y	None	Spectrachem		
PP147.3	North Cape Formation	Pecks Point S	40.57292	172.63373		Clast	granite: light		Gm	A1	N		Spectrachem		
PP150.1	North Cape Formation	Pecks Point S	40.57292	172.63373		Clast	Green volcanic (?) clast		Gm	A1	N		Spectrachem		
PP150.2	North Cape Formation	Pecks Point S	40.57292	172.63373		Clast	Green volcanic (?) clast		Gm	A1	N		Spectrachem		
PP151.1	North Cape Formation	Pecks Point S	40.57292	172.63373		Clast	granite: dark		Gm	A1	N		Spectrachem		
PP151.2	North Cape Formation	Pecks Point S	40.57292	172.63373		Clast	granite: dark		Gm	A1	N		Spectrachem		
PP151.3	North Cape Formation	Pecks Point S	40.57292	172.63373		Clast	granite: dark		Gm	A1	N		Spectrachem		
PP153	North Cape Formation	Pecks Point N	40.56885	172.62675		Sed	fine to medium sandstone	860.3	Sh	A1	Y	Plag/K-spar	Chemostrat	P3	
PP156.1	North Cape Formation	Pecks Point N	40.56900	172.62732		Clast	granite: dark, foliated		Gm	A1	N		Spectrachem, UC		
PP156.2	North Cape Formation	Pecks Point N	40.56900	172.62732		Clast	granite: dark		Gm	A1	N		Spectrachem		
PP157.2	North Cape Formation	Pecks Point N	40.56900	172.62732		Clast	granite: light		Gm	A1	N		Spectrachem, UC		
PP158	North Cape Formation	Pecks Point N	40.56900	172.62732		Clast	Green volcanic (?) clast		Gm	A1	N		Spectrachem, UC		
PP164	North Cape Formation	Pecks Point S	40.57150	172.63129		Sed	medium to coarse sandstone	758.7	St	A1	Y	Plag/K-spar			
PP165	North Cape Formation	Pecks Point S	40.57124	172.63069		Clast	grey metasedimentary		Gm	A1	N		Spectrachem, UC		
PP166.1	North Cape Formation	Pecks Point S	40.57124	172.63069		Clast	granite: dark		Gm	A1	Y	Plag/K-spar	Spectrachem, UC		
PP166.2	North Cape Formation	Pecks Point S	40.57124	172.63069		Clast	granite: dark		Gm	A1	Y	Plag/K-spar	Spectrachem, UC		

Sample	Unit	Location	Latitude (WGS 84 °S)	Longitude (WGS 84 °E)	Elevation (m)	Sample type	Field description	Calculated thickness from basement (m)	Lithofacies	Lithofacies association	Thin section Y/N	Thin section stain	Geochem laboratory	Petrofacies	Notes
PP167	North Cape Formation	Pecks Point S	40.57124	172.63069		Clast	granite: light		Gm	A1	Y	Plag/K-spar	Spectrachem, UC		
PP168.2	North Cape Formation	Pecks Point S	40.57124	172.63069		Clast	Green volcanic (?) clast		Gm	A1	N		Spectrachem		
PP170	North Cape Formation	Pecks Point S	40.57124	172.63069		Clast	Green-grey soft silt/sandstone		Gm	A1	Y	None			
PP173	North Cape Formation	Pecks Point S	40.57124	172.63069		Clast	Red granite		Gm	A1	Y	None	Spectrachem, UC		
PP174	North Cape Formation	Pecks Point S	40.57165	172.63258		Sed	fine to medium sandstone	739.9	St	A1	Y	Plag/K-spar			
PP175	North Cape Formation	Pecks Point				Sed	medium sandstone	850	St	A1	Y	Plag/K-spar			
PP176	North Cape Formation	Pecks Point N	40.56875	172.62827		Sed	siltstone and fine sandstone	839.4	St	A1	Y	Plag/K-spar	Chemostrat	P3	Unweathered
PP177	North Cape Formation	Pecks Point N	40.56877	172.62840		Sed	fine sandstone	839.5	St	A1	Y	Plag/K-spar			
PP178	North Cape Formation	Pecks Point S	40.57137	172.63086		Sed	siltstone	884	Ml	A2	N		Chemostrat	P3	
PP180	North Cape Formation	Pecks Point S	40.57151	172.63144		Sed	medium sandstone	756.7	St	A1	Y	Plag/K-spar			Poor thin section
PP182	North Cape Formation	Pecks Point S	40.57240	171.63351		Clast	grey metasedimentary		Gm	A1	N		Spectrachem, UC		
PP183.1	North Cape Formation	Pecks Point S	40.57240	171.63351		Clast	granite: light		Gm	A1	N		Spectrachem		
PP183.2	North Cape Formation	Pecks Point S	40.57240	171.63351		Clast	granite: light		Gm	A1	N		Spectrachem		
PP184.1	North Cape Formation	Pecks Point S	40.57240	171.63351		Clast	granite: dark		Gm	A1	Y	None	Spectrachem, UC		
PP187	North Cape Formation	Pecks Point S	40.57240	171.63351		Clast	Green volcanic (?) clast		Gm	A1	Y	None	Spectrachem, UC		
PP188	North Cape Formation	Pecks Point S	40.57240	171.63351		Clast	Red granite		Gm	A1	N		Spectrachem		
PP190	North Cape Formation	Pecks Point S	40.57240	171.63351		Sed	medium sandstone	723.8	St	A1	Y	Plag/K-spar	Chemostrat	P3	
PP288	North Cape Formation	Pecks Point S	40.57089	172.63063		Clast	granite: dark, non-foliated, equigranular		Gm	A1	Y	None			
PP289	North Cape Formation	Pecks Point S	40.57089	172.63063		Clast	granite: light, no biotite, equigranular		Gm	A1	Y	None	Spectrachem		
PP295	North Cape Formation	Pecks Point N	40.56880	172.62836		Sed	medium sandstone	841.2	St	A1	Y	K-spar			
PP296	North Cape Formation	Pecks Point N	40.56879	172.62799		Sed	medium sandstone	845.5	Sp	A1	Y	K-spar			
PP299	North Cape Formation	Pecks Point N	40.56897	172.62694		Sed	very coarse sandstone	857.5	St	A1	Y	K-spar			
PP301	North Cape Formation	Pecks Point N	40.56865	172.62640		Sed	medium sandstone	867	St	A1	Y	K-spar			
PP304	North Cape Formation	Pecks Point N	40.56866	172.62637		Sed	medium sandstone	869.3	St	A1	Y	K-spar			
PP426	North Cape Formation	Pecks Point S	40.57295	172.63393		Sed	medium sandstone	716.8	St	A1	Y	None			
PP427	North Cape Formation	Pecks Point S	40.57251	172.63367		Sed	medium sandstone	721.9	St	A1	Y	None			
PP428	North Cape Formation	Pecks Point S	40.57181	172.63306		Sed	medium sandstone	730.9	St	A1	Y	None			
PP429	North Cape Formation	Pecks Point S	40.57143	172.63228		Sed	medium to coarse sandstone	742.8	St	A1	Y	None			
PP430	North Cape Formation	Pecks Point S	40.57295	172.63393		Clast	(basalt?)		Gm	A1	Y	None			
PR192	Rakopi Formation	Paturau River	40.68299	172.48506		Sed	siltstone	10.5	Mc	O	N		Chemostrat	P1	
PR193	Rakopi Formation	Paturau River	40.68299	172.48506		Sed	very fine sandstone	11	Mc	O	N		Chemostrat	P1	
PR194	Rakopi Formation	Paturau River	40.67920	172.48384		Sed	very fine sandstone	101	Mc	R	N		Chemostrat	P1	
PR195	Rakopi Formation	Paturau River	40.67920	172.48384		Sed	very fine sandstone	103	Mc	R	N		Chemostrat, Spectrachem	P1	
PR196	Rakopi Formation	Paturau River	40.67920	172.48384		Sed	siltstone	104	Sc	R	N		Chemostrat	P1	
PR199	Rakopi Formation	Paturau River	40.67077	172.47702		Sed	medium sandstone	317	Sm	R	Y	Plag/K-spar	Chemostrat	P2	Thin section labelled SS099
PR200	Rakopi: Otimataura Conglomerate	Paturau River	40.68246	172.48485		Sed		15.5	Sm	O	Y	Plag/K-spar			
PR201	Rakopi Formation	Paturau River	40.67797	172.48259		Sed	siltstone	145		R	N		Chemostrat	P1	
PR252	Rakopi Formation	Paturau River	40.67332	172.47910		Sed	carbonaceous siltstone	246	Z	R	N		Chemostrat	P2	

Sample	Unit	Location	Latitude (WGS 84 °S)	Longitude (WGS 84 °E)	Elevation (m)	Sample type	Field description	Calculated thickness from basement (m)	Lithofacies	Lithofacies association	Thin section Y/N	Thin section stain	Geochem laboratory	Petrofacies	Notes
Pu203	Farewell Formation	Puponga (river)	40.52448	172.73679	-18	Sed	medium sandstone	1435.9	St	FG	Y	K-spar	Chemostrat	P5	
Pu205.1	Farewell Formation	Puponga (river)	40.52461	172.73677	1	Sed	organic rich mudstone	1440.5		FG	N		Chemostrat, Spectrachem	P5	
Pu207	Farewell Formation	Puponga (river)	40.52477	172.73705	-13	Sed	medium to coarse sandstone	1454.3	Sm	FG	Y	Plag/K-spar	Chemostrat	P5	
Pu210	Farewell Formation	Puponga (river)	40.52477	172.73705	-13	Clast	Cream soft sediment		Gm	FG	N		Spectrachem, UC		
Pu212	Farewell Formation	Puponga (river)	40.52477	172.73705	-13	Clast	Grey soft sandstone		Gm	FG	N		Spectrachem, UC		
Pu213	Farewell Formation	Puponga (river)	40.52477	172.73705	-13	Clast	Green crystalline clast		Gm	FG	Y	None	Spectrachem, UC		
Pu214	Farewell Formation	Puponga (river)	40.52477	172.73705	-13	Clast	grey metasedimentary		Gm	FG	Y	None	Spectrachem, UC		
Pu215	Farewell Formation	Puponga (river)	40.52495	172.73706	-12	Sed		1458.7	Sh	FG	Y	K-spar	Chemostrat	P5	
Pu216	Farewell Formation	Puponga (river)	40.52503	172.73721	-5	Sed		1464.6	St	FG	Y	Plag/K-spar			
Pu218	Farewell Formation	Puponga (river)	40.52517	172.73747	-2	Sed		1475.7	St	FG	Y	K-spar	Chemostrat	P5	
Pu219	Farewell Formation	Puponga (river)	40.52515	172.73763	-5	Sed		1480	Gp	FG	Y	Plag/K-spar			
Pu221	Farewell Formation	Puponga (river)	40.52514	172.73781	-5	Sed		1490.4	Si	FI	Y	K-spar	Chemostrat	P6	Outcrop is iron stained
Pu223	Farewell Formation	Puponga (river)	40.52515	172.73747		Clast	granite: light		Gm	FG	N		Spectrachem, UC		
Pu225.1	Farewell Formation	Puponga (from salt marsh)	40.52595	172.73721	3	Clast	White weathered granite		Gm	FG	Y	None	Spectrachem, UC		2 duplicates submitted to geochem
Pu226	Farewell Formation	Puponga (from salt marsh)	40.52595	172.73721	3	Clast	Cream metasediment		Gm	FG	Y	Plag/K-spar			
Pu227	Farewell Formation	Puponga (from salt marsh)	40.52595	172.73721	3	Clast	Cream soft sediment		Gm	FG	Y	None			
Pu228	Farewell Formation	Puponga (from salt marsh)	40.52595	172.73721	3	Clast	granite: light		Gm	FG	Y	None	Spectrachem, UC		
TH231	Farewell Formation	Te Hapu Rd, Westhaven	40.60637	172.51938		Sed	siltstone	1289.5		FM	N		Spectrachem	P4	
TH232	Farewell Formation	Te Hapu Rd, Westhaven	40.60671	172.51910		Sed					Y	None			
TH235	Farewell Formation	Te Hapu Rd	40.61396	172.51363		Sed	medium to coarse sandstone	1130.3	St	FM	Y	Plag/K-spar			
TH236	Farewell Formation	Te Hapu Rd	40.61239	172.51353		Sed	coarse sandstone	1152.5	St	FM	Y	Plag/K-spar			
TH240	Farewell Formation	Te Hapu Rd	40.61270	172.51360		Sed	medium sandstone	1142.5	St	FM	Y	Plag/K-spar			
TH241	Farewell Formation	Te Hapu Rd	40.61105	172.51498		Sed	medium sandstone	1213.3	St	FM	Y	Plag/K-spar			
TH415	Farewell Formation	Te Hapu Rd	40.61504	172.51328	85	Sed	fine sandstone	1128.6	Sw	FM	Y	None			
TH417	Farewell Formation	Te Hapu Rd	40.61320	172.51181		Sed	medium sandstone	1012.1	St	FM	Y	None			
TH419	Farewell Formation	Te Hapu Rd	40.61843	172.51054	19	Sed	medium sandstone	1001.5	Sw	FM	Y	None			
TH421	North Cape?	Te Hapu Rd	40.61843	172.51054	19	Sed	medium sandstone	999.7	Sm	A3	Y	None			
TH422	North Cape?	Te Hapu Rd	40.61893	172.50946	12	Sed	fine sandstone	1021.8	St	FM	Y	None			
Wh242	Farewell Formation	Whararikimid	40.50445	172.67331	1	Sed		1180	St	FG	Y	Plag/K-spar			
Wh244	Farewell Formation	Whararikis	40.50626	172.66519	1	Sed		1222.2	Sm	FS	Y	Plag/K-spar			
Wh245	Farewell Formation	Whararikis	40.50579	172.66606	11	Sed		1228.4	Sp	FG	Y	Plag/K-spar			
Wh255	Farewell Formation	Whararikis	40.50655	172.66498		Clast	Green crystalline clast, fine grained		Gm	FG	Y	None			
Wh256	Farewell Formation	Whararikis	40.50655	172.66498		Clast	granite: dark, non-foliated, equigranular		Gm	FG	Y	None	Spectrachem		
Wh260	Farewell Formation	Whararikis	40.50655	172.66498		Clast	granite: dark, non-foliated, porphyritic		Gm	FG	Y	None	Spectrachem		
Wh266	Farewell Formation	Whararikis	40.50655	172.66498		Clast	granite: dark, foliated, porphyritic		Gm	FG	Y	None	Spectrachem		
Wh267	Farewell Formation	Whararikis	40.50655	172.66498		Clast	granite: dark, foliated, porphyritic		Gm	FG	N		Spectrachem		

Sample	Unit	Location	Latitude (WGS 84 °S)	Longitude (WGS 84 °E)	Elevation (m)	Sample type	Field description	Calculated thickness from basement (m)	Lithofacies	Lithofacies association	Thin section Y/N	Thin section stain	Geochem laboratory	Petrofacies	Notes
Wh268	Farewell Formation	Whararikí S	40.50657	172.66472		Sed	coarse sandstone	1217.3	Gp	FG	Y	K-spar			
Wh269	Farewell Formation	Whararikí S	40.50644	172.66579		Sed	medium sandstone	1212.8	Sp	FG	Y	K-spar			
Wh271	Farewell Formation	Whararikí S	40.50655	172.66498		Clast	Green crystalline clast, white phenocrysts		Gm	FG	Y	None	Spectrachem		
Wh272	Farewell Formation	Whararikí S	40.50655	172.66498		Clast	Green crystalline clast, white phenocrysts		Gm	FG	Y	None			
Wh273	Farewell Formation	Whararikí S	40.50655	172.66498		Clast	granite: red, equigranular		Gm	FG	Y	None	Spectrachem		
Wh274	Farewell Formation	Whararikí S	40.50644	172.66579		Clast	Green crystalline clast, fine grained		Gm	FG	N				
Wh275	Farewell Formation	Whararikí S	40.50644	172.66579		Clast	Green crystalline clast, black phenocrysts		Gm	FG	Y	None	Spectrachem		
Wh276.1	Farewell Formation	Whararikí S	40.50644	172.66579		Clast	Green crystalline clast, white phenocrysts		Gm	FG	Y	None	Spectrachem		
Wh276.2	Farewell Formation	Whararikí S	40.50644	172.66579		Clast	Green crystalline clast, white phenocrysts		Gm	FG	Y	None	Spectrachem		
Wh276.3	Farewell Formation	Whararikí S	40.50644	172.66579		Clast	Green crystalline clast, white phenocrysts		Gm	FG	Y	None			
Wh277.1	Farewell Formation	Whararikí S	40.50644	172.66579		Clast	Red volcanic		Gm	FG	Y	None	Spectrachem		
Wh278.1	Farewell Formation	Whararikí S	40.50644	172.66579		Clast	red, fine grained		Gm	FG	Y	None			
Wh283	Farewell Formation	Whararikí S	40.50644	172.66579		Clast	granite: dark, foliated, porphyritic		Gm	FG	Y	None	Spectrachem		
Wh285	Farewell Formation	Whararikí S	40.50644	172.66579		Clast	Quartzite		Gm	FG	Y	None			

APPENDIX C: CLAST COUNT DATA

Table C.1 Clast count field data

Location description	Formation	Latitude (WGS 84 °S)	Longitude (WGS 84 °E)	Texture	Notes	Sample number(s)	Grey metasediment	Cream metasediment	Vein quartz/quartzite	Fresh, foliated granitoid	Fresh, non-foliated granitoid	WEATHERED granitoid	Green volcanics	Other volcanics	Soft grey siltstones	Soft grey sandstones	Cream siltstone	Schist/foliated metamorphics	Chert	Matrix	SUM clasts
Maori Point	North Cape	40.58039	172.62572	Poor to moderate sorting	Includes both pebble horizons.		115	0	17	0	47	0	15	0	0	0	0	7	0	57	**201**
Maori Point	North Cape	40.48044	172.62569	ms matrix, mp clasts, subrounded, rod shaped	RECOUNT		150	3	31	1	26	0	4	0	0	0	0	0	0	62	**215**
Maori Point	North Cape	40.48044	172.62569	cs matrix, cp clasts, moderate sorting, subround-round, rod shaped	RECOUNT	MP037-MP043, MP342-MP362	149	1	22	1	28	0	5	0	6	4	0	0	0	40	**216**
Pecks Point S	North Cape	40.57292	172.63373			PP147.1-PP151.1	52	0	4	0	19	0	11	0	0	0	0	0	0	20	**86**
Pecks Point S	North Cape	40.57292	172.63383		RECOUNT		132	0	26	0	39	0	13	0	10	0	0	4	0	18	**224**
Pecks Point S	North Cape	40.57292	172.63383	ms matrix, cp clasts, subangular - subround, rod shaped	RECOUNT		142	0	37	0	20	0	5	1	5	1	0	0	0	35	**211**
Pecks Point S	North Cape	40.5724	172.63351				118	0	22	0	52	0	13	0	4	0	0	5	0	57	**214**
Pecks Point S	North Cape	40.57124	172.63069	vcp clasts	Surface weathered, hard to see	PP165-PP173	112	0	26	0	38	1	9	0	10	0	0	5	0	55	**201**
Pecks Point S	North Cape	40.57124	172.63069	ms matrix, cp clasts, subrounded, rod shaped	RECOUNT		144	0	31	1	24	0	0	0	2	0	0	1	0	32	**203**
Pecks Point N	North Cape	40.569	172.62732	cp clasts		PP154-PP161	110	0	23	0	35	4	19	0	11	0	0	5	0	87	**207**
Nguroa Road	North Cape	40.53508	172.63934	vcs matrix, vcp clasts, moderate sorting, subround-round, rod shaped		NR365-NR375	139	2	11	0	37	0	8	0	0	0	0	0	0	64	**197**
Moki Point	North Cape	40.58139	172.57295	granule - fp clasts, moderate sorting	Channel. Granule-fine pebble, unimodal, moderately sorted	Mo027-Mo028	135	2	37	0	20	1	6	0	0	0	0	6	0	60	**207**
Moki Point S	Farewell				Farewell Formation, from JUST above contact	Mo251, Mo015-Mo019	129	0	28	0	14	0	7	0	0	0	0	3	3	99	**184**
Oyster Point	Farewell	40.56664	172.59700		46m elevation. On track down to beach	OP071-OP077	139	0	5	2	6	0	0	0	0	0	0	1	0	99	**153**
Whararíki S	Farewell	40.50584	172.66638	cs matrix, cp clasts, moderate to well sorting, subround-round, rod shaped	Taken on bedding surface. Clasts well-mod sorted.	Wh254-Wh267, Wh270-Wh285	173	2	19	0	0	10	3	0	3	10	4	0	0	28	**224**
Whararíki mid	Farewell	40.50428	172.67331				155	6	14	1	0	4	3	0	8	5	3	4	0	20	**203**
Whararíki N	Farewell	40.50094	172.68008				147	3	22	2	1	4	0	0	3	3	15	1	0	66	**201**
Green Hills S	Farewell	40.50840	172.65013	vcp clasts, subround-round, rod shaped		GH384-GH386	137	5	25	0	20	2	17	0	3	0	2	0	1	42	**212**

Location description	*Formation*	*Latitude (WGS 84 °S)*	*Longitude (WGS 84 °E)*	*Texture*	*Notes*	*Sample number(s)*	*Grey metasediment*	*Cream metasediment*	*Vein quartz/quartzite*	*Fresh, foliated granitoid*	*Fresh, non-foliated granitoid*	*WEATHERED granitoid*	*Green volcanics*	*Other volcanics*	*Soft grey siltstones*	*Soft grey sandstones*	*Cream siltstone*	*Schist/foliated metamorphics*	*Chert*	*Matrix*	*SUM clasts*
Green Hills N	Farewell	40.50677	172.65497	cs matrix, vcp-cob clasts, moderate sorting, subround-round, rod shaped		GH377-GH383	136	2	10	0	10	19	8	4	0	10	8	1	0	69	**208**
Pillar Point	Farewell	40.50760	172.71212		lower middle on west side of conglomerate tracked across road	Pi124.1-Pi124.2	147	5	15	0	0	16	1	0	11	13	10	2	0	134	**220**
Pillar Point	Farewell	40.50717	172.71373		in small cutting	Pi112-Pi114	187	1	15	0	0	2	2	0	4	0	2	0	0	40	**213**
Pillar Point	Farewell	40.50459	172.71326		near top	Pi081-Pi086	177	0	7	0	0	3	0	0	13	0	8	0	0	37	**208**
Puponga	Farewell	40.52477	172.73705	cs matrix, vcp clasts, round, rod shaped	Clasts aligned.	Pu208-Pu214	157	0	11	0	0	17	1	0	5	14	8	0	0	76	**213**
Puponga	Farewell	40.52515	172.73781			Pu222-Pu228	146	1	14	0	0	6	1	0	5	4	23	2	0	75	**202**

APPENDIX D: CLAST PETROLOGY

Table D.1: Petrograaphic composition of conglomerate clast samples. Composition in percentage of thin section. Values are estimated, except for point-counted samples in Table D.2.

Sample	*Field description*	*Polished?*	*Staining*	*Rock textures*	*Degree of alteration*	*Petrographic name*	*quartz*	*alkali feldspar*	*plagioclase*	*muscovite*	*biotite*	*chlorite*	*amphibole*	*clinopyroxene*	*opaques*	*apatite*	*titanite*	*tourmaline*	*other heavy*	*glass shards*	*vesicle*	*groundmass*	*lithics*	*SUM*
GH382	grey metasedimentary	N	Kspar	Well sorted fine-grained subangular sand. All feldspars altered to grey clay (can't differentiate k-spar and plag).		fine sandstone	40	55			5													100
Mo017	vein quartz	N	Kspar	Interlocking, sutured qz with strongly undulose extinction. Medium grained.		quartzite	95			<1													5	100
MP037	grey metasedimentary	N	Kspar	Equigranular fine sand quartz with minor micas. Polygonal/**mosaic** quartz, straight extinction		quartzite	90	2		5	3						<1	<1						100
MP352	green metasedimentary	N	Kspar	Volcanic? Quartz siltstone with few fine sand grains of rounded (embayed?) plag, kspar, qz. Matrix has clusters of brown clay/opaques. Opaques are square.		siltstone																		
NR370	green metasedimentary	N	Kspar	Quartz siltstone with few fine sand grains of plag, kspar, qz. Matrix has clusters of brown clay/opaques.		siltstone																		
Pu214	grey metasedimentary	N	Kspar	fine sand grains in silt matrix. Sutured quartz boundaries, strongly undulose extinction. Foliated. Matrix supported		fine sandstone	90	10	0	<1														100
Pu226	cream metasedimentary	N	Plag	Very fine sand grains with sutured grain boundaries. Undulose qz extinction		very fine sandstone	79	20		1														100
Pu228	quartzite	N	Kspar	sutured strongly undulose quartz fs grains in silt matrix. Grain supported. No titanite, apatite, tourmaline		very fine sandstone	75	15	7					3				<1						100
Wh277.1	red metasedimentary	N	Kspar	Subangular strongly undulose quartz grains, well sorted. Stain picks up clay along grain boundaries, also opaques.		fine sandstone	97	<1	3															100
Wh285	quartzite	N	Kspar	Qz grains with strongly undulose extinction. Sutured grain boundaries. Loosely foliated (qz slightly tabular)		fine sandstone	85	15	0	<1	<1													100
GH379	Black volcanic	N	N	Plag totally replaced by fine grey mineral. Quartz embayed	high	Highly altered volcanic	10		20													70		100
MP040.1	Green volcanic	Y	N	Porphyritic. Tabular plag phenocrysts saussuritised, sericitised and albitised. No original twinning. Chl replacing amphibole phenocrysts. Vesicle rimmed by quartz. Groundmass V.fine grained sericite, quartz, zoisite chlorite	moderate	Moderately altered porphyritic andesite/basalt	0		20			1									5	74		100

Sample	Field description	Polished?	Staining	Rock textures	Degree of alteration	Petrographic name	quartz	alkali feldspar	plagioclase	muscovite	biotite	chlorite	amphibole	clinopyroxene	opaques	apatite	titanite	tourmaline	other heavy	glass shards	vesicle	groundmass	lithics	SUM
MP040.2	Green volcanic	N	N	Porphyritic, weakly flow banded. Almost entirely replaced by v. fine grained silica/albite/sericite. Amps shown by chlorite, opaques. Embayed quartz	very high	Very highly altered volcanic																		
MP040.3	Green volcanic	Y	N	Silicified tuff: equgranular, very coarse sand. Tuff - silicified glass shards. Embayed quartz. Seritised plag. Chloritsed amp.	moderate	Silicified alkali feldspar tuff	10	10					1							5		74		100
MP040.4	Green volcanic	Y	N	Porphyritic. Completely sericitised plag phenocrysts. Chloritised amphible. Clinopyroxene phenocrysts rims replaced by chlorite. Groundmass v.fine grained quartz, zoisite, sericite	moderate	Moderately altered porphyritic andesite/basalt			15				10	5								70		100
MP354	Green volcanic	N	N	Porphyritic, weakly flow banded. Plag phenocrysts embayed, fractured, albitised and sericitised. Chloritised amphibole. Groundmass has microlites and very fine grained sericite, albite	moderate	Moderately altered porphyritic andesite/basalt			30				5									65		100
MP355	Green volcanic	N	N	Equigranular medium grained. Alkali feldspar altered, difficult to tell from plag	low	Silicified rhyolite	60	25		1	14													100
NR372	Green volcanic	N	N	Porphyritic. Alkali feldspar altered with remnant perthite. Plag seritised, but have poly twinning. Glassy groundmass replaced by chlorite in some places, otherwise is fine grained albite, sericite, quartz, biotite.	moderate	Moderately altered porphyritic andesite/basalt		5	30		3		2									60		100
OP074	Green volcanic	Y	N	Porphyritic, hypabyssal. Embayed quartz. Groundmass is medium to fine grained plag, bio, chl, opaques, qz	very low	Porphyritic andesite/basalt	1		25				5									69		100
Pi306	Green volcanic	N	N	Porphyritic. Embayed quartz, completely albitised plag, chloritized amphibole. Groundmass is medium quartz xtls in fine grained albite, chlorite, zoisite	high	Highly altered volcanic	15	0	10				10									65		100
Pi307.1	Green volcanic	N	N	Silicified and chloritised groundmass, only hints of primary porphyritic texture remain	very high	Very highly altered volcanic																		0
Pi307.2	Green volcanic	N	N	Porphyritic. Completely saussuritized plag, chloritised amphibole. Groundmass very fine grained quartz, sericite, zoisite chlorite	high	Highly altered porphyritic andesite/basalt			15				15									70		100
Pi307.3	Green volcanic	N	N	Equigranular coarse grained?. Or angular plag phenos? Highly silicified - see chert in DRM124. Qz and chlorite in voids.	very high	Very highly altered volcanic																		0
PP430	Black volcanic	N	N	Plag completely sericitised, whole thing is very fine grained sericite, biotite, silica, albite. Voids filled w/ qz.	very high	Very highly altered volcanic																		0
Pu213	Red volcanic	N	N	Totally replaced by fine grained sericite, zoisite, albite, silica. Some tabular forms could be plag phenos.	very high	Very highly altered volcanic																		0

Sample	Field description	Polished?	Staining	Rock textures	Degree of alteration	Petrographic name	quartz	alkali feldspar	plagioclase	muscovite	biotite	chlorite	amphibole	clinopyroxene	opaques	apatite	titanite	tourmaline	other heavy	glass shards	vesicle	groundmass	lithics	SUM
Pu227.1	Green volcanic	N	N	Very fine grained albite, sericite, zoisite, silica. Angular forms poss plag phenos.	very high	Very highly altered volcanic																		0
Wh255	Green volcanic	N	N	Porphyritic, weakly flow banded. Tabular plagioclase sericitised and albitised. Chloritised amphibole. Groundmass disseminated opaques, v.fine grained sericite, zoisite chlorite	moderate	Moderately altered porphyritic andesite/basalt	0		25			15											60	100
Wh260	Green volcanic	N	N	Very fine grained albite, sericite, zoisite, silica. Angular forms poss plag phenos.	very high	Very highly altered volcanic																		0
Wh271	Green volcanic	N	N	Porphyritic. Embayed quartz. Alkali feldspar heavily seritised, but some show simple twins. Plag sericitised but still shows twinning. Chloritised amphibole. Groundmass is fine grained quartz, chlorite, feldspar, opaques	low	Porphyritic rhyolite	3	6	5				1										85	100
Wh272	Green volcanic	N	N	Porphyritic. Plag phenocrysts sericitised and albitised some with original twinning. Chloritised amphibole. Groundmass disseminated opaques, v.fine grained sericite, zoisite chlorite	moderate	Moderately altered porphyritic andesite/basalt	0		25			10		3									62	100
Wh275	Green volcanic	N	N	Porphyritic. Plag completely saussuritized. Amphibole completely chloritised. Groundmass v.fine grained sericite, zoisite chlorite	high	Highly altered porphyritic andesite/basalt	0	0	15				1										84	100
Wh276	Green volcanic	N	N	Porphyritic. Tabular plag phenocrysts sericitised and albitised, some w/ original twinning. Euhedral amphibole chloritised. Groundmass very fine grained quartz, feldspar, chlorite	low	Porphyritic andesite/basalt	0		25				5								5	65	100
Wh276.2	Green volcanic	N	K-spar	Porphyritic, weakly flow banded. Embayed quartz. Sericitised plag still shows twinning. Chloritised amphibole. Groundmass fine grained quartz, chlorite, feldspar, opaques	Very low	Porphyritic andesite/basalt	1	2	5				<1									92	100
Wh276.3	Green volcanic	N	Kspar	Porphyritic medium grained. Very embayed quartz, pag, k-spar phenocrysts. Groundmass medium grained plag, kspar, disseminated chlorite	very low	Porphyritic andesite/basalt	5	5	30													60	100
Wh278.1	Green volcanic	N	Kspar	Very fine grained brown sericite, clays. Angular forms poss plag phenos. Vesicular	very high	Very highly altered volcanic																		0
BR399	Aplite	N	Kspar	one half thin section is aplitic. Myrmekite		Aplitic monzo-granite	43.5	30.6	16.7	8.3	0.9						0							100
KR396	weakly foliated granitoid	N	Kspar	Weakly foliated with some qz ribbons, and foliation shown by micas. Some microcline.		Weakly foliated syeno-granite	33.0	38.7	16.0	2.8	9.4	<1		<1			<1							100
KR397	Aplite	N	Kspar	Mostly aplitic, equigranular, one end is coarse equigranular with micas.		Aplitic quartz-rich granitoid	61.7	26.3	10.5	0.0	1.5						0							100

Sample	Field description	Polished?	Staining	Rock textures	Degree of alteration	Petrographic name	quartz	alkali feldspar	plagioclase	muscovite	biotite	chlorite	amphibole	clinopyroxene	opaques	apatite	titanite	tourmaline	other heavy	glass shards	vesicle	groundmass	lithics	SUM
MP038	Dark granitoid	N	Kspar	Feldspar phenocrysts in a foliated, fine-grained matrix. Strongly undulose quartz. Microcline and perthite.		Foliated monzo-granite	30	45	20		5						0							100
MP342	light granitoid	N	Kspar	equigranular course grained		Equigranular granodiorite	22.8	18.8	47.5	0.0	5.9	5.0					0							100
MP356	light granitoid	N	Kspar	equigranular course grained. Perthitic K-spar. Red-brown opaques		Equigranular syeno-granite	35	45	15						5									100
NR368	Dark granitoid	N	Kspar	equigranular course grained		Equigranular alkali feldspar granite	40	55	5		<1	<1			<1		0							100
OP072	Foliated granite	N	N	Foliation - alignment of micas. K-spar phenocrysts in groundmass of qz and mica		Foliated quartz-rich granitoid	50	32	0	5	10				3	<1								100
OP075	light granitoid	Y	N	Equigranular, interlocking crystals		Equigranular syeno-granite	30	64	5		1						<1							100
P81311-F	Green Hills clast	N	Kspar	Fine grained ?granite, w/ fine qz groundmass and large, round qz phenos or recrystallised qz? Also bio and sericitised k-spar		Equigranular syeno-granite	45	35	10	5	5													100
P81313-A	Green Hills clast	N	Kspar	Equigranular weathered granite w/ qz and altered kspar, minor plag		Equigranular monzo-granite	30	40	30			<1					<1							100
P81313-C	Green Hills clast	N	Kspar	Foliated/deformed granite w/ qz groundmass, K-spar phenos, abundant, deformed musc and bio		Foliated syeno-granite	30	45	5	10	10													100
P81313-E	Green Hills clast	N	Kspar	Equigranular weathered granite w/ qz and altered kspar, minor plag		Equigranular monzo-granite	20	50	30		<1	<<1			<1	<<1	<1							100
P81315-B	Green Hills clast	N	Kspar	Foliated, biotite-rich granite, w/ k-spar phenocrysts and minor plag		Foliated quartz-rich granitoid	55	25	10	2	8													100
Pi311	White weathered granite	N	Kspar	Equigranular course grained. Core lots of Fe oxide ppts.	low	Equigranular syeno-granite	35	55	10								0							100
Pi312.1	White weathered granite	N	Kspar	Kspar phenocrysts in fine, foliated matrix, with quartz ribbons. Plag highly altered to sericite.	low	Foliated syeno-granite	35	45	10	4	5	1												100
Pi314	Porphyritic weathered granite	N	Kspar	Thin section too broken up		Equigranular alkali feldspar granite	35.4	56.3	4.2	0.0	4.2													100
PP147.2	light granitoid	N	Kspar	equigranular medium grained. Strongly undulose extinction. Microcline.		Equigranular monzo-granite	25	40	30		5	<1												100
PP166.1	Dark granitoid	N	Plag	Porphyritic, w/ qz phenocrysts.		Porphyritic quartz-rich granitoid	55.0	21.9	9.3	2.6	11.3	0.0			0.0									100
PP166.2	Dark granitoid	N	Plag	foliation - alignment of micas/amp		Foliated quartz monzonite	16	40	30	5	5				4	<1								100

Sample	*Field description*	*Polished?*	*Staining*	*Rock textures*	*Degree of alteration*	*Petrographic name*	*quartz*	*alkali feldspar*	*plagioclase*	*muscovite*	*biotite*	*chlorite*	*amphibole*	*clinopyroxene*	*opaques*	*apatite*	*titanite*	*tourmaline*	*other heavy*	*glass shards*	*vesicle*	*groundmass*	*lithics*	*SUM*
PP167	Light granitoid	N	Plag	interlocking equant kspar and quartz. Sutured grain boundaries.		Equigranular alkali feldspar granite	30	69	0	<1	1				0	<1	<1							100
PP175		N	Kspar	equigranular course grained		Equigranular monzo-granite	20.5	47.2	30.7		1.6						0							100
PP184.1	Dark granitoid	Y	N	equigranular, non-foliated		Equigranular syeno-granite	30	45	20	<1	5				<1	0	0							100
PP187	Granitoid	N	Kspar	No foliation. Slight variation in grain size. Qz clustered together. Qz has strongly undulose extinction. Microcline.		Equigranular monzo-granite	49	30	20		1						0	<1						100
PP288	Dark granitoid	N	Kspar	Kspar, perthitic, phenocrysts in aplitic, foliated matrix. Undulose quartz.		Foliated syeno-granite	45	35	15	5							0							100
PP289	Light granitoid	N	Kspar	equigranular medium grained. Microcline.		Equigranular syeno-granite	25	60	14		1						0							100
Pu225	White weathered granite	N		Interlocking equigranular crystals		Equigranular syeno-granite	30	69	0	0	0				1	0	0							100
Wh256	Dark granitoid	N	Kspar	equigranular course grained		Equigranular monzo-granite	20	50	30		<1						0							100
Wh266	Dark granitoid	N	Kspar	Fine grained, strongly foliated. Strongly undulose quartz, sutured boundaries		Foliated monzo-granite	40	30	20	7	3													100
Wh273	Red granitoid	N	Kspar	equigranular course grained. Perthitic K-spar		Equigranular monzo-granite	30	44	25								1							100
Wh283	Dark granitoid	N	Kspar	Feldspar phenocrysts in a foliated, fine-grained matrix. Strongly undulose quartz. Microcline.		Equigranular monzo-granite	30.2	26.7	25.6	0.0	17.4													100

Table D.2: Petrograaphic composition of conglomerate granitoid clast samples, with visually estimated and point counts compared. Data presented as percentage of whole rock.

Sample	*Method*	*quartz*	*alkali feldspar*	*plagioclase*	*muscovite*	*biotite*	*chlorite*	*opaques*	*apatite*	*titanite*	*tourmaline*	*SUM*
BR399	Estimate	39	40	20	1					0		100
BR399	Point count	43.5	30.6	16.7	8.3	0.9						100
KR396	Estimate	37	40	20		3	<1	<1		<1		100
KR396	Point count	33.0	38.7	16.0	2.8	9.4		0				100
KR397	Estimate	58	25	15	1	1				0		100
KR397	Point count	61.7	26.3	10.5		1.5		0				100
MP342	Estimate	20	30	35		5	10			0		100
MP342	Point count	22.8	18.8	47.5		5.9	5.0					100
PP166.1	Estimate	55	32	5	0	5		3	0			100
PP166.1	Point count	55.0	21.9	9.3	2.6	11.3		0.0				100
PP175	Estimate	25	40	30		5				0		100
PP175	Point count	20.5	47.2	30.7		1.6					<1	100
Pu225	Estimate	30	69	0	0	0		1	0	0		100
Pu225	Point count	34.0	53.0	13.0								100
Wh283	Estimate	35	42	15		8						100
Wh283	Point count	30.2	26.7	25.6		17.4						100

APPENDIX E: CLAST XRF RESULTS

Table E.1: Spectrachem Ltd. laboratory, major element data. Duplicate samples (split of crushed powder samples) in bold.

Sample	*Formation*	*Hand sample*	*SiO_2 (wt.%)*	*TiO_2 (wt.%)*	*Al_2O_3 (wt.%)*	*Fe_2O_3 T (wt.%)*	*MnO (wt.%)*	*MgO (wt.%)*	*CaO (wt.%)*	*Na_2O (wt.%)*	*K_2O (wt.%)*	*P_2O_5 (wt.%)*	*LOI (wt.%)*	*SUM*
Mo017	Farewell	Vein quartz	98.67	0.04	0.39	0.07	0.01	0.05	0.02	0.07	0.07	0.01	0.20	99.61
Mo028	North Cape	Grey metasediment	81.48	0.25	10.22	1.32	0.05	0.80	0.07	1.46	3.03	0.03	1.53	100.23
MP037	North Cape	Grey metasediment	90.02	0.25	5.27	0.38	0.01	0.12	0.03	1.62	1.70	0.02	0.47	99.89
OP076	**Farewell**	**Grey metasediment**	**94.56**	**0.23**	**2.36**	**0.69**	**0.01**	**0.30**	**0.04**	**0.37**	**0.64**	**0.04**	**0.59**	**99.81**
OP076	**Farewell**	**Grey metasediment**	**94.49**	**0.23**	**2.33**	**0.69**	**0.01**	**0.30**	**0.04**	**0.35**	**0.63**	**0.05**	**0.57**	**99.67**
Pi124.1	Farewell	Cream metasediment	91.21	0.22	5.10	0.22	0.01	0.14	0.02	0.16	1.30	0.01	1.31	99.69
Pi124.2	Farewell	Cream metasediment	90.91	0.18	5.48	0.34	0.01	0.20	0.01	0.14	1.33	0.01	1.32	99.92
PP165	North Cape	Grey metasediment	83.29	0.41	8.66	0.99	0.01	0.53	0.06	2.18	2.41	0.03	0.89	99.44
PP182	North Cape	Grey metasediment	59.02	0.72	17.21	6.48	0.12	4.74	2.72	5.06	0.41	0.26	2.99	99.74
Pu214	Farewell	Grey metasediment	93.86	0.19	3.37	0.21	0.01	0.11	0.02	0.25	0.72	0.02	1.18	99.93
Pu228	Farewell	Quartzite	94.83	0.23	2.92	0.13	0.01	0.09	0.02	0.23	0.59	0.02	0.74	99.81
Pi083.1	Farewell	Cream siltstone	82.54	0.41	12.11	0.24	0.01	0.03	0.02	0.11	0.09	0.04	4.54	100.14
Pi083.2	Farewell	Cream siltstone	77.15	0.86	15.64	0.21	0.01	0.08	0.02	0.13	0.63	0.04	5.28	100.06
Pu210	Farewell	Cream siltstone	67.41	0.91	21.21	0.62	0.01	0.28	0.04	0.41	1.28	0.02	7.60	99.78
Pu212	Farewell	Cream siltstone	86.05	0.42	8.22	0.20	0.01	0.14	0.02	0.30	1.75	0.01	2.46	99.58
MP040.1	North Cape	Green volcanic clast	68.20	0.63	14.20	4.96	0.07	3.05	0.85	3.01	1.63	0.04	3.16	99.78
MP040.2	North Cape	Green volcanic clast	70.92	0.59	15.47	0.88	0.01	0.47	0.16	2.07	6.32	0.07	2.52	99.47
MP040.3	North Cape	Green volcanic clast	76.39	0.35	12.44	2.55	0.01	0.55	0.14	3.53	1.95	0.06	2.24	100.20
MP040.4	North Cape	Green volcanic clast	65.98	0.72	16.90	3.39	0.03	1.28	1.18	6.75	1.40	0.13	2.07	99.83
PP150.2	North Cape	Green volcanic clast	61.37	0.79	17.48	6.62	0.12	3.36	0.28	5.69	0.82	0.08	3.14	99.76
PP158	North Cape	Green volcanic clast	58.54	0.98	17.61	9.15	0.08	3.15	1.02	3.59	1.98	0.15	3.74	99.99
PP168.2	North Cape	Green volcanic clast	66.30	0.63	15.88	4.68	0.06	2.10	2.09	5.62	0.56	0.05	1.94	99.90
Pu213	Farewell	Green volcanic clast	79.42	0.18	12.52	1.41	0.01	0.28	0.02	0.27	3.00	0.02	2.85	99.99
BR399	Rakopi	granite: light, equigranular	75.92	0.04	13.26	0.49	0.01	0.08	0.25	3.03	5.96	0.03	0.56	99.63
GH379	Farewell	dark igneous w/ white xtls	49.53	1.30	26.30	8.15	0.08	2.07	0.59	0.69	2.88	0.41	8.01	100.01
GH381	Farewell	granite: light, equigranular	77.03	0.12	12.75	0.21	0.04	0.10	0.26	4.44	4.42	0.02	0.24	99.62
GH382	Farewell	fine white igneous, black xtls	63.54	0.82	21.57	1.94	0.07	1.25	0.37	2.00	1.79	0.20	6.31	99.84
Mo027	North Cape	granite: red	72.41	0.30	15.37	1.22	0.01	0.46	0.25	3.65	4.33	0.08	1.47	99.54
MP038	North Cape	granite: dark	71.48	0.35	15.11	1.76	0.02	0.42	0.66	3.92	5.05	0.04	0.93	99.75
MP039	North Cape	granite: light	70.97	0.27	16.09	0.61	0.01	0.13	0.90	4.65	5.09	0.03	0.80	99.55
MP343	North Cape	granite: light, equigranular	73.70	0.23	14.05	1.66	0.02	0.36	0.94	3.70	4.28	0.05	0.52	99.50
MP356	North Cape	granite: light, equigranular	76.00	0.11	13.28	0.52	0.01	0.05	0.16	4.38	4.85	0.02	0.35	99.74
NR366	Farewell	granite: light, equigranular	75.08	0.12	13.61	0.70	0.07	0.13	0.44	4.64	4.57	0.02	0.23	99.61

Sample	*Formation*	*Hand sample*	*SiO_2 (wt.%)*	*TiO_2 (wt.%)*	*Al_2O_3 (wt.%)*	*Fe_2O_3T (wt.%)*	*MnO (wt.%)*	*MgO (wt.%)*	*CaO (wt.%)*	*Na_2O (wt.%)*	*K_2O (wt.%)*	*P_2O_5 (wt.%)*	*LOI (wt.%)*	*SUM*
NR368	Farewell	granite: dark, non-foliated, porphyritic	76.69	0.12	12.98	0.28	0.02	0.10	0.17	4.39	4.74	0.01	0.22	99.72
OP071	Farewell	granite: dark	69.51	0.37	15.53	3.12	0.05	0.52	0.91	3.91	4.98	0.05	0.69	99.63
OP072	Farewell	granite: foliated	73.80	0.29	14.15	1.74	0.02	0.34	0.36	2.34	5.49	0.03	1.33	99.87
OP075	Farewell	granite: light	76.63	0.12	13.01	0.25	0.02	0.08	0.22	4.21	4.85	0.02	0.29	99.69
Pi085	Farewell	weathered granitoid	75.82	0.15	14.61	0.09	0.02	0.03	0.02	0.22	5.65	0.02	3.28	99.91
Pi306	Farewell	weathered granitoid	70.57	0.95	20.22	0.27	0.01	0.05	0.03	0.10	0.35	0.06	7.15	99.77
Pi312.1	Farewell	weathered granitoid	69.01	0.46	19.62	0.68	0.01	0.09	0.02	0.25	4.26	0.02	5.33	99.76
PP147.1	North Cape	granite: light	77.36	0.10	12.53	0.55	0.01	0.08	0.15	3.95	4.48	0.02	0.52	99.74
PP147.2	North Cape	granite: light	71.73	0.18	16.09	0.63	0.03	0.25	1.50	5.38	3.31	0.03	0.46	99.58
PP147.3	North Cape	granite: light	71.84	0.19	15.95	0.62	0.02	0.27	1.13	5.62	3.37	0.02	0.49	99.53
PP151.1	North Cape	granite: dark	74.80	0.26	13.42	1.45	0.01	0.35	0.79	3.07	4.41	0.04	1.19	99.78
PP151.2	North Cape	granite: dark	77.56	0.12	12.49	0.25	0.01	0.06	0.15	3.96	4.75	0.01	0.41	99.77
PP151.3	North Cape	granite: dark	68.66	0.23	17.03	0.95	0.02	0.21	1.30	4.48	6.15	0.03	0.52	99.58
PP156.1	North Cape	granite: dark	72.40	0.32	14.40	2.01	0.02	0.51	0.47	3.24	4.81	0.02	1.26	99.46
PP156.2	North Cape	granite: dark	58.40	1.78	17.91	4.57	0.04	1.94	0.95	3.73	5.45	0.14	4.57	99.48
PP157.2	North Cape	granite: light	72.75	0.32	14.56	1.06	0.01	0.30	0.29	3.21	5.25	0.04	1.72	99.53
PP166.1	North Cape	granite: dark	72.47	0.27	15.12	0.65	0.02	0.22	0.72	4.37	5.46	0.03	0.45	99.77
PP166.2	North Cape	granite: dark	71.65	0.32	15.20	2.05	0.02	0.49	0.61	4.40	4.66	0.02	0.56	99.96
PP167	North Cape	granite: light	73.58	0.10	14.45	0.27	0.01	0.18	0.65	2.09	7.76	0.04	0.63	99.75
PP173	North Cape	granite: red	73.62	0.33	14.43	0.40	0.01	0.23	1.04	3.80	5.12	0.05	0.55	99.58
PP183.1	North Cape	granite: light	70.90	0.37	15.17	2.45	0.03	0.61	0.51	3.85	4.72	0.03	1.20	99.84
PP183.2	North Cape	granite: light	71.97	0.39	14.65	2.18	0.04	0.54	0.99	4.26	3.92	0.04	0.92	99.90
PP184.1	North Cape	granite: dark	73.12	0.23	14.11	1.34	0.02	0.23	0.73	3.98	4.85	0.04	0.63	99.28
PP187	North Cape	Pegmatite	82.24	0.04	9.64	0.17	0.01	0.08	0.47	2.06	4.64	0.01	0.28	99.64
PP188	North Cape	granite: red	71.02	0.23	16.13	0.55	0.01	0.09	0.18	5.50	5.20	0.03	0.66	99.60
PP289	North Cape	granite: light, no biotite, equigranular	65.04	0.30	19.87	0.15	0.01	0.06	1.22	5.26	7.40	0.02	0.32	99.65
Pu223	Farewell	granite: light	71.70	0.96	17.45	0.61	0.01	0.32	0.05	0.76	1.01	0.04	6.89	99.80
Pu225	**Farewell**	**White weathered granite**	**76.71**	**0.17**	**14.09**	**0.11**	**0.01**	**0.04**	**0.02**	**0.27**	**4.98**	**0.01**	**3.41**	**99.83**
Pu225	**Farewell**	**White weathered granite**	**76.74**	**0.17**	**14.08**	**0.11**	**0.01**	**0.04**	**0.02**	**0.29**	**4.96**	**0.01**	**3.41**	**99.84**
Wh256	Farewell	granite: dark, non-foliated, equigranular	76.40	0.11	13.38	0.21	0.03	0.11	0.29	4.58	4.72	0.02	0.24	100.08
Wh260	Farewell	granite: dark, non-foliated, porphyritic	82.77	0.20	9.53	2.58	0.04	0.35	0.04	0.38	1.89	0.02	1.99	99.78
Wh266	Farewell	granite: dark, foliated, porphyritic	73.28	0.24	14.47	1.15	0.01	0.24	0.20	3.27	5.59	0.02	0.85	99.31
Wh267	Farewell	granite: dark, foliated, porphyritic	62.38	0.64	18.41	4.36	0.05	0.98	1.20	4.54	5.32	0.21	1.30	99.39

Sample	Formation	Hand sample	SiO_2 (wt.%)	TiO_2 (wt.%)	Al_2O_3 (wt.%)	Fe_2O_3T (wt.%)	MnO (wt.%)	MgO (wt.%)	CaO (wt.%)	Na_2O (wt.%)	K_2O (wt.%)	P_2O_5 (wt.%)	LOI (wt.%)	SUM
Wh273	Farewell	granite: red, equigranular	77.23	0.12	12.77	0.24	0.01	0.08	0.21	4.33	4.66	0.02	0.29	99.96
Wh283	Farewell	granite: dark, foliated, porphyritic	68.27	0.42	16.27	3.09	0.05	0.77	1.04	4.25	4.33	0.12	1.20	99.81
KR396	Separation Point Suite (Knuckle Hill)	weathered granitoid	69.21	0.30	17.92	1.43	0.02	0.38	0.57	3.88	2.82	0.09	2.87	99.48
KR397	Separation Point Suite (Knuckle Hill)	aplite	76.48	0.03	13.38	0.26	0.02	0.05	0.35	4.68	4.12	0.01	0.31	99.67

Table E.2: Spectrachem Ltd. laboratory, trace element data. Duplicate samples in bold.

Sample	Granitoid grouping	As (ppm)	Ba (ppm)	Ce (ppm)	Cr (ppm)	Cu (ppm)	Ga (ppm)	La (ppm)	Nb (ppm)	Ni (ppm)	Pb (ppm)	Rb (ppm)	Sc (ppm)	Sr (ppm)	Th (ppm)	U (ppm)	V (ppm)	Y (ppm)	Zn (ppm)	Zr (ppm)
Mo017		<1	15	26	<1	<1	1	12	2	<1	4	4	<2	6	2	<1	7	4	4	22
Mo028		1	300	37	41	9	16	17	14	9	31	92	10	53	13	3	45	15	31	135
MP037		2	704	35	22	<1	3	28	6	1	14	43	5	72	8	1	19	15	5	239
OP076		**1**	**684**	**62**	**40**	**<1**	**3**	**41**	**6**	**1**	**10**	**25**	**2**	**29**	**8**	**1**	**20**	**14**	**10**	**321**
OP076		**1**	**698**	**69**	**46**	**<1**	**3**	**44**	**5**	**<1**	**9**	**27**	**4**	**29**	**8**	**2**	**19**	**14**	**11**	**311**
Pi124.1		1	330	46	22	<1	6	25	6	3	6	44	5	14	7	1	27	9	6	201
Pi124.2		1	329	38	21	<1	6	22	5	2	3	49	5	8	4	2	23	10	11	156
PP165		1	676	52	38	<1	10	21	9	2	13	82	7	78	8	3	38	15	14	344
PP182		3	288	64	38	28	16	38	10	12	8	12	19	986	7	1	180	22	76	120
Pu214		2	280	50	17	<1	5	20	5	2	16	22	6	12	5	1	23	13	10	202
Pu228		<1	251	44	31	<1	5	26	5	1	5	45	2	8	9	2	22	11	8	206
Pi083.1		14	79	61	53	10	13	32	20	1	26	6	11	74	18	6	66	51	3	334
Pi083.2		5	78	140	87	2	17	74	18	2	10	28	15	28	21	5	100	49	5	293
Pu210		10	374	20	49	2	21	6	15	16	11	41	23	18	12	4	143	21	18	149
Pu212		1	598	25	48	<1	9	15	9	<1	11	37	10	26	6	2	56	9	7	500
MP040.1		1	340	56	52	1	15	19	15	11	10	54	22	222	8	3	121	16	55	177
MP040.2		2	861	190	6	<1	18	132	17	4	27	218	4	207	30	6	37	43	34	399
MP040.3		3	471	71	12	5	12	39	13	1	7	76	6	165	13	2	35	25	22	187
MP040.4		3	297	47	23	1	16	33	13	4	16	47	14	865	7	2	105	9	41	147
PP150.2		2	320	73	53	2	18	36	16	13	20	26	23	256	6	3	175	17	83	132
PP158		2	624	39	32	<1	19	24	5	10	13	56	25	313	2	1	253	18	68	58
PP168.2		1	276	58	37	<1	14	30	12	10	11	18	18	833	11	1	96	8	58	137
Pu213		2	471	112	16	<1	23	53	29	2	3	70	13	9	14	4	46	70	33	355
BR399	BR399	3	236	18	<1	<1	17	11	13	<1	40	209	3	55	7	2	8	18	8	30
GH379	High LOI	6	524	49	32	32	34	30	28	22	18	112	12	68	13	4	111	17	106	738
GH381	S3	2	53	52	<1	<1	18	26	17	<1	15	219	<2	33	23	2	4	6	16	114
GH382	High LOI	1	211	40	<1	3	15	24	15	10	18	90	12	131	16	5	72	16	79	382
Mo027	High LOI	1	103	128	7	<1	19	75	9	6	13	176	2	366	14	2	27	12	30	176
MP038	A	1	609	123	6	<1	18	73	20	2	25	219	10	224	30	3	20	18	34	255
MP039	S2	1	1250	11	<1	<1	18	10	17	<1	14	124	<2	468	14	2	11	6	11	206
MP343	A	2	784	28	2	<1	13	26	11	3	26	121	2	244	14	1	16	7	26	177
MP356	S3	1	118	148	<1	<1	18	127	17	<1	9	260	4	59	21	3	7	15	11	104

Sample	Granitoid grouping	As (ppm)	Ba (ppm)	Ce (ppm)	Cr (ppm)	Cu (ppm)	Ga (ppm)	La (ppm)	Nb (ppm)	Ni (ppm)	Pb (ppm)	Rb (ppm)	Sc (ppm)	Sr (ppm)	Th (ppm)	U (ppm)	V (ppm)	Y (ppm)	Zn (ppm)	Zr (ppm)
NR366	S3	1	176	36	<1	<1	23	17	48	<1	40	383	4	97	46	11	6	7	22	139
NR368	S3	<1	95	59	<1	<1	18	36	18	1	11	237	<2	40	29	2	4	7	18	114
OP071	A	2	567	104	4	<1	19	70	24	1	28	207	4	224	34	4	16	8	38	305
OP072	High LOI	2	757	67	3	<1	19	37	21	3	29	246	2	177	26	2	20	7	29	234
OP075	A	2	86	27	<1	<1	18	15	18	<1	11	256	3	31	21	2	6	4	13	120
Pi085	High LOI	<1	33	34	19	<1	20	19	22	2	18	213	6	15	25	3	30	7	9	155
Pi306	High LOI	3	79	220	76	<1	21	126	21	2	26	19	23	66	25	6	122	76	7	311
Pi312.1	High LOI	2	602	77	30	1	20	43	26	3	34	113	12	101	36	6	67	12	19	329
PP147.1	S3	3	48	43	5	<1	19	26	20	1	8	234	<2	20	17	1	8	13	12	94
PP147.2	S1	1	956	<5	<1	<1	20	15	5	1	23	81	<2	944	4	<1	11	1	30	115
PP147.3	S1	<1	980	14	<1	<1	17	10	4	1	18	99	5	755	6	2	6	2	29	125
PP151.1	High LOI	3	825	57	4	<1	15	28	16	1	26	120	4	223	18	3	15	6	17	211
PP151.2	S3	1	47	59	5	<1	19	23	20	1	13	259	2	14	21	2	4	13	10	119
PP151.3	S1	<1	1775	10	3	<1	17	6	5	1	28	128	2	527	9	1	10	3	16	397
PP156.1	High LOI	<1	932	109	4	<1	18	55	20	3	15	233	3	147	26	5	15	8	28	277
PP156.2	High LOI	2	983	39	43	6	27	30	38	22	16	172	11	757	25	5	103	7	80	539
PP157.2	High LOI	2	627	110	6	<1	17	63	20	<1	18	208	2	186	26	2	17	13	18	251
PP166.1	S1	1	798	18	3	<1	18	16	12	1	13	135	2	221	8	1	6	5	17	239
PP166.2	A	1	545	86	2	<1	18	57	19	2	17	183	1	227	15	2	17	14	31	224
PP167	S1	1	1588	34	<1	<1	14	19	8	1	19	210	5	535	7	2	5	6	11	47
PP173	S1	<1	692	79	3	<1	14	48	8	3	14	93	7	425	7	1	12	5	24	173
PP183.1	High LOI	1	573	82	8	<1	18	46	20	2	20	221	4	228	27	3	20	18	36	243
PP183.2	A	3	494	64	8	<1	18	31	22	2	17	178	4	220	27	3	21	16	52	283
PP184.1	A	3	1031	102	2	1	16	64	16	<1	14	154	2	208	17	2	9	12	13	209
PP187	S2	1	698	8	19	<1	11	<5	2	5	14	156	1	317	24	4	1	2	6	69
PP188	A	2	416	106	<1	<1	19	53	19	<1	20	128	<2	100	17	2	11	18	16	364
PP289	S2	<1	1061	39	<1	<1	21	32	14	1	12	321	<2	600	15	4	15	7	5	224
Pu223	High LOI	28	283	109	59	27	20	62	16	1	39	36	23	27	14	4	128	24	27	170
Pu225	**High LOI**	**2**	**37**	**26**	**14**	**<1**	**21**	**15**	**23**	**1**	**20**	**257**	**5**	**12**	**11**	**3**	**22**	**5**	**5**	**162**
Pu225	**High LOI**	**1**	**42**	**32**	**13**	**<1**	**19**	**17**	**24**	**2**	**20**	**254**	**9**	**12**	**11**	**4**	**18**	**4**	**4**	**162**
Wh256	S3	2	73	43	2	<1	19	13	13	3	13	231	<2	44	21	2	6	5	21	111
Wh260	High LOI	1	1416	29	<1	6	10	21	22	<1	8	53	6	38	9	2	7	22	98	257
Wh266	A	2	767	76	1	<1	16	53	19	2	23	232	2	183	35	4	20	15	20	213
Wh267	High LOI	1	1060	61	<1	3	21	43	20	32	20	113	8	395	13	4	34	19	62	344
Wh273	S3	2	41	61	<1	<1	19	31	18	1	14	226	2	26	25	3	8	13	14	119
Wh283	High LOI	2	740	63	13	<1	19	42	19	12	23	174	6	270	20	4	29	10	57	294
KR396	BASEMENT	1	959	33	2	<1	19	36	10	2	22	73	6	564	7	2	12	2	51	224
KR397	BASEMENT	1	55	11	<1	<1	22	<5	6	<1	31	164	3	79	3	2	3	2	20	55

APPENDIX F: DUPLICATE ANALYSES

Data from International Standard Reference material analysed at the laboratories has been requested from Chemostrat Ltd. and Spectrachem Ltd. but as of publication is not available.

Table F.1: all duplicate samples, including samples sent to two laboratories and duplicate powder samples sent to the same laboratory. Samples sent to Spectrachem and UC laboratories were crushed powder samples, and duplicates were from a split of the same prepared powder. Samples sent to Chemostrat were unprepared rock samples, duplicates with Spectrachem are rock samples divided in half.

Sample	Lab	SiO2 (%)	TiO2 (%)	Al2O3 (%)	Fe2O3T (%)	MnO (%)	MgO (%)	CaO (%)	Na2O (%)	K2O (%)	P2O5 (%)	LOI (%)	As	Ba	Ce	Cr	Cu	Ga	La	Nb	Ni	Rb	Sc	Sr	Th	U	V	V	Y	Zn	Zr
Mo017	UC	98.93	0.04	0.45	0.11	<0.01	<0.05	0.02	<0.1	0.07	<0.01	0.29																			
Mo017	Spectra	98.67	0.04	0.39	0.07	0.01	0.05	0.02	0.07	0.07	0.01	0.20																			
MP037	UC	90.04	0.25	5.47	0.41	<0.01	<0.05	0.02	1.58	1.69	<0.01	0.50																			
MP037	Spectra	90.02	0.25	5.27	0.38	0.01	0.12	0.03	1.62	1.70	0.02	0.47																			
MP038	UC	71.22	0.35	15.47	1.77	0.02	0.28	0.66	4.14	4.97	0.03	1.06																			
MP038	Spectra	71.48	0.35	15.11	1.76	0.02	0.42	0.66	3.92	5.05	0.04	0.93																			
OP071	UC	68.82	0.37	15.97	3.06	0.05	0.38	0.91	4.16	4.95	0.04	1.24																			
OP071	Spectra	69.51	0.37	15.53	3.12	0.05	0.52	0.91	3.91	4.98	0.05	0.69																			
OP072	UC	73.28	0.29	14.46	1.74	0.02	0.19	0.35	2.46	5.46	0.02	1.65																			
OP072	Spectra	73.80	0.29	14.15	1.74	0.02	0.34	0.36	2.34	5.49	0.03	1.33																			
OP075	UC	76.21	0.13	13.37	0.28	0.02	<0.05	0.22	4.50	4.83	<0.01	0.42																			
OP075	Spectra	76.63	0.12	13.01	0.25	0.02	0.08	0.22	4.21	4.85	0.02	0.29																			
OP076	UC	94.77	0.24	2.41	0.71	0.01	0.15	0.04	0.22	0.62	0.03	0.70																			
OP076	UC	94.85	0.23	2.43	0.71	0.01	0.16	0.04	0.22	0.63	0.03	0.62																			
OP076	Spectra	94.56	0.23	2.36	0.69	0.01	0.30	0.04	0.37	0.64	0.04	0.59	1	684	62	40	<1	3	41	6	1	10	25	2	29	8	1	20	14	10	321
OP076	Spectra	94.49	0.23	2.33	0.69	0.01	0.30	0.04	0.35	0.63	0.05	0.57	1	698	69	46	<1	3	44	5	<1	9	27	4	29	8	2	19	14	11	311
Pi106	Spectra	69.21	0.83	18.17	2.44	0.02	1.08	0.03	0.24	2.57	0.03			627	103	114	12	24	55	16	21	127	13	60	15	4	136		34	44	215
Pi106	Chemo	67.78	0.88	18.59	2.62	0.02	1.24	0.27	0.17	2.60	0.03			1028.02	98.52	116.63	20.51	24.97	52.62	16.36	31.26	154.74	14.29	80.07	16.54	3.70	137.63		35.92	61.70	290.49
PP156.1	UC	71.59	0.32	14.83	2.01	0.01	0.36	0.48	3.50	4.78	0.01	1.09																			
PP156.1	Spectra	72.40	0.32	14.40	2.01	0.02	0.51	0.47	3.24	4.81	0.02	1.26																			
PP157.2	UC	73.16	0.33	14.92	1.07	<0.01	0.15	0.29	3.36	5.19	0.03	1.47																			
PP157.2	Spectra	72.75	0.32	14.56	1.06	0.01	0.30	0.29	3.21	5.25	0.04	1.72																			
PP158	UC	58.44	0.99	17.87	9.02	0.08	3.01	1.00	3.79	1.92	0.14	3.71																			
PP158	Spectra	58.54	0.98	17.61	9.15	0.08	3.15	1.02	3.59	1.98	0.15	3.74																			
PP165	UC	83.48	0.41	9.01	1.02	0.01	0.39	0.05	2.21	2.41	0.02	0.93																			
PP165	Spectra	83.29	0.41	8.66	0.99	0.01	0.53	0.06	2.18	2.41	0.03	0.89																			
PP166.1	UC	71.95	0.27	15.57	0.68	0.01	0.08	0.71	4.69	5.44	0.01	0.48																			
PP166.1	Spectra	72.47	0.27	15.12	0.65	0.02	0.22	0.72	4.37	5.46	0.03	0.45																			
PP166.2	UC	70.89	0.32	15.56	2.03	0.02	0.34	0.61	4.66	4.65	<0.01	0.87																			

Sample	Lab	SiO2 (%)	TiO2 (%)	Al2O3 (%)	Fe2O3T (%)	MnO (%)	MgO (%)	CaO (%)	Na2O (%)	K2O (%)	P2O5 (%)	LOI (%)	As	Ba	Ce	Cr	Cu	Ga	La	Nb	Ni	Rb	Sc	Sr	Th	U	V	V	Y	Zn	Zr
PP166.2	Spectra	71.65	0.32	15.20	2.05	0.02	0.49	0.61	4.40	4.66	0.02	0.56																				
PP167	UC	73.13	0.11	14.91	0.31	<0.01	<0.05	0.65	2.15	7.72	0.03	0.85																				
PP167	Spectra	73.58	0.10	14.45	0.27	0.01	0.18	0.65	2.09	7.76	0.04	0.63																				
PP173	UC	73.14	0.33	14.92	0.43	0.01	0.09	1.04	4.07	5.11	0.03	0.70																				
PP173	Spectra	73.62	0.33	14.43	0.40	0.01	0.23	1.04	3.80	5.12	0.05	0.55																				
PP182	UC	58.60	0.73	17.73	6.38	0.12	4.70	2.71	5.37	0.40	0.26	2.93																				
PP182	Spectra	59.02	0.72	17.21	6.48	0.12	4.74	2.72	5.06	0.41	0.26	2.99																				
PP184.1	UC	73.10	0.23	14.67	1.34	0.02	0.07	0.73	4.29	4.83	0.03	0.66																				
PP184.1	Spectra	73.12	0.23	14.11	1.34	0.02	0.23	0.73	3.98	4.85	0.04	0.63																				
PP187	UC	82.00	0.04	10.14	0.21	<0.01	<0.05	0.48	2.10	4.60	<0.01	0.36																				
PP187	Spectra	82.24	0.04	9.64	0.17	0.01	0.08	0.47	2.06	4.64	0.01	0.28																				
PR195	Spectra	67.31	0.73	17.87	3.23	0.02	1.72	0.09	0.23	3.81	0.09			1372	72	107	40	24	42	16	33	195	18	78	17	5	138		39	114	189
PR195	Chemo	67.15	0.76	17.58	3.33	0.02	1.66	0.34	0.18	3.47	0.08			1532.54	90.15	93.84	34.56	22.91	45.11	14.11	34.71	184.39	16.06	79.86	16.42	3.88	131.81		35.83	117.59	169.87
Pu205	Spectra	56.44	0.81	21.92	0.88	0.01	0.46	0.04	0.32	2.27	0.06			638	118	97	71	28	68	16	20	134	15	104	18	5	120		80	32	165
Pu205	Chemo	56.65	0.82	22.17	0.85	0.00	0.54	0.19	0.25	2.24	0.06			793.44	105.88	96.54	51.63	28.06	55.55	15.23	26.44	143.11	17.35	97.27	17.13	4.94	138.86		61.41	46.03	131.95
Pu210	UC	67.23	0.93	21.93	0.64	<0.01	0.16	0.03	0.38	1.27	<0.01	7.39																				
Pu210	Spectra	67.41	0.91	21.21	0.62	0.01	0.28	0.04	0.41	1.28	0.02	7.60																				
Pu212	UC	86.27	0.43	8.64	0.24	<0.01	<0.05	0.01	0.17	1.75	<0.01	2.44																				
Pu212	Spectra	86.05	0.42	8.22	0.20	0.01	0.14	0.02	0.30	1.75	0.01	2.46																				
Pu213	UC	79.43	0.19	12.88	1.42	0.01	0.15	0.01	0.17	2.99	<0.01	2.71																				
Pu213	Spectra	79.42	0.18	12.52	1.41	0.01	0.28	0.02	0.27	3.00	0.02	2.85																				
Pu214	UC	93.71	0.19	3.66	0.25	<0.01	<0.05	0.02	<0.1	0.73	<0.01	1.37																				
Pu214	Spectra	93.86	0.19	3.37	0.21	0.01	0.11	0.02	0.25	0.72	0.02	1.18																				
Pu223	UC	72.06	0.97	18.06	0.65	<0.01	0.18	0.05	0.77	1.00	0.03	6.13																				
Pu223	Spectra	71.70	0.96	17.45	0.61	0.01	0.32	0.05	0.76	1.01	0.04	6.89																				
Pu225	UC	76.32	0.17	14.65	0.15	<0.01	<0.05	0.02	0.21	4.96	<0.01	3.45																				
Pu225	UC	75.98	0.18	14.70	0.15	<0.01	<0.05	0.02	0.20	4.96	<0.01	3.78																				
Pu225	Spectra	76.71	0.17	14.09	0.11	0.01	0.04	0.02	0.27	4.98	0.01	3.41	2	37	26	14	<1	21	15	23	1	20	257	5	12	11	3	22	5	5	162
Pu225	Spectra	76.74	0.17	14.08	0.11	0.01	0.04	0.02	0.29	4.96	0.01	3.41	1	42	32	13	<1	19	17	24	2	20	254	9	12	11	4	18	4	4	162
Pu228	UC	94.91	0.24	3.19	0.17	<0.01	<0.05	0.01	0.13	0.59	<0.01	0.70																				
Pu228	Spectra	94.83	0.23	2.92	0.13	0.01	0.09	0.02	0.23	0.59	0.02	0.74																				

Table F.2: Standard deviation of duplicate geochemical analyses. The different results from the samples sent to Chemostrat and Spectrachem (Pi106, PR195, Pu205, see highlight) are likely because the duplicates are from two pieces of a heterogenous rock sample, rather than split homogenous crushed powders.

Sample	SiO2	TiO2	Al2O3	Fe2O3T	MnO	MgO	CaO	Na2O	K2O	P2O5	LOI	As	Ba	Ce	Cr	Cu	Ga	La	Nb	Ni	Rb	Sc	Sr	Th	U	V	V	Y	Zn	Zr
Mo017	0.18	0.00	0.04	0.03			0.00		0.00		0.06																			
MP037	0.01	0.00	0.14	0.02			0.00	0.03	0.01		0.02																			
MP038	0.19	0.00	0.25	0.00	0.00	0.10	0.00	0.15	0.06	0.01	0.09																			
OP071	0.48	0.00	0.31	0.04	0.00	0.10	0.00	0.18	0.02	0.01	0.39																			
OP072	0.37	0.00	0.22	0.00	0.00	0.11	0.01	0.09	0.02	0.01	0.23																			
OP075	0.30	0.01	0.26	0.02	0.00		0.00	0.21	0.01		0.09																			
OP076	0.17	0.00	0.05	0.01	0.00	0.08	0.00	0.08	0.01	0.01	0.06	0.10	0.00	9.90	4.95	4.24		0.00	2.12	0.71		0.71	1.41	1.41	0.00	0.00	0.71	0.71	0.00	0.71
Pi106	1.01	0.03	0.30	0.13	0.00	0.11	0.17	0.04	0.02	0.00			283.56	3.17	1.86	6.02	0.69	1.68	0.25	7.26	19.62	0.91	14.19	1.09	0.21	1.15		1.36	12.52	53.38
PP156.1	0.58	0.00	0.30	0.01	0.00	0.11	0.00	0.18	0.02	0.01	0.12																			
PP157.2	0.29	0.00	0.26	0.01		0.11	0.01	0.10	0.04	0.01	0.18																			
PP158	0.07	0.01	0.18	0.10	0.00	0.10	0.02	0.14	0.04	0.01	0.02																			
PP165	0.13	0.00	0.25	0.02	0.00	0.09	0.01	0.02	0.00	0.01	0.03																			
PP166.1	0.37	0.00	0.32	0.02	0.00	0.10	0.00	0.22	0.01	0.01	0.02																			
PP166.2	0.54	0.00	0.26	0.01	0.00	0.11	0.00	0.19	0.01		0.22																			
PP167	0.32	0.00	0.33	0.03			0.00	0.05	0.03	0.01	0.16																			
PP173	0.33	0.00	0.35	0.03	0.00	0.10	0.00	0.19	0.01	0.01	0.10																			
PP182	0.30	0.01	0.36	0.07	0.00	0.03	0.01	0.22	0.01	0.00	0.04																			
PP184.1	0.01	0.00	0.40	0.00	0.00	0.11	0.00	0.22	0.01	0.01	0.02																			
PP187	0.17	0.00	0.35	0.03			0.00	0.03	0.03		0.05																			
PR195	0.11	0.02	0.21	0.07	0.00	0.04	0.18	0.03	0.24	0.00			113.52	12.83	9.31	3.85	0.77	2.20	1.34	1.21	7.50	1.37	1.31	0.41	0.79	4.38		2.24	2.54	13.53
Pu205	0.15	0.01	0.18	0.03	0.00	0.06	0.11	0.04	0.02	0.00			109.92	8.57	0.32	13.70	0.04	8.81	0.54	4.55	6.44	1.66	4.76	0.62	0.04	13.34		13.15	9.92	23.37
Pu210	0.13	0.01	0.51	0.02		0.08	0.01	0.02	0.01		0.15																			
Pu212	0.16	0.01	0.30	0.03			0.00	0.10	0.00		0.02																			
Pu213	0.00	0.00	0.26	0.00	0.00	0.10	0.01	0.07	0.01		0.10																			
Pu214	0.11	0.00	0.21	0.03			0.00		0.00		0.14																			
Pu223	0.26	0.01	0.43	0.02		0.09	0.00	0.01	0.01	0.01	0.54																			
Pu225	0.36	0.00	0.34	0.03	0.00	0.00	0.00	0.04	0.01	0.00	0.18	0.71	3.54	4.24	0.71		1.41	1.41	0.71	0.71	0.00	2.12	2.83	0.00	0.00	0.71	2.83	0.71	0.71	0.00
Pu228	0.05	0.01	0.19	0.03			0.00	0.07	0.01		0.03																			

APPENDIX G: SANDSTONE PETROLOGY

Table G.1: sandstone composition point count results, as total counts.LA: lithofacies association; M: matrix; Q: quartz; Plag: plagioclase; K spar: alkali feldspar; L: lithic.

Sample	*Formation*	*LA*	*grain size (phi)*	*Step length (mm)*	*Part of slide counted*	*Point count notes*	*M: silt*	*M: clay - vf silt*	*M: void*	*M: clay, brown*	*M: Fe oxide*	*M: organics*	*M: micrite*	*M: sparry calcite*	*Q straight*	*Q undulose*	*Q polycrystalline*	*Q polycrystalline bladed*	*Plag: polysynthetic twins*	*Plag: deformation twins*	*Plag: highly altered*	*Plag: no pink staining*	*Plag, pink stained*
BR408	Otimatau ra	R	2.5	0.5	yellow stain		7	20	19	0	0	52			54	75	14	0	0	0	0		
BR409	Otimatau ra	R	2.5	0.5	yellow stain	interlocking qz and musc	1	9	30	0	2	4			49	198	0	0	1	0	0		
BR412	Otimatau ra	R	0.5	0.5	yellow stain		18	57	7	0	0	5			8	23	23	5	0	0	0		
PR200	Otimatau ra	O	1.5	0.75	Unstained (pink)		13	27	4	0	0	0			72	65	24	4	0	1	0		0
BR404	Rakopi	R	0.5	0.5	yellow stain		78	18	8	0	37	0			43	62	17	0	10	0	0		
BR425	Rakopi	R	2.5	0.5	all		2	27	29	1	9	0			88	33	9	0	23	0	8		
KR004	Rakopi	R	1.6	0.5	Unstained (pink)		15	65	19	3	1				91	86	15	2	26	22	2		
KR005	Rakopi	R	2.3	0.5	pink stained	Mudstone lenses skipped over	43	139	8	77	0	0			65	81	5	0	19	29	6		45
KR006	Rakopi	R	2.6	0.5	pink stained		9	115	0	22	0				82	79	6	1	23	12	2		42
KR009	Rakopi	R	1.8	0.5	pink stained		4	86	33	25	0				77	67	4	0	29	33	15		100
PR199	Rakopi	R	2.5	0.5	Unstained (pink)	Pink stain has washed over everything, including qz	18	117	15	0	0	0			111	127	10	0	2	3	0		0
Mo021	North Cape	A3	0.87	0.6	pink stained		3	60	48	2	1	0			105	70	9	2	11	25	1		39
Mo023	North Cape	A3	2.2	0.3	pink stained		17	154	4	2	0	1			84	102	4	1	14	13	0		31
MP029	North Cape	A2	1.5	0.5	yellow stain		4	27	32	0	71	0			79	36	11	0	24	2	6		
MP031	North Cape	A2	1.5	0.5	all	thin section small	6	34	32	0	16	0			57	34	6	0	35	1	13		
MP032	North Cape	A1	1.5	0.5	yellow stain		2	10	62	0	9	0			84	47	6	0	22	0	16		
MP035	North Cape	A1	1.5	0.5	yellow stain		5	12	67	7	8	0			79	59	5	1	32	0	6		
MP036	North Cape	A1	2.5	0.5	yellow stain		1	8	44	7	30	0			76	25	3	0	10	0	3		
MP044	North Cape	A1	0.5	0.5	yellow stain		1	10	63	0	15	0			64	33	8	0	19	0	12		
MP335	North Cape	A1	1.5	0.5	yellow stain		9	11	62	1	8	0			55	35	1	0	12	0	3		

Sample	Formation	LA	grain size (phi)	Step length (mm)	Part of slide counted	Point count notes	M: silt	M: clay - vf silt	M: void	M: clay, brown`	M: Fe oxide	M: organics	M: micrite	M: sparry calcite	Q straight	Q undulose	Q polycrystalline	Q polycrystalline bladed	Plag: polysynthetic twins	Plag: deformation twins	Plag: highly altered	Plag: no pink staining	Plag, pink stained
MP336	North Cape	A1	0.5	0.5	yellow stain		2	3	45	0	4	0			55	21	13	3	12	2	6		
MP338	North Cape	A2	0.5	0.5	yellow stain		2	0	76	0	54	0			63	33	7	0	18	0	7		
MP339	North Cape	A2	-0.5	0.5	yellow stain		13	10	70	2	24	0			31	23	4	0	17	5	5		
MR045	North Cape	A3	1.5	0.5	yellow stain		4	9	43	2	19	0			107	45	4	0	14	2	2		
MR048	North Cape	A1	1.5	0.5	yellow stain		2	11	64	0	44	0			116	52	12	1	15	3	2		
MR051	North Cape	A1	2.5	0.5	yellow stain		4	17	81	0	15	0			103	43	4	1	24	1	0		
MR052	North Cape	A3	2.5	0.5	yellow stain		1	9	124	0	18	0			97	49	5	0	17	1	2		
MS053	North Cape	A2	3.5	0.5	yellow stain		0	13	29	0	22	0			96	40	2	0	8	0	0		
MS055	North Cape	A2	3.5	0.5	yellow stain		5	13	28	0	122	0			76	39	4	0	8	1	20		
MS056	North Cape	A1	1.5	0.5	yellow stain		0	8	39	1	70	0			102	81	10	0	0	4	0		
OP057	North Cape	A2	2.6	0.5	pink stained		0	89	2	0	0	0			87	39	2	0	5	27	9		82
OP061	North Cape	A3	0.44	1	All		73	47	15	0	0	1			126	50	9	1	6	17	2		23
OP326	North Cape	A2	1.5	0.5	yellow stain		26	64	20	0	3	0			82	57	5	1	5	2	0		
OP327	North Cape	A3	1.5	0.5	yellow stain		36	68	21	9	0	0			96	36	7	0	11	0	0		
OP328	North Cape	A3	1.5	0.5	yellow stain		29	103	7	0	27	0			92	43	8	0	4	0	0		
OP329	North Cape	A3	0.5	0.5	yellow stain		24	85	11	0	17	2			80	71	23	1	6	0	0		
PM383	North Cape	A3	1.5	0.5	yellow stain		17	78	19	0	1	0			62	51	12	0	10	0	3		
PP146	North Cape	A1	1.7	0.5	Unstained (pink)		2	7	13	11	0				71	69	2	0	34	19	4		0
PP153	North Cape	A1	2.7	0.25	pink stained		3	21	45	54	0				75	87	4	0	27	26	3		76
PP164	North Cape	A1	1.7	0.4	pink stained		1	4	98	3	0	0			51	58	2	0	13	5	5		74
PP174	North Cape	A1	1.99	0.5	All	TS ground very thin	1	41	2	18	0	0			49	59	0	0	21	6	0		
PP175	North Cape	A1	1.9	0.3	pink stained		2	11	136	20	0	0			22	114	3	1	28	20	5		63
PP176	North Cape	A1	2.4	0.3	Unstained (pink)	Only counted vfs portion, not zst	26	82	31	4	0	0			94	115	5	3	18	21	2		0
PP177	North Cape	A1	1.9	0.5	All		4	9	45		17	0			59	47	12	0	38	0			80

Sample	Formation	LA	grain size (phi)	Step length (mm)	Part of slide counted	Point count notes	M: silt	M: clay - vf silt	M: void	M: clay, brown`	M: Fe oxide	M: organics	M: micrite	M: sparry calcite	Q straight	Q undulose	Q polycrystalline	Q polycrystalline bladed	Plag: polysynthetic twins	Plag: deformation twins	Plag: highly altered	Plag: no pink staining	Plag, pink stained
PP180	North Cape	A1	1.9	0.5	All	Skipped over most of TS due to holes/fracturing	0	5	2	6					19	37	1	0	15	2	1		3
PP190	North Cape	A1	1.1	0.5	All		12	7	58	4					77	85	18	0	42	0			18
PP295	North Cape	A1	-0.5	0.5	all		0	3	115	0	14	0			45	36	7	0	29	1	7		
PP296	North Cape	A1	-0.5	0.5	yellow stain		0	0	111	0	18	0			33	53	5	3	14	2	0		
PP299	North Cape	A1	0.5	0.5	yellow stain		43	10	55	0	15	0			41	81	12	0	20	2	0		
PP301	North Cape	A1	1.5	0.5	yellow stain		3	9	62	10	18	0			64	72	5	0	25	2	3		
PP304	North Cape	A1	1.5	0.5	yellow stain		19	19	56	0	26	0			56	50	24	1	21	0	5		
PP426	North Cape	A1	0.5	0.5	yellow stain		1	4	50	0	24	0			55	36	4	4	16	0	8		
PP427	North Cape	A1	1.5	0.5	yellow stain		1	2	70	0	2	0			46	72	4	2	19	0	8		
PP428	North Cape	A1	0.5	0.5	yellow stain		0	1	68	0	1	0			40	59	12	0	25	2	13		
PP429	North Cape	A1	1.5	0.5	yellow stain		3	3	69	0	9	0			77	56	18	0	21	1	15		
TH421	Farewell	A3	3.5	0.5	yellow stain		1	19	30	1	0	0			88	33	0	0	3	0	0		
GH376	Farewell	FG	1.5	0.5	yellow stain		9	84	18	0	6	0			74	50	9	0	0	2	0		
Mo014	Farewell	FS	0.29	0.8	All		25	29	66	2	0	0			116	51	6	1	20	26	4		25
Mo025	Farewell	FS	1.1	0.7	pink stained		14	57	21	0	0	0			111	29	10	0	7	20	3		48
Mo026	Farewell	FS	1.3	0.6	pink stained	TS v. broken up, skipped over holes	16	54	6	5	2	0			99	55	4	0	11	27	1		68
Mo250	Farewell	FS	-0.49	1	All		1	21	34	0	0	0			85	53	6	2	7	13	0		3
NR363	Farewell	FG	0.5	0.5	yellow stain		5	37	17	0	19	0			37	25	10	0	6	0	3		
NR364	Farewell	FG	1.5	0.5	yellow stain		6	14	31	0	21	0			51	58	4	0	13	0	12		
OP058	Farewell	FS	0.97	0.5	pink stained		18	50	65	1		0			88	66	7	0	26	0			56
OP065	Farewell	FS	0.97	0.75	pink stained		29	21	16		0	0			82	39	1	0	17	27	4		40
OP069	Farewell	FS	-0.063	1	All		10	20	39	0	0	0			102	49	14	0	19	28	4		12
OP070	Farewell	FS	2	0.5	pink stained		52	41	24	0	3	0			67	46	13	2	22	0			95
OP331	Farewell	FS	0.5	0.5	yellow stain		5	50	18	0	1	0			80	44	11	0	22	1	2		

Sample	Formation	LA	grain size (phi)	Step length (mm)	Part of slide counted	Point count notes	M: silt	M: clay - vf silt	M: void	M: clay, brown`	M: Fe oxide	M: organics	M: micrite	M: sparry calcite	Q straight	Q undulose	Q polycrystalline	Q polycrystalline bladed	Plag: polysynthetic twins	Plag: deformation twins	Plag: highly altered	Plag: no pink staining	Plag, pink stained
P81312	Farewell	FG	1.5	1	All		101	136	7	16	0	0			85	156	7	0	15	14	4	5	
Pi079	Farewell	FI	0.5	1	All (pink)	Broken TS, no coverslip. Grains well rounded. Matrix has brownish glauconite, red iron oxide, and voids (possibly from glauc or clays falling out)	0	0	66	1	68	0			87	144	32	8	1	0	0		1
Pi080	Farewell	FG	0.5	0.5			21	51	12	4					145	35	16		8	0			24
Pi088	Farewell	FG	1	0.5		Large greywacke clast poss skewing results	9	64	25	3		1			125	75	17	1	8	0			34
Pi089	Farewell	FG	0.5	0.5	pink stained	One large greywacke sandstone	94	34	14						149	63	1		7	0			40
Pi092	Farewell	FG	1	0.5	pink stained		13	79	12	26					104	80	21	0	12	0			41
Pi095	Farewell	FG	1.5	0.5	Yellow stain		4	79	9	8	0	0			68	70	6	0	10	0	0		
Pi097	Farewell	FG	1.5	0.5	pink stained	Poor quality thin section	15	40	4	0		0			65	12	10	0	2	0			33
Pi099	Farewell	FG	1.5	0.5	yellow stain		2	110	16	0	24	0			58	73	13	2	1	0	0		
Pi100	Farewell	FG	1.5	0.5	pink stained		24	97	40	12		5			103	62	26	2	7	0			50
Pi110	Farewell	FG	1.5	0.5	Yellow stain		13	45	13	17	0	0			81	60	3	0	2	1	0	0	
Pi115	Farewell	FG	-0.5	1	yellow stain		2	18	6	0	0	0	0	0	44	39	2	0	1	2	2	0	0
Pi125	Farewell	FG	1.5	0.5	Yellow stain		16	99	14	5	0	2			83	48	11	3	0	0	0		
Pi127	Farewell	FG	1.5	0.5	Yellow stain		18	95	3	1	6	0			75	66	15	0	1	0	0		
Pi128	Farewell	FG	2.5	0.5	Yellow stain		11	59	2	2	0	0			83	58	6	0	1	3	0		
Pi130	Farewell	FG	2.5	0.5	Yellow stain		19	46	4	5	0	0			38	62	4	0	3	2	0		
Pi134	Farewell	FG	1.5	0.5	Yellow stain		43	154	31	0	0	0			37	50	5	1	1	5	0		
Pi136	Farewell	FG	0.5	0.5	Yellow stain		7	42	7	5	2	0			75	68	2	0	0	0	0		
Pi138	Farewell	FG	2.5	0.5	Yellow stain		29	64	0	1	1	0			70	44	4	0	2	3	0	0	
Pi142	Farewell	FG	1.5	0.5	Yellow stain		16	47	6	0	1	0			48	24	8	0	6	0	2		
Pi144	Farewell	FG	1.5	0.5	Yellow stain		23	45	8	11	0				48	58	4	1	9	1	2		
Pu203	Farewell	FG	1.5	0.5	yellow stain		8	65	31	76	72	0			89	67	11	0	0	0	0		
Pu207	Farewell	FG	0	1	All	Large fpeb of q mud skewing results, also granule of h bf ss	3	46	15	3	0	0			100	99	10	6	3	11	0		16
Pu215	Farewell	FG	0.5	0.5	yellow stain		15	74	33	0	0	2			87	83	22	0	4	0	0		

Sample	Formation	LA	grain size (phi)	Step length (mm)	Part of slide counted	Point count notes	M: silt	M: clay - vf silt	M: void	M: clay, brown`	M: Fe oxide	M: organics	M: micrite	M: sparry calcite	Q straight	Q undulose	Q polycrystalline	Q polycrystalline bladed	Plag: polysynthetic twins	Plag: deformation twins	Plag: highly altered	Plag: no pink staining	Plag, pink stained
Pu216	Farewell	FG	0.5	0.8	All		23	72	12	4	1	0			157	91	11	1	5	26	3		18
Pu218	Farewell	FG	1.5	0.5	yellow stain		14	121	5	0	4	2			99	81	14	1	0	0	0		
Pu219	Farewell	FG	-0.5	1	All	Small TS, broken up on one side	10	40	3	1	0	0			78	65	2	1	3	18	0		13
Pu221	Farewell	FI	1.5	0.5	yellow stain	Grains very well rounded and well sorted in Fe oxide matrix	0	0	34	0	67	0			80	76	13	4	0	0	0		
TH235	Farewell	FM	1.5	0.7	pink stained		14	29	25	2					52	113	0	3	24	20	6		11
TH236	Farewell	FM	0	1	All		15	25	31	2	0	0			34	142	3	3	13	7	1		2
TH240	Farewell	FM	1.5	0.7	Unstained (pink)	Grains are fractured, possibly diagenetic?	34	27	47	2	1	0			70	99	2	2	18	13	2		0
TH241	Farewell	FM	1.5	0.5	pink stained		0	62	31	5	0	0			40	93	4	0	4	10	0		54
TH415	Farewell	FM	2.5	0.5	yellow stain		5	128	3	0	1	5			57	56	5	0	0	2	1		
TH417	Farewell	FM	1.5	0.5	yellow stain		9	18	21	0	0	0			78	30	0	0	0	0	4		
TH419	Farewell	FM	2.5	0.5	yellow stain		3	44	5	0	1	1			70	60	4	0	5	0	4		
TH422	Farewell	FM	1.5	0.5	yellow stain	One glauc grain passed by	1	26	4	0	0	0			55	51	6	0	4	0	3		
Wh242	Farewell	FG	0.5	1	All		4	100	8	4	1				143	79	16	1	0	10	2		18
Wh244	Farewell	FS	1.5	0.8	All	Staining didn't work. Lots of glue bubbles and broken up TS	3	92	13	2	3				100	75	6	0	17	23	10		0
Wh245	Farewell	FG	1.5	0.7	All	TS v. broken up. Mostly counted unstained side.	15	30	0	4	0	0			40	71	7	0	4	3	0		16
Wh268	Farewell	FG	1.5	0.5	yellow stain		52	38	33	0	0	0			60	102	2	0	20	0	3		
Wh269	Farewell	FG	1.5	0.5	yellow stain		3	24	36	0	1	0			69	88	6	0	12	0	7		
MatPu	Matapo Greensand		2.5	1	All		0	0	10	0	0	0	155	19	4	12	0	0		1	0	0	
MatSH	Matapo Greensand		3.5	0.75	All		0	0	6	0	0	0	140	26	8	16	0	0		1	0	0	
KR392	Bay Schist?		3.5	0.5	yellow stain	Schist?	0	0	0	0	0	1		47	110	46	0	0	1	0	0		
KR393	Bay Schist?		3.5	0.3	yellow stain	Schist?	0	0	3	0	0	0		36	109	49	0	0	0	0	0		
KR394	Bay Schist?		3.5	0.5	yellow stain	Schist?	0	0	0	0	0	0		0	69	61	1	0	0	0	0		

Table G.1 cont: sandstone composition point count results, as total counts.LA: lithofacies association; M: matrix; Q: quartz; Plag: plagioclase; K spar: alkali feldspar; L: lithic.

Sample	Plag, no yellow staining	Microcline pink stained	Microcline yellow stain	Microcline, wavy	Microcline, not stained	K spar	Kspar yellow stain	K spar perthite	K spar: wavy	K spar, sericitised/altere	K spar simple twins	K spar myrmetic texture	L: chert	L: quartzite	L: metasediment	L: very fine sandstone	L: siltstone, poorly sorted	L: siltstone q dominated`	L siltstone, w/ fine h bf musc	L: mudstone with quartz	L: mudstone with illite	L: litharenite	L schist	L: green-brown volcanic	L: black volcanic	L: plutonic (Q)	L: plutonic (K)	L: plutonic (P)	L: plutonic (musc)	L: plutonic (biotite)	L: plutonic (chl)	Musc	Biotite	Chlorite	Amphibole	Other heavy minerals	Glauconite	Bioclast	Opaques	Total counts
BR408	0		0	0	0		6	0	0	0	0	0	0	0	1	72	0	3	6	3	20	0	0	1	0	3	0	0	1	0	0	23	3	0	0	0	0		2	385
BR409	0		0	0	0		8	0	0	0	0	0	0	0	0	8	0	3	3	1	5	0	2	1	0	0	0	0	0	0	0	42	0	0	0	0	0		6	373
BR412	2		2	0	0		3	5	0	0	0	0	0	0	4	100	14	3	1	3	28	0	0	0	0	22	1	0	4	0	0	2	3	0	0	0	0		0	343
PR200		0		0	0	1		0	0	0	0	0	4	7	11	53	6	17	34	25	7		161	1	0	2	0	0	1	0	0	3	2	1		0	0		5	551
BR404	7		34	1	0		62	8	0	0	0	0	1	0	0	21	4	0	1	5	6	0	0	1	0	4	2	3	0	0	0	0	0	0	0	0	0		0	433
BR425	10		9	0	0		65	0	0	1	3	1	0	0	0	16	2	2	10	2	21	0	3	11	0	2	0	1	0	0	0	0	3	0	0	0	0			391
KR004				18	21	17		16	4	25	1	2	3	1	1	15	1	11	16	4	4		25	15	0	2	3	0	4	0	0	0	0	8	0	0	6	0	0	570
KR005		12		7	4	5		12	4	16	11	1	3	0	4	9	0	3	6	0	1		2	6	0	1	2	0	1	0	0	5	9	0	0	0	2		1	644
KR006		9		7	14	3		10	5	46	7	1	8	0	1	1	0	1	8	0	2		2	0	0	2	0	0	1	0	0	10	55	9	0	0	0		3	598
KR009		2		6	0	9		21	4	25	4	1	5	1	1	3	0	3	9	0	0		7	7	0	3	5	0	1	1	0	0	9	0	0	0	2		0	602
PR199		0		8	28	35		18	2	4	0	0	2	4	2	27	1	9	36	1	3		12	4	1	4	0	0	1	0	0	1	15	5	0	0	1		6	633
Mo021		1		4	24	15		17	8	16	0	2	5	2	2	28	0	5	25	1	0		2	38	4	5	6	2	2	0		1	22	0	0	0	0		0	613
Mo023		7		1	7	15		12	2	4	0	0	5	1	2	14	0	10	20	2	24		12	5	0							8	53		1	1	0		3	636
MP029	8		6	6	0		39	0	0	7	0	1	0	0	0	20	1	3	9	1	4	0	1	6	0	3	1	2	0	0	0	1	2	0	0	0	7			420
MP031	2		4	11	0		24	1	0	3	0	0	0	0	0	12	1	2	13	0	0	0	1	12	0	1	1	0	0	0	0	0	5	0	0	0	8		0	335
MP032	5		11	3	0		55	0	0	1	0	0	0	0	1	7	0	4	12	0	2	0	2	5	1	1	1	0	0	1	0	1	17	1	0	0	4		0	393
MP035	2		6	2	0		81	7	0	19	0	0	0	0	0	32	0	2	11	1	4	0	3	27	2	2	4	0	1	1	0	1	3	1	0	0	12		1	506
MP036	7		5	3	2		72	0	0	11	0	0	0	0	0	14	0	2	15	1	5	0	0	6	0	2	1	0	3	0	0	0	6	1	0	0	1		1	365
MP044	12		34	0	0		45	13	0	0	0	0	0	0	8	20	2	5	11	1	4	0	0	11	0	1	1	0	2	0	0	0	5	0	0	0	4		0	404
MP335	7		12	1	0		65	1	0	3	0	0	0	0	0	26	0	0	3	4	5	0	2	11	0	0	0	0	0	0	0	0	16	0	0	0	3		0	356
MP336	10		22	3	0		37	0	0	0	2	0	1	1	1	15	0	0	6	0	4	0	3	12	1	6	4	2	0	0	0	0	11	0	0	0	1		0	308
MP338	13		13	10	0		34	3	0	5	1	1	1	4	1	13	1	5	8	1	11	0	2	11	0	8	11	4	0	0	0	0	2	0	0	0	1		0	424
MP339	2		18	5	0		39	14	0	1	0	0	0	0	1	46	1	2	1	2	11	0	8	14	2	10	8	2	0	0	0	0	2	0	0	0	1		1	395

Sample	Plag, no yellow staining	Microcline pink stained	Microcline yellow stain	Microcline, wavy	Microcline, not stained	K spar	Kspar yellow stain	K spar perthite	K spar: wavy	K spar, sericitised/altere	K spar simple twins	K spar myrmetic texture	L: chert	L: quartzite	L: metasediment	L: very fine sandstone	L: siltstone, poorly sorted	L siltstone q dominated`	L siltstone, w/ fine h bf musc	L: mudstone with quartz	L: mudstone with illite	L: litharenite	L schist	L: green-brown volcanic	L: black volcanic	L: plutonic (Q)	L: plutonic (K)	L: plutonic (P)	L: plutonic (musc)	L: plutonic (biotite)	L: plutonic (chl)	Musc	Biotite	Chlorite	Amphibole	Other heavy minerals	Glauconite	Bioclast	Opaques	Total counts
MR045	4		15	0	0		44	0	0	14	0	1	4	0	2	15	0	2	9	1	13		5	3	0	2	1	0	2	2	0	1	49	1		0	3		1	445
MR048	12		18	4	0		55	5	0	8	0	2	5	1	3	8	1	1	11	3	8		8	8	1	6	2	0	2	1	0	0	5	0		0	12		0	512
MR051	2		15	12	0		39	3	0	7	1	0	4	0	0	13	0	1	9	2	6		2	13	0	5	2	0	2	3	0	1	14	0	0	0	12		0	461
MR052	9		5	3	0		40	1	0	7	1	0	2	0	1	17	3	1	18	0	3		3	13	0	4	4	0	2	4	0	4	14	0	0	0	7		0	489
MS053	1		2	0	0		80	0	0	0	0	0	0	0	0	8	0	2	11	0	0		0	3	0	2	1	0	8	13	0	10	42	1	0	0	7		0	401
MS055	6		15	2	0		56	0	0	2	0	2	0	0	0	14	2	1	8	0	3	0	3	6	0	2	1	0	1	0	0	3	14	0	0	0	5		0	462
MS056	5		25	3	0		40	30	0	0	0	0	0	0	0	5	0	0	6	0	0		1	0	0	30	13	0	4	0	2	5	7	0		0	1		0	492
OP057		3		4	3	8		11	7	6	0	1	8	0	3	1	0	4	15	0	3		6	2	0	0	2	0		0		10	110	0	0	0	0		2	551
OP061		5		10	22	28		16	7	3	0	2	10	2	6	12	0	8	14	6	5		4	3	0	13	8	0	3	0		0	5	1	1	0	0		4	568
OP326 NC	3		15	2	0		70	7	3	3	0	0	0	0	0	22	3	1	16	1	4	1	3	11	0	3	1	2	0	0	0	0	6	0	0	0	0		0	442
OP327	4		23	0	0		61	1	2	4	0	0	2	0	1	24	3	5	32	5	5		5	12	0	1	1	0	4	0	0	2	34	0	0	0	0		1	516
OP328	2		20	10	0		44	3	0	5	0	0	3	0	0	35	11	4	14	0	2		4	17	0	2	1	0	0	0	0	3	34	2	0	0	0		2	531
OP329	2		34	11	0		62	17	0	2	0	0	0	0	4	16	2	5	15	4	5	3	10	17	0	3	6	0	1	0	0	3	3	0	1	0	0		0	546
PM383	19		18	2	0		71	2	0	0	0	0	0	2	0	16	2	1	5	0	6	0	5	20	0	0	0	0	0	0	0	3	8	2	0	0	0		0	435
PP146		0		18	21	23		16	2	24	0	6	4	4	2	38	0	4	12				1	9	0	1	3	2	1	0	0	9	26	0		0	1		1	460
PP153		8		14	0	22		8	0	24	3	4	0	0	3	4	0	2	23	0	0			3	0	0	0	0	0	0	0	9	62	1		0	2		4	617
PP164		22		28	2	16		8	1	7	2	2	1	0	5	16	0	0	15	0	0		5	16	0	4	7	0	2	0	0	5	20	0	0	0	4		1	503
PP174				33	18	10		16	0	20	3	1	0	0	0	6	0	2	11	0	0		0	0	0	1	0	0	1	0	0	4	10	0		0	2		1	336
PP175		8		35	10	9		4	1	22	7	3	4	0	3	13	2	1	29	2	2		1	7	0	7	6	3	1	5	0	2	50	0	0	0	2		1	665
PP176		0		23	19	42		17	5	35	8	5	4	0	4	7	1	0	19	0	1		4	2	0	0	1	0	0	0	0	14	14	5	0	4	0		10	645
PP177		18				15				11		3			5	5		3	27				6	25	1							5	16	1		0	3		1	456
PP180		0		10	7	10		9	0	16	1	0	0	1	1	1	0	1	7	1	0		0	2	0	0	1	0	0	0	0	9	8	0	0	0	0		0	176
PP190		54				35				15		5			3	6	1	5	21	0	0		8	25	11	7	4	0				3	21	1		0	5		2	472
PP295	7		31	0	0		22	5	0	0	0	0	0	3	0	103	9	1	16	1	14	0	5	48	0	1	2	3	1	0	0	0	2	0	1	0	1		0	533

Sample	Plag, no yellow staining	Microcline pink stained	Microcline yellow stain	Microcline, wavy	Microcline, not stained	K spar	Kspar yellow stain	K spar perthite	K spar: wavy	K spar, sericitised/altere	K spar simple twins	K spar myrmetic texture	L: chert	L: quartzite	L: metasediment	L: very fine sandstone	L: siltstone, poorly sorted	L siltstone q dominated`	L siltstone, w/ fine h bf musc	L: mudstone with quartz	L: mudstone with illite	L: litharenite	L schist	L: green-brown volcanic	L: black volcanic	L: plutonic (Q)	L: plutonic (K)	L: plutonic (P)	L: plutonic (musc)	L: plutonic (biotite)	L: plutonic (chl)	Musc	Biotite	Chlorite	Amphibole	Other heavy minerals	Glauconite	Bioclast	Opaques	Total counts
PP296	11		30	6	0		21	20	0	5	0	0	0	0	0	50	6	6	16	13	1	14	0	28	0	8	28	4	3	0	0	0	0	0	0	7		0	516
PP299	3		25	2			46	7	0	7	0	0	4	1	3	21	9	7	10	10	1	4	1	38	2	3	9	14	1	0	0	1	7	0	0	0	0	0	515
PP301	12		8	4	0		64	2	0	2	1	0	0	0	1	24	1	7	45	5	0		6	21	0	4	10	2	2	1	0	1	23	0		0	0	0	519
PP304	4		39	12	0		42	10	0	1	0	0	0	0	3	57	3	4	12	1	3		4	22	2	7	5	1	1	0	0	0	3	0	0	0	0	0	513
PP426	7		13	1	0		23	2	0	1	0	0	0	6	0	25	4	2	13	1	10	0	4	31	0	9	2	2	1	1	0	0	18	1	0	0	3	0	382
PP427	18		15	0	0		51	0	0	0	0	0	0	0	2	15	2	4	7	0	2	0	2	10	0	3	1	2	0	1	0	0	9	0	0	0	7	0	377
PP428	5		11	4	0		55	0	0	1	0	0	0	3	0	15	1	0	8	1	4	0	2	19	0	5	3	1	1	0	0	0	9	0	0	0	3	0	372
PP429	8		16	2	1		52	1	0	2	0	0	0	2	4	17	3	3	8	5	3	1	6	18	0	5	4	4	0	0	0	1	13	1	0	0	3	0	455
TH421	1		7	2	0		54	0	0	0	0	0	0	0	0	5	0	1	9	0	2	0	0	0	0	3	0	0	0	0	0	1	85	0	0	0	0	1	346
GH376	0		25	2	0		65	3	0	0	0	0	0	1	4	27	1	1	2	4	6	0	3	18	0	1	2	0	1	0	0	1	16	0	0	0	0	1	436
Mo014		10		11	24	6		29	11	2	0	2	7	5	7	28	1	3	11	3	9		5	9	0	5	9	2	3	0		1	13	0		0	0		587
Mo025		6		4	13	6		5	3	3	1	1	3	0	6	16	0	7	18	3	0		6	27	1	2	5	0	1	0	0	1	21	3		0	0	1	483
Mo026		8		12	7	9		17	4	3	0	2	2	5	6	18	3	10	21	0	1		10	12	0	2	0	0	0	0		5	41	0	3	0	0	0	549
Mo250		0		9	9	14		20	3	3	2	1	9	7	5	42	5	10	18	2	7		3	6	0	5	3	0	0	0		0	1	0	1	0	0		410
NR363	9		11	3	0		47	1	0	1	0	0	0	6	1	37	7	2	8	3	37	0	5	8	0	6	7	0	0	0	0	0	11	0	0	0	0	0	369
NR364	15		15	1	0		48	3	0	0	0	0	0	2	0	20	0	2	7	5	10	0	2	11	0	2	0	0	1	1	0	1	8	0	0	0	0	0	364
OP058		40				3				8		1			6	21	1	8	27	1	0		5	33	5	1		1				1	31	0		0	0	2	572
OP065		17		6	5	3		13	1	1	2	0	2	2	3	6	0	3	21				9	16	0	1	2			1		5	25	1		0	0		421
OP069		11		12	23	9		54	15	1	3	1	4	5	5	9	5	4	27	2	2		4	17	0	4	4	2		1		0	6	0	2	0	0		529
OP070		42				12				3		0			8	4	0	4	29	0	0		2	16	9							7	55	3		1	0	4	564
OP331	11		6	4	0		53	2	0	3	0	0	2	0	1	5	0	2	19	1	3	2	1	11	0	8	0	1	1	3	0	4	27	1	0	0	0	0	405
P81312			24	6	0		41	6	13	0	0	0	3	0	2	33	2	6	28	5	5		3	0	0	2	1	0	0	0	0	3	8	1	1	0	0	1	740
Pi079		0		4	13	6		17	0	3	1	0	0	24	0	6	0	0	0	2	1		0	0	0	7	7	0	0	0	0	0	0	0		0	114	3	616
Pi080		6				22									1	1		13	9	7			15	0	0											0	0		390

Sample	Plag, no yellow staining	Microcline pink stained	Microcline yellow stain	Microcline, wavy	Microcline, not stained	K spar	Kspar yellow stain	K spar perthite	K spar: wavy	K spar, sericitised/altere	K spar simple twins	K spar myrmetic texture	L: chert	L: quartzite	L: metasediment	L: very fine sandstone	L: siltstone, poorly sorted	L: siltstone q dominated`	L siltstone, w/ fine h bf musc	L: mudstone with quartz	L: mudstone with illite	L: litharenite	L schist	L: green-brown volcanic	L: black volcanic	L: plutonic (Q)	L: plutonic (K)	L: plutonic (P)	L: plutonic (musc)	L: plutonic (biotite)	L: plutonic (chl)	Musc	Biotite	Chlorite	Amphibole	Other heavy minerals	Glauconite	Bioclast	Opaques	Total counts
Pi088		13				9									6	7		2	1	47			2	0	0							1				0	0		1	451
Pi089		13				13										58		2		5				0	0	4						1				0	0			498
Pi092		30				17									7	6	2	11	6		1		12	0	0							5	1			1	0		8	495
Pi095	18			1			45	0	0	0	0	0	0	0	1	21	0	15	4	13	1		8	0	0	0	0	0	2	1	0	2	4	0	0	0	0		0	390
Pi097		6				2									0	3		8	2	1			0	0	0								3			0	0			206
Pi099	4		5	0	0		42	0	0	0	0	0	0	0	0	18	0	5	5	2	4	0	2	7	0	1	0	0	0	0	0	1	2	0	0	0	0		0	397
Pi100		15				4									4	5	0	2	2	7	1		4	0	0							1	6	2		0	0		11	492
Pi110	3		15	5	0		19	0	3	0	0	0			3	25	3	14	10	3	1		6	0	0				3			0	3	1	0	0	0			352
Pi115	2	0	2	2	1	0	16	8	0	1	0	1	0	0	0	32	0	11	1	11	0		1	8	1	0	0	0	0	0	0	0	0	0	0	0	0	0	214
Pi125	3		16	2	0		40	0	0	0	0	0	1	0	5	15	0	2	20	3	3		4	1	1	0	0	0	0	1	0	3	12	0	0	0	0		1	414
Pi127	1		23	9	0		46	1	0	0	0	0	1	0	2	14	1	1	10	1	4		3	1	0	0	0	0	2	1	0	2	10	0	0	1	0			414
Pi128	2		11	6	0		38	0	1	0	0	0	0	0	0	16	0	2	22	1	0		6	0	0	0	0	0	1	0	0	0	18	1		0	0		23	373
Pi130	7		12	10	0		58	0	5	0	0	0	0	0	2	11	0	2	19	6	5		5	0	0	0	1	0	0	7	0	1	28	0	0	0	0		1	363
Pi134	0		23	3	0		21	0	1	0	0	0	0	0	0	14	4	4	7	2	19		6	1	0	4	1	0	4	2	0	1	17	0		0	0		1	462
Pi136	1		18	24	0		36	0	0	0	0	1	2	0	0	24	2	2	13	2	4		6	4	0	0	1	0	0	0	0	1	8	1		0	0			358
Pi138	6		15	2	0		54	0	1	0	0	0	1		2	11	0	1	18	2	1		11	0	0	0	1	0	0	1	0	7	41	0		0	0			393
Pi142	12		10	1	0		65	0	0	0	0	0	0	1	0	11	1	1	7	2	8	0	0	5	1	1	0	0	0	0	0	1	26	0	0	0	0		0	311
Pi144	9		17	4	0		36	0	2	0	0	0	0	0	1	15	0	6	37	5	1		3	5	0	1	2	1	0	0	0	3	15	0	0	0	0		0	373
Pu203	0		13	1	0		50	0	0	1	0	0	1	0	1	14	7	3	7	3	25	0	1	4	2	0	0	1	0	0	0	4	3	0	2	0	0		4	566
Pu207		2		3	8	13		0	0	0	0	0	0	4	4	42	5	14	19	57	13		6	0	3	1	0	0	0	0	0	1	1	0	0	0	0		2	510
Pu215	0		30	3	0		35	0	0	0	0	0	0	0	0	35	15	12	7	13	23	0	3	0	0	3	4	0	0	0	0	2	1	0	0	0	0		1	507
Pu216		6		3	7	29		3	7	0	0	0	1	5	7	23	6	10	3	13	18		7	2	1	0	0	0	0	0	0	5	0	0	0	0	0		2	582
Pu218	2		13	0	0		69	0	0	0	0	0	0	0	1	56	6	3	26	6	10	0	5	1	0	1	0	0	0	0	0	1	0	0	0	0	0		0	541
Pu219		3		1	10	12		1	1	2	0	0	1	3	0	26	6	14	16	8	9		0	0	5	0	0	0	0	0	0	0	0	0	0	0	0		1	353

Sample	Plag, no yellow staining	Microcline pink stained	Microcline yellow stain	Microcline, wavy	Microcline, not stained	K spar	Kspar yellow stain	K spar perthite	K spar: wavy	K spar, sericitised/altere	K spar simple twins	K spar myrmetic texture	L: chert	L: quartzite	L: metasediment	L: very fine sandstone	L: siltstone, poorly sorted	L: siltstone q dominated`	L siltstone, w/ fine h bf musc	L: mudstone with quartz	L: mudstone with illite	L: litharenite	L schist	L: green-brown volcanic	L: black volcanic	L: plutonic (Q)	L: plutonic (K)	L: plutonic (P)	L: plutonic (musc)	L: plutonic (biotite)	L: plutonic (chl)	Musc	Biotite	Chlorite	Amphibole	Other heavy minerals	Glauconite	Bioclast	Opaques	Total counts
Pu221	0		5	0	0		15	0	0	0	0	0	0	0	0	1	0	0	0	0	0	0	0	0	0	0	1	0	0	0	0	0	0	0	0	7		0	303
TH235		4		30	14	17		30	2	7	3	1	6	5	11	29	11	5	20	0	2		10	7	0	5	3	5	1	0	0	1	14	0	0	0	0		8	550
TH236		1		42	47	14		15	0	7	0	1	14	0	5	53	0	10	26	3	0		5	2	0	6	7	4	1	1	0	1	3	0	0	0	0		2	548
TH240		2		44	24	33		4	1	4	2	3	3	5	9	50	1	11	26	1	2		4	3	0	1	1	2	1	0	0	2	28	0	0	0	0		1	585
TH241		6		2	4	4		1	2	0	1	0	3	0	2	14	9	9	20	1	4		5	0	0	2	1	0	1	1	0	5	50	1	0	0	0		0	451
TH415	5		16	0	0		55	0	0	0	0	0	0	2	1	11	0	3	11	2	1	0	9	3	0	5	1	0	0	1	0	3	43	3	0	0	0		1	439
TH417	4		18	2	0		62	0	0	0	0	0	0	0	0	3	0	0	7	0	2	0	1	1	0	0	2	0	0	0	0	5	67	1	0	0	0		0	335
TH419	2		6	0	0		35	0	0	0	0	0	0	1	1	20	1	6	13	0	11	0	5	7	0	0	0	0	1	0	0	3	39	1	0	0	0		2	351
TH422	4		9	0	0		37	0	0	0	0	0	0	0	2	14	0	2	9	3	1	0	10	1	0	0	0	0	1	2	0	5	87	0	0	0	0		0	337
Wh242		5		28	26	19		1	4	0	1	1	0	1	6	29	5	9	19	15	13		9	4	2	1	1	0	1			3	12	0	0	0	0		5	606
Wh244		0		20	45	42		24	0	20	5	2	2	1	3	17	0	4	10	3	0		12	1	0	4	2	2	1	0	0	2	26	12	0	0	0		4	608
Wh245		13		12	33	15		2	0	0	2	0	1	1	0	16	0	3	5	6	1		0	0	0	0	0	0	0	0	0	0	14	0	0	0	0		0	314
Wh268	12		15	4	0		89	4	0	2	0	0	1	0	1	15	1	2	16	5	4		2	3	0	2	0	1	1	1	0	1	12	0		0	1		0	505
Wh269	11		17	6	0		79	1	0	4	0	1	1	0	0	13	2	4	21	7	4		7	18	0	1	2	0	3	2	0	0	24	0		0	1		0	475
MatPu		0		1	3	5		0	0	0	0	0	0	0	0	0	0	0	0				0	0	0	0	0	0	0	0	0	1	0	0	0	0	67	18	2	298
MatSH		0		3	1	2		2	0	1	0	0	0	0	0	0	0	1	0	0	0		0	0	0	0	0	0	0	0	0	0	0	0	0	0	165	13	35	420
KR392	7		0	0			20	0	0	0	1	0	0	0	0	0	0	0	0	0	0	0	0	0	0	0	0	0	0	0	0	0	67	0	0	0	0		0	300
KR393	0		0	0			5	0	0	0	0	0	0	0	0	0	0	0	0	0	0	0	0	0	0	0	0	0	0	0	0	0	97	0	0	0	0		4	303
KR394	0		0	0			1	0	0	0	0	0	0	0	0	0	0	0		0		0	0	0	0	0	0	0	0	0	0	0	167	0	0	0	0		301	301

APPENDIX H: SEDIMENTARY GEOCHEMISTRY DATA

Table H.1: ICP-OES data from Chemostrat Ltd.

Grain size abbreviations: mud=mudstone, zst=siltstone, vfs=very fine sandstone, fs=fine sandstone, ms=medium sandstone, cs=coarse sandstone, vcs=very coarse sandstone, m-cs=medium to coarse sandstone, c-vcs=coarse to very coarse sandstone

Sample	Latitude (WGS 84 °S)	Longitude (WGS 84 °E)	Total thickness (m)	Grain size	Formation	lithofacies association	Al2O3	SiO2	TiO2	Fe2O3	MnO	MgO	CaO	Na2O	K2O	P2O5	S	Sc
PR192	40.68299	172.48506	10.5	zst	Otimataura	O	13.30	70.66	0.82	3.88	0.02	1.28	0.22	0.15	2.47	0.06	69.18	12.63
PR193	40.68299	172.48506	11.0	vfs	Otimataura	O	11.46	76.79	0.74	2.29	0.02	1.05	0.32	0.14	2.18	0.04	65.40	11.20
PR194	40.6792	172.48384	101.0	vfs	Rakopi	R	16.40	60.93	0.77	2.24	0.01	0.97	0.25	0.22	3.19	0.06	7.81	15.32
PR195	40.6792	172.48384	103.0	vfs	Rakopi	R	17.58	67.15	0.76	3.33	0.02	1.66	0.34	0.18	3.47	0.08	33.11	16.06
PR196	40.6792	172.48384	104.0	zst	Rakopi	R	12.67	72.45	0.79	3.19	0.04	1.13	0.27	0.14	2.31	0.10	30.49	11.18
PR199	40.67077	172.47702	317.0	fs	Rakopi	R	15.96	71.90	0.52	2.09	0.02	0.76	0.30	0.50	3.28	0.07	32.38	5.78
PR201	40.67797	172.48259	145.0	zst	Rakopi	R	17.72	66.24	0.83	3.84	0.02	1.66	0.19	0.19	3.33	0.06	27.73	16.63
PR252				mud	Rakopi	R	15.18	60.52	0.82	9.97	0.21	1.34	0.59	0.13	2.30	0.32	54.73	13.40
MP029	40.58115	172.62813	618.0	ms	North Cape	A2	12.02	70.44	0.31	3.37	0.02	0.69	1.21	3.03	3.17	0.17	354.97	4.85
MP031	40.58082	172.62744	627.5	ms	North Cape	A2	14.04	69.91	0.36	1.75	0.01	0.75	1.25	3.59	3.00	0.05	152.85	6.26
MP032	40.58088	172.62671	638.0	ms	North Cape	A1	14.60	69.49	0.42	2.51	0.03	1.26	1.37	3.86	2.89	0.07	131.02	7.42
MP035	40.57991	172.62515	673.0	ms	North Cape	A1	12.54	74.03	0.30	2.01	0.01	0.69	1.11	3.22	3.27	0.07	354.08	4.80
MP044	40.58039	172.62572	656.5	cs	North Cape	A1	11.85	74.66	0.27	1.03	0.01	0.44	0.85	3.22	3.51	0.02	183.19	4.17
OP057	40.57153	172.59999	970.0	vfs	North Cape	A2	15.57	60.18	0.70	6.69	0.06	1.89	0.64	2.62	3.28	0.07	233.50	12.31
OP059	40.57036	172.59875	1021.9	zst	North Cape	A3	15.48	74.55	0.78	2.74	0.03	1.14	0.53	1.07	2.89	0.11	85.67	9.59
OP061	40.57072	172.59903	996.0	cs	North Cape	A3	12.19	79.23	0.41	1.05	0.01	0.46	0.41	1.26	3.67	0.06	78.74	3.59
OP063	40.57109	172.59926	975.8		North Cape	A2	16.40	66.81	0.76	3.94	0.04	1.40	0.48	0.93	2.84	0.13	124.61	10.65
OP064	40.57127	172.59962	905.4		North Cape	A2	16.18	65.54	0.82	5.75	0.04	1.67	0.77	1.87	2.31	0.10	158.93	13.44
PP146	40.57292	172.63373	717.0	ms	North Cape	A1	15.00	67.53	0.72	5.62	0.01	0.72	0.99	3.66	2.97	0.13	252.96	9.78
PP153	40.56885	172.62675	860.3	fs	North Cape	A1	15.22	70.52	0.43	2.52	0.02	1.03	1.44	4.47	2.75	0.08	152.90	7.07
PP176	40.56875	172.62827	839.4	fs	North Cape	A1	15.09	68.62	0.95	3.02	0.03	1.10	1.32	3.32	2.51	0.06	874.51	11.94
PP178	40.57137	172.63086	665.0		North Cape	A2	17.51	66.41	0.65	4.07	0.05	2.02	0.81	3.29	2.59	0.06	832.92	10.30
PP190	40.5724	171.63351	723.8	ms	North Cape	A1	13.44	73.36	0.56	3.51	0.01	0.62	0.99	3.23	3.13	0.11	245.43	6.08
OP058	40.57021	172.59891	1001.5	cs	Farewell	FS	13.71	78.17	0.46	1.49	0.02	0.57	0.67	1.34	3.60	0.02	91.03	4.95
OP067	40.56845	172.59706	1240.3	fs	Farewell	FS	19.25	70.14	0.81	3.62	0.03	1.53	0.54	0.55	3.20	0.03	95.47	13.35
OP070	40.56842	172.59563	1106.3	ms	Farewell	FS	15.45	71.83	0.53	2.28	0.04	1.01	0.88	2.12	3.85	0.06	95.36	6.43

Sample	Latitude (WGS 84 °S)	Longitude (WGS 84 °E)	Total thickness (m)	Grain size	Formation	lithofacies association	Al2O3	SiO2	TiO2	Fe2O3	MnO	MgO	CaO	Na2O	K2O	P2O5	S	Sc
Pi079	40.50451	172.71342	1508.3	cs	Farewell	FI	6.42	83.20	0.16	3.78	0.00	0.34	0.20	0.13	1.87	0.02	121.64	2.62
Pi080	40.50455	172.71336	1504.3	cs	Farewell	FG	16.35	75.39	0.40	0.39	0.00	0.14	0.38	0.14	2.23	0.02	40.78	6.54
Pi088	40.50467	172.71317	1488.8	m-cs	Farewell	FG	11.94	80.12	0.35	0.59	0.00	0.24	0.26	0.13	2.06	0.01	62.34	4.73
Pi092	40.50481	172.71266	1463.1	m-cs	Farewell	FG	14.48	78.35	0.39	0.81	0.01	0.29	0.26	0.16	2.68	0.02	71.67	5.61
Pi095	40.50512	172.7126	1445.6	ms	Farewell	FG	18.66	71.87	0.58	1.10	0.01	0.54	0.30	0.16	2.69	0.03	58.08	8.28
Pi099	40.50569	172.71336	1418.6	ms	Farewell	FG	17.65	68.41	0.87	1.27	0.01	0.54	0.32	0.14	2.44	0.03	43.01	8.44
Pi104	40.50637	172.71396	1386.7	ms	Farewell	FG	16.71	69.78	0.62	2.49	0.01	0.63	0.31	0.18	2.77	0.02	101.76	7.48
Pi106	40.50651	172.71414	1377.5	zst	Farewell	FG	18.59	67.78	0.88	2.62	0.02	1.24	0.27	0.17	2.60	0.03	64.70	14.29
Pi110	40.50717	172.71358	1313.7	ms	Farewell	FG	13.74	76.90	0.53	1.13	0.01	0.43	0.14	0.17	2.60	0.02	29.60	5.32
Pi115	40.50721	172.71327	1304.4	vcs	Farewell	FG	13.19	76.27	0.43	1.14	0.01	0.45	0.16	0.19	3.18	0.02	34.69	5.15
Pi120	40.50731	172.71268	1289.0	zst	Farewell	FG	18.78	62.66	0.92	1.98	0.01	1.05	0.16	0.21	2.78	0.03	24.83	14.53
Pi125	40.5075	172.71233	1261.0	ms	Farewell	FG	15.43	72.89	0.70	2.57	0.01	0.40	0.17	0.20	3.27	0.02	182.14	6.42
Pi127	40.50778	172.71213	1248.2	ms	Farewell	FG	14.75	72.94	0.55	1.60	0.02	0.69	0.15	0.17	3.16	0.02	29.85	6.52
Pi128	40.50806	172.71181	1225.9	fs	Farewell	FG	15.57	67.63	0.60	6.01	0.08	0.79	0.19	0.21	3.38	0.02	56.06	6.08
Pi130	40.50835	172.71167	1187.6	fs	Farewell	FG	16.30	70.45	0.68	1.83	0.02	0.76	0.33	0.75	3.18	0.02	43.56	6.52
Pi134	40.50952	172.70952	1150.5	ms	Farewell	FG	16.23	70.57	0.70	2.17	0.02	0.68	0.23	0.58	3.27	0.04	60.40	7.12
Pi138	40.50984	172.70914	1136.1	fs	Farewell	FG	17.22	64.68	0.64	3.78	0.03	1.19	0.36	0.66	3.06	0.03	75.24	8.17
Pi142	40.51028	172.70879	1112.1	ms	Farewell	FG	17.95	69.53	0.62	1.83	0.02	0.80	0.36	1.30	3.71	0.02	77.38	5.96
Pi145	40.51056	172.70876	1100.0	zst	Farewell	FG	17.01	69.32	0.81	3.35	0.02	1.33	0.29	0.62	2.88	0.04	112.44	11.83
Pu203	40.52448	172.73679	1435.9	ms	Farewell	FG	15.52	72.77	2.30	1.53	0.06	0.29	0.17	0.43	2.31	0.04	105.40	10.51
Pu205	40.52461	172.73677	1440.5	mud	Farewell	FG	22.17	56.65	0.82	0.85	0.00	0.54	0.19	0.25	2.24	0.06	39.78	17.35
Pu207	40.52477	172.73705	1454.3	c-vcs	Farewell	FG	13.25	79.95	0.53	0.34	0.00	0.19	0.18	0.23	2.26	0.02	22.43	6.62
Pu215	40.52495	172.73706	1458.7	cs	Farewell	FG	13.06	79.35	0.43	0.26	0.00	0.16	0.16	0.24	2.23	0.02	29.62	6.31
Pu218	40.52517	172.73747	1475.7	ms	Farewell	FG	13.00	78.51	0.42	0.43	0.00	0.18	0.17	0.32	2.08	0.02	45.32	5.17
Pu221	40.52514	172.73781	1490.4	ms	Farewell	FI	4.08	83.07	0.12	7.54	0.01	0.19	0.19	0.35	1.28	0.28	110.45	3.28

Table H.2: ICP-MS data from Chemostrat Ltd. laboratory

Sample	Ba	Be	Ce	Co	Cr	Cs	Cu	Dy	Er	Eu	Ga	Gd	Hf	Ho	La	Lu	Mo	Nb	Nd	Ni	Pr	Rb	Sm	Sr	Ta	Tb	Th	Tm	U	V	Y	Yb	Zn	Zr
PR192	1194.86	2.19	89.55	4.94	81.85	11.63	21.87	5.81	3.54	1.40	17.49	6.48	7.34	1.27	44.03	0.51	1.32	13.60	39.85	22.91	10.44	141.53	7.48	39.08	1.22	1.03	15.35	0.52	3.71	113.57	36.04	3.38	72.12	269.74
PR193	1368.70	1.81	80.82	4.05	73.85	10.32	32.84	5.11	3.08	1.26	14.97	5.62	8.70	1.06	39.68	0.44	3.21	12.81	35.54	19.79	9.41	114.76	6.62	45.61	1.11	0.87	14.21	0.46	3.62	102.08	30.25	2.92	54.27	316.81
PR194	1613.46	2.91	84.33	5.91	86.49	17.28	10.76	5.85	3.41	1.37	21.52	6.27	4.79	1.26	41.53	0.48	1.62	13.42	37.37	21.41	9.87	176.39	7.04	66.13	1.16	0.98	13.97	0.51	3.31	124.25	34.51	3.21	42.82	165.85
PR195	1532.54	2.68	90.15	7.70	93.84	12.10	34.56	6.22	3.52	1.55	22.91	6.70	4.86	1.29	45.11	0.50	2.46	14.11	39.63	34.71	10.66	184.39	7.57	79.86	1.21	1.06	16.42	0.53	3.88	131.81	35.83	3.31	117.59	169.87
PR196	1216.84	2.13	79.17	15.34	70.63	7.61	22.36	4.90	2.94	1.14	15.92	5.28	7.04	1.09	38.60	0.43	6.11	13.22	33.58	27.31	9.02	121.77	6.02	81.21	1.14	0.82	12.67	0.45	3.46	97.40	29.48	3.06	83.61	262.30
PR199	1183.87	1.24	50.61	4.64	37.60	3.98	11.52	1.98	1.18	0.91	16.19	2.90	3.54	0.42	25.54	0.16	0.73	10.22	21.68	14.54	5.86	115.75	3.62	181.64	0.78	0.38	7.96	0.18	1.94	53.17	11.70	1.11	45.41	130.85
PR201	1618.46	2.85	96.23	7.42	101.87	11.98	54.91	6.53	3.76	1.70	23.22	7.35	5.71	1.35	47.81	0.52	4.13	14.63	43.24	32.11	11.40	174.81	8.39	71.71	1.29	1.12	17.56	0.55	4.21	149.84	38.24	3.55	99.66	199.14
PR252	963.78	3.01	77.15	13.24	90.49	7.70	33.41	5.58	3.18	1.45	18.66	6.08	6.10	1.16	36.23	0.45	1.26	14.09	34.33	44.33	8.86	109.43	6.91	98.96	1.16	0.95	15.65	0.47	4.21	105.40	31.77	3.06	114.42	221.87
MP029	1392.53	2.19	34.10	3.93	25.94	3.50	13.08	2.01	1.16	0.78	13.50	2.26	2.53	0.43	19.67	0.17	1.57	6.44	13.83	6.74	3.73	100.66	2.70	436.94	0.55	0.33	5.83	0.18	2.77	60.02	11.63	1.14	32.71	89.91
MP031	1382.93	1.51	42.18	2.45	22.21	3.17	4.90	1.55	0.79	0.85	14.65	2.44	3.25	0.30	20.95	0.11	0.60	6.02	18.17	5.32	4.85	93.77	3.27	468.61	0.50	0.32	5.98	0.12	1.51	44.95	7.21	0.77	24.65	123.20
MP032	1258.08	2.02	53.13	5.73	26.51	2.86	8.32	2.28	1.14	1.06	16.17	3.39	3.01	0.43	26.77	0.15	1.31	6.67	24.12	11.15	6.37	89.53	4.32	463.62	0.56	0.46	8.88	0.15	1.74	57.83	11.19	1.04	71.59	108.23
MP035	1121.49	2.14	38.03	3.39	25.63	3.63	8.34	1.59	0.94	0.67	13.47	2.12	2.21	0.33	21.48	0.14	0.91	5.69	13.98	6.90	3.94	104.86	2.46	443.66	0.51	0.28	5.04	0.14	1.98	51.79	9.27	0.94	25.88	79.59
MP044	1191.92	1.57	37.07	2.06	18.41	3.30	7.34	1.28	0.63	0.66	13.94	2.03	2.12	0.24	17.78	0.09	0.51	5.47	14.23	4.33	3.89	106.16	2.52	405.58	0.47	0.27	5.15	0.10	1.11	31.05	6.55	0.62	27.39	74.51
OP057	841.28	2.50	53.14	12.79	48.81	8.53	18.99	2.97	1.59	1.11	21.64	4.04	4.90	0.60	26.42	0.23	2.14	9.23	25.58	27.00	6.60	160.84	4.80	254.97	0.81	0.56	7.23	0.23	1.75	115.01	15.72	1.43	134.25	187.14
OP059	1335.98	2.16	78.56	7.53	82.47	6.30	21.47	4.50	2.57	1.48	17.41	5.63	11.62	0.93	38.15	0.40	0.98	14.21	34.66	24.25	9.08	114.36	6.43	141.74	1.17	0.80	13.59	0.40	3.30	79.38	27.26	2.55	75.46	461.14
OP061	1341.31	0.99	42.45	5.45	28.34	2.92	8.30	1.98	1.06	0.83	10.92	2.56	3.23	0.39	19.75	0.16	2.08	10.06	18.04	17.72	4.91	109.86	3.13	281.14	0.80	0.36	7.93	0.17	1.90	34.25	11.24	1.03	31.71	119.64
OP063	973.92	2.13	72.31	9.50	84.13	6.67	28.14	4.26	2.41	1.43	18.88	5.16	7.30	0.88	36.53	0.36	2.13	13.70	32.80	32.40	8.60	117.36	6.02	160.68	1.11	0.75	12.23	0.36	3.03	107.47	24.78	2.29	97.61	278.58
OP064	741.40	1.98	54.43	10.49	82.06	7.34	18.04	4.01	2.39	1.19	17.45	4.49	7.97	0.85	24.66	0.38	2.62	9.01	25.47	26.21	6.52	96.63	5.19	208.03	0.76	0.71	9.54	0.35	2.42	110.59	23.63	2.39	109.37	306.88
PP146	865.28	2.09	71.17	3.12	67.88	3.39	19.38	3.63	1.88	1.38	16.79	4.47	5.28	0.69	25.74	0.25	2.59	10.72	26.98	9.91	6.77	89.42	5.84	411.85	0.89	0.66	9.60	0.27	2.41	86.81	14.74	1.71	53.88	213.42
PP153	1040.01	1.91	33.66	3.45	29.04	3.68	7.02	1.49	0.89	0.70	15.73	2.10	3.51	0.30	16.83	0.14	1.63	6.82	14.68	10.90	3.96	84.39	2.55	485.94	0.53	0.28	5.79	0.14	1.40	58.65	8.55	0.86	29.28	125.01
PP176	1030.02	1.93	88.92	7.33	63.36	4.29	23.95	4.37	2.47	1.65	17.36	6.01	8.44	0.91	42.88	0.34	2.71	13.20	40.21	19.48	10.73	88.82	7.32	416.92	1.19	0.83	14.92	0.36	3.06	85.13	24.16	2.34	87.93	332.70
PP178	682.05	2.15	95.19	11.79	53.63	4.65	17.64	12.72	6.96	3.43	18.08	12.77	5.08	2.63	37.18	0.91	3.12	8.07	62.75	21.18	13.60	87.21	13.76	267.35	0.68	2.15	7.06	1.01	2.24	84.14	74.85	6.43	142.21	185.06
PP190	993.15	1.47	37.56	2.56	33.27	2.96	14.57	1.53	0.79	0.76	14.53	2.31	5.75	0.30	19.88	0.13	0.89	8.76	16.11	8.02	4.34	97.08	2.91	468.07	0.76	0.31	10.09	0.12	1.56	60.00	7.60	0.82	35.26	235.55
OP058	1517.38	1.26	42.73	4.00	29.26	3.18	11.75	1.75	1.02	0.86	14.58	2.57	3.23	0.36	21.80	0.14	0.65	9.38	18.09	11.65	4.98	102.66	3.18	291.94	0.77	0.34	7.09	0.15	1.68	44.26	10.45	0.98	55.65	119.33
OP067	1550.46	2.56	78.54	11.07	99.58	10.96	35.73	4.52	2.50	1.51	22.24	5.45	6.62	0.92	32.61	0.36	0.67	14.96	33.47	36.30	8.60	141.75	6.51	126.77	1.23	0.81	15.10	0.38	3.18	112.10	24.73	2.35	106.14	249.66
OP070	1406.40	1.77	51.43	6.18	35.31	4.39	15.02	2.08	1.15	0.99	17.30	3.09	3.79	0.42	27.95	0.16	0.95	10.28	21.81	14.24	6.00	127.95	3.73	344.99	0.83	0.41	9.49	0.17	1.90	56.40	11.51	1.07	74.05	137.86
Pi079	648.25	1.88	5.74	2.72	173.91	2.25	4.65	0.57	0.37	0.16	7.01	0.43	2.83	0.13	3.40	0.08	2.62	5.33	2.25	17.89	0.66	69.31	0.47	66.69	0.40	0.08	6.14	0.08	1.61	381.32	3.83	0.50	42.46	93.91
Pi080	1099.09	2.20	34.33	1.42	60.78	1.78	6.04	2.12	1.22	0.74	16.56	2.67	2.91	0.45	16.76	0.16	0.59	8.11	16.02	10.63	4.23	55.39	3.13	130.03	0.66	0.38	6.29	0.17	2.74	68.12	12.89	1.13	13.40	108.23
Pi088	1273.02	1.45	31.56	2.16	36.13	2.02	6.64	2.01	1.24	0.73	13.25	2.37	2.58	0.45	15.71	0.17	2.56	7.61	14.36	12.34	3.73	54.63	2.62	125.45	0.63	0.35	5.98	0.17	1.40	52.38	13.53	1.11	12.98	96.05
Pi092	1215.40	1.51	49.78	3.96	39.44	2.23	11.74	2.41	1.38	0.93	14.84	3.17	2.94	0.50	25.60	0.18	2.81	8.46	20.34	19.51	5.59	69.81	3.64	144.49	0.66	0.46	6.97	0.21	1.62	56.91	15.14	1.27	28.98	107.11
Pi095	1096.95	2.37	65.94	5.04	57.00	3.53	18.11	3.65	2.11	1.36	20.59	4.70	4.27	0.77	34.26	0.28	3.10	10.70	30.06	26.42	7.97	84.49	5.44	133.39	0.81	0.65	7.86	0.32	2.16	75.91	23.06	1.92	52.52	163.22
Pi099	1249.54	2.15	78.51	3.87	70.21	3.03	12.90	4.14	2.26	1.56	20.35	5.25	5.42	0.84	38.27	0.31	2.94	17.17	35.43	20.63	9.41	81.86	6.35	137.57	1.38	0.77	13.30	0.33	3.05	93.72	24.54	2.07	107.04	206.49
Pi104	1171.65	1.96	60.00	4.41	73.58	3.85	14.87	3.33	1.99	1.15	19.74	4.24	5.62	0.73	30.16	0.28	3.41	11.99	27.13	21.83	7.23	97.80	4.86	141.84	0.93	0.60	8.69	0.33	2.38	97.41	21.76	1.90	43.09	215.45
Pi106	1028.02	2.86	98.52	6.37	116.63	27.02	20.51	5.55	3.29	1.66	24.97	6.54	7.82	1.21	52.62	0.51	3.39	16.36	42.09	31.26	11.22	154.74	7.48	80.07	1.30	0.99	16.54	0.49	3.70	137.63	35.92	3.27	61.70	290.49
Pi110	822.92	1.28	44.20	2.15	37.29	2.64	4.90	2.17	1.26	0.90	14.66	2.91	2.87	0.46	21.91	0.18	0.38	9.26	19.26	9.22	5.17	74.59	3.25	143.81	0.80	0.40	8.45	0.19	1.73	52.87	13.18	1.23	22.79	102.59
Pi115	1138.92	1.37	56.33	3.96	37.39	2.03	7.85	2.35	1.27	1.08	14.07	3.52	3.88	0.46	29.43	0.18	0.41	9.06	25.01	12.44	6.61	79.88	4.37	206.97	0.81	0.44	8.48	0.18	1.50	49.46	13.05	1.20	49.22	164.14
Pi120	764.57	3.34	118.59	4.31	105.12	12.95	85.42	6.90	3.88	2.00	23.18	8.24	7.08	1.43	59.12	0.55	0.57	15.60	51.16	21.29	13.66	132.54	9.28	66.77	1.28	1.22	16.35	0.58	3.28	115.08	41.62	3.70	56.59	263.71
Pi125	975.87	1.56	62.00	2.41	52.11	3.47	16.10	2.83	1.52	1.17	17.25	4.07	6.20	0.55	31.44	0.22	0.71	13.57	27.72	11.48	7.40	97.73	4.92	163.07	1.13	0.54	9.52	0.23	2.35	57.51	16.19	1.45	30.03	243.09
Pi127	977.27	1.44	67.99	3.82	41.16	3.42	6.60	2.86	1.57	1.24	16.44	4.18	3.25	0.57	33.27	0.21	0.37	10.81	29.71	11.04	8.00	98.50	5.03	164.46	0.84	0.55	10.13	0.23	2.19	58.67	16.96	1.43	37.94	117.87
Pi128	923.42	2.14	62.12	4.65	41.55	3.76	13.23	3.20	1.66	1.37	17.76	4.54	3.64	0.64	32.83	0.23	0.38	11.81	30.88	13.87	7.98	115.26	5.33	158.90	0.99	0.61	7.91	0.24	2.06	59.45	18.47	1.50	79.31	130.14
Pi130	895.05	1.59	57.66	4.46	51.78	3.83	11.52	2.38	1.38	1.08	18.50	3.64	5.09	0.49	29.26	0.20	0.55	12.32	25.57	13.41	6.83	101.73	4.36	218.69	0.96	0.48	9.80	0.20	2.11	89.41	13.94	1.34	43.74	201.95
Pi134	1269.79	1.45	63.37	4.47	61.59	4.02	12.15	2.72	1.46	1.13	16.81	3.91	6.13	0.54	31.22	0.20	0.55	13.03	27.82	14.43	7.46	101.73	4.82	210.74	1.10	0.56	12.33	0.22	2.15	68.65	14.55	1.41	43.10	246.11
Pi138	1120.93	1.97	70.06	8.50	50.69	6.45	20.59	3.15	1.63	1.33	20.68	4.53	5.19	0.61	35.36	0.22	1.66	11.17	31.56	24.86	8.39	120.00	5.49	191.38	0.78	0.60	10.93	0.23	2.43	81.82	16.64	1.53	93.60	194.01
Pi142	970.38	1.67	51.45	5.50	48.01	3.60	18.07	2.27	1.20	0.95	18.62	3.17	4.52	0.45	25.95	0.17	1.47	12.37	22.61	21.10	6.12	104.59	4.07	250.97	1.07	0.43	10.30	0.18	2.11	77.71	12.04	1.13	57.52	168.56
Pi145	1104.95	2.16	88.38	7.64	81.45	13.05	20.98	4.74	2.73	1.41	18.91	5.78	7.63	0.98	42.67	0.37	2.44	14.09	38.05	26.09	10.06	119.40	6.97	94.26	1.15	0.84	14.45	0.40	3.75	94.59	27.66	2.64	64.88	277.89
Pu203	901.74	2.15	168.93	4.11	181.62	1.89	28.83	6.04	3.21	2.68	17.75	9.67	23.19	1.18	78.71	0.48	1.14	42.05	74.20	14.44	19.76	67.96	12.36	134.97	3.75	1.23	46.92	0.48	8.27	76.49	32.78	3.06	187.65	965.12
Pu205	793.44	9.46	105.88	8.78	96.54	20.87	51.63	8.23	5.65	2.31	28.06	9.07	3.75	1.90	55.55	1.13	1.08	15.23	50.61	26.44	13.02	143.11	9.73	97.27	1.18	1.36	17.13	0.90	4.94	138.86	61.41	5.94	46.03	131.95
Pu207	908.24	1.54	48.31	1.24	43.18	1.85	4.19	2.58	1.47	0.98	14.43	3.27	3.52	0.53	24.34	0.20	0.55	10.43	22.12	6.79	5.83	67.72	3.98	134.27	0.78	0.47	8.58	0.21	1.68	53.75	15.09	1.39	6.43	125.32
Pu215	906.64	1.47	65.69	1.10	43.62	1.62	10.41	2.98	1.56	1.28	14.48	4.18	2.92	0.60	31.54	0.21	0.40	8.47	28.53	7.31	7.66	66.80	5.24	149.27	0.60	0.57	8.36	0.23	1.59	54.40	16.18	1.43	6.36	105.00
Pu218	825.21	1.19	46.35	1.32	40.26	1.59	5.23	2.26	1.37	0.90	14.41	3.05	3.11	0.49	23.64	0.20	0.65	8.20	20.46	6.72	5.41	62.62	3.58	140.33	0.61	0.42	7.68	0.21	1.52	47.35	14.45	1.31	13.27	112.85
Pu221	377.94	0.83	17.49	3.95	87.57	1.19	2.16	1.05	0.61	0.38	3.98	1.14	1.97	0.22	8.54	0.09	0.65	3.76	6.62	34.36	1.86	42.20	1.29	68.31	0.29	0.18	4.53	0.10	2.38	170.20	5.91	0.62	33.98	63.56